RAINFALL AND RUNOFF ESTIMATION USING HYDROLOGICAL MODELS AND ANN TECHNIQUES

ATHESIS SUBMITTED

FOR THE AWARD OF THE DEGREE OF

DOCTOR OF PHILOSCOPHY

IN

CIVIL ENGINEERING

BY

JANHABI MEHER
(ROLL NO. 510CE101)

NATIONAL INSTITUTE OF TECHNOLOGY
ROURKELA-769008, INDIA

July-2014

National Institute of Technology Rourkela
Rourkela-769008

CERTIFICATE

This to certify that the thesis entitled "**Rainfall and Runoff Estimation using Hydrological Models and ANN Techniques"** being submitted by **Mrs. Janhabi Meher** for the award of the degree of Doctor of Philosophy (Civil Engineering) of NIT Rourkela, is a record of bonafide research work carried out by her under my supervision and guidance.

To the best of our knowledge, the matter embodied in the thesis has not been submitted to any other university or institution for the award of any degree or diploma.

Date:
Place: Rourkela

Dr. Ramakar Jha
Professor
Department of Civil Engineering
NIT Rourkela

Dedicated to

My Family

ACKNOWLEDGEMENT

First and foremost I convey my thanks to National Institute of Technology, Rourkela for providing me the degree of Doctor of Philosophy in Civil Engineering.

I feel glad to offer my sincerest gratitude and respect to my supervisor Prof. Ramakar Jha, Water Resources Department for his invaluable advice, and guidance from the foundational stage of this research and providing me extraordinary experiences throughout the work.I truly appreciate his esteemed guidance and encouragement from beginning to the end of the thesis. I consider myself extremely fortunate to have had the opportunity of associating myself with him.

I wish to express my sincere thanks to Prof. N. Roy, Chairman of doctoral committee and the doctoral committee members Prof. K. K. Khatua, Prof. B.K. Pal and Prof. D. P. Tripathy, for their valuable suggestions and instructions in my work.

I would like to express my gratitude to all the faculty and staff members of the Department of Civil Engineering, National Institute of Technology, Rourkela for their continuous support and moral inspiration.

I am also thankful to my friends, of Civil Engineering Department NIT., Rourkela for their helping hands during the project.

Last but not the least; I am especially indebted to my parents, husband and son for their unwavering support, love and invariable source of motivation.

Janhabi Meher

ABSTRACT

Water is one of the most important natural resources and a key element in the socio-economic development of a State and Country. Water resources of the world in general and in India are under heavy stress due to increased demand and limitation of available quantity. Proper water management is the only option that ensures a squeezed gap between the demand and supply. Rainfall is the major component of the hydrologic cycle and this is the primary source of runoff. Worldwide many attempts have been made to model and predict rainfall behaviour using various empirical, statistical, numerical and deterministic techniques. They are still in research stage and needs more focussed empirical approaches to estimate and predict rainfall accurately. Various spatial interpolation techniques to obtain representative rainfall over the entire basin or sub-basins have also been used in the past. In the present work, estimation of mean rainfall over the Mahanadi basin lying in Odisha and its sub-basins has been done using different deterministic and geo-statistical methods including nearest neighbourhood, Spline, Inverse-distance weighting, and Kriging techniques. Different thematic maps for the study area have been developed for water resources assessment, planning and development analysis.

Further, rainfall generated runoff is very important in various activities of water resources development and management. The method of transformation of rainfall to runoff is highly complex, dynamic, nonlinear, and exhibits temporal and spatial variability. It is further affected by many parameters and often inter-related physical factors. Determining a robust relationship between rainfall and runoff for a watershed has been one of the most important problems for hydrologists, engineers, and agriculturists. Many approaches are being used to estimate runoff, in which the soil conservation service curve number (SCS-CN) method (SCS 1956) converts rainfall to surface runoff (or rainfall-excess) using a CN derived from

watershed characteristics and 5-days antecedent rainfall is one. In this study, simulation and critical evaluation of daily runoff has been done using various rainfall-runoff models based on (a) existing SCS-CN Model: NEH (1954) with remote sensing data as input, MS model (2002), Michel model (2005), and Sahu Model (2007), and (b) proposed FD-PE model (2014), MM-SCS model (2014), and ANN-MLP model (2014) techniques.

It is understood that, the CN value for estimating runoff potential for planning purposes at watershed, sub-basin and basin level is often a policy decision. The available approaches utilize either daily, weekly, half-monthly or monthly data or average physical characteristics of watersheds. Derivation of Curve Numbers for 1-day, 2-day, 3-day, 4-day, 5-day, 6-day, 7-day, 10-day, 15-day, 20-day, 25-day and 30-day runoff data has been done in the present work and equations are derived to obtain curve numbers and estimate runoff.

Monthly data are very useful for the planning, development and management of available water resources. Development of SARIMA and MLP-ANN models for monthly rainfall forecasting for Mahanadi basin lying in Odisha and its sub-basins has been done. Further, application of forecasted model to predict monthly runoff and their performance evaluation using different error statistics and correlation coefficient is done.

TABLE OF CONTENTS

LIST OF FIGURES

LIST OF TABLES

CHAPTER 1

INTRODUCTION

1.1 BACKGROUND

Water is one of the most important natural resources and a key element in the socio-economic development of a State and Country. Water influences every sphere of the environment supporting life on earth. Its varying availability in time and space is a matter of concern to the mankind since fresh water is not an ever-present resource. Water resources of the world in general and in India are under heavy stress due to increased demand and limitation of available quantity. Proper water management is the only option that ensures a squeezed gap between the demand and supply. Sustainable water management of a river basin is required to ensure a long-term stable and flexible water supply to meet crop water demands as well as growing municipal and industrial water demands. Water resources structures need appropriate planning to ensure the fulfilment of the goals of water management. Water resources management requires a systems approach that includes not only all of the hydrological components, but also the links, relations, interactions, consequences, and implications among these components. Human modifications of the environment, including land cover change, irrigation, and flow regulation, now occur on scales that significantly affect seasonal and yearly hydrologic variations. A thorough knowledge and understanding of the different hydrological phenomena and hydrological cycle as a whole is required in studying the implications of these changes.

1.2 RAINFALL ANALYSIS

Rainfall is the major component of the hydrologic cycle and is the primary source of runoff (Beven, 2001b). Rainfall is essentially required to fulfil various demands including agriculture, hydropower, industries, environment and ecology. It is implicit that the rainfall is

a natural phenomenon occurring due to atmospheric and oceanic circulation (local convection, frontal or orographic pattern) and has large variability at different spatial and temporal scales. However, this input is subjected to uncertainty and stochastic errors (Jakeman and Hornberger, 1993; Beven, 2001a). Worldwide many attempts have been made to model and predict rainfall behaviour using various empirical, statistical, numerical and deterministic techniques (Namias, 1968; Koteshwaram and Alvi, 1969; Ramamurthy et al. 1987; Jha and Jaiswal, 1992; Chiew et al, 1993; Kuo and Sun, 1993; Langu, 1993; Meher and Jha, 2011(a); Meher and Jha, 2011(b)). They are still in research stage and needs more focussed empirical approaches to estimate and predict rainfall accurately.

These data are usually collected using rain gauges, and therefore they are point precipitation data. However, the application of a single rain gauge as precipitation input carries lots of uncertainties regarding estimation of runoff (Faur`es et al., 1995 and Chaubey et al., 1999).This creates a lot of problem for the discharge prediction, especially if the rain gauge is located outside the basin (Schuurmans and Bierkens, 2007).As a result, some utilities such as hydrological modelling (Syed et al., 2003; Kobold and Su˘selj, 2005; Gabellani et al., 2007; Cole and Moore, 2008; Collischonn, et al., 2008; Ruelland et al., 2008; Moulin et al., 2009) need rainfall data that are spatially continuous. The quality of such result is therefore estimated by the quality of the continuous spatial rainfall (Singh, 1997; Andr´eassian et al., 2001; Kobold and Su˘selj, 2005; Leander et al., 2008; Moulin et al., 2009). Various spatial interpolation techniques to obtain representative rainfall over the entire basin or sub-basins have also been used in the past.

The justification underlying spatial interpolation is the assumption that points closer together in space are more likely to have similar values than points that are more distant. This observation is known as Tobler's First Law of Geography (Tobler, 1970). Spatial interpolation is a very important component of many geographical information systems

(GIS), frequently used as a tool to aid spatial decision making both in (1) physical and human geography and (2) related disciplines, such as hydrology and water resources planning and management. Many of the techniques of spatial interpolation are two-dimensional developments of the one-dimensional methods originally developed for time series analysis (Ripley, 1981).

Once the spatial interpolation is done by different methods, the rainfall data may be used to predict rainfall by time series analysis. The main development of time series models is done by Box and Jenkins (1970) and further discussed in some other resources (Chatfild, 1996; Montgomery and Johnson, 1967). Many attempts have been made in the recent past to model and forecast rainfall using various techniques, with the use of time series techniques proving to be the most common (Gorman and Toman, 1966; Salas et al., 1980; Galeati, 1990; Lall and Bosworth, 1993; Hsu *et al*., 1995, Davidson, *et.al*., 2003). In time series analysis it is assumed that the data consists of a systematic pattern (usually a set of identifiable components) and random noise (error) which usually makes the pattern difficult to identify. Time series analysis techniques usually involve some method of filtering out noise in order to make the pattern more salient. The time series patterns can be described in terms of two basic classes of components: trend and seasonality. The trend represents a general systematic linear or (most often) nonlinear component that changes over time and does not repeat or at least does not repeat within the time range captured by the data. The seasonality may have a formally similar nature; however, it repeats itself in systematic intervals over time. Those two general classes of time series components may coexist in real-life data. The ARIMA model is an important forecasting tool, and is the basis of many fundamental ideas in time-series analysis. An autoregressive model of order p is conventionally classified as AR (p) and a moving average model with q terms is known as MA (q). A combined model that contains p

autoregressive terms and *q* moving average terms is called ARMA (*p*,*q*) (Gujarati, 1995). If the object series is differenced *d* times to achieve stationarity, the model is classified as ARIMA (*p, d, q*), where the letter "I" signifies "integrated". Thus, an ARIMA model is a combination of an autoregressive (AR) process and a moving average (MA) process applied to a non-stationary data series. ARIMA modeling has been successfully applied in various water and environmental management applications (Meher and Jha, 2013).

Many applications of ANN can be found in water resource and environmental engineering literature. Some of these studies include groundwater simulation by Nourani et al. (2008), river flow modeling by Kisi (2004a, 2007) and Cigizoglu and Kisi (2005), water quality modeling by Onkal-Engin et al. (2005), hydrological time series modeling by Jayawardena et al. (2006) and rainfall and runoff modeling by Tokar and Johnson (1999). There are many approaches to estimate rainfall and rainfall generated runoff. Among all, ANN has also been considered as one of the reliable methods to estimate rainfall and rainfall generated runoff at basin and sub-basin scales. The application of the ANN in time series for forecasting is relatively new (Mirko & Christian 2000). It is primarily based on the ability of neural networks to approximate nonlinear functions. This technique corresponds to human neurological system, which consists of a series of basic computing elements, called as neurons, interconnected together to form a network (Rummelhart & McClelland 1996). The parallel-distributed processing architecture of ANN has proved to be a very powerful computational tool which is now being used in several fields to model the dynamic processes successfully (Mirko & Christian 2000; Mary 2002) including the rainfall (Singh & Chowdhury 1986; Cigizoglu 2002). This technique has the ability to learn and generalize from examples to produce meaningful solutions.

1.3 RUNOFF ANALYSIS

Further, rainfall generated runoff is very important in various activities of water resources development and management, such as: flood control and its management, irrigation scheduling, design of irrigation and drainage works, design of hydraulic structures, hydro-power generation, and so on. The method of transformation of rainfall to runoff is highly complex, dynamic, nonlinear, and exhibits temporal and spatial variability. It is further affected by many parameters and often inter-related physical factors. It is a common experience that for a given amount of rainfall on a watershed, the event produces a high or low runoff depending on (besides other parameters): the small or large time interval/duration, with the infiltration and evaporation losses depending significantly on how long the water remains in the watershed.

Determining a robust relationship between rainfall and runoff for a watershed has been one of the most important problems for hydrologists, engineers, and agriculturists. Many approaches are being used to estimate runoff, in which the soil conservation service curve number (SCS-CN) method (SCS 1956) converts rainfall to surface runoff (or rainfall-excess) using a CN derived from watershed characteristics and 5-days antecedent rainfall is one. Being conceptual, the runoff curve number method is simple, and this is at the root of its popularity. On the other hand, the runoff curve number method has not fared well among the supporters of alternative models, which include the physically based models (Smith 1976). Ponce and Hawkins (1996) critically examined the curve number method and clarified its conceptual and empirical basis. The curve number method is an infiltration loss model; where infiltration is the most important loss for short term storm analysis, although it may also account for interception and surface storage losses through its initial abstraction feature, which are usually of secondary importance. As originally developed, the method is not intended to account for evaporation and evapo-transpiration, which are long term losses and are the most important for seasonal or annual yield evaluations (Ponce and Hawkins, 1996).

Many researchers have demonstrated that potential retention from rainfall and runoff data has variable components and is not a constant for a watershed (Hjelmfelt et al. 1982; McCuen 2002), and varies with rainfall. As a result, CN value varies monthly, seasonally and annually. In a similar manner CN varies at daily, weekly and half-monthly basis too. Besides daily and monthly CN values, weekly, ten days and half-monthly CN are also required for various purposes such as agriculture, flood control, drought mitigation etc. Therefore, such studies are very important.

Remote Sensing and GIS techniques are being increasingly used for planning, development and management of natural resources. GIS technology helps in integrating various data sets and spatial analysis for decision making. Data acquired through remote sensing satellite can help us in mapping land and other resources in spatial and temporal domain. These technologies presently being used for solving watershed related problems like watershed planning, development and management, aim to harness all natural resources for sustainable development. Thus Remote Sensing and GIS together provide information base for efficient management of water resources. Some researchers integrated the SCS-CN model into the GIS/RS system to extend the model applicability to complex watersheds with high temporal and spatial variability in soil and land use (Zhan and Huang, 2004; Geetha *et al*., 2007).

A lot of studies on application of ANN for stream flow prediction are also found in the literature. ANN is defined according to its model inputs and its architecture: the number of layers, the number of nodes in each layer, the activation function in each layer, and the manner in which the layers are interconnected. However, one of the most unresolved questions in modelling of the rainfall-runoff process when applying ANNs is what architecture should be used to map the process effectively. The selection requires choosing an appropriate input vector, besides the hidden units and weights. Unlike the physically based models, the sets of variables that influence the system are not known a priori. Therefore, the

selection of an appropriate input vector that will allow an ANN to map to the desired output vector successfully is not a trivial task. In most of the applications that are reported, this has been done by a trial- and error-procedure (Fernando and Jayawardena, 1998). Sudheer et al. (2002) outlined a procedure for selecting an appropriate input vector in ANN rainfall-runoff models, based on statistical pre-processing of the data set. The proposed methodology has been illustrated by presenting an application of the procedure to an Indian River basin. The results reported by some researchers have also been analyzed to check the effectiveness of the proposed algorithm and then they concluded that their proposed algorithm would easily lead to a more compact network, thus avoiding a long trial- and-error procedure.

Keeping above in view, a comprehensive study on rainfall estimation and rainfall generated runoff estimation has been done in Mahanadi river system lying in Odisha and its five sub-basins (Sundargarh, Kesinga, Kantamal, Salebhata, and Tikarpara) with the following objectives.

1.4 OBJECTIVES

1. Development of Thematic maps for Mahanadi Basin lying in Odisha and its sub-basins for water resources assessment, planning and development analysis.
2. Estimation of mean rainfall over the Mahanadi basin lying in Odisha and its sub-basins using different deterministic and geo-statistical methods including nearest neighbourhood, Spline, Inverse-distance weighting, and Kriging techniques.
3. Simulation and critical evaluation of daily runoff using various rainfall-runoff models based on (a) existing SCS-CN Model: NEH (1954) with remote sensing data as input, MS model (2002), Michel model (2005), and Sahu Model (2007), and (b) proposed FD-PE model (2014), MM-SCS model (2014), and ANN-MLP model (2014) techniques in Mahanadi basin lying in Odisha and its sub-basins.

4. Simulation and critical evaluation of monthly runoff using various rainfall-runoff models used above and applicable for monthly data set in Mahanadi basin lying in Odisha and its sub-basins.
5. Performance evaluation of all the models using different error statistics and correlation coefficient for daily and monthly rainfall-runoff data.
6. Derivation of Curve Numbers for 1-day, 2-day, 3-day, 4-day, 5-day, 6-day, 7-day, 10-day, 15-day, 20-day, 25-day and 30-day runoff data. Moreover, equations are derived to obtain curve numbers and resulting runoff for any number of days ranging between 1 to 30 days.
7. Development of SARIMA and MLP-ANN models for monthly rainfall forecasting for Mahanadi basin lying in Odisha and its sub-basins. Application of forecasted model to predict monthly runoff and their pperformance evaluation using different error statistics and correlation coefficient.

1.5 SKETCH OUT OF THE CHAPTERS

In view of the above objectives the present work has been divided into different Chapters.

Chapter 1 describes concise introduction of the topic, objectives and sketch out of the chapters.

Chapter 2 provides comprehensive literature review on rainfall interpolation methods, rainfall forecasting techniques and runoff estimation techniques.

Chapter 3 describes various salient features of Mahanadi river basin lying in Odisha and its sub basins (Sundargarh, Kesinga, Kantamal, Salebhata, Tikarpara and Naraj). Data collection part is also included in this chapter.

Chapter 4 shows delineation of the thematic maps for the study area having different Themes and required to be used for analysis in next chapters as input theme and variable.

Chapter 5 computes different deterministic and geo-statistical spatial rainfall interpolation techniques for calculation of rainfall over individual sub-basin of the study area.

Chapter 6 evaluates daily runoff using various existing and proposed rainfall-runoff models. This section thoroughly presents the methods applied for derivation of CN for runoff computation. A comparative study of the proposed methods with previously developed models has also been presented. Finally developmental procedure and validation of a CN equation with the best applied method has been described.

Chapter 7 derives Curve Numbers for different rainfall and runoff durations varying from 1 day to 30-day period to obtain curve numbers and resulting runoff.

Chapter 8 describes SARIMA and ANN models for rainfall forecasting. This section describes about application of these models for monthly forecasting of rainfall and utilization of the forecasted rainfall for monthly runoff computations.

Chapter 9 is the Conclusions of all the findings.

CHAPTER 2

LITERATURE REVIEW

2.1 INTRODUCTION

Assessment, simulation and prediction of rainfall and corresponding runoff are essential for stakeholders and policy makers to plan or adopt the required policies. There are various techniques available in the literature to assess, simulate and predict hydrological variables. However, the selection of these techniques normally depends on the objectives of the study, availability of required input data, the quality of available models and some pre- defined assumptions. According to Makridakis et al., (1998) each method is different in terms of accuracy, scope, time horizon and the cost. To facilitate an adequate level of accuracy, the developer has to be responsive to the characteristics of different methods, and determine if a particular method is appropriate for the undertaken situation before embarking its usage in real application. As a result, the choice of a model is one of the important factors that will influence the forecasting accuracy. In the following sections literature review on the application of various hydrological and ANN models for rainfall and runoff assessment, simulation and prediction has been summarized.

2.2 SPATIAL INTERPOLATION OF RAINFALL

The application of point rain gauge as precipitation input carries lots of uncertainties regarding estimation of runoff (Faur`es et al., 1995 and Chaubey et al., 1999), which, in turn, creates problem for the discharge prediction, especially if the rain gauge is located outside the basin (Schuurmans and Bierkens, 2007). For such reasons, some utilities such as hydrological modeling (Syed et al., 2003; Kobold and Su˘selj, 2005; Gabellani et al., 2007; Cole and Moore, 2008; Collischonn, et al., 2008; Ruelland et al., 2008; Moulin et al., 2009) need rainfall data that are spatially continuous and the quality of results are by the quality of the

continuous spatial rainfall (Singh, 1997; Andr´eassian et al., 2001; Kobold and Su˘selj, 2005; Leander et al., 2008; Moulin et al., 2009).

Many of the techniques of spatial interpolation are two-dimensional developments of the one-dimensional methods originally developed for time series analysis (Ripley, 1981).

Karnieli and Gurion (1990) applied kriging technique for mapping and evaluating precipitation data for the State of Arizona, as the classical methods for interpolating and spatial averaging of precipitation fields fail to quantify the accuracy of the estimate.

Annual and monthly rainfall data from the Algarve region (Portugal) are interpolated by Hutchinson (1998) using 100 daily square root transformed rainfall values across the USA using two dimensional thin plate smoothing splines. The distribution of precipitation usually relates to orographic factors, and this makes the use of topographic data advantageous for spatial rainfall interpolation.

Goovaerts (2000) and Lloyd (2005) applied elevation as secondary data to incorporate into multivariate geo-statistics for monthly and annual rainfall and compared these results with those of deterministic methods.

Goovaerts (2000) used two types of techniques: (1) methods that use only rainfall data recorded at 36 stations (the Thiessen polygon, inverse square distance, and ordinary kriging); and (2) algorithms that combine rainfall data with a digital elevation model (linear regression, simple kriging with varying local means, kriging with an external drift, co-located ordinary cokriging), and concluded that for low-density networks of rain gages geostatistical interpolation outperforms deterministic techniques.

Kastelec and Kosmelj (2002) found an appropriate method for the spatial interpolation of mean yearly precipitation (MYP) into a regular grid with 1 km resolution, for Slovenia, using the universal kriging method.

Naoum and Tsanis (2004) selected the appropriate interpolation technique used in studying rainfall spatial variability of the country of Switzerland by developing a GIS-based Decision Support System (DSS). They found that the ordinary Kriging with exponential model and Universal Kriging with linear drift model showed consistent performance and provided reliable estimates regardless of the number of gages or the cell size used in the interpolation.

Lloyd (2005) did mapping monthly precipitation in Great Britain from sparse point data using techniques (i) moving window regression, (ii) inverse distance weighting, (iii) ordinary kriging, (iv) simple kriging with a locally varying mean and (v) kriging with an external drift (KED). MWR, SKlm and KED make use of elevation data.

Kottek and Rubel (2008) applied ordinary areal kriging for interpolation to compile a global precipitation product by incorporation of daily ground rain gauge measurements so that an improvement of the global precipitation data accuracy would be possible.

Hofstra et al. (2008) compared six interpolation methods e.g. global and local kriging, two versions of angular distance weighting, natural neighbor interpolation, regression, 2D and 3D thin plate splines, and conditional interpolation, for the interpolation of daily precipitation, mean, minimum and maximum temperature, and sea level pressure from station data over Europe from 1961 to 1990 and selected global kriging as the best performing method overall, for use in the development of a daily, high-resolution, long-term, European data set of climate variables.

Taesombat and Sriwongsitanon (2009) introduced the thin plate spline (TPS) technique for daily areal rainfall approximation in the Upper Ping river basin and found that the spline technique proved to provide more accurate results of rainfall estimation than the two conventional techniques, the isohyetal and Thiessen polygon techniques. Global daily precipitation analyses are mainly based on satellite estimates, often calibrated with monthly ground analyses or merged with model predictions.

Tao et al. (2009) analyzed some rainfall series from 30 rain gauges located in the Great Lyon area, including annual, month, day and intensity of 6mins, aiming at improving the understanding of the major sources of variation and uncertainty in small scale rainfall interpolation in different input series and found that the model and the parameters of Kriging should be different for the different rainfall series, even if in the same study area. Again they found that to the small region with high density of rain gauges, the Kriging method superiority is not obvious, IDW and the Spline interpolation result can be better. Finally, they concluded that the different methods will be suitable for the different research series, and it must be determined by the data series distribution.

Geostatistical interpolation of daily rainfall for 30-year daily rainfall data of 70 rain gages in the hilly landscape of the Ourthe and Ambleve catchments in Belgium was done by Ly et al. (2011). For geostatistical algorithms, seven semi-variogram models were fitted to daily sample semi-variogram on a daily basis and found that between the seven semi-variogram models used, the Gaussian model was the most frequently best fit.

Luo et al. (2011) chose ordinary co-kriging (OCK) to integrate altitude into the estimation of monthly precipitation. On the other hand, another three commonly used methods, including Thiessen polygon, inverse distance weighted (IDW) and ordinary kriging (OK), were also adopted to compare the spatial monthly rainfall estimation performance of OCK with other methods especially for different correlation between rainfall and elevation.

Mair and Fares (2011) used traditional and geostatistical interpolation methods such as Thiessen polygon, IDW, linear regression, ordinary kriging and simple kriging with varying local means to estimate wet and dry season rainfall and compared them in assessing rainfall spatial variability across the mountainous leeward portion of the island of O'ahu ,Hawai'i. From ordinary kriging interpolation map, they found that the areas of greatest rainfall deficit are confined to the mountainous region of west O'ahu.

Regarding the spatial interpolation of rainfall, Chen and Liu (2012) used the inverse distance weighting (IDW) method to estimate the rainfall distribution in the middle of Taiwan. Besides, they evaluated the relationship between interpolation accuracy and two critical parameters of IDW: power value and radius of influence (search radius).

2.3 RAINFALL PREDICTION MODELS

2.3.1 Based on ARIMA Modeling

Time series analysis is one of the most popular forms of data-driven modeling in rainfall and stream flow forecasting. Most "time series" models belong to the class of linear time series forecasting, because they postulate a linear dependency of the future value on the past values. The most popular univariate models are the autoregressive moving average (ARMA) model and its derivatives, which include the autoregressive (AR), autoregressive integrated moving average (ARIMA), seasonal ARIMA, periodic ARMA, threshold AR, and fractionally integrated ARMA models (Adamowski and Karapataki,2010). These univariate time series models including autoregressive integrated moving average (ARIMA) models and derivatives have long been applied in rainfall and stream flow forecasting, particularly in the modeling of monthly rainfall and streamflow (Noakes et al. 1985; Salas 1992; Abrahart and See 2000; Wang et al. 2009).

Delleur and Kavvas(1978) developed a non-seasonal ARIMA model suitable for both generation of monthly rainfall series and forecasting and a seasonal ARIMA model suitable only for forecasting of one or two months ahead basin average rainfall series, which was obtained by Thiessen polygon method.

Chang et al. (1984) used a binary discrete autoregressive moving average (B-DARMA) process to model the sequences of wet and dry days which are obtained from daily precipitation time series.

Mateos et al. (2002) compared ARMA and discrete linear transfer function noise (DLTFN) model to fit monthly accumulated rainfall series and found that performance of the DLTFN model is better than that of ARMA model.

Weesakul and Lowanichchai (2005) developed ARIMA models most appropriate to forecast annual rainfall in all regions of Thailand with acceptable accuracy, which are able to fulfill the requirement for agricultural water allocation planning.

Singhrattna et al. (2005) adopted the traditional parametric linear regression approach ARIMA and a nonparametric regression technique to forecast of Thailand summer monsoon rainfall at 2–5 months' lead time and found that the nonparametric method showed improved skill in the extreme years.

Nail and Momani (2009) forecasted the monthly rainfall time series of Amman, Jordan using seasonal ARIMA which was not found appropriate to forecast peak values of monthly rainfall data.

Otok and Suhartono (2009) developed Adaptive Splines Threshold Autoregressive (ASTAR) which is a nonlinear time series model and Single Input Transfer Function model which is a linear multi-variate time series model to forecast monthly rainfall series of Indonesia, and they found the two methods better than ARIMA model while comparing both methods to ARIMA model.

Rabenja et al. (2009) used ARMA, ARIMA and SARIMA models to foresee the evolution of the monthly rainfall and found that the SARIMA model is the more adapted for the forecasting of monthly rainfall.

Tularam and Ilahee (2010) studied the relationship between temperature and rainfall variations in eastern Queensland with the use of time series (ARIMA) and spectral method and concluded that the daily temperature and daily rainfall were not related directly, while daily temperature range and rainfall were.

Magar and Jothiprakash (2011) developed and compared MLR models and ARIMA models using time-series lumped rainfall data derived from the Koyna watershed in Maharashtra, India to predict the inflow. Lumped rainfall data was derived using each station time series and Thiessen polygon method. They concluded that both the MLR and ARIMA models performed equally well for sufficiently longer rainfall data.

Sovoe (2011) forecasted the Volta river basin's long term rainfall event using Integrated Geographic Information System (GIS) and Autoregressive Integrated Moving Average (ARIMA) model. Historical spatial variation of the rainfall was modeled using Geographic Information System (GIS), through which monthly rainfall total for each sub-catchment was generated from a Thiessen polygon map.

Martins et al. (2011) modeled the daily flow sequence of the Benue River, Nigeria using Autoregressive Integrated Moving Average (ARIMA) and its two derivatives, the ARMA and the Periodic Autoregressive (PAR) models and it was found that ARMA model was unable to robustly simulate high flow regimes unlike the periodic AR (PAR).

Ashri et al. (2011) simulated the synthetic runoff data using the stochastic ARMA model by applying catchment average rainfall calculated using station based synthetic daily rainfall data and Thiessen polygons method. Synthetic daily rainfall data was generated using the stochastic Lag-one Markov Chain model.

Few hybrid models by combining ARIMA model with other models have been developed to improve performance of the ARIMA model. A hybrid model consisting of Singular Spectrum

Analysis (SSA) and ARIMA is proposed by Zhang et al. (2011) for medium and long-term hydrological runoff forecasting.

2.3.2 Based on ANN Modeling

Simple regression and multiple linear regression (MLR) are frequently used as rainfall and river flow forecasting methods. They have the advantage that they are comparatively simple and can easily be implemented. However, they are somewhat limited in their ability to forecast in certain situations, especially in the presence of nonlinear relationships and high levels of noisy data (Adamowski and Karapataki, 2010).

In recent years, the applications of artificial neural network (ANN) techniques in hydrological modeling have received increasing attention. The ANN has the capability to identify complex nonlinear relationships between input and output data sets without the necessity of understanding the nature of the phenomena and without making any underlying assumptions regarding linearity or normality (Abudu et al., 2011). ANN also has the capability to handle noisy data.

ANN was used by Sahai et al. (2000) to predict the seasonal and monthly mean summer monsoon rainfall over the whole of India, using only rainfall time series as inputs.

Toth et al. (2000) developed ARMA model, ANN and KNN method to forecast rainfall, using which the average areal rainfall over the watershed was computed with the Thiessen polygons method and was routed through a rainfall-runoff model. They compared performance of the three methods based on both forecasted rainfall and flow and concluded that the ARMA model provided best accuracy in flow forecasting.

Kihoro et al.(2004) comparatively evaluated performance of ANN to the univariate time series forecasting model ARIMA in forecasting various monthly time series data and showed that the ANN are relatively better than ARIMA models in forecasting ability but the nature of

the data may influence the results. Somvanshi et al. (2006) made a comparative study of complexity of the nature and behavior of annual rainfall record as obtained by ARIMA and ANN techniques and revealed that ANN model outperformed ARIMA model.

Iseri et al. (2005) computed the partial mutual information between August rainfall in Fukuoka, Japan and hydro-climatic variables in order to identify the predictors and forecasted August rainfall with the identified predictors using ANN.

Kumar et al. (2007) adopted ANN for individual months and for seasonal rainfall prediction using climate indices as predictor variables.

Hung et al. (2009) developed a rainfall forecast model using ANN technique and the ANN model was found to be efficient in fast computation and capable of handling the noisy and unstable data.

Karamouz et al. (2009) compared ANN with Statistical Down-Scaling Model (SDSM) for rainfall prediction and concluded that the SDSM performance is better than the ANN model, even though, in comparison, it is a more data intensive model than ANN.

Dastorani et al. (2010) applied ANN as well as ANFIS models to predict future precipitation in the hyper arid region of Yazd in Iran and found comparable prediction performance of these tools.

Khalili et al. (2011) used ANNs to obtain a forecasting model for the daily rainfall of Mashhad, Iran using only the past information of system and got satisfactory prediction performance. But Geetha and Selvaraj (2011) used ANN to predict monthly rainfall in Chennai and concluded that ANN could not predict the sharp peak values.

Sumi et al. (2011) proposed a hybrid multi-model approach for daily rainfall forecasting where other models such as step-wise linear regression, partial least square regression, multivariate adaptive regression spline and radial basis kernel gaussian process were used along with multi layer perceptron(MLP) ANN with quasi Newton optimization techniques.

2.4 RUNOFF SIMULATION MODELS

2.4.1 Based on SCS-CN Method

Long-term observations on stream flow are generally not available at desired locations, and these records often contain data missing attributable to variety of reasons. Therefore, many hydrological models have been developed in the past (Singh 1989; Singh and Frevert 2006) for transformations of rainfall into stream flow because of easy availability of rainfall data for longer time periods at different locations. In many of these models, soil conservation service curve number (SCS-CN) model has been widely used for surface runoff computations.

Yu (1998) provided a theoretical framework in which the SCS method can be tested. They showed that the proportionality between retention and runoff and the SCS equation would follow if the temporal distribution of rainfall intensity and the spatial distribution of the maximum rate of infiltration are independent and described by exponential probability distributions. In particular, they showed that the maximum retention S could be seen as the product of the spatially averaged maximum rate of infiltration and the effective storm duration.

Mishra and Singh (1999) modified the existing SCS-CN method by taking 0.5(P - Ia) in place of (P - Ia) .The existing SCS-CN method and the proposed modification are compared and the modified version is found to be more accurate than the current version.

Akhondi (2001) used curve number method in estimating flood utilizing geographical information system in north Karoon River field.

Mishra et al. (2004) modified the existing SCS-CN method, which is based on the Soil Conservation Service Curve Number (SCS-CN) methodology but incorporates the antecedent moisture in direct surface runoff computations and named it as MS model. They evaluated the modified version and by comparing with the existing SCS-CN method they found that the modified MS model performs far better than the existing SCS-CN model. In 2005, they

applied the MS model with its eight variants at field using a large set of rainfall-runoff events and revealed that the performance of the existing version of the SCS-CN method was significantly poorer than that of all the model variants.

Some researchers integrated the SCS-CN model into the GIS/RS system to extend the model applicability to complex watersheds with high temporal and spatial variability in soil and land use (Zhan and Huang, 2004; Geetha *et al*., 2007). Moreover, a great number of researchers carried our researches using GIS technique in order to determine curve number and runoff quantity in different regions in the world.

Tekeli et al. (2006) determined the digits of curve number for the study area using the instruments of GIS and RS. Yaghoobzadeh (2008) provided curve number map by merging the land usability, soil texture and slope maps in GIS and by the help of SCS table.

Mishra *et al*. (2006) employed a large dataset from 84 small watersheds (0.17– 71.99 ha in area) in the USA to investigate a number of *I*a-*S* relationships that incorporated antecedent moisture as a function of antecedent precipitation.

Jain *et al*. (2006) reviewed the *I*a-*S* relationship and proposed a new non-linear relationship that incorporated storm rainfall and Ponce and Hawkins (1996) suggested that the fixed initial abstraction ratio 0.20 may not be the most appropriate number and that it should be interpreted as a regional parameter.

Geetha et al. (2007) proposed two new modified models based on the existing SCS-CN concept, to carry out long-term hydrologic simulation. In Model I, CN is varied with respect to the AMC, whereas Model II computes CN variation by considering the antecedent moisture amount, by which pore space available for water retention *S* can be computed. They found that these models are capable of simulating stream flow. Better and satisfactory performance of Model II is attributed to the CN variation that varies with AMA and

advantageously obviates the sudden jumps in the curve number values with antecedent moisture conditions.

Mishra et al. (2008) presented a rain duration-dependent procedure based on the popular Soil Conservation Service Curve Number (SCS-CN) methodology for computation of direct surface runoff from long duration rains. Curve numbers were derived from long-term daily rainfall-runoff data, and antecedent moisture condition (AMC) related with antecedent duration. The derived runoff curve numbers exhibited a strong dependency on the storm duration and the reasonable match of the observed runoff with those due to the proposed approach was better than those from the original SCS-CN method.

Soulis et al. (2009) analyzed the fundamental mechanism for the generation of surface runoff, as well as to investigate the SCS-CN method applicability in a watershed presenting forested land covers with very permeable soils. The interpretation of the analysis results supports the hypothesis that in watersheds covered with permeable soils, the impervious part of the watershed is dominant in the direct runoff generation process. In such watersheds, the linear runoff response provides better results than the SCS-CN method.

Soulis et al. (2009) further analyzed the runoff generation mechanism and has shown that for some extreme rainfall intensity storm events, the permeable part of the watershed may partly participate in the runoff production. In this case, the linear formula significantly underestimates the total runoff.

Reshma et al.(2010) developed a hydrological model to simulate runoff from sub-watersheds using SCS curve number based unit hydrograph methods and another hydrological model to route the runoff from sub-watersheds to outlet of watersheds by Muskingum-Cunge method. Remote sensing and GIS techniques have been used to estimate the spatial variation of the hydrological parameters and it was found that the developed model has reasonably simulated the hydrographs of runoff at the outlet of watershed.

The applicability of the SCS-CN model to a small watershed on the Loess Plateau of China with high spatial heterogeneity was studied by Bo et al. (2011). They quantified the most appropriate *I*a*/S* value by the inverse method. The value of *I*a*/S*, which is traditionally set equal to 0.2, was modified until the model yielded the best performance. Finally, this value of the initial abstraction ratio was assumed for the runoff estimation. They found that the relative error rapidly decreased with increasing *I*a*/S* when it was less than 0.15, while it was almost stable when the *I*a*/S* value was between 0.15 and 0.30.

To overcome the slope limitation of the SCS-CN method, Gupta et al. (2012) modified the SCS-CN method to correct it for steep slopes. They incorporated antecedent moisture using Mishra et al. (2005a) approach. Furthermore, a hydrological model for runoff modeling should have two essential components such as generation of runoff and routing of runoff. The SCS-CN method is a static model and does not take into account routing phase of the runoff.

A hybrid technique was used by Gupta et al.(2012) ,combining a modified SCS-CN method with a physically distributed two-dimensional (2D) overland flow model to extend the SCS-CN method for accounting for the routing phase of the runoff.

Soulis and Valiantzas (2012) proposed a two-CN system considering the theoretical analysis of SCS-CN method, the systematic analysis using synthetic data and the detailed case studies. They concluded that the observed correlation between the calculated CN value and the rainfall depth in a watershed can be attributed to the soils and land cover spatial variability of the watershed and that the proposed two-CN system can sufficiently describe the CN-rainfall variation observed in natural watersheds.

Yu (2012) tested the assumption of proportionality, hence, the runoff equation for the SCS method, and aims to validate the foundation of the method. They further showed that the product of the effective storm duration and the maximum infiltration rate is a good predictor of the maximum retention parameter in the SCS method, and this interpretation of the

maximum retention provides an effective method to estimate storm runoff amount and peak runoff rate, which is an alternative approach to prediction of runoff amount and peak runoff rate.

Tedela et al. (2012) compared SCS-CN tabulated curve numbers with watershed curve numbers determined by five procedures using gauged rainfall and runoff for forested watersheds of the mountainous eastern United States. These procedures include the median, geometric mean, arithmetic mean, nonlinear, least squares fit, and standard asymptotic fit. They found substantial uncertainties in using the curve number method for estimating runoff from un-gauged watersheds. They concluded that runoff estimates using tabulated curve numbers are unreliable and that curve number selection requires independent calibration to watersheds representative of regional landscape and hydrologic characteristics. In un-gauged watersheds presenting forested land covers with very permeable soils, the runoff coefficient can be accurately estimated using land cover and soil survey using remote sensing and GIS, as well as a numerical soil water flow model (Soulis et al., 2009).

Again, the original conceptualization of the curve number method did not account for the influence of forest management practices. Tedela et al. (2012) calculated curve numbers for forested watersheds in the Appalachian Mountains of the eastern United States, by comparing curve numbers calculated for the growing and dormant seasons, as well as by investigating curve numbers change between the precutting and post-forest-cutting hydrologic effect periods. They concluded that curve number analysis does not consider major processes that regulate forest hydrologic responses; thus, the method is not reliable in the development of policies and standards for managing eastern United States hardwood forest runoff.

Many researchers have applied SCS-CN model for basin-scale water resources planning and management. With the help of GIS technique, Kumar and Rajput (2013) assessed the surface hydro-environmental loss as surface runoff of water which is received in the Pahuj river basin

area, and passes out within a short time period. Pahuj River is a tributary of Sind River in Datia district of Madhya Pradesh.

Kabiri et al. (2013) compared the parameters of some storm events of Klang watershed, Malaysia using SCS Curve Number and Green-Ampt methods for estimation of runoff losses in Unit hydrograph method developed by HEC-HMS software for runoff and flood modeling and showed that there was no significant difference between the SCS-CN and Green-Ampt loss method.

Chauhan et al. (2013) studied the availability and demand of water in Mula reservoir project , a major irrigation project on the river of Mula, a sub-tributary of Godavari, generating geo-database using Remote Sensing and GIS, to develop SCS-CN based long term hydrological simulation model for computation of inflow to reservoir.

Even one study was found for rooftop rainwater harvesting using SCS-CN method. Singh et al. (2013) explored the suitability of SCS-CN model and its variants, i.e., Hawkins SCS-CN model (for l_a=0.05), Michel SCS-CN model (Michel et al. 2005) and their comparison with SWMM-ASRC model (Heany et al. 1976), and CGWB approach for rooftop storm water yields developed (annual storm runoff coefficients) ASRCs using these models, in the selection of roofs in order to maximize their rain water harvesting (RWH) potential.

Zlatanovic and Gavric(2013) calculated morphometric characteristics for each catchment, first manually using topographic maps and then automatically using the pre-processed DEM based on SRTM data and scripting capabilities of GIS. The transformation of excess rainfall into direct runoff was simulated using a modified SCS dimensionless unit hydrograph and flow rates obtained by automated methods proved to be slightly higher than those manually obtained. The results showed that the estimation of actual runoff is much more sensitive to the quality of input data (i.e. soil, land use, rainfall etc.) and showed minor differences that are insignificant compared to the time and resources saved with the automated techniques.

Panahi (2013) conducted a scientific analysis and evaluation in order to quantitatively study and predict the runoff resulting from precipitation, and proposed a model for estimating runoff and determining potential sites of runoff production of the study area by using experimental methods. SCS-CN experimental method was utilized, due to its precision and efficiency. By preparing CN, runoff production potential of the region was determined.

2.4.2 Based on Artificial Neural Network

Fernando and Jayawardena (1998) developed an ANN rainfall-runoff model using hourly data of rainfall and runoff for an experimental catchment in Kamhonsa in Japan. They presented a qualitative examination of the cross-correlation curves between the rainfall and runoff to decide on the input vector.

Tokar and Johnson (1999) used ANN for flow modeling, and presented a qualitative examination of the cross-correlation matrix between the rainfall and runoff to decide on the input vector.

Multilayered perceptrons (MLPs) are the simplest and most commonly used neural network architectures. MLPs can be trained using many different learning algorithms. Tokar and Markus (2000) used MLP for Fraser River in Colorado, US for flow forecast of 1 month ahead.

Zealand et al. (1999) used MLP Winnipeg River system in Canada for Flow forecast of 1–4 weeks ahead.

Imrie et al. (2000) suggested that activation functions with higher limiting amplitude produce better results.

Sudheer et al. (2002) proposed a methodology for selecting an appropriate input vector in ANN rainfall runoff models. The method utilizes the statistical properties such as cross-correlation, auto-correlation and partial-auto-correlation of the data series in identifying a

unique input vector that best represents the process for the basin, and a standard algorithm for training. The methodology presented by Sudheer et al. (2002), therefore is more comprehensive, and the decision is based on clearly defined rules and can be applied for any ANN rainfall-runoff model development.

A lot of hybrid models by combining ANN model with other models have been found in literature, which has been developed to improve performance of the ANN model. Brath et al. (2002) coupled a deterministic rainfall-runoff model with univariate time-series analysis techniques used both for forecasting the future rainfall values to be provided as input to the hydrological model and for updating the discharges issued by the hydrological model. Improvement in discharge forecasts was assessed and it was found that for rainfall forecasting except ANNs other techniques allowed significant improvements in flood forecasting accuracy.

Tseng et al. (2002) combined the seasonal ARIMA model and the neural network back propagation (BP) model to forecast seasonal time series data with seasonality and found that the SARIMABP model outperforms the SARIMA model and the BP model.

Hsieh et al. (2003) applied MLR (multiple linear regression) and feed-forward artificial neural network (ANN) models using principal components of large-scale climatic indices to predict the seasonal volume of the Columbia River; ANN and MLR predictions were essentially identical, implying that the detectable relationships in the short sample size were linear.

Many people have compared performance of ANN with other models for stream flow prediction. Jain and Indurthy (2003) modeled an event-based rainfall-runoff process using the statistical unit hydrograph (UH) theory, statistical regression, and the ANN. A comparative analysis of all of the modeling techniques revealed that the ANN is the most suitable

technique and can be very efficient in modeling an event-based rainfall-runoff process for determining peak discharge and time to the peak discharge very accurately.

Jain and Srinivasalu (2004) presented a new class of model called gray box model that integrate deterministic and ANN techniques, which was found to perform better than the purely black box type ANN rainfall runoff model.

Anctil and Lauzon (2004) used MLP with Kohonen network for 6 different basins in US, Canada, and France for 1day ahead flow forecast.

Huang et al. (2004) developed an ANN model for daily, monthly, quarterly and yearly flow forecasting, using long-term observations of rainfall and river flow in the Apalachicola River, USA.

Anctil and Rat (2005) used MLP with Levenberg-Marquardt (LM) algorithm for 47 watersheds of France and United States for 1day ahead flow forecast.

Wu et al. (2005) used MLP for North Buffalo Creek watershed in North Carolina, US for Flow forecast of 1 and 3 h ahead.

Risley et al. (2005) found that PCR (principal components regression) outperformed ANN methods under almost all circumstances of forecasting Klamath River seasonal runoff.

Some people have compared performance of ANN with ARIMA also for stream flow prediction. Mohammadi et al. (2005) developed an ANN model to predict the spring season inflow to the Karaj reservoir, Iran and by comparing the ANN model with ARIMA model and regression analysis method they found the ANN model best among all.

An integrated modeling framework is proposed by Jain and Srinivasalu (2006) using conceptual techniques and ANN technique to develop the rainfall-runoff relationship and to model the different segment of the decomposed flow hydrograph.

Srivastava et al. (2006) also used MLP and SWAT for West Fork Brandywine Basin in PA, US for 1 month ahead flow and base-flow forecast.

Solomatine et al. (2007) used MLP for Bagmati catchment in Nepal and Sieve catchment in Italy for 1hour, 3 hour and 1 day ahead flow forecast.

Sallehuddin et al.(2007) proposed a approach called GRANN ARIMA., hybridizing linear ARIMA and nonlinear GRANN(Gray Relational ANN) models and concluded that GRANN ARIMA can be used as an alternative tool for forecasting time series data for better forecasting accuracy.

Nayak et al. (2007) explored the potential of integrating neural network and fuzzy logic, effectively to model the rainfall-runoff process from rainfall and runoff information. The integration is achieved through representing fuzzy system computations in a genetic artificial neural network (ANN) architecture, which is functionally equivalent to a fuzzy inference system. The performance of the proposed model is found to be comparable to that of an adaptive neural based fuzzy inference system (ANFIS).

Bustami et al. (2007) used ANN model to predict water level from precipitation with its missing data simulated using ANN and this ANN model was found better compared to the ANN model used to predict water level from precipitation with its missing data calculated using normal ratio formula or from precipitation with missing data.

The study of long-term discharge prediction using ANN and other data-driven models were presented by Cheng et al. (2008), Lin et al. (2006), Wang et al. (2009), and Wu et al. (2009). Data-driven models, such as artificial neural networks (ANNs), have been often used instead of physically based models because of their simplicity and promising capability to simulate input-output relations (Wu et al. 2005).

Akhtar et al. (2009) used ANN as flow forecasting models using hydrologically pre-processed spatial precipitation data. The applied pre-processing includes GIS-based different methods of spatial and time integration of the remotely sensed rainfall data, on the basis of flow path and travel time information. It is found that the spatially distributed ANN, with

one-day previous discharge and preprocessed rainfall, successfully forecasted flow of Ganges river basin.

Mukerji et al. (2009) compared the efficiency of ANN, adaptive network-based fuzzy inference system (ANFIS), and adaptive neuro-GA integrated system (ANGIS) models for flood forecasting in the Ajay basin of Jharkhand and found the ANFIS model worked with better accuracy.

Duc (2009) simulated monthly runoffs of Dong Nai river basin, Viet Nam by using ANN models and when the results were compared with those from Tank, Harmonic and Thomas & Fiering models, ANN model was clearly better than the other traditional models.

An ANN model was developed by El-Shafie et al. (2011) to predict rainfall runoff relationship and it was indicated through comparative study that the ANN method is more suitable to predict runoff than MLR model.

Modarres (2009) used ANN with four hidden layers for Plasjan Basin in Iran to forecast flow of 1–2 days ahead.

Demirel et al. (2009b) used MLP and SWAT for Pracana Basin, Portugal for 1day ahead flow forecast.

Adamowski and Krapataki (2010) trained MLPs using Levenberg-Marquardt (LM), resilient back-propagation (RP), and conjugate gradient Powell-Beale (CGPB) learning algorithms for peak weekly water-demand forecasting in Nicosia and mentioned that there are a number of advantages associated with using the LM, RP, and CGPB learning algorithms. Furthermore, it was mentioned that the RP and CBPB learning algorithms have not been explored earlier for use in short-term urban water-demand forecasting and concluded that LM ANNs are more accurate than CGPB and RP ANNs, as well as MLR (multiple linear regression), for urban weekly peak water-demand forecasting in Nicosia.

Adamowski and Krapataki (2010) compared three types of ANNs: LM, RP, and CGPB. MLR was also used in their study because it is one of the most widely used techniques for water-demand forecasting .They concluded that LM ANNs are more accurate than CGPB and RP.

Previous experimental comparisons for streamflow forecasting, such as those of Shamseldin et al. (2002) and Shrestha et al. (2005), indicated that transfer functions are pretty much interchangeable as long as they are of sigmoid shape.

Yonaba et al. (2010) compared six MLP architectures based on three different nonlinear transfer functions tangent sigmoid, bipolar logistic and elliot sigmoid used in the hidden layer, and either the same nonlinear transfer function or the linear transfer function used in the output layers for multistep ahead stream flow prediction over lead times from 1 to 5 days and found that all MLPs have shown good performance. They confirmed the universal approximation theorem that a linear transfer function is suitable for the output layer, as usage of a nonlinear transfer function in the output layer failed in improving performance values in their study and endorsed the tangent sigmoid as the most pertinent transfer function for streamflow forecasting, over the bipolar (logistic) and Elliott sigmoids.

Abudu et al. (2010) investigated the application of PLSR (partial least square regression) in seasonal streamflow forecasting for snowmelt-dominated basins in the western United States.

Abudu et al. (2010) applied both time series non-seasonal and seasonal ARIMA models and Jordan-Elman ANN models in forecasting one-month-ahead stream flow and observed no significant difference in model performance using the time series ARIMA and Jordan-Elman ANN models.

Birinci and Akay (2010) compared the performance of the Radial Basis Function Neural Network (RBFNN) model with MLR and ARIMA models for daily mean flow prediction and found that the RBFNN model is better than other two models for long term continuous data.

The strong hydrologic non-linearity and the strong storage characteristics cannot be modeled adequately by a system-based model and therefore require a conceptual model while the mild hydrologic linearity is satisfactorily modeled by the simple linear models or lumped hydrologic models.

Hybrid modeling, an integration of different models by definition, may combine forecasts from different individual models and integrate them into models that provide better forecasting solutions than just using a single model (Abudu et al., 2011). This approach is essentially a modeling of errors by combined application of several models and can focus on the mismatch between model results and observations (Solomatine and Price, 2004).

Monthly streamflow during spring-summer runoff season in the Rio Grande Headwaters Basin in Colorado was forecasted by Abudu et al.(2011) using a transfer-function noise model and then, forecasts of TFN models were modified using an ANN model denoted as hybrid TFN and ANN. The results indicated that the hybrid TFN and ANN approach improved forecast accuracy significantly when compared with single TFN and ANN models. Song et al. (2012) developed a hybrid model of neural network with the conceptual XAJ model to simulate the rainfall-runoff relationship of Yanduhe Basin. In the absence of the significant signature of periodicity and seasonality (e.g., event based simulation), the classic ANN or GP technique may be sufficient for the modeling. On the other hand, the WGP and WGPNN models are appropriate when the study process contains non-stationary and long-term patterns (seasonality).

Nourani et al. (2012) presented two hybrid models, wavelet–genetic programming (WGP) approach and wavelet–genetic programming neural network (WGPNN) approach to highlight the seasonal patterns of a time series. Further Nourani et al. (2012) presented an integrated ANN and geomorphological genetic programming based on observed time series and

spatially varying geomorphological parameters. The efficiency of the integrated approach was increased by including geomorphological features of the watershed.

Kar et al. (2012) developed a flood forecasting model for Ayeyarwady River Basin of Myanmar applying ANN multilayered feed forward network along with the Takagi-Sugeno (TS) fuzzy inference model, to forecast the stage from 1 to 4 days in advance. The fuzzy model performed better than the ANN model when modelling the peak values. Kar et al. (2012) presented the ANN and fuzzy approaches and it was observed that with the selected model structure for the development of flood forecasting models for the selected forecasting station, in all cases ANN and fuzzy techniques provide a good workable soft computing based flood forecasting model and the T-S (Takagi-Sugeno) fuzzy model (Takagi and Sugeno 1985) performs better than the MLFF (multilayered feed forward) network. When tested for peak flood modeling, the fuzzy model shows promising results in comparison with the ANN model as the sequence of most of the intermediate stages are properly modeled through the fuzzy model.

Demirel et al. (2012) calibrated the ANN model by using the BP algorithm to predict flow heights for a lead time of 12 h and proposed an ANN-cluster analysis (CA) coupling procedure for model validation.

Tiwari et al. (2012) improved performance of ANN for forecasting daily river discharge for 1- to 5-day lead time in the Mahanadi River basin by using neural units with higher-order synaptic operation (NU-HSO). While, NNs with NU-HSO were compared with conventional NNs of neural units with linear synaptic operation (NU-LSO) for forecasting daily river discharge, it was found that NNs of neural units with quadratic synaptic operation (NU-CSO) and NNs of neural units with cubic synaptic operation (NU-QSO) achieved better performance even with a lower number of hidden neurons.

2.5 CONCLUSION

Regarding spatial interpolation of rainfall methods it can stated that the semivariogram model and the parameters of Kriging should be different for the different rainfall series, even if in the same study area. Again to the small region with high density of rain gauges, the Kriging method superiority is not obvious, IDW and the Spline interpolation result can be better. But for large regions with low-density networks of rain gages geostatistical interpolation outperforms deterministic techniques Finally, it can be concluded that the different methods will be suitable for the different research series, and it must be determined by the data series distribution.

For rainfall prediction using ARIMA model it can be concluded that ARIMA models performance is not much better than MLR models for sufficiently longer rainfall data. But for shorter time series ARIMA models outperform linear regression models. Further ANN models perform better than ARIMA models especially in the presence of nonlinear relationships and high levels of noisy data. However sometimes ANN cannot predict the sharp peak values. Therefore atmospheric models such as Statistical Down-Scaling Model (SDSM) have also been adopted whose performance is better than the ANN model, even though, in comparison, it is a more data intensive model than ANN.

Soil conservation service curve number (SCS-CN) model has been widely used for surface runoff computations. In SCS-CN method the observed correlation between the calculated CN value and the rainfall depth in a watershed can be attributed to the soils and land cover spatial variability of the watershed. Therefore runoff estimates using tabulated curve numbers are unreliable and that curve number selection requires independent calibration to watersheds representative of regional landscape and hydrologic characteristics. This can be done using land cover and soil survey using remote sensing and GIS. Runoff has also been predicted using ANN and in most of the cases it has outperformed the statistical models. But in some cases the ARMA and ARIMA models provided better accuracy in runoff forecasting based on forecasted rainfall. To increase forecasting accuracy of ANN models, linear ARIMA and nonlinear GRANN (Gray Relational ANN) models have been hybridized.

CHAPTER 3

THE STUDY AREA AND DATA COLLECTION

3.2 THE STUDY AREA

3.2.1 Mythology

The literal meaning of Mahanadi River is “large size river”. At origin of Mahanadi River, which is located near the Ashram (place of stay in remote area) of Maharshi (Saint) Shrangi, it is called as holy Ganga. It is said that once all the sages of this area came at this place for taking holy bath in Mahakumbh (festival). The Maharshi was under meditation and penance at that time. The sages waited for several days to draw the attention of the Maharshi but the Maharshi’s meditation was not disrupted. Thereafter, the sages went for the holy bath. While returning after the bath, all the sages brought some holy water with them. Finding that Maharshi Shrangi was still in the meditation, they filled the Maharshi’s kamandal (vessel) with water, and returned to their native places. After some time, when the meditation of the Maharshi Shrangi was disrupted, the water of the kamandal fell down on the ground with the stroke of his hand. This water began to flow towards east and was converted into a stream. This stream was called as Mahanadi which is said to fulfill the desires of millions of people.

3.2.2 Location

Mahanadi river is the second major river in peninsular India after Godavari with respect to the water potential and flood producing capacity and is located in East Central India within geographical co-ordinates of 80º30’ to 86º50’ E and 19º20’ to 23º35’ N (Figure 3.1). Mahanadi river basin is the largest river of Odisha State and extends over an area of 141589 sq. km which is nearly 4.3% of the total geographical area of India and covers five different states namely Maharashtra, Madhya Pradesh, Chhattisgarh, Odisha and Jharkhand (CWC, 2009). Mahanadi River originates from a fall of Pharsiya village near Nagri town in Dhamtari district of Chattisgarh at an elevation of 442 m above mean sea level. About 65580 km^2 of the basin lying in Odisha extending within geographical co-ordinates of 82º to 86º E and 19º30’ to 22º30’ N approximately, (Figure 3.1) has been considered in the present work.

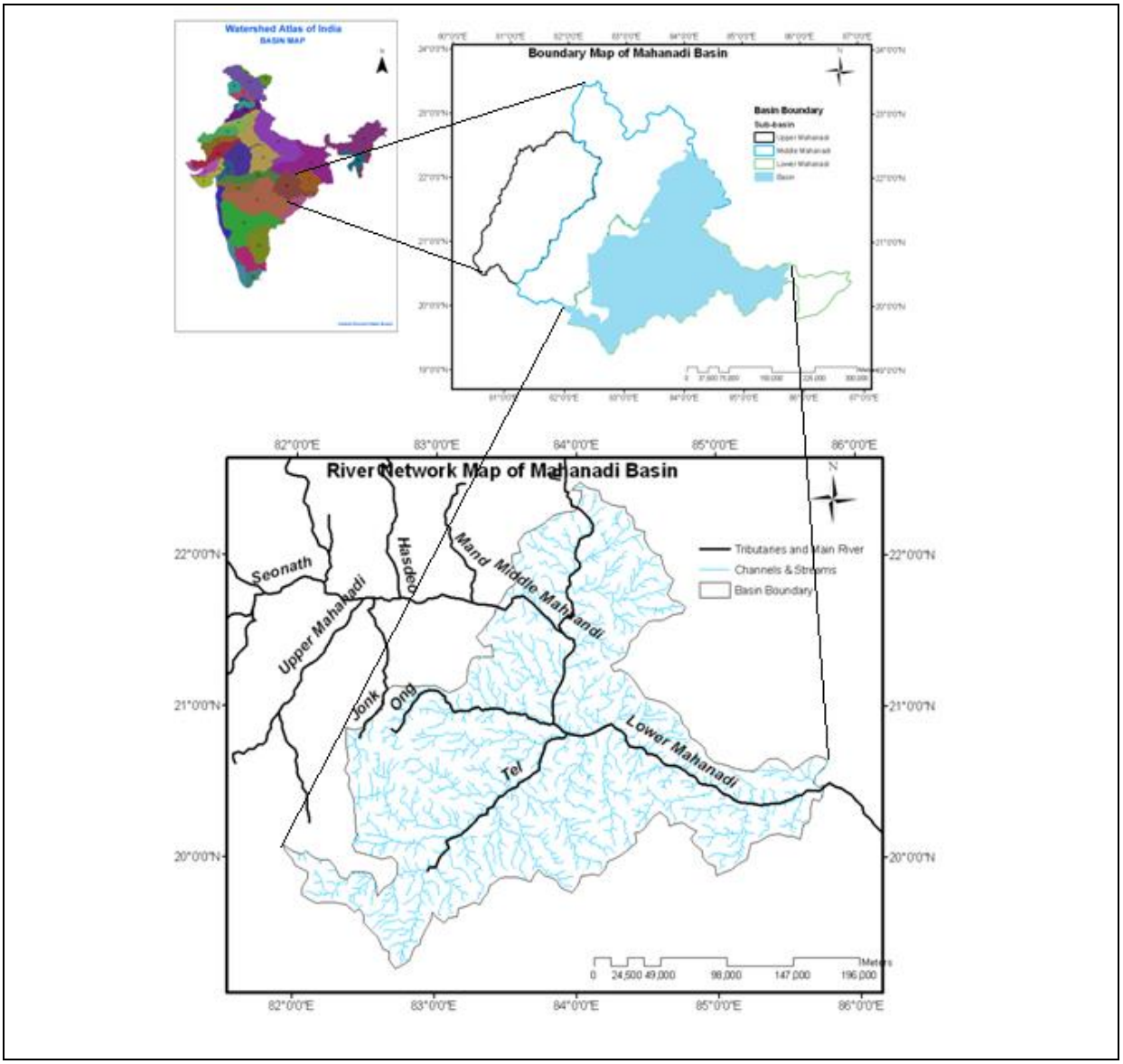

Figure 3.1: Location of Mahanadi Basin lying in Odisha, INDIA

The total length of the river from its origin to confluence at the Bay of Bengal is about 851 km, of which 357 km is in Chhattisgarh and 494 km is in Orissa. Drainage density of the basin is extremely thick. During its traverse, a number of tributaries join the river on both the banks. Principal tributaries of the tributary joining on Odisha are Ib, Ong and Tel (CWC, 2009). The tributary upstream of Hirakud dam is Ib, whereas Ong and Tel are the downstream tributaries as shown in Figure 3.1. Average annual flow (cumecs) of the three tributaries Ib, Ong and Tel lying in the study area is given in Table 3.1. The average annual

flow of the basin measured at different places such as Sarangarh, Sambalpur, Sonepur and Munduli are 30586, 41816, 54881 and 66640 cumecs, respectively.

Table 3.1: Basic Characteristics of major tributaries of Mahanadi basin lying in Odisha

Major Tributaries	State of Origin	Catchment Area(sq. km)	Distance(km)	Average Annual Flow (cumecs)
Ib	Chattisgarh	12,447	251	9003
Ong	Odisha	5,128	204	2220
Tel	Odisha	22,818	296	11716

The river enters in Odisha through Jharsuguda district after covering about half of its total length. Before Sambalpur, it meets its tributary Ib. The Ib, which is the third largest tributary of Mahanadi, rises in village Pandrapat, District Raigarh (Chhattisgarh) and drains Raigarh district of Chhattisgarh and three districts of Orissa, namely Sundargarh, Jharsuguda and Sambalpur. After Sambalpur Mahanadi river takes a southernly turn and it is joined by the Ong. The Ong drains Sartaipali, Padampur and Bijepur area of Balangir and Bargarh districts of Odisha. The southernly turn of the river continues up to Sonepur, where it meets with its tributary the Tel. The Tel, which is the second largest tributary of Mahanadi River and the largest of the study area, rises in village Jorigam of Koraput district of Odisha and drains Deobhog, Bhawanipatna and Balangir area of six districts of Odisha namely Rayagada, Kalahandi, Nuapada, Balangir, Boudh and Kandhamal. Other tributaries meeting the river in Odisha in this section are Jeera and Bheden.

Further downstream Udayagiri and Phulbani areas are drained by the tributary Salki which meets Mahanadi on the right bank upstream of Boudh. It then turns East and skirts the boundaries of the Boudh districts and forces a tortuous way between ridges and ledges in a

series of rapids until it reaches Dholpur of this district. The rapids end here and the river rolls towards the Eastern Ghats, forcing its way through them via the 64 km long Satkosia Gorge. The Satakosia Gorge ends at Barmul of Nayagarh district. Dense forests cover the hills flanking the river at Barmul. Daspalla, Nayagrah and Bolgarh areas are drained by the tributaries Kuanria and Kusumi. Boudh, Barmul, Banki and Kaimundi are situated on the right bank and Baramba, Athgarh, Narsinghpur are situated on the left bank of Mahanadi of this section. The area of this region is 50,745 km^2. Around 83 small and big channels carry flood water of this section to Mahanadi.

The river then traverses Cuttack district in an east-west direction and enters the coastal plains of Odisha at Naraj, which is the head of delta and about 320 km downstream of Hirakud dam. Naraj is about 11 km from Cuttack and here the river pours down between two hills. A barrage has been constructed at Naraj to regulate the river's flow into Cuttack city. After Naraj the river splits into several branches. Just before entering Cuttack city, it gives off a large distributary called the Kathjodi. The city of Cuttack stands on the spit separating the two channels Mahanadi and Kathjodi. The Mahanadi River enters the Bay of Bengal via several channels at Paradeep , Jagatsinghpur district. The Kathjodi then branches into Kathjodi, Surua, Biluakahi, Devi, Kandal, Taunla and numerous other small channels which flow down and create the Kathjodi, Surua, Devi-Biluakhai, Devi-Kandal, Devi-Taunla islands and other small islands, which again join together and fall into the Bay of Bengal after entering Puri district. All these Islands are flood prone. The Kathjodi itself falls into the Bay of Bengal as a river called the Jotdar. Another distributary Kuakhai has bifurcated into Kushabhadra, Bhargabi and Daya. Kusabhadra has an independent mouth to the Bay of Bengal whereas Bharagabi and Daya reunite and discharge into Chilika Lake. Similarly, another distributary Birupa has bifurcated into Genguti and Birupa and forms the Birupa-

Genguti Island .These two branches flow into Kimiria and finally to the Brahmani River at Krushnanagar and enters the Bay of Bengal at Dhamra, Jagatsinghpur district. Other distributaries of Mahanadi include Chitrotpala, Luna, Karandia, Paika and Sukapaika which form a number of islands. All these Islands are flood prone. In between these tributaries there are several drainage channels. To name a few important ones are Gobari, Alaka, Baghuni, Kula, Prachi, Dhanua and Nuna etc. All these drainage channels are prone to tidal effect near the Bay of Bengal. The combined Delta formed by numerous distributaries of the Mahanadi and the Brahmani, is one of the largest delta in India.

Mahanadi and its branches in this region are all embanked on both sides. However some embankments in Kathjodi from Khannagar to Mattagajapur and the Mahanadi right embankment from Jobra to the downstream end of Cuttack need further strengthening. The main river in this region divides into a number of branches. During the course of Delta formation, some islands have been formed between various channels and those islands are subjected to continual flooding during the monsoon due to spill of the channels.

3.1.3 Water Resources

Mahanadi is mainly rain fed river and the water availability undergoes large seasonal fluctuations. The National Commission for Integrated Water Resources Development estimated the basin-wise average annual flow in Indian River systems as 1953 km^3, out of which average annual flow of Mahanadi river basin is 66.88 km^3 /year. Utilizable water resource is the quantum of withdrawal water from its place of natural occurrence. The utilizable annual surface water of the country is 690 km^3, out of which 49.99 km^3 /year is the utilizable flow of Mahanadi river basin, utilized for drinking and irrigation purposes. Total replenishable groundwater resource of the country is assessed as 431.89%. After allotting 15% of this quantity for drinking, and 6 km^3 for industrial purposes, the remaining can be

utilized for irrigation purposes. Thus, the available groundwater resource for irrigation is 361 km^3, of which utilizable quantity (90%) is 325 km^3 (Kumar et al., 2005). Total replenishable ground water resources of Mahanadi river basin is 16.46 km^3/year, out of which 2.47 km^3/year ground water has provision for domestic, industrial and other uses, so 13.99 km^3/year ground water is made available for irrigation. Therefore net draft of ground water resources of the basin is 0.97 km^3 /year. Balance ground water potential of the basin is 13.02 km^3 /year and level of ground water development (%) per year is 6.95 km^3.

The volume of the total renewable water resources (TRWR) of India is 1,887 km3. The TRWR is the sum of internally renewable water resources (IRWR) and the flow generated outside the national borders (600 km^3). The volume of potentially utilizable surface water resources (the part of the water resources that can be captured for first-time use and subsequent reuse at downstream with all possible physical and economic means) of India is about 690 km^3. The total volume of potentially utilizable water resources (PUWR), including groundwater, of India is about 1,033 km^3. Total renewable water resources of Mahanadi basin is 66.9 km^3/year and its per capita availability is 2463 m^3.Potentially utilizable water resources of the basin is 63.6 km^3/year, out of which surface water and ground water resources are 50 and 13.6 km^3/year respectively and per capita availability of the potentially utilizable water resources is 2341 m^3.As per the assessment made in 2001 by Orissa Community Tank Development and Management Society, average annual surface water inflow of Mahanadi river basin (in BCM) is 59.155, out of which inside Odisha and outside Odisha flows are 29.90 and 29.255 respectively. As per the topography and geological limitations 75% of the average annual flow can be utilized. 75% dependable flow of the basin (in BCM) is 48.732, out of which inside Odisha and outside Odisha flows are 25.508 and 23.225 respectively.

India's aggregate water withdrawal in 1995 was estimated at about 650 km^3 (IWMI 2003). Of this, 91 percent was withdrawn for agriculture sector, 4 percent for the domestic sector, and 5 percent for the industrial sector. Total water withdrawal of Mahanadi basin is 19.9 km^3, of which 91%, 5% and 4% water is withdrawn for agriculture, domestic and industrial sectors respectively.

3.1.5 Discharge

Twenty number of gauge and discharge observation sites have been installed and operated by Central Water Commission, Government of India, to measure these hydrological variables. Out of these twenty sites, at 13 observation sites, sediment is also measured. The mean annual river flow of the basin (in MCM) is 66 640. The entire flow is only due to rainfall in the region since there is no contribution from either snowfall or snowmelt. The average annual discharge is 1895 m3/sec, with a maximum of 6352 m^3 /sec occurring during the months of July, August and September. Minimum discharge is 759 m^3 /sec and occurs during the months October through June.

Average annual runoff for 2006-2007 at Tikarpada (terminal site) gauging station of the basin has been measured as 61945 MCM for a catchment area of 124450 sq. km., out of which the monsoon and non-monsoon water flow are 56562 and 5383 MCM respectively. Peak water level of 74.980 m recorded at this site has occurred on 30/08/1982 with discharge of 41400 cumecs. Maximum discharge of 30863 cumecs observed at this site has occurred on 29/08/1978(CWC, 2009).

3.1.5 Problem of Floods and Droughts in Mahanadi Basin

The spatial distribution of rainfall pattern of the basin highlights the chance of occurrence of flood in the downstream sub-catchments, while upstream sub-catchments set-off the threat of drought. This basin is highly vulnerable to flood, and has been affected by catastrophic flood

disasters almost annually. The monsoon of 2001 topped to the worst hit flood ever recorded in this basin for the past century, which inundated 38% of its geographical area. Ironically, this basin suffered one of its worst droughts in the same year, affecting 11 million people, and two-thirds of its area (CSE, 2003) (Asokan et al, 2008).

The catchment area of Mahanadi is divided into two distinct reaches (i) Upper Mahanadi and (ii) Mahanadi Delta. The upstream catchment of Mahanadi is mountainous and has a steep slope. The catchment lies directly on the south west monsoon track and as such receives heavy rainfall during summer monsoon. Besides, the catchment area close to the sea is prone to heavy rain brought about by the cyclones generated in the Bay during September-November. Thus the catchment has the potential of producing very high flood. The delta area is plain and has a flat slope. Due to flat topography of the delta area the excess flood water is not discharged to the sea quickly and as a consequence, Mahanadi Delta area gets flooded when peak flood discharge exceeds a certain limit. Upper Mahanadi area above Naraj does not have any significant flood problem due to topography excepting few places in IB, Bheden and Tel tributary catchments (OSWP, 2004).

3.1.7 Geology and Rock

Mahanadi basin predominantly consists of Archaean rocks represented by folded Khondalites, Granite gneisses and Charnockite. They are inter-banded and the first two appear to grade into one another. Field relationship of these rocks is complex and it is difficult to assign any age relationship. It is generally agreed that the rocks were deposited during Archaean era (2000 - 2500 Million years) and were folded and metamorphosed by at least two tectonic activities. The rocks have experienced metamorphic conditions of amphibolite facies to granulite facies. Magmatization appears to have played a major role in resulting present state of rocks. The area has been reported to have experienced block faulting during Gondwana times and area upstream of Badmul appears to be a Graben. In general

downstream part of the river lying in Odisha is dominated by silicate rocks of metamorphic origin (Ghose et al, 2011).

3.1.7 Rainfall

Rainfall is dominated by the summer monsoon (June through September) with an average annual rainfall in the basin is 1,463 mm (1,663 mm - 1,331 mm). During the remainder of the year, rainfall is extremely low, rarely exceeding 30 mm per month. The spatial variation in rainfall is moderate in the basin. Average annual rainfall in the most upstream part of the basin is about 1000 mm, increasing toward the central basin part (1300 mm) and further in the most downstream coastal belt of the basin (1700 mm) (Asokan et al,2010).

3.1.8 Temperature

Temperature variation of the basin is from 7°C to 45.5°C (CWC, 2009). Summer temperatures are around 29ºC and winter temperatures of 21ºC. In winter the mean daily minimum temperature varies from 4°C to 12°C. In summer the mean daily maximum temperature varies from 42°C to 45.5°C (Dadhwal et al., 2010).December is the coldest month with the mean minimum temperature ranging from 10° C to 13.7° C. May is the hottest month in this region where the mean maximum temperature ranges from 38° C over the hills to 43° C in the plains. As compared to eastern portion and delta area, western portions record the lowest and highest temperatures during winter and summer respectively. The diurnal range of temperatures during July-August is of the order of 5° C to 6° C and the same during winter is up to a maximum order of 14° C to 16° C.

3.1.9 Relative Humidity

The highest relative humidity in the basin varies between 68% and 87% and occurs during July/August. The lowest relative humidity occurs during April/May and varies between 9%

and 45%. The average highest relative humidity in the basin is 82% and the average lowest relative humidity is 31.6%.

3.1.10 Evaporation and Evapo-transpiration

Monthly Evaporation of the basin ranges from 40 mm in winter to 360 mm in summer (CWC, 2009). However, the average daily pan evaporation of the basin varies from 2.4 to 14.6 mm (Tiwari et al, 2012). The Indian Meteorological Department has reported that the basin has a high rate of yearly evapo-transpiration varying from 1520 mm in the east to 1740 mm in the west.

3.1.11 Physiography and Soil

Physiographically, the basin can be divided in to four well-defined physical regions, namely, the northern plateau, the Eastern Ghat, the coastal plain and the erosional plains of central table land. The Northern Plateau and the Eastern Ghats are well-forested hilly regions. The Coastal Plain stretching over the districts of Cuttack and Puri covers the large delta formed by the river Mahanadi and is a fertile area well suited for intensive cultivation. The interior coastal plain has a relatively low elevation and relief is extremely low. The erosion plain of the Central Table Land is the central interior region of the basin, traversed by the river and its tributaries. The average elevation of the drainage basin is 426 m with a maximum of 877 m and a minimum of 193 m.

The Mahanadi River basin with its tributaries flowing in Odisha like IB, Jira, Ong and Tel are covered by central table land region of Odisha, which covers an area of 24% of the state comprising of districts Balangir, Nuapada, Kalahandi, Kandhamal, Boudh, Sonepur, Dhenkanal, Angul, Sambalpur, Deogarh, Bargarh ,Jharsuguda and Sundargarh. The deltaic part of Mahanadi river basin is comprised by coastal plain region of Odisha, which covers an area of 26% of the state .The districts of the Mahanadi basin under this coastal plain region are Cuttack, Jagatsinghpur, Jajpur, Kendrapara, Puri, Nayagarh, Khordha and Ganjam.

The delta of Mahanadi River starts from Cuttack. The Mahanadi Delta is formed by the network of the rivers Mahanadi and Brahmani. The delta covers a coastline of 200 km, which stretches from south near Chilika to north up to Dhamra River. The Delta covers an area of 9,500 sq km accounting for merely 7% of state's geographical area. The Mahanadi Delta is a basin of huge amount of silt deposit that drains a large land mass of the Indian subcontinent into the Bay of Bengal. The alluvial valley is wide and relatively flat with a meandering river channel that changes its course. The delta's landforms are mainly denuded hills and erosion plains, whose depressions contain water bodies. The central part of the delta is distinct for its extensive plains, leeves and paleochannels. The coastal parts contain spits, bars, lakes, creeks, swamps, beaches, tidal flat and mangroves. Mahanadi River drains into Bay of Bengal at Paradeep port. The main branchs of Mahanadi River are Kathajodi, Kuakhai, Birupa, Debi, Daya and Bhargabi, which meet Bay of Bengal at Paradip and Nuagarh (Devi estuary). The tidal estuarine part of the river covers a length of 40 km and has a basin area of 9 km^2. Based on physical characteristics, the estuary has been characterized as a partially mixed coastal plain estuary.

Primary soils available in the basin are Black soil, Red soil, Yellow soil, Brownish Red to Yellowish Red soil and Dark Gray Coastal alluvial soil (CWC, 2009). The main soil types found in the basin are Red and Yellow soils. The soil of the basin is predominantly sandy loam, however; sandy clay loam and clay loam are also present. Mixed red and black soils occur in parts of the Balangir, Sambalpur and Sundargarh districts of Odisha. Laterite soil is found in the lower parts of Odisha. The deltaic soil is found in the coastal plains of the Basin.

3.2.12 Land use and Land cover

The Mahanadi River flows slowly for 851 km and deposits more silt than any other river in the Indian subcontinent. Prior to the construction of Hirakud dam, the river carried a huge amount of silt to its mouth. As a result, its delta had one of the highest yields per acre in the

whole of India. Its delta also features one of the largest mangrove forests in Indian peninsular. Today this productive plain of Mahanadi valley are home to intensive rice cultivation, and is a main rice producing area of the eastern coast of India. Mahanadi valley is best known for its fertile soil and flourishing agriculture, which primarily depends on a network of canals that arise from the river. Rice, oilseeds and sugarcane are the principal crops cultivated in the Mahanadi valley.

The basin has a culturable area of about 79,900 km^2 which is about 57% of the basin area and 4% of the total culturable area of the country. Major crops cultivated in the basin are rice and wheat. Except in the coastal plains of Odisha, the basin has an extensive area under forests. The sparse vegetation of the highlands contrasts with the moderately luxuriant vegetation of the river valleys. The coastal plains of Odisha, with a high incidence of rainfall, are predominantly rice growing areas. As per Land Use Classification for 1999-2000, the reporting area for land utilization is classified into (i) forest area (ii) area not available for cultivation (iii) other uncultivated lands excluding fallow land (iv) fallow land (v) net area sown (vi) total cropped area and (vii) area sown more than once. The land utilization pattern of Mahanadi river basin comprises 37.275% forest area, 10.432% area not available for cultivation, 9.137% area for other uncultivated lands excluding fallow land, 4.967% fallow land and 38.187% net sown area. Besides the total cropped area is 44.696% and the area sown more than once is 6.508%. The major part of the basin is under agriculture land use, where rice and wheat are the predominant crops. The cultivable area of Mahanadi river basin is irrigated by different sources of irrigation such as canal, tank, tube well, other well and by other sources also. The percentage of gross irrigated area by canal, tank, tube well, other well and other sources in Mahanadi river basin are 23.050, 8.463, 12.380, 18.056, 38.048 respectively. The percentage of net irrigated area by canal, tank, tube well, other well and

other sources in Mahanadi river basin are 5.644, 2.944, 17.905, 60.341, 13.164 respectively(CWC, 2009).

In Odisha, the Hirakud dam with its reservoir, built in 1956 with a gross water storage capacity of 8136×10^6 m^3, is an engineered water storage structure that facilitates different human water uses, including water use for irrigation in the basin. Agricultural areas in the basin are cultivated throughout the year. The cropping seasons are broadly classified into Kharif (rain fed cultivation) and Rabi (irrigated cultivation) seasons. The Kharif season extends from June till November and the Rabi season spans from December till May. Out of the total annual irrigation water demand of 11km^3 in the basin, the Kharif season utilizes 7km^3 and Rabi season demands 4km^3.Major land use and associated water use changes that have taken place in this basin in the 20th century are related to intense irrigation of agricultural areas (Asokan, 2013).

3.2 DATA COLLECTION

The study area consists of thirty rain gauge stations, to monitor daily rainfall. Besides, fifteen stations monitor rainfall data twice daily and five stations monitor hourly rainfall data. Moreover, other climatic variables such as temperature, pressure, relative humidity and sunshine duration, are also measured at some of these stations in daily, twice daily and hourly intervals. In addition to the very dense rain gauge network, special care was also given to the quality of the discharge measurements. The basin consists of twenty four water level recording stations measuring water level at three times a day, of which six stations measure water level at hourly interval and twenty two stations record stage and discharge thrice a day. Very frequent stage-discharge measurements secure the accuracy of discharge measurements. All the stations are operated by Water Resources Department, Govt. of Odisha, whose characteristics are given in Table 3.2. Daily rainfall data for the period of ten years

(01/01/2000 to 30/04/2009) has been collected from these sites of Water Resources Department, Govt. of Odisha. Rainfall data (in mm) was available for twenty three stations of Odisha. Daily rainfall data were summed up to get monthly rainfall series for the period of ten years. Location of these rainfall stations are shown in Figure 3.3.

Table 3.2 Characteristics of OWRD rainfall stations and discharge sites

Site	Establishment Year	Rainfall Data used for	Discharge Data used for	River/Tributary	Catchment Area(km^2)	Longitude	Latitude
Dasapalla	2000	✓		Mahanadi		84.84	20.32
Patora	1999	✓		Mahanadi,Jonk	342	82.46	20.74
Bargaon	1999	✓	✓	Mahanadi,Tel	1062	83.33	20.41
Takla	2000	✓	✓	Mahanadi,Tel	1093	82.85	20.31
Gorla		✓		Mahanadi		83.58	20.61
Tulaghat	1999	✓	✓	Mahanadi,Roul	1165	83.61	20.32
Burat	1999	✓	✓	Mahanadi,Tel	713	83.49	20.17
Chatikuda	1999	✓	✓	Mahanadi,Tel	290	83.27	19.97
Icchapur	1999	✓		Mahanadi,Tel	145	82.63	20.60
Surubali	2000	✓	✓	Mahanadi,Tel	1628	83.95	20.17
Magurbeda	1999	✓	✓	Mahanadi,Tel	1230	83.38	20.75
Baghupali	2000	✓	✓	Mahanadi	1085	83.88	21.19
Sagada	2000	✓		Mahanadi	1106	84.07	20.69
Bisipada	2000	✓	✓	Mahanadi	1657	83.23	20.40
Bansajal	2000	✓	✓	Mahanadi	140	84.25	21.11
Kadaligarh	2000	✓	✓	Mahanadi	170	84.31	20.94
Sagjuri	2000	✓		Mahanadi	350	84.06	21.05
Rampur	2000	✓	✓	Mahanadi	1310	84.02	21.73
Maneswar	2000	✓	✓	Mahanadi	340	83.96	20.45
Naraj	1966	✓	✓	Mahanadi	132085	85.76	20.47
Takara	2000	✓	✓	Mahanadi	1386	84.78	20.38
Madhupur	2000	✓		Mahanadi	124	84.83	20.31
Badapandusar	2000	✓	✓	Mahanadi	1204	85.18	20.16
Gania	2000	✓		Mahanadi	126122	85.08	20.39
Tumulibud	2000	✓	✓	Mahanadi	686	84.03	21.89

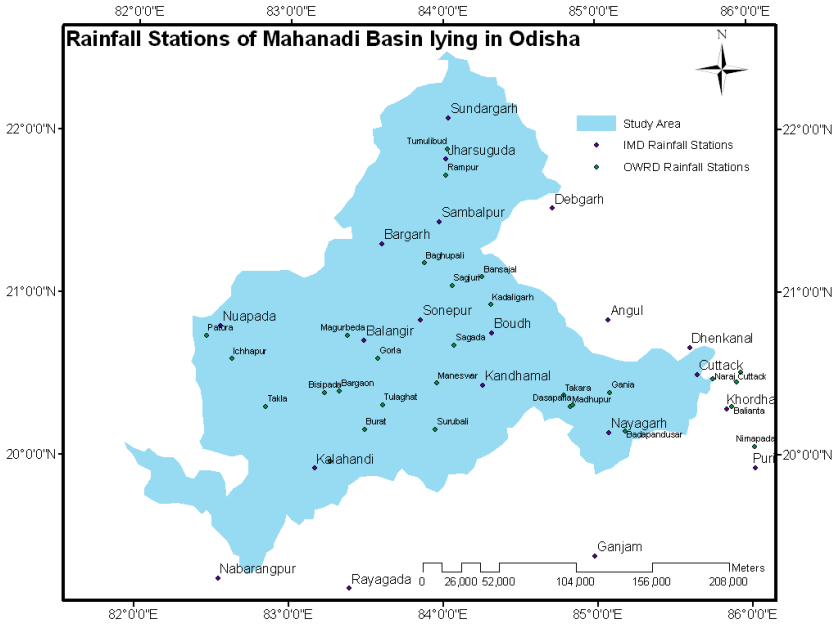

Figure 3.3 Location of rainfall stations of Mahanadi Basin

Further monthly rainfall data of twenty three stations of India Meteorological Department (IMD) for time period of 2009-2012 were collected from "Odisha Rainfall Monitoring System" monthly rainfall report. Name and location of these rainfall stations are shown in Figure 3.3.Rainfall data of twenty three stations are utilized for development of SCS-CN based runoff computation model. For development of sub-basin level runoff computation model, rainfall data of twenty three IMD stations and discharge data of the five CWC stations were utilized. Time series plots of daily and monthly rainfall data of two representative stations are shown in Figure 3.4.

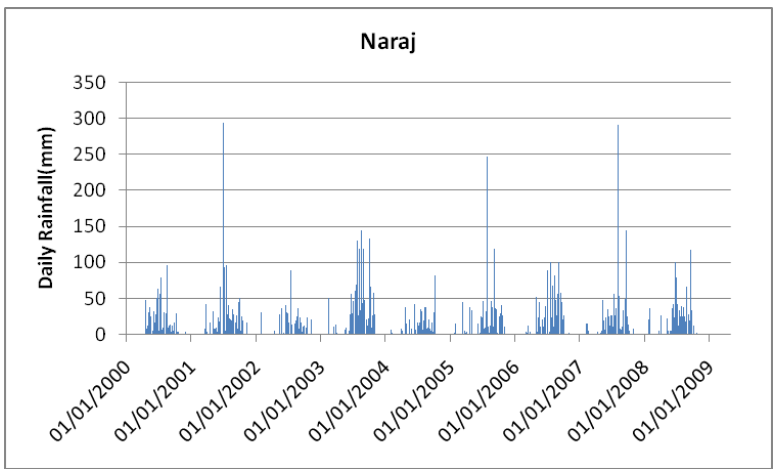

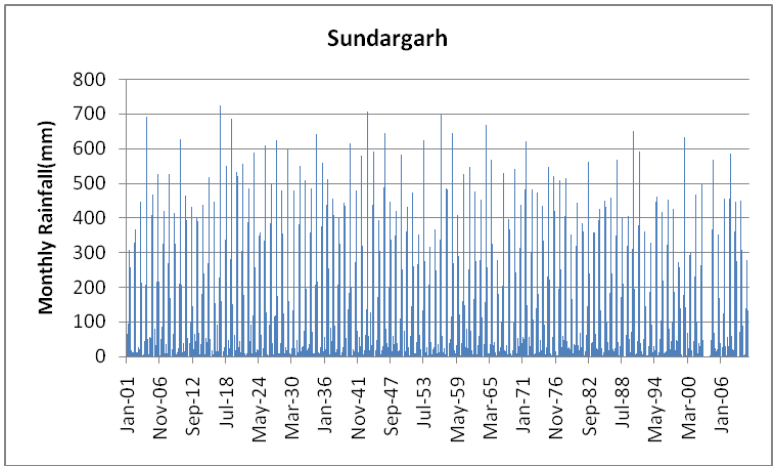

Figure 3.4: Time Series Plots of Daily and Monthly Rainfall Data

Daily discharge data for the period of ten years (01/01/2000 to 30/04/2009) has been collected from these sites of Water Resources Department, Govt. of Odisha. Discharge data (in m^3/s) was available for seventeen stations of Odisha. Daily discharge data were summed up to get monthly discharge series for the period of ten years. Location of these discharge sites is shown in Figure 3.4. Besides, daily discharge data for the period from 01/12/1999 to 31/12/2012 of five stations, namely Kesinga, Kantamal, Salebhatta, Sundargarh and Tikarpada of Odisha, installed and operated by Central Water Comission, Govt. of India was also collected. Daily discharge data of these five stations were summed up to get monthly discharge series of the same period. Discharge data (Q in cumec) was converted into runoff data (in mm) using the relation (Q*86.4/A), where A is the catchment area (in km^2) of the station. Location of these five discharge sites is shown in Figure 3.5. Table 3.3 provides the saliet feature of CWC discharge site.

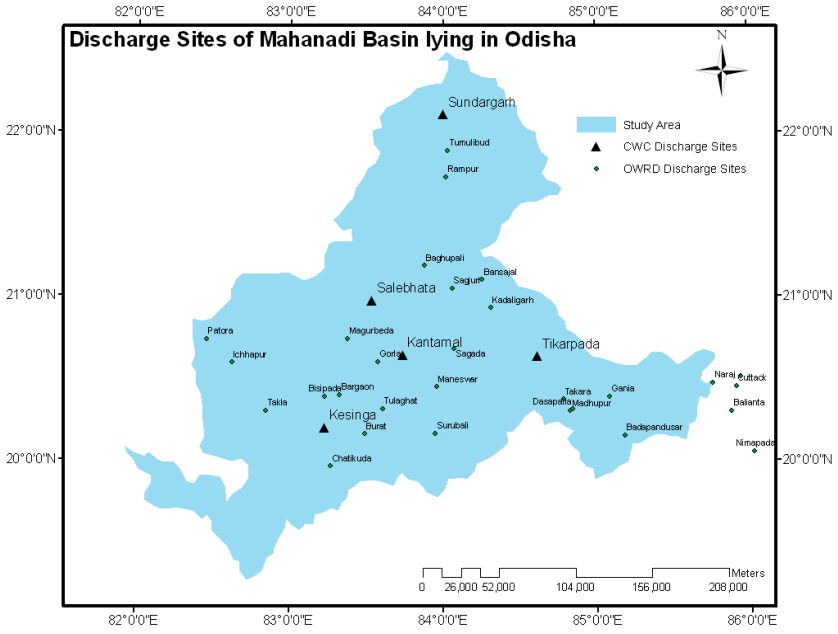

Figure 3.5: Location of Discharge Sites of Mahanadi Basin

Table 3.3: Characteristics of CWC discharge sites

Site	River/Tributary	Catchment Area(km^2)	Longitude	Latitude	Elevation (m)
Kantamal	Tel	19600	83.74	20.65	118
Kesinga	Tel	11960	83.23	20.20	166
Salebhatta	Ong	4650	83.54	20.98	130
Sundargarh	Ib	5870	84.00	22.11	214
Tikarpada	Lower Mahanadi	124450	84.61	20.64	50

The discharge data of the seventeen stations (marked in Table 3.2) are used for the analysis and time series plots of daily and monthly discharge data of two representative stations are shown in Figure 3.6.

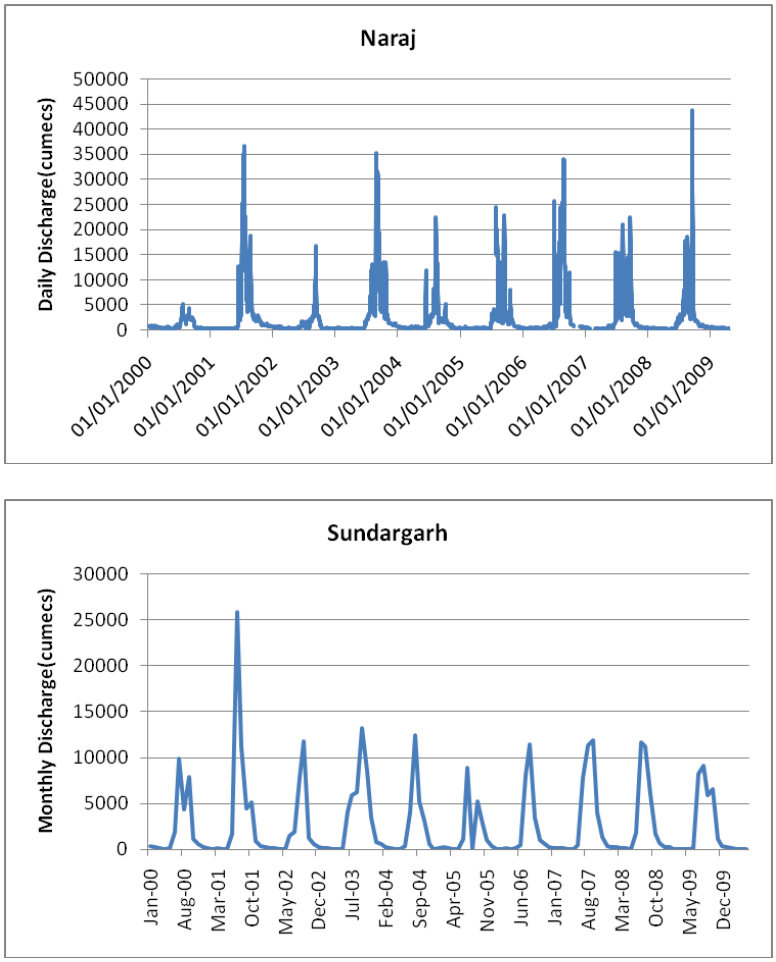

Figure 3.6: Time Series Plots of Daily and Monthly Discharge Data

CHAPTER 4

DEVELOPMENT OF THEMATIC MAPS WITH REMOTE SENSING AND GIS SUPPORT

4.1 INTRODUCTION

Spatial variability is at the heart of geography, a field dedicated to understanding where things are and why. It is also a critical component in understanding many complex systems, particularly those which include interactions between wildly disparate sets of forces. Water systems, for example, can act as a powerfully unifying resource. To truly assess water resources in their most holistic sense, one needs to include the many aspects of hydrological cycle, from meteorology to surface hydrology to soil sciences to groundwater to limnology to aquatic ecosystems. And that is just physical system. The thematic map developed from a variety of perspectives of the basin provides a view of the water shed and are being used for hydrological analysis.

4.2 DEVELOPMENT OF BASIN AND SUB-BASIN MAPS

In the present study, the basin area of Mahanadi river system lying in Odisha and its sub-basins are delineated using Arc Soil and Water Assessment Tool (Arc-SWAT) model. Arc-SWAT is a tool of Geographic Information Systems (GIS) based software called Arc-GIS. Arc-SWAT which is a graphical user interface of SWAT in Arc-GIS delineates the basin into sub-basins and hydrologic response units (HRUs) using the digital elevation model (DEM) map, land use map, soil map and slope map. For modeling purposes, the basin is divided into number of sub-basins. The use of sub-basins in a simulation is particularly beneficial when different areas of the basin are dominated by different land uses or soils, which may have impact on hydrology.

The conventional method of drainage basin delineation is obtained by using the topographic map. The basin divide is drawn starting from the outflow profile, drawing a line perpendicular to the contour lines, encompassing the headwaters and the entire stream network. This is usually done using scanned maps in CAD or GIS software, where the polygon properties can be easily calculated. But this conventional method is a little time consuming. The method used in this study uses the depression-less preprocessed digital elevation model and the calculated flow accumulation grid to determine which of the grid elements (or cells) drain into the specified output profile, or "pour point". These are the cells that comprise the catchment area, and a polygon can easily be generated for direct calculation of area and perimeter.

The Arc-SWAT requires one spatial raster data set: digital elevation model (DEM). This map is created in the "Polyconic" projection with the resolution in meters and elevation in meters. The digital elevation model (DEM) used in the present study, is GTOPO30, downloaded from the site http://eros.usgs.gov/elevation-products. GTOPO30 is a global digital elevation model (DEM) with a horizontal grid spacing of 30 arc seconds (approximately 1 kilometer). GTOPO30 is derived from several raster and vector sources of topographic information. GTOPO30, completed in late 1996, is developed over a three year period through a collaborative effort led by staff at the U.S. Geological Survey's Center for Earth Resources Observation and Science (EROS). The study area is extracted from the GTOPO30 and imported to the ArcGIS software for its delineation into sub-basins using "watershed delineation" tool. This tool allows delineation of the basin into sub-basins based on an automatic procedure using DEM data. This tool uses and expands Arc-GIS and spatial analyst extension functions to perform basin delineations. As the GTOPO30 DEM has a spatial resolution of 1 km, it does not provide enough detail to allow the interface to accurately

predict the location of the stream network. Therefore a stream network dataset in a polyline vector format is superimposed onto the DEM to define the location of the stream network. The stream network improved hydrographic segmentation and sub-basin boundary delineation. The flow direction and accumulation map is prepared from the DEM by filling the sinks and calculating the flow direction and flow accumulation grids. Duration of this process depends up on spatial resolution of the DEM. In the present case, it is a process of just few minutes. This process is necessary when defining streams from the DEM. Then the stream network is created, from which sub-basins and sub-basin outlets are generated. Sub-basin outlets are the points in the drainage network of a sub-basin where stream flow exits the sub-basin area. Adding outlets at the location of monitoring stations is useful for comparison of measured and predicted flow. In the present case, discharge data for twenty seven discharge sites are available for the study area, so these sites are added as sub-basin outlets. Then the basin outlet is defined and the basin is delineated in to fifty four sub-basins according to both the linking stream added outlets and manually added outlets.

Further according to location of discharge sites and magnitude of discharge, the basin is demarcated into seven major sub-basins namely, Sundargarh, Hirakud, Kesinga, Kantamal, Salebhatta, Tikarpada and Naraj, with catchment areas1524.918, 7372.37, 10086.5, 9960.579, 3944.771, 19172.27, 9526.295 km^2 respectively. To avoid confusion, henceforth the fifty-four sub-basins will be termed as watersheds and the above mentioned seven major sub-basins will be termed as sub-basins. The maps generated from Arc-SWAT during the basin delineation process are presented in Figure 4.1.

Further it was observed in the stream link and stream order maps that some portions of the river drainage network (such as lower left corner) are not connected to their subsequent networks and therefore these portions have been eliminated from the further analysis.

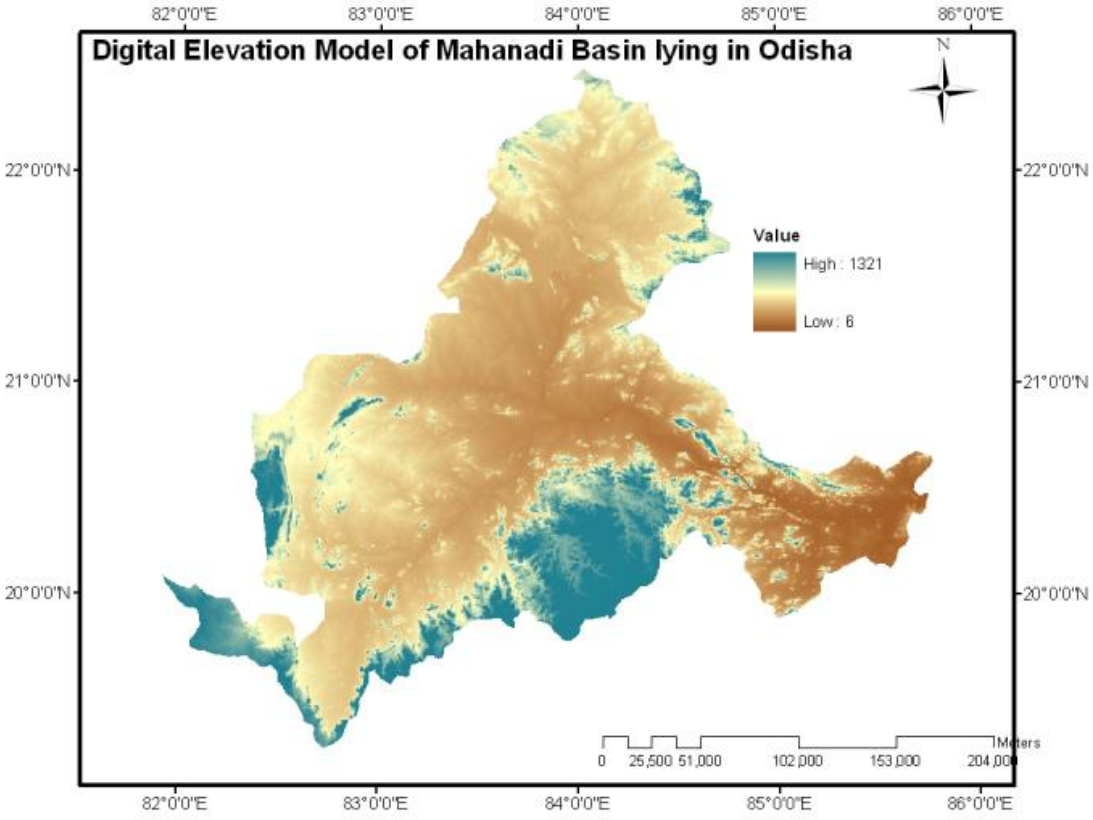
Digital Elevation Model of Mahanadi Basin lying in Odisha
N
Value
High : 1321
Low : 6
82°0'0"E
83°0'0"E
84°0'0"E
85°0'0"E
86°0'0"E
22°0'0"N
21°0'0"N
20°0'0"N
0 25,500 51,000 102,000 153,000 204,000
Meters

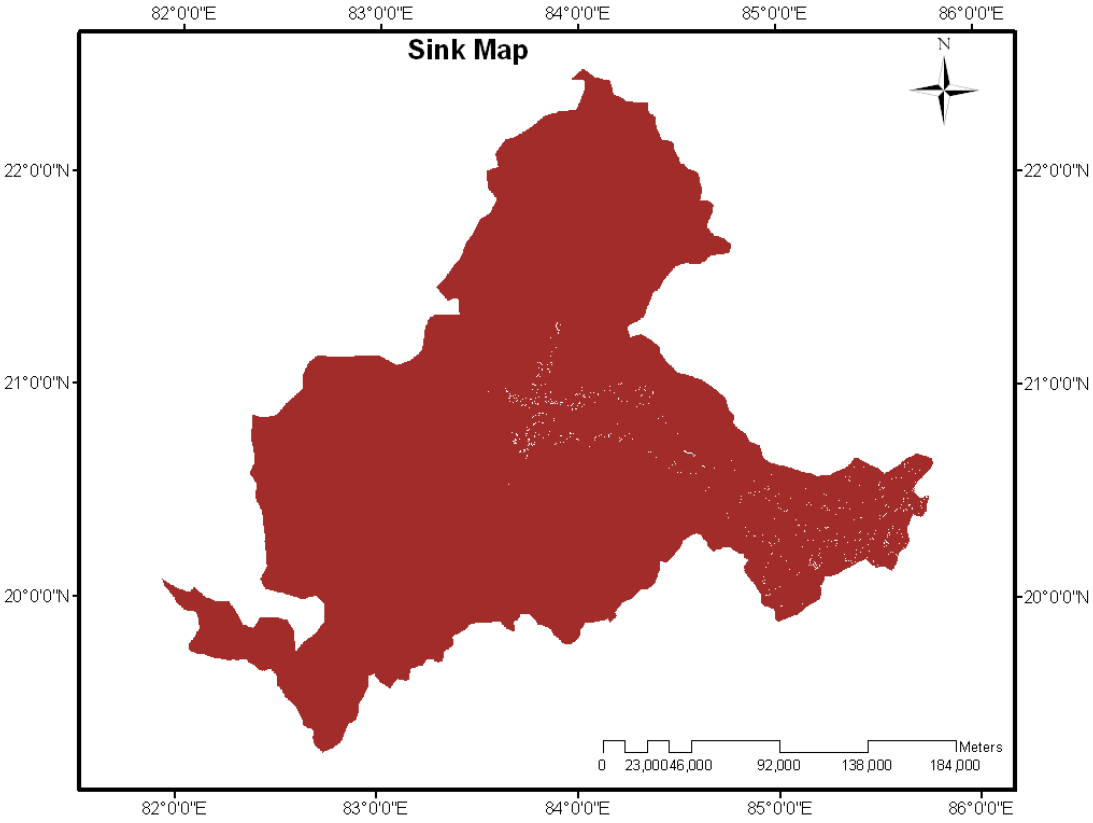
Sink Map
N
82°0'0"E
83°0'0"E
84°0'0"E
85°0'0"E
86°0'0"E
22°0'0"N
21°0'0"N
20°0'0"N
0 23,00046,000 92,000 138,000 184,000
Meters

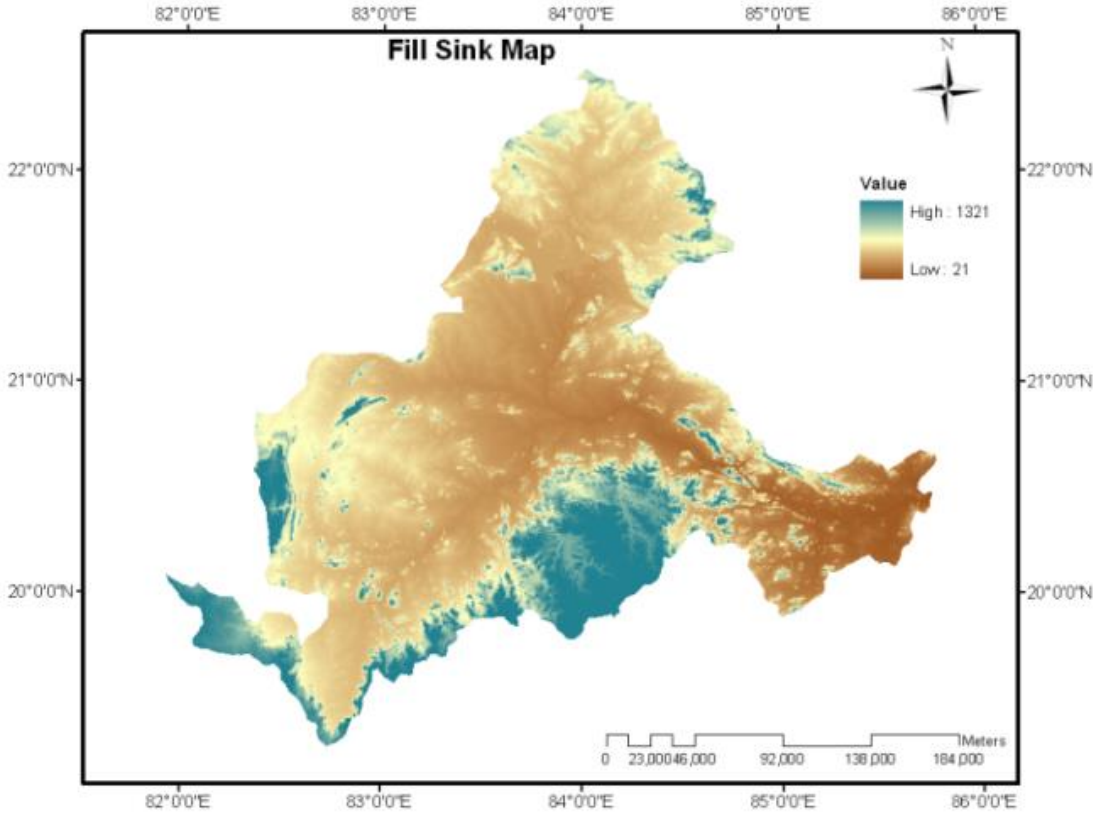
Fill Sink Map
82°0'0"E
83°0'0"E
84°0'0"E
85°0'0"E
86°0'0"E
22°0'0"N
21°0'0"N
20°0'0"N
N
Value
High : 1321
Low : 21
0 23,000 46,000 92,000 138,000 184,000
Meters

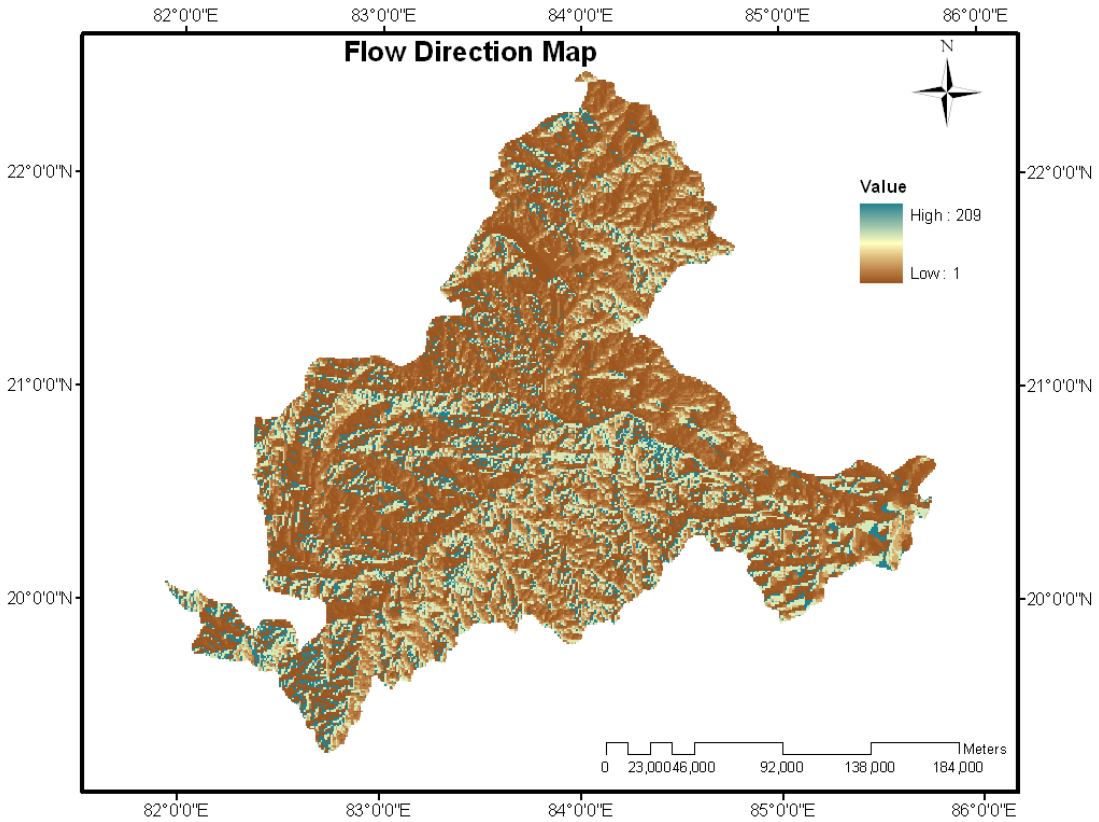
Flow Direction Map
82°0'0"E
83°0'0"E
84°0'0"E
85°0'0"E
86°0'0"E
22°0'0"N
21°0'0"N
20°0'0"N
N
Value
High : 209
Low : 1
0 23,000 46,000 92,000 138,000 184,000
Meters

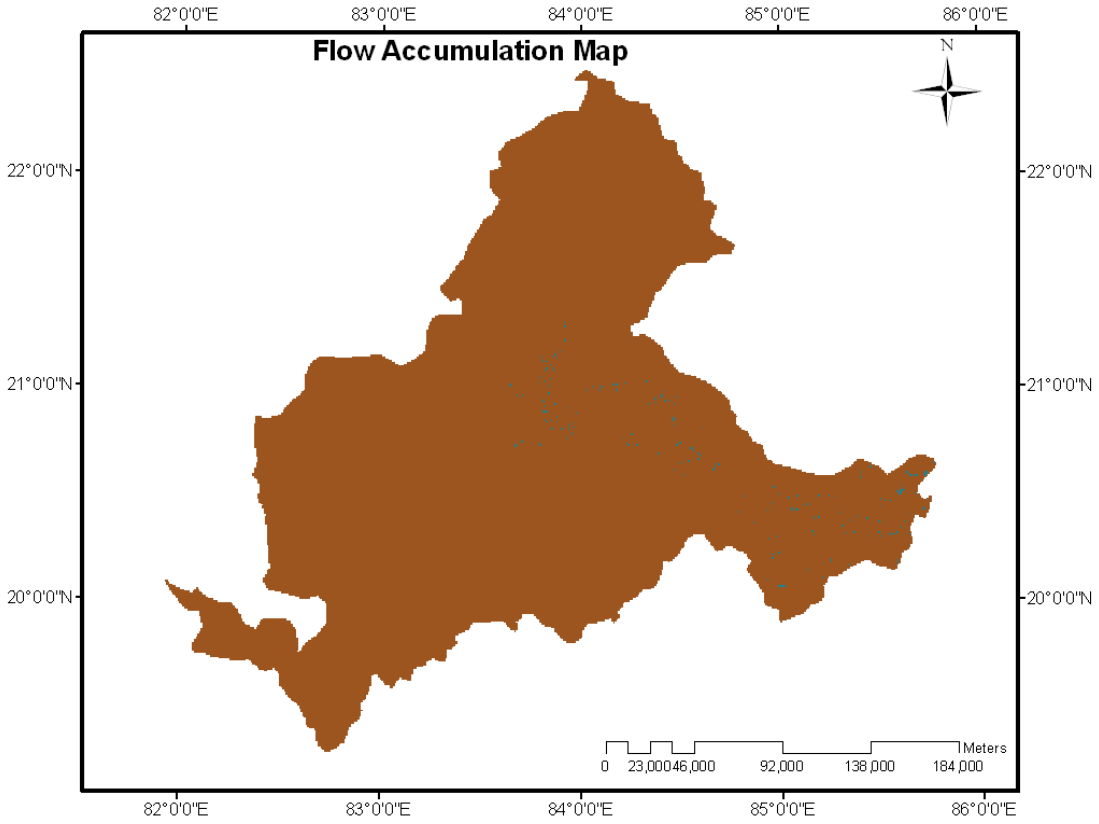
Flow Accumulation Map
N
82°0'0"E
83°0'0"E
84°0'0"E
85°0'0"E
86°0'0"E
22°0'0"N
21°0'0"N
20°0'0"N
0 23,000 46,000 92,000 138,000 184,000
Meters

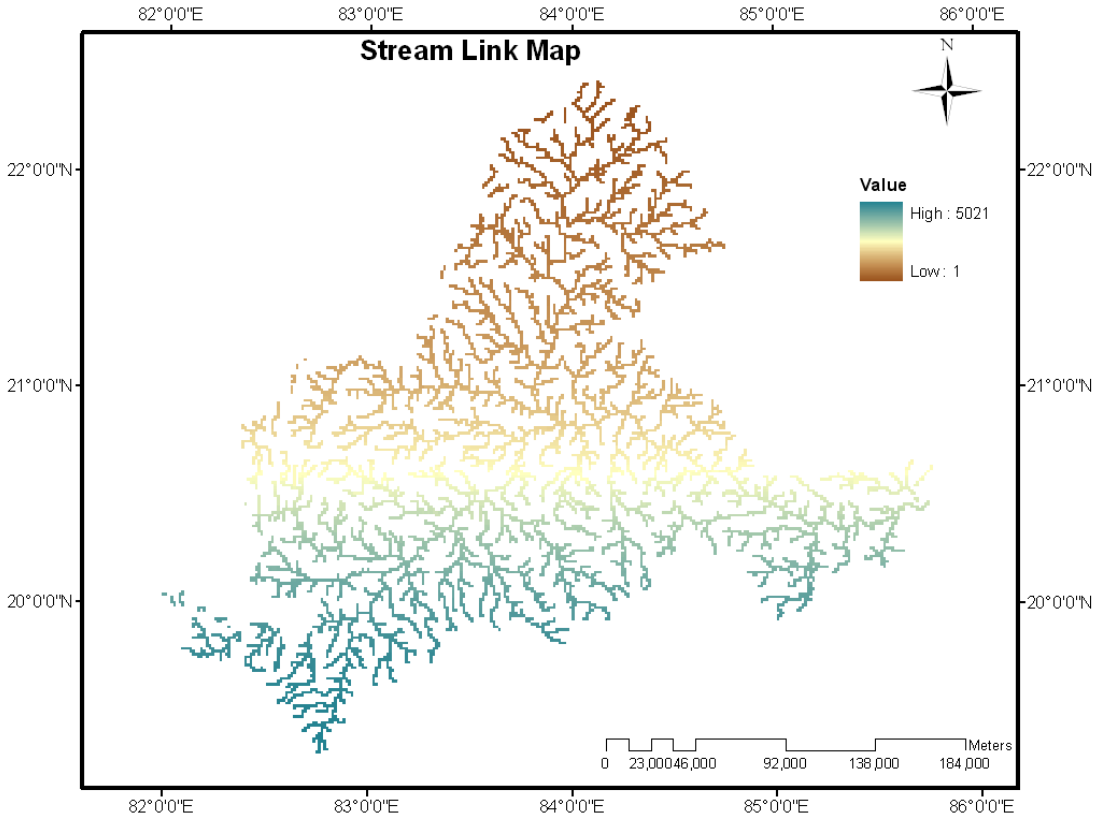
Stream Link Map
N
Value
High : 5021
Low : 1
82°0'0"E
83°0'0"E
84°0'0"E
85°0'0"E
86°0'0"E
22°0'0"N
21°0'0"N
20°0'0"N
0 23,000 46,000 92,000 138,000 184,000
Meters

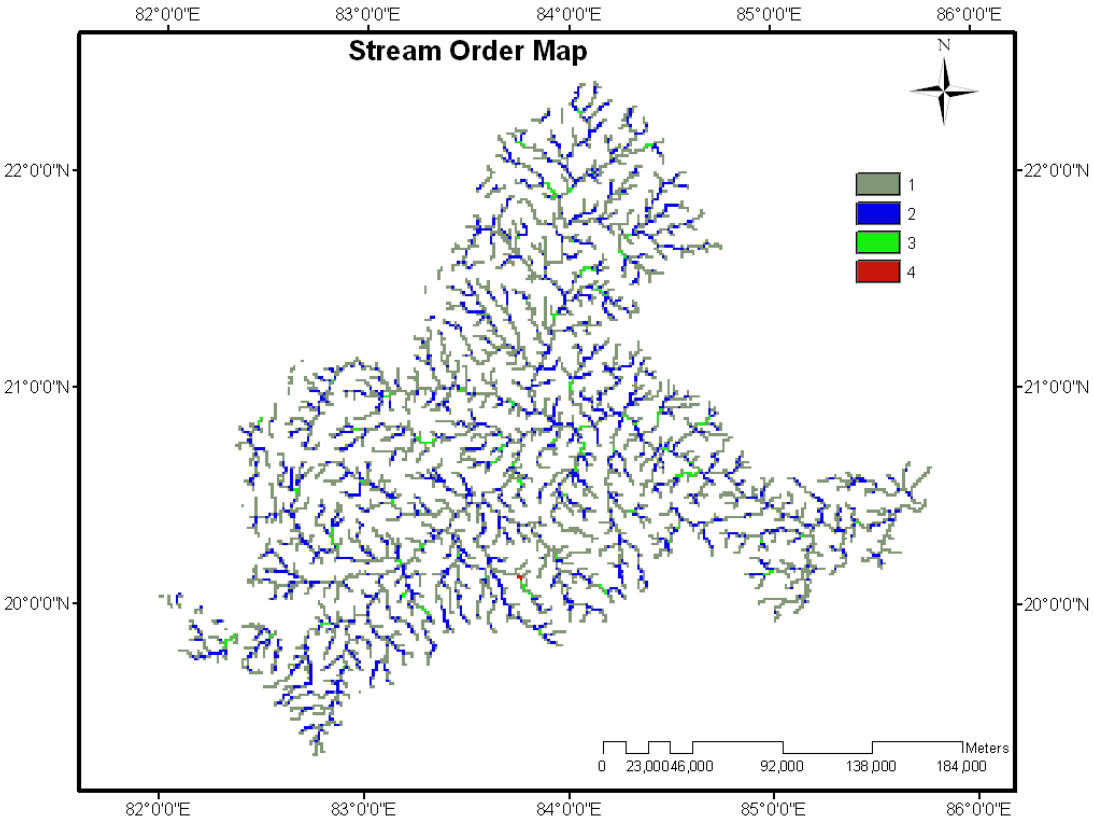
Stream Order Map
N
1
2
3
4
82°0'0"E
83°0'0"E
84°0'0"E
85°0'0"E
86°0'0"E
22°0'0"N
21°0'0"N
20°0'0"N
0 23,000 46,000 92,000 138,000 184,000
Meters

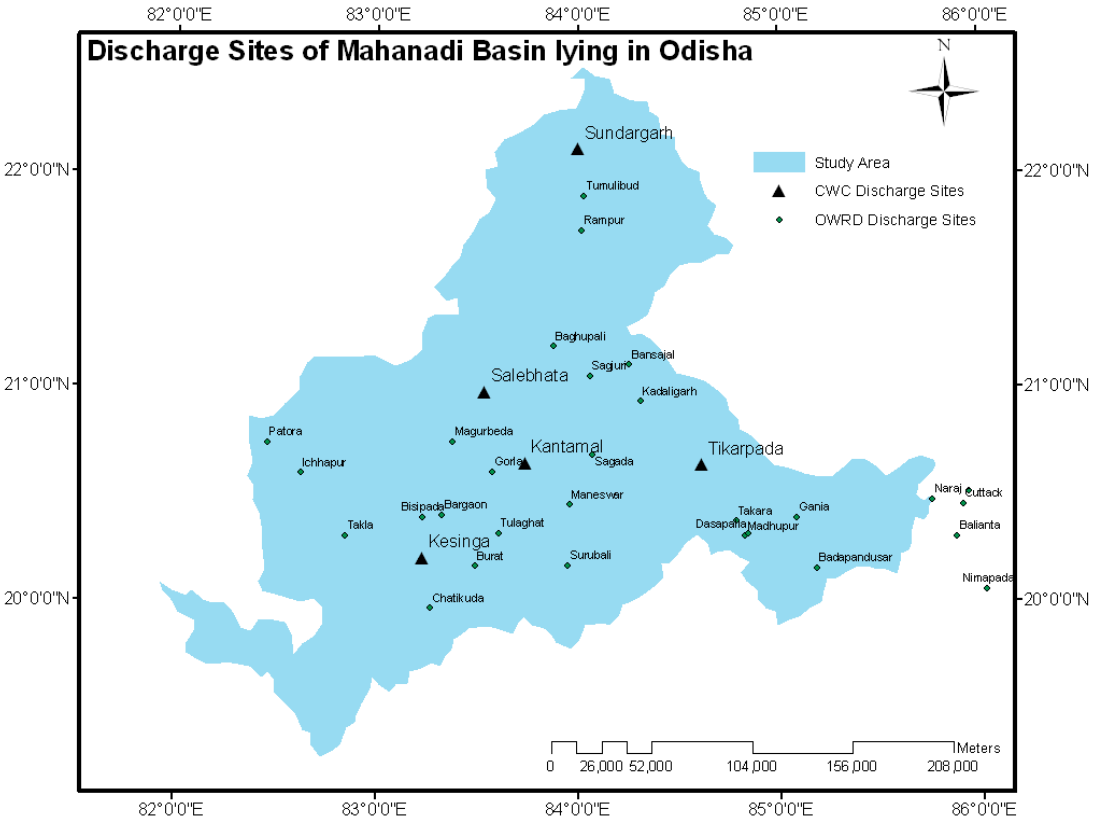
Discharge Sites of Mahanadi Basin lying in Odisha
N
Study Area
CWC Discharge Sites
OWRD Discharge Sites
Sundargarh
Tumulibud
Rampur
Baghupali
Bansajal
Sagjuri
Salebhata
Kadaligarh
Patora
Magurbeda
Kantamal
Tikarpada
Ichhapur
Gorla
Sagada
Maneswar
Bisipada
Bargaon
Takara
Gania
Takla
Tulaghat
Dasapalla
Madhupur
Kesinga
Burat
Surubali
Badapandusar
Chatikuda
Nimapada
Narsi
Cuttack
Balianta
82°0'0"E
83°0'0"E
84°0'0"E
85°0'0"E
86°0'0"E
22°0'0"N
21°0'0"N
20°0'0"N
0 26,000 52,000 104,000 156,000 208,000
Meters

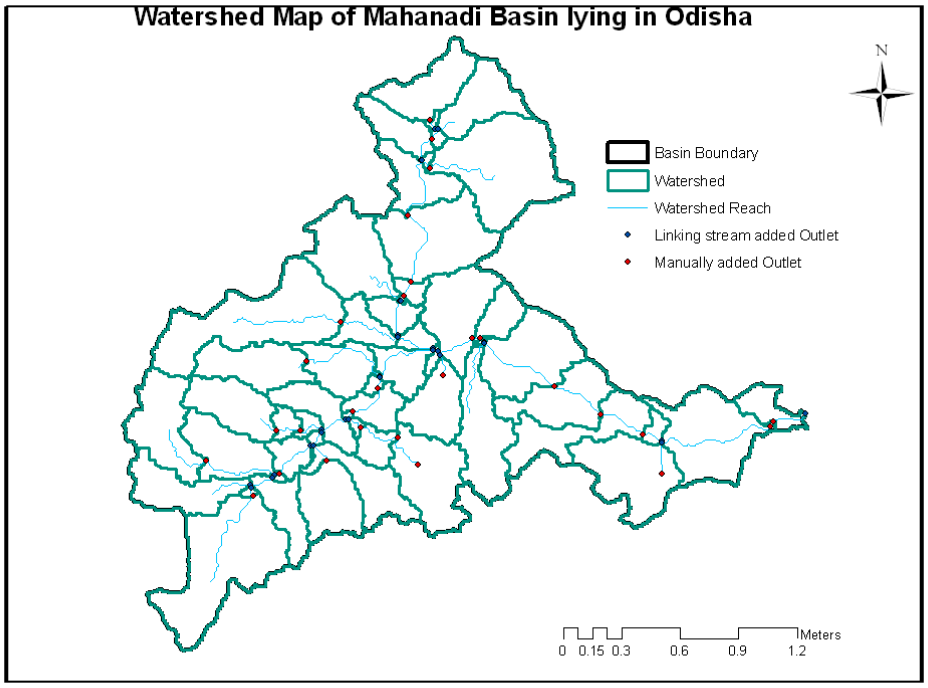

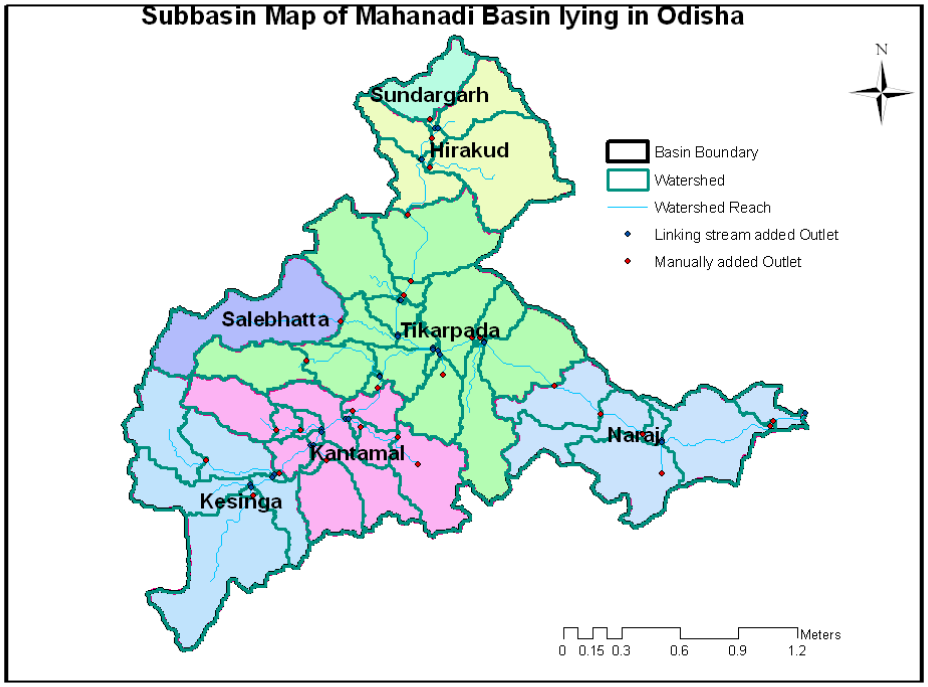

Figure 4.1: Basin and sub-basin maps of the Study Area generated stepwise in Arc-SWAT

4.3 ESTIMATION OF BASIN AND SUB-BASIN PARAMETERS

The basin area is one of the most important watershed characteristic for hydrologic design. It is the horizontal projection of the entire surface of the catchment, and is the area or reception of rainfall. Moreover, the catchment perimeter is the most straightforward variable. The mean elevation, or mean altitude, of a catchment is manually calculated from the weighted mean of the sum of partial volumes between contour lines (Zavoianu, 1985). When using digital elevation models, the calculation of mean elevation is done by using the median value (numerical value separating the higher and lower half of the sample) and the median is obtained from the entire sample of catchment cell elevations. The longest flow path, or length of the stream, is the distance measured along the stream channel from the source to outlet, a distance which may be measured on the topographic map. The average slope of a catchment, as an independent variable, is calculated as the weighted mean of all the elementary surfaces between two consecutive contour lines. The catchment area, catchment perimeter, mean elevation, longest flow path and average slope of the fifty four watersheds of the study area is given in Appendix I.

4.4 DELINEATION OF THEMATIC MAPS

Land use and soil are two important variables in addition to DEM or contour map of the study area. Both the maps along with the river network maps delineated for the study area are shown in Figure 4.2. All thematic maps developed would be used for further analysis.

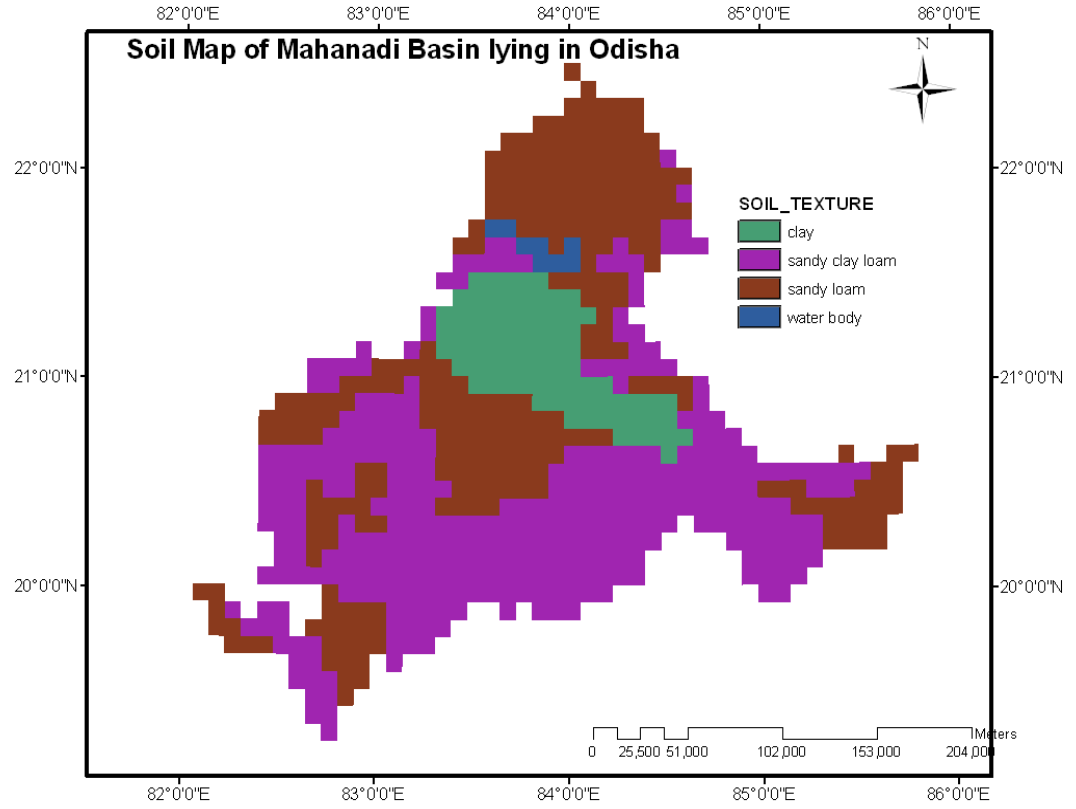
Soil Map of Mahanadi Basin lying in Odisha
82°0'0"E
83°0'0"E
84°0'0"E
85°0'0"E
86°0'0"E
22°0'0"N
21°0'0"N
20°0'0"N
N
SOIL_TEXTURE
clay
sandy clay loam
sandy loam
water body
0 25,500 51,000 102,000 153,000 204,000
Meters

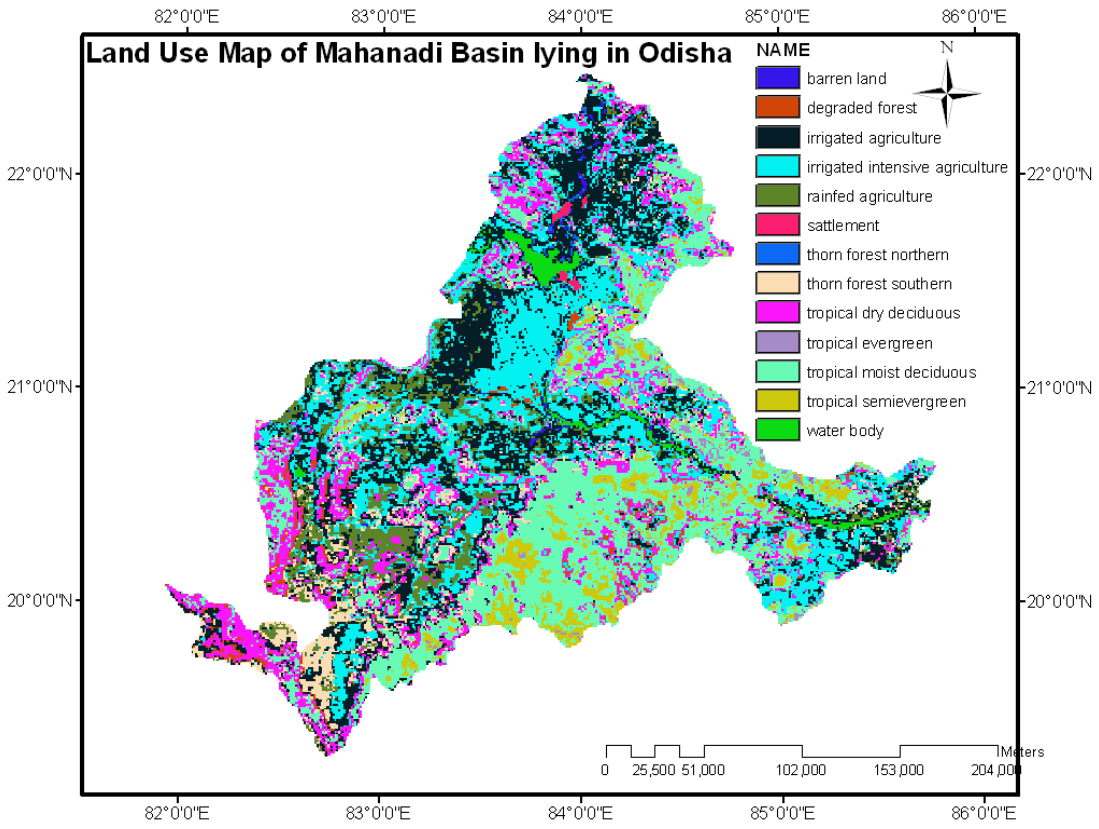
Land Use Map of Mahanadi Basin lying in Odisha
82°0'0"E
83°0'0"E
84°0'0"E
85°0'0"E
86°0'0"E
22°0'0"N
21°0'0"N
20°0'0"N
N
NAME
barren land
degraded forest
irrigated agriculture
irrigated intensive agriculture
rainfed agriculture
sattlement
thorn forest northern
thorn forest southern
tropical dry deciduous
tropical evergreen
tropical moist deciduous
tropical semievergreen
water body
0 25,500 51,000 102,000 153,000 204,000
Meters

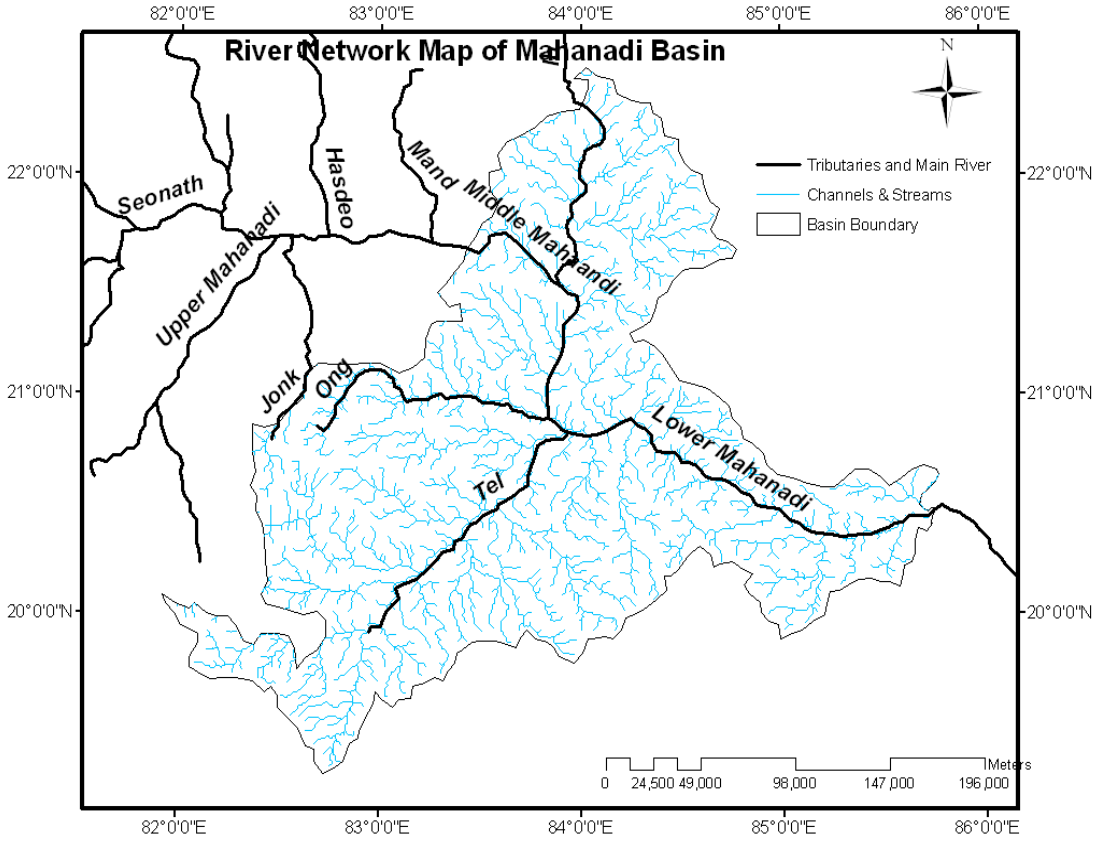

Figure 4.2: Soil, Landuse and River netwrok map of the study area

4.5 CONCLUSION

Using DEM and shape files of the basin, it was delineated into seven major subbasins according to the location of discharge stations applying ARC-SWAT within the environment of ARC-GIS and then parameters of each subbasin, such as catchment area, catchment perimeter, mean elevation, longest flow path and average slope were estimated for runoff simulation.

CHAPTER 5

ESTIMATION OF MEAN RAINFALL BY SPATIAL INTERPOLATION

5.1 INTRODUCTION

The application of point rain gauge as precipitation input carries lots of uncertainties regarding estimation of runoff (Faur`es et al., 1995 and Chaubey et al., 1999), which, in turn, creates problem for the discharge prediction, especially if the rain gauge is located outside the basin (Schuurmans and Bierkens, 2007). For such reasons, some utilities such as hydrological modeling(Syed et al., 2003; Kobold and Su˘selj, 2005; Gabellani et al., 2007; Cole and Moore, 2008; Collischonn, et al., 2008; Ruelland et al., 2008; Moulin et al., 2009) need rainfall data that are spatially continuous and the quality of results are by the quality of the continuous spatial rainfall (Singh, 1997; Andr´eassian et al., 2001; Kobold and Su˘selj, 2005; Leander et al., 2008; Moulin et al., 2009).

Spatial interpolation is a technique in which with given values of a variable at a set of sample points, values of variable at every point can be predicted. For any unknown point, some form of weighted average of the values at surrounding points is taken to predict the value at the point where it is unknown. In other words, a continuous surface is created from a set of points. This type of interpolated surface is often called a statistical surface. Elevation data, precipitation, temperature, snow accumulation and ground water table are types of data that can be computed using interpolation. The basic premise behind interpolation is “Everything is related to everything else, but near things are more related than distant things"(Waldo Tobler, 1970), and therefore in interpolation near points generally receive higher weights than far away points.

In order to generate a continuous map, for example, a digital elevation map from elevation points measured with a GPS device, a suitable interpolation method is required to be used to optimally estimate the values at those locations where no samples or measurements are taken. The results of the interpolation analysis can then be used for the analyses and modeling of the whole area. A very basic problem in spatial analysis is interpolating a spatially continuous variable from point samples. But interpolation should not be used when there isn't a meaningful value of the variable at every point within the region of interest, i.e. when points represent merely the presence of events, interpolation does not make sense.

The generation of continuous surfaces starting from irregularly distributed data can be performed by different methods but the difficulty is the choice of the one that best reproduces the actual surface (Caruso and Quarta, 1998). Regarding the rainfall, indirect methods of creation of continuous surface based on the measurement of related auxiliary variables have been provided since the 1960s by ground-based meteorological RADARs and by remote sensing devices installed on satellite platforms. The certainty and reliability of such indirect methodologies for hydrological purposes have yet to be estimated. The methodologies must be calibrated and validated using historical data (Lanza et al., 2001). A number of interpolation techniques have been described in the literature, which reproduce the spatial continuity of rainfall fields based on rain gauge measurement. These methods can be generally classified into two main groups: deterministic methods and geo-statistical methods. Some commonly used methods are briefly introduced here. Spatial interpolation is generally carried out by estimating a regionalized value at un-sampled points based on a weight of observed regionalized values. The general formula for spatial interpolation is as follows:

$$Z_g = \sum_{i=1}^{ns} \lambda_i Z s_i \qquad (5.1)$$

Where Zg is the interpolated value at the required points, Zs_i is the observed value at point i, ns is the total number of observed points and $\lambda = (\lambda_i)$ is the weight contributing to the interpolation. The problem lies in calculating the weights, λ, which will be used in the interpolation. The different methods for computing the weights with their outcome for the study area are being presented in the following sections.

5.2 DETERMINISTIC METHODS

5.2.1 Thiessen Polygon method or Nearest Neighborhood method

The Thiessen polygon method assumes that the estimated values can take on the observed values of the closest station. The Thiessen polygon method is also known as the nearest neighbor (NN) method (Nalder et al., 1998). Nearest neighbor methods have been intensively investigated in the field of statistics and in pattern recognition procedures. Despite their inherent simplicity, nearest neighbor algorithms are considered versatile and robust. Although more sophisticated alternative techniques have been developed since their inception, nearest neighbor methods remain very popular. A nearest neighbor algorithm typically involves selecting a specified number of data vectors similar in characteristics to the vector of interest. One of these vectors is randomly re-sampled to represent the vector of the given time step in the simulation period. In the context of weather data simulation, the nearest neighbor approach involves simultaneous sampling, with replacement, weather variables, like precipitation and temperature, from the observed data. To generate weather variables for a new day, t+1, days with similar characteristics to those simulated for the previous day t are first selected from the historical record. One of these nearest neighbors is then selected according to a defined probability distribution or kernel and the observed values for the day subsequent to that nearest neighbor are adopted as the simulated values for day t+1.

Models based on the NN approach can easily be extended to multisite simulation of weather data while keeping the spatial correlation structure virtually intact. The spatial dependencies are preserved because the same day's weather is adopted as the weather for all stations. Apart from the spatial dependencies, temporal dependence is likely to be preserved as the simulated values for day t +1 are conditioned on the values for the previous day t. Further, the cross-correlation among the variables at any given site is automatically preserved as a block of variables, rather than a single variable, is resampled from the observed data. Monthly rainfall interpolation map of the study area from January to December generated by nearest neighbor method is shown in Figure 5.1.

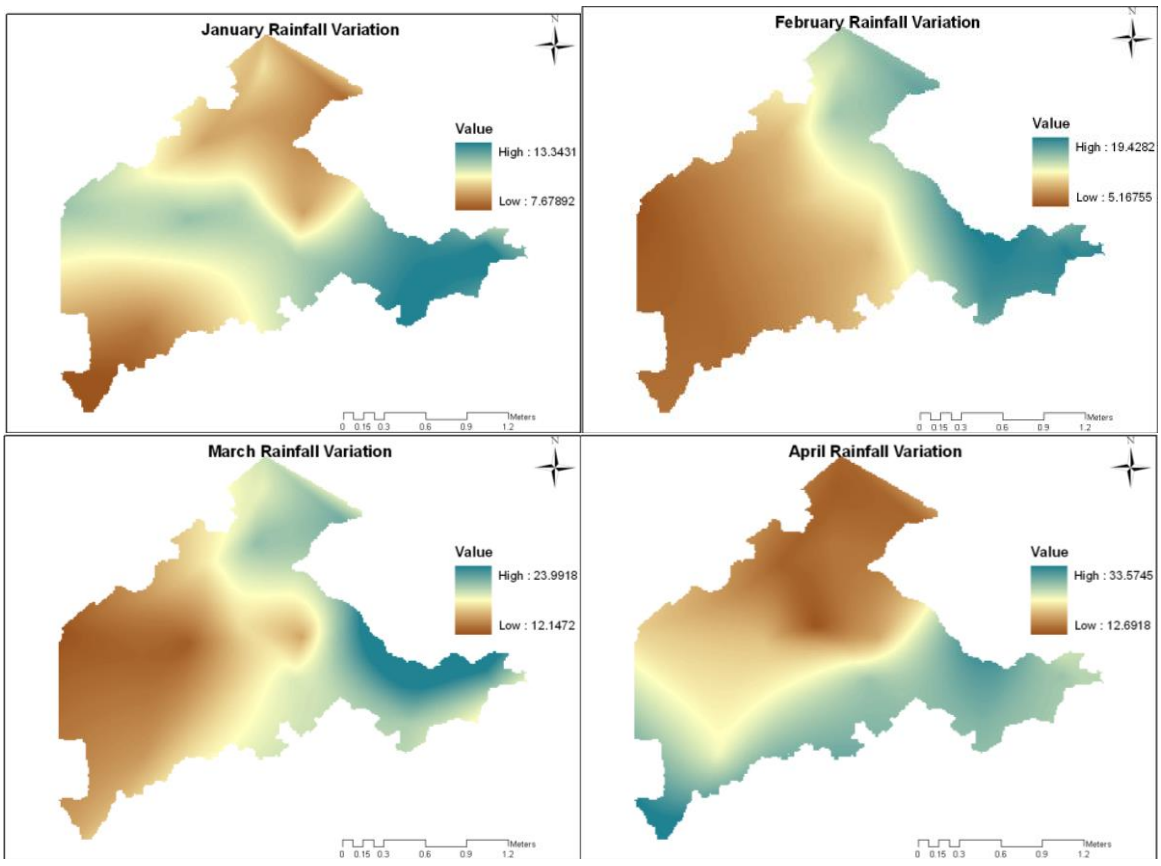

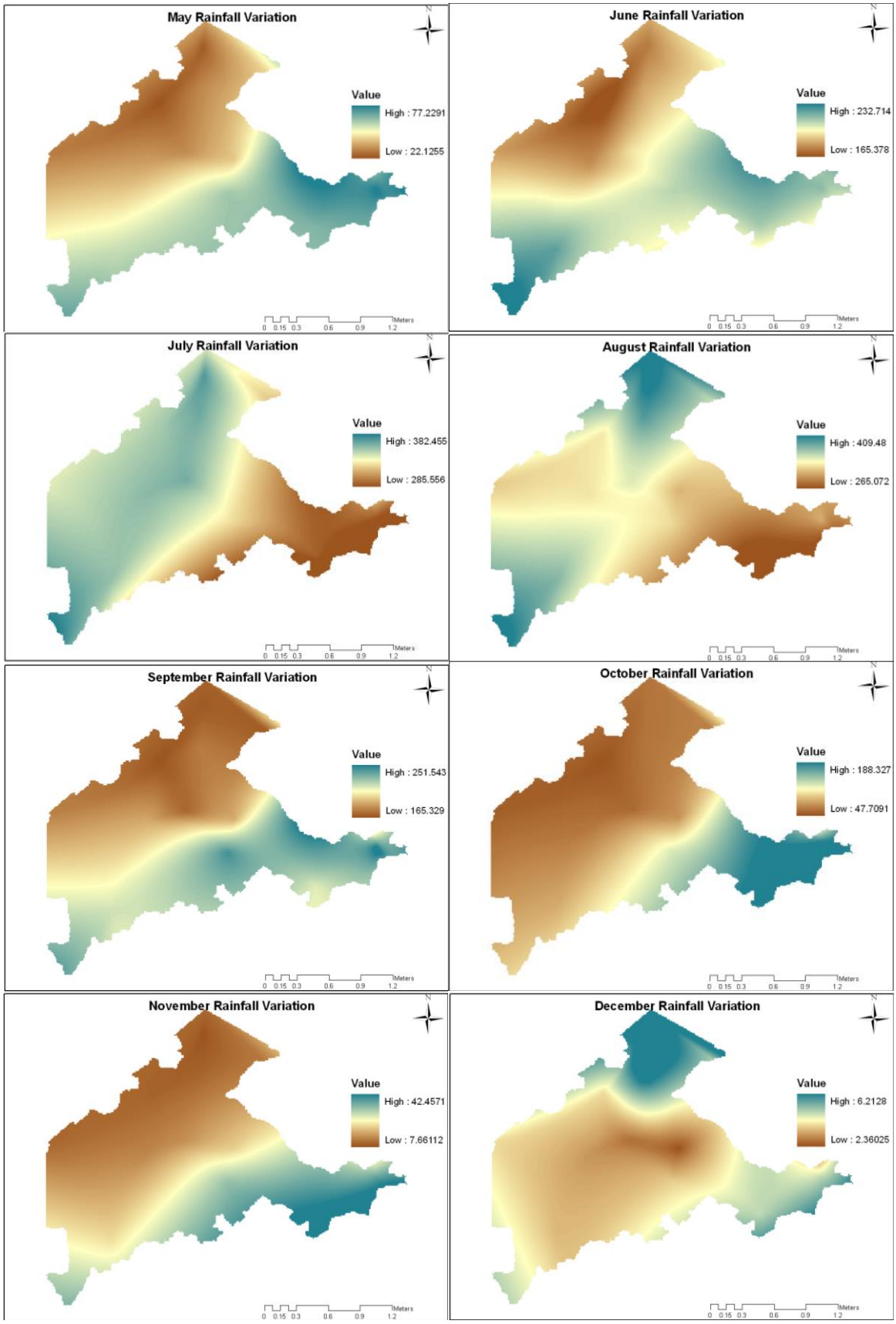

Figure 5.1: Monthly rainfall Interpolation by Nearest Neighbor Method

It is to be noted that, the polygon must be changed every time a station is added or deleted from the network (Chow, 1964). The deletion of a station is referred to as “missing rainfall”. This method, although more popular than the method of taking the simple average of the number of stations, is not suitable for mountainous regions, because of the orographic influence of the rain (Goovaerts, 1999).

5.2.2 Inverse Distance Weighting (IDW) Method

The Inverse Distance Weighting (IDW) method is based on the functions of the inverse distances in which the weights are defined by the opposite of the distance and normalized so that their sum equals one. The weights decrease as the distance increases. This method is more complex than the previous methods, since the power of the inverse distance function must be selected before the interpolation is performed. A low power leads to a greater weight towards a grid point value of rainfall from remote rain gauges. As the power tends toward zero, the interpolated values will approximate the areal-mean method, while for higher levels of power, the method approximates the Thiessen method (Dirks et al., 1998). There is a possibility of including elevation weighting along with distance weighting, known as Inverse Distance and Elevation Weighting (IDEW). IDEW provides more suitable results for mountainous regions where topographic impacts on precipitation are important (Masih et al., 2011).The general formula of IDW is:

$$\hat{Z}(s_o) = \sum_{i=1}^{N} \lambda_i Z(s_i) \qquad (5.2)$$

where $\hat{Z}(s_o)$ is the predicted value for location s_o, N is the number of measured sample points surrounding the prediction location, λ_i are the weights assigned to each measured point, $Z(s_i)$ is the observed value at the location s_i. The formula to determine the weights is the following:

$$\lambda_i = d_{io}^{-p} / \sum_{i=1}^{N} d_{io}^{-p}; \sum_{i=1}^{N} \lambda_i = 1 \quad (5.3)$$

Monthly rainfall interpolation map of the study area from January to December generated by inverse distance weighting method is shown in Figure 5.2. However, daily rainfall interpolation map of the study area by IDW is shown in Figure 5.3.

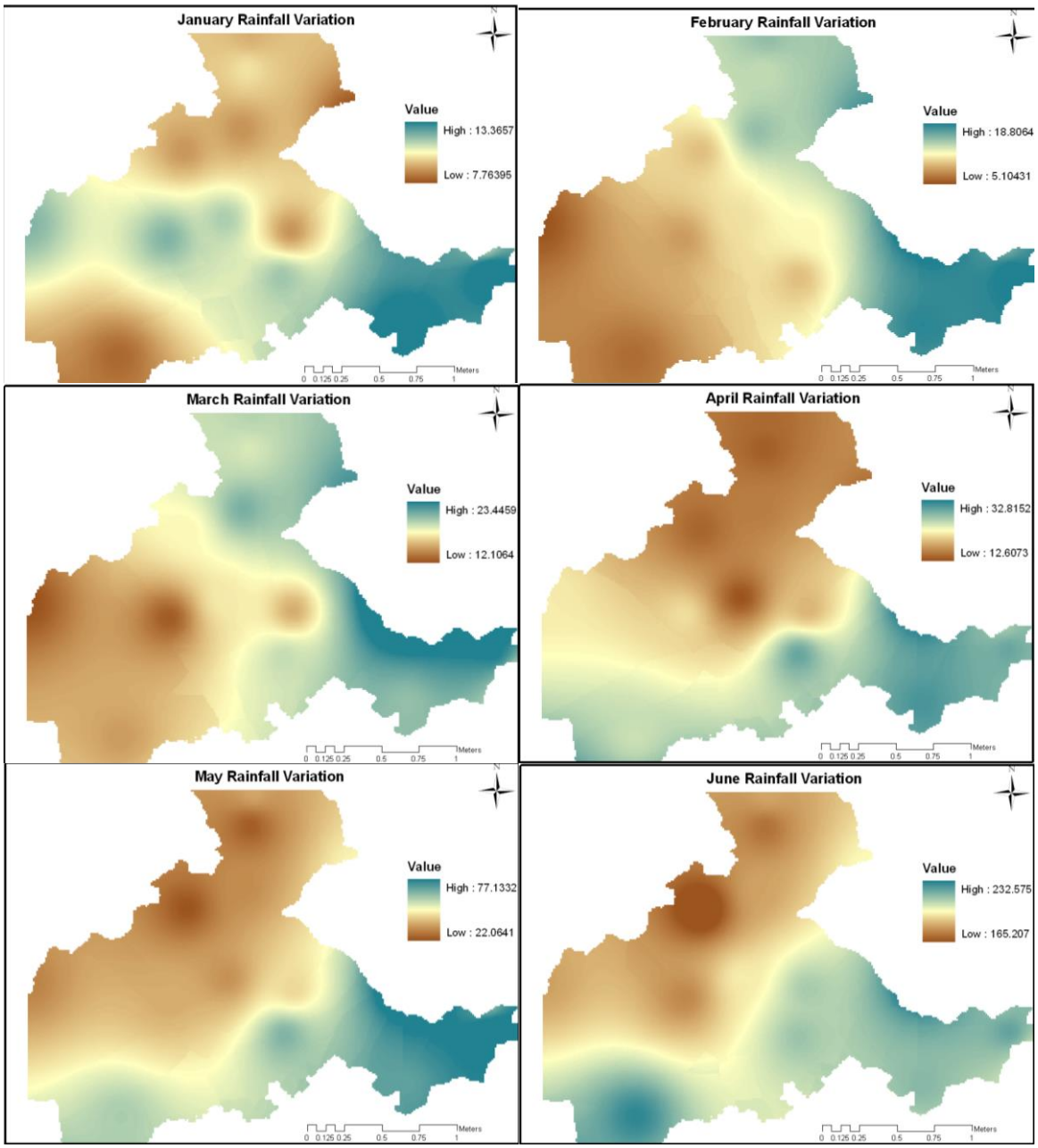

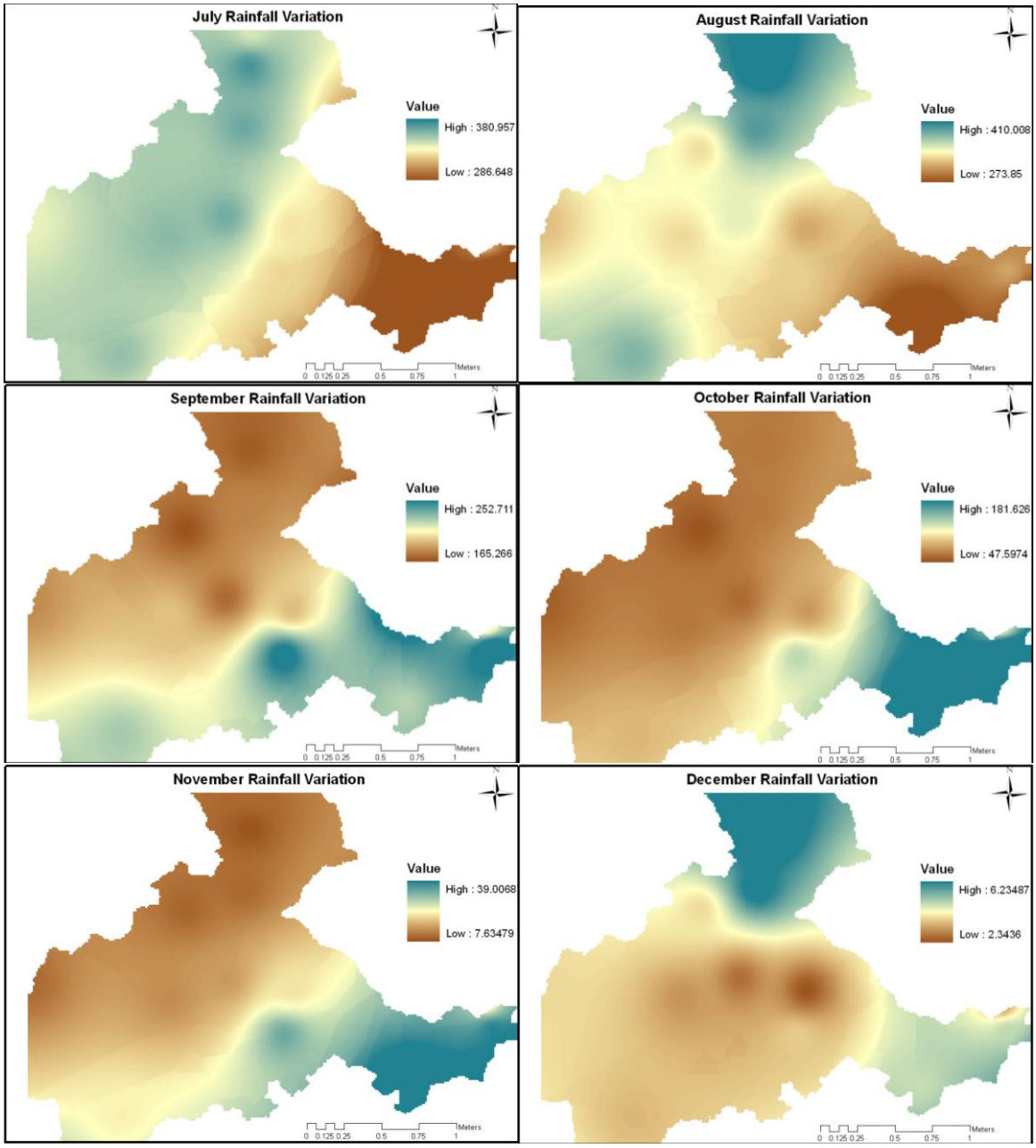

Figure 5.2: Monthly Rainfall Interpolation by Inverse Distance Weighting Method

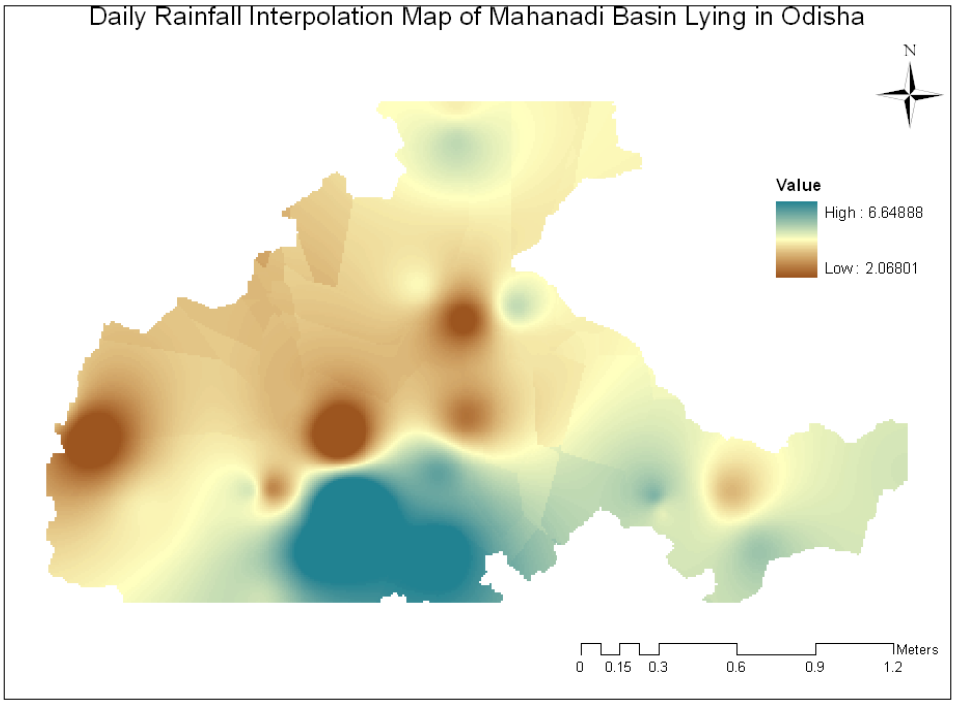

Figure 5.3: Daily Rainfall Interpolation by Inverse Distance Weighting Method

There are a few areas of concern with the IDW and other non-statistical averaging methods. First, the range of the interpolated values is constrained by the range of the measured values, i.e., no interpolated values will fall outside the observed data range. This means that high or low points of the area under consideration will be missed if they are not sampled. Also, because of the nature of the averaging formula, areas outside of the sampled area will flatten to the mean value.

5.2.3 Spline Method

The spline interpolation method is based on a mathematical model for surface estimation that fits a minimum-curvature surface through the input points. The method fits a mathematical function to a specified number of the nearest input points, while passing through the sample points. Spline can generate sufficiently accurate surfaces from only a few sampled points and they retain small features. Spline works best for gently varying surfaces like temperature.

There are two variations of Spline: regularized and tension. A regularized Spline incorporates the first derivative (slope), second derivative (rate of change of slope), and third derivative (rate of change in the second derivative) into its minimization calculations. Although a tension Spline uses only first and second derivatives, it includes more points in the Spline calculations, which usually creates smoother surfaces but increases computation time. As in the present study area, 23 interpolation points for monthly data and 25 interpolation points for daily data are considered, therefore regularized spline is considered adequate to create a smooth surface.The general formula is:

$$Z_{(x,y)} = T_{(x,y)} + \sum_{j=1}^{N} \lambda_j R(r_j) \quad (5.4)$$

where N is the number of sampled points used for the estimation,λ is coefficient of linear equations,r_j is distance from the sample of point and T is determined by the user. Monthly rainfall interpolation map of the study area from January to December generated by regularized Spline method is shown in Figure 5.4. However, daily rainfall interpolation map of the study area by regularized spline is shown in Figure 5.5.

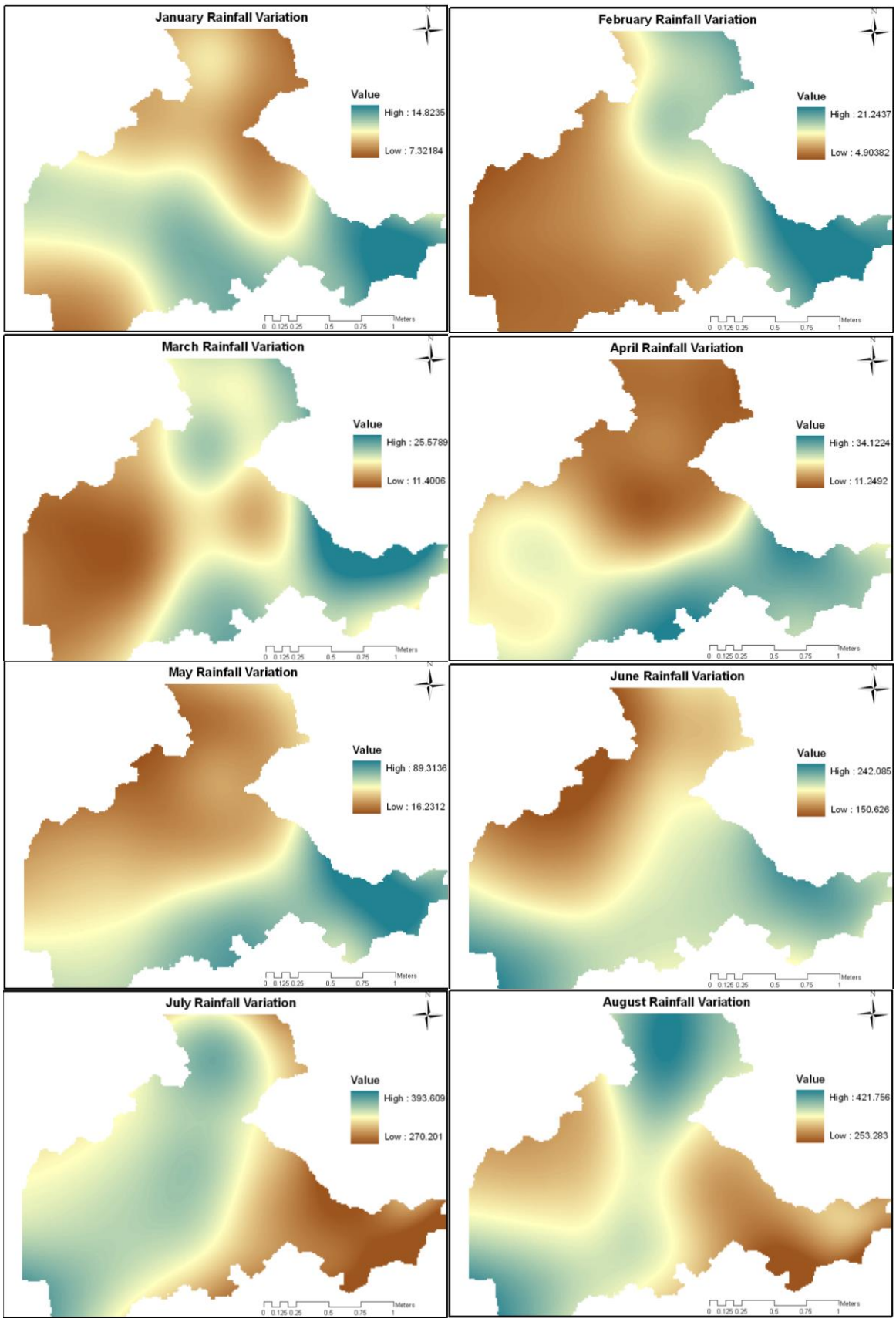
January Rainfall Variation
Value
High : 14.8235
Low : 7.32184
February Rainfall Variation
Value
High : 21.2437
Low : 4.90382
March Rainfall Variation
Value
High : 25.5789
Low : 11.4006
April Rainfall Variation
Value
High : 34.1224
Low : 11.2492
May Rainfall Variation
Value
High : 89.3136
Low : 16.2312
June Rainfall Variation
Value
High : 242.085
Low : 150.626
July Rainfall Variation
Value
High : 393.609
Low : 270.201
August Rainfall Variation
Value
High : 421.756
Low : 253.283

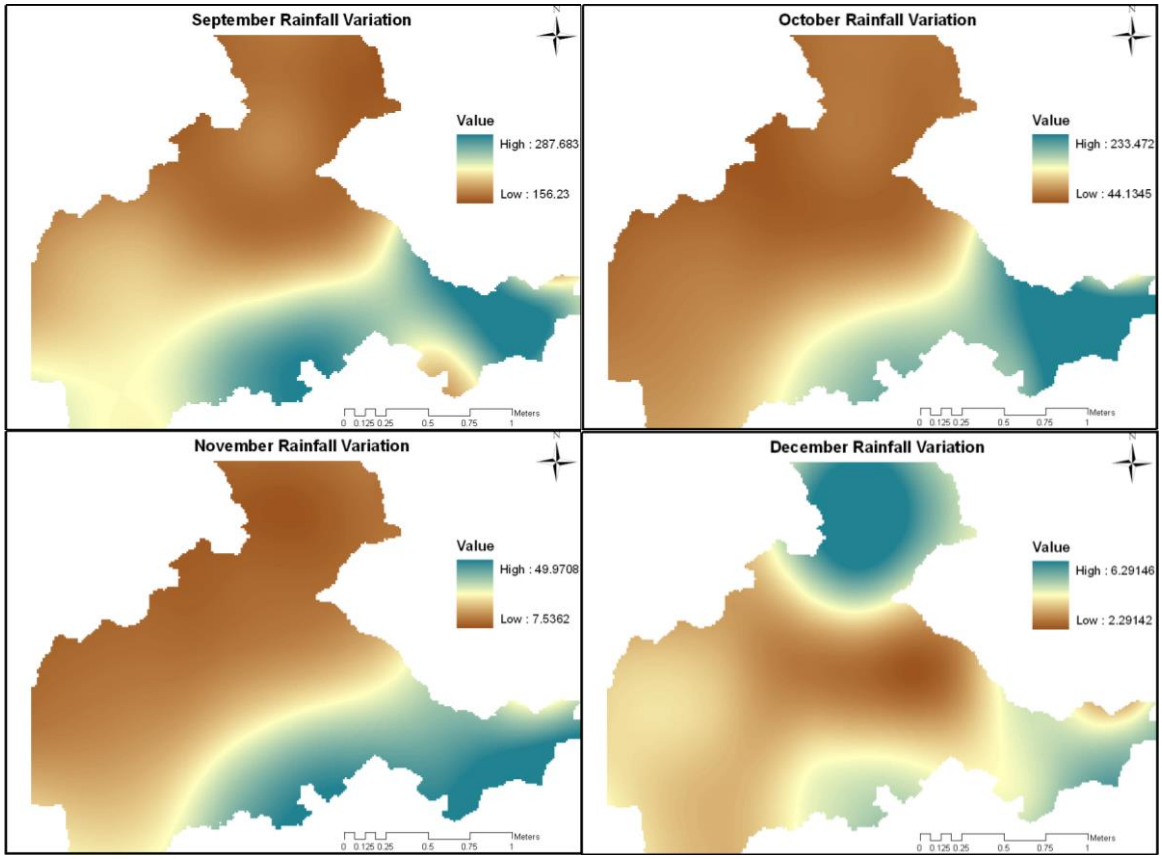

Figure 5.4: Monthly Rainfall Interpolation by Regularized Spline Method

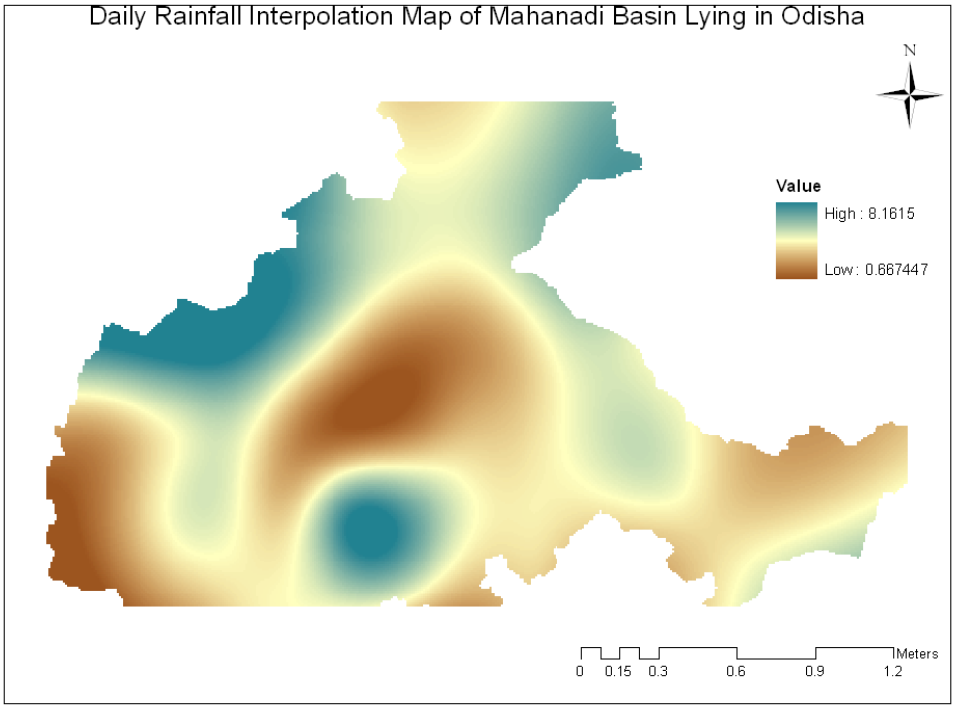

Figure 5.5: Daily Rainfall Interpolation by Regularized Spline Method

This method is not appropriate if there are large changes in the surface within a short distance, because it can overshoot estimated values (Ruelland et al., 2008). Unlike IDW methods, the values predicted by Spline are not constrained to the range of measured values, i.e., predicted values can be above the maximum or below the minimum measured value.

5.3 GEOSTATISTICAL METHODS

5.3.1 Kriging Method

The second group of spatial interpolation methods for measuring rainfall is the geo-statistical methods, which constitutes a discipline connecting mathematics and earth sciences. The Kriging method is an example of a group of geo-statistical techniques used to interpolate the value of a random field. Matheron (1971) named and formalized this method in honour of

Daniel G. Krige, a South African mining engineer who pioneered the field of geo-statistics. The Kriging method is based on statistical models involving autocorrelation. Autocorrelation refers to the statistical relationships between measured points. The geo-statistical methods have the capability of producing a prediction surface and provide some measures of the certainty and accuracy of the predictions. In this method, the value of the variable is estimated for a particular point using a weighted sum of the available point observations. The weights of the data are chosen so that the interpolation is unbiased and the variance is minimized. In general, the Kriging system must be Linear, Authorized, Unbiased and Optimal (LAUO). Kriging is the first method of interpolation to take into account the spatial dependence structure of the data. There are several types of Kriging, which differ according to the form applied to the mean of the interest variable: (a) when it is assumed that the mean is constant and known, simple Kriging (SK) is applied; (b) where the mean is constant but unknown, ordinary Kriging (ORK) is applied; (c) where the mean is assumed to show a polynomial function of spatial coordinates, universal Kriging (UNK). So, in contrast to the other two types, this last type of Kriging is not stationary with regard to the mean.

Stationarity defines itself here by the constancy of the mean, but also by the covariance between two observations that depend only on the distance between these observations. All the different types of Kriging apply the stationarity of the covariance, or, more generally, the semi-variogram. This function, which represents the spatial dependence structure of the data, must be estimated and modelled before making the interpolation. First of all, the experimental semi-variogram can be calculated as being half the squared difference between paired values to the distance by which they are separated:

$$\hat{\gamma}(h) = \frac{1}{2N(h)} \sum_{i=1}^{N(h)} \left(Zs_i - Z(s_i + h)\right)^2 \qquad (5.5)$$

where N(h) is the number of pairs of data locations at distance h apart.

In practice, the average squared distance can be obtained for all pairs separated by a range of distances and these average squared differences can be plotted against the average separation distance. A theoretical model might then be fitted to the experimental semi-variogram **(Figure 5.6)** and the coefficient of this model (nugget effect, sill and range) can be used for a Kriging equation system.

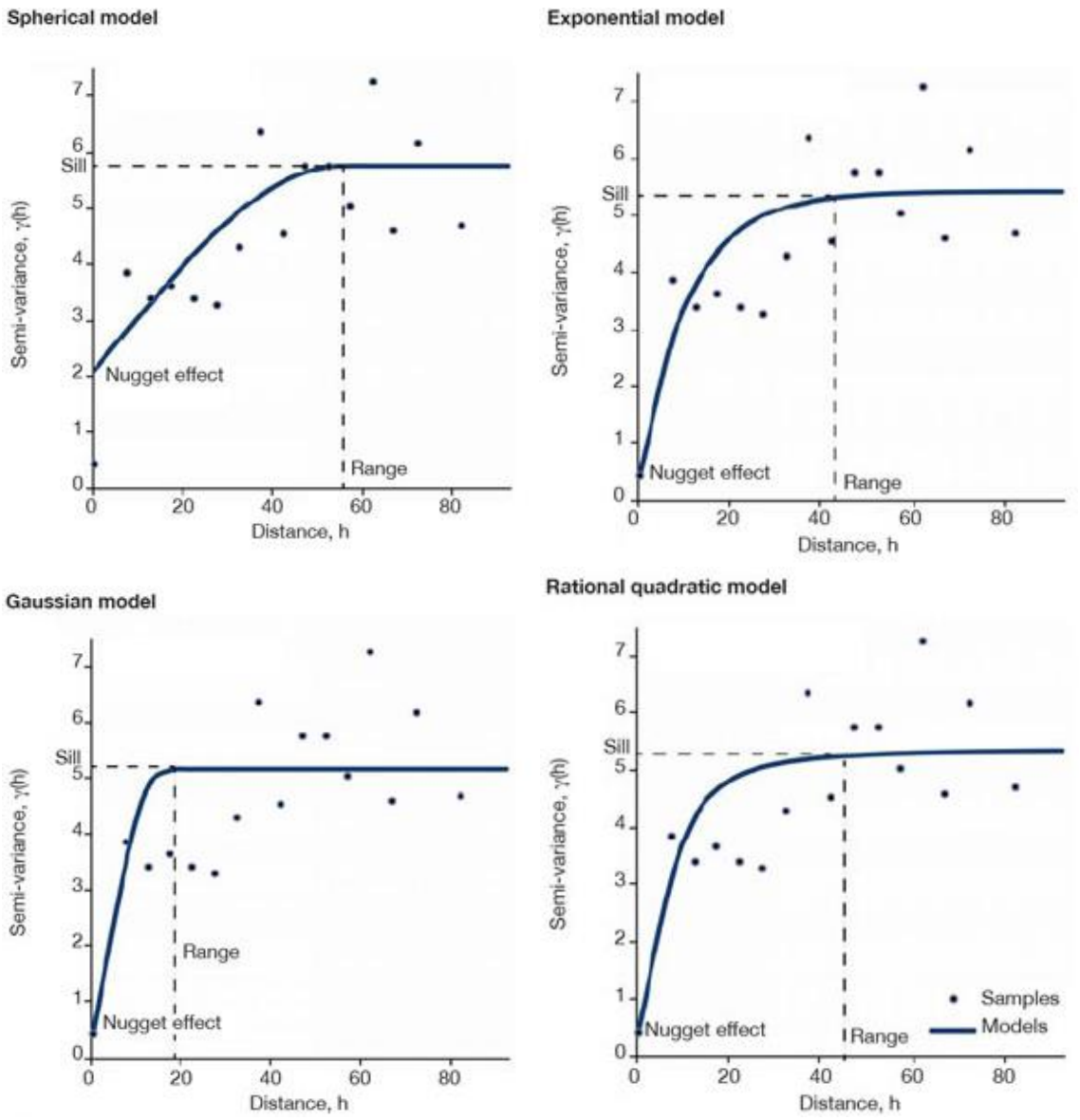

Figure 5.6: Experimental semi-variogram and coefficients of Kriging method (source: Goovaerts, 2000)

The kriging method encompasses several ways of integrating auxiliary variables:

– if the mean is not constant, but we can estimate the mean at locations in the domain of interest, then this locally varying mean can be used to inform estimation using Simple Kriging; this is referred to as Simple Kriging with a Locally varying mean (SKL) (Goovaerts, 2000);

– Kriging with External Drift (KED) assumes that the mean of the interest variable depends on auxiliary variables; the theory behind KED is in fact the same as the theory behind universal kriging, which also contains a non-constant mean. The drift is defined externally through certain auxiliary variables (Hengl et al., 2003);

– in order to better meet the assumptions of stationarity, linear regression may be carried out against secondary variables to remove first order trends. The residuals can be used to generate a new variogram and then ordinary kriging can be applied to these residuals. The resulting estimates can be added to the trend to give the estimated values. This technique has been termed Residual Kriging (RK) or Detrended Kriging (DK).

– the other type of kriging, Ordinary Cokriging (OCK), involves estimating the variable of interest by the weighted linear combination of its observations and the observations of the auxiliary variables. This technique requires the study of the spatial dependence between variables in addition to the study of simple spatial dependences.

A detailed presentation of geostatistical theories can be found in Cressie (1991); Goovaerts (1997); Chilès et al. (1999) and Webster et al. (2007).

Many previous studies in monthly or yearly steps have used only one theoretical model for each time step (Hevesi et al., 1992; Goovaerts, 2000; Boer et al., 2001; Todini, 2001;

Marqu´ınez et al., 2003; Lloyd, 2005). In this study, the semi-variogram models are fitted for monthly rainfall data of 112 year and daily rainfall data of nine years.

In order to do this, existing theoretical models, circular, spherical, exponential, gaussian and linear models are used. For each month, four semi-variogram models for all the 23 raingauge stations considered are generated. Semi-variance increased according to the separation distance, explaining that two rainfall data close to each other are more similar, and their squared difference are less significant than those that are farther apart.

The semi-variogram model is generated by observing the coefficient of determination (r^2) and residual sum of squared error (RSSE) values through the validation procedure with a trial-and-error approach for different lag sizes and lag intervals (Goovaerts 1997). The lag sizes and number of lags varied because of a general rule of thumb, in which the lag size times the number of lags should be less than one-half of the largest distance between data pairs (Johnston et al. 2010). The optimum model parameters (sill, nugget, and range) corresponding to the lowest RSSE and highest R^2 value are noted as 1.37, 0.0 and 0.58, respectively. Among the five semi-variogram models, e.g. circular, spherical, exponential, gaussian and linear, the exponential model estimated lowest RSSE and highest r^2 values. Therefore, exponential semi-variogram model is selected for monthly rainfall interpolation.

Higher error is obtained from interpolation by linear with linear drift universal Kriging. So this technique is not considered for further analysis. Interpolation using Linear with quadratic drift universal Kriging is also performed, but it estimates negative values in most of the cases. Monthly rainfall interpolation map of the study area from January to December generated by Ordinary Kriging method is shown in Figure 5.7. However, daily rainfall interpolation map of the study area by ordinary kriging is shown in Figure 5.8.

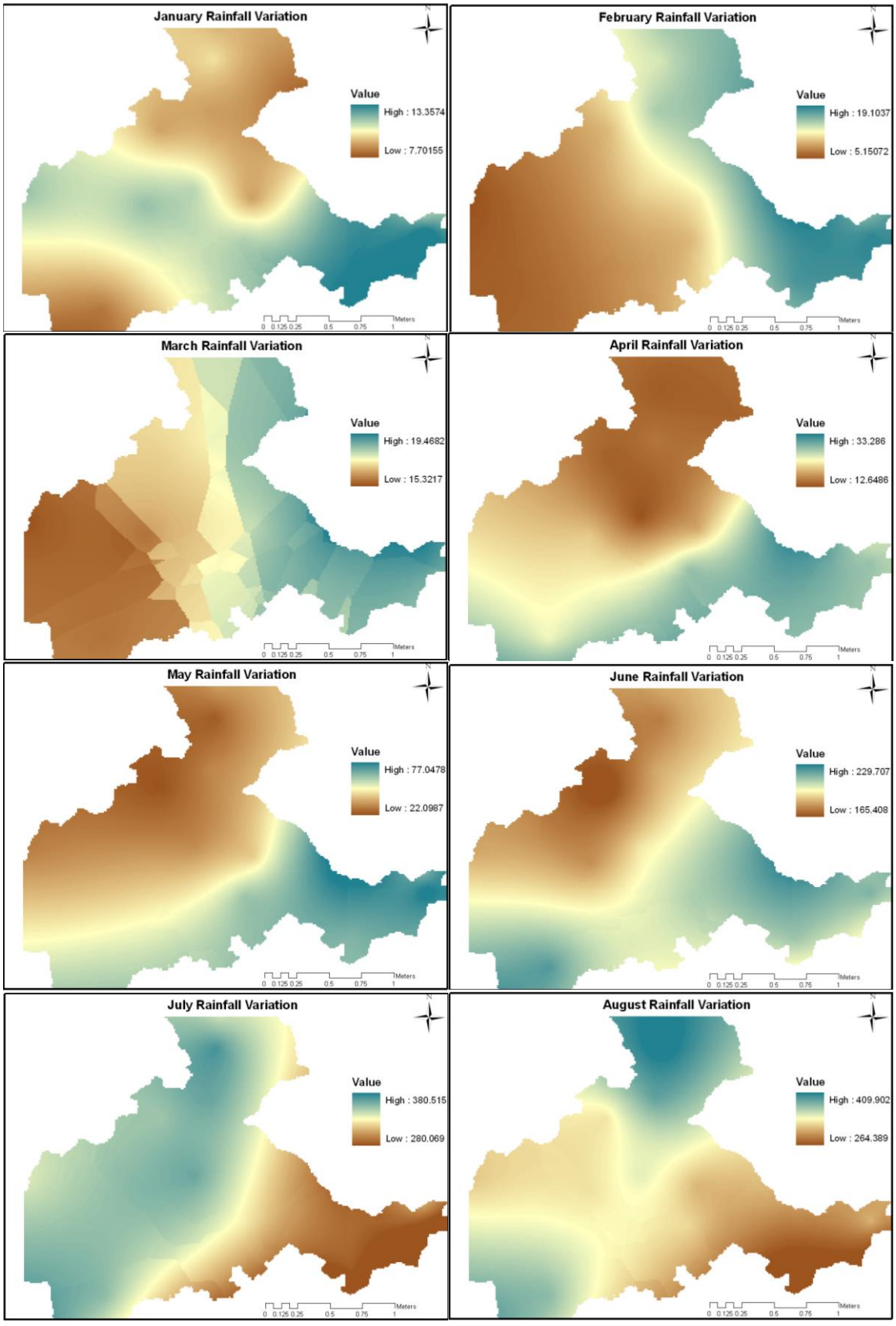
January Rainfall Variation
Value
High : 13.3574
Low : 7.70155
February Rainfall Variation
Value
High : 19.1037
Low : 5.15072
March Rainfall Variation
Value
High : 19.4682
Low : 15.3217
April Rainfall Variation
Value
High : 33.286
Low : 12.6486
May Rainfall Variation
Value
High : 77.0478
Low : 22.0987
June Rainfall Variation
Value
High : 229.707
Low : 165.408
July Rainfall Variation
Value
High : 380.515
Low : 280.069
August Rainfall Variation
Value
High : 409.902
Low : 264.389

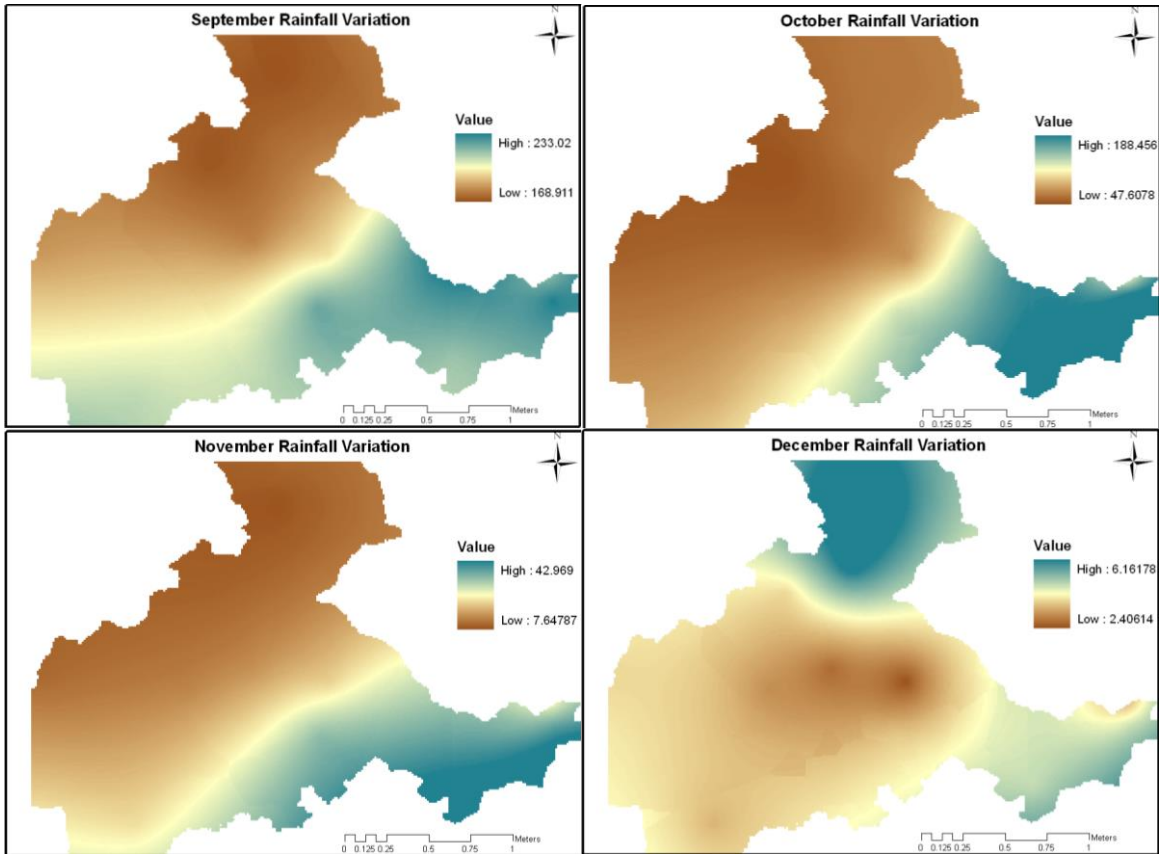

Figure 5.7: Monthly Rainfall Interpolation by Ordinary Kriging Method

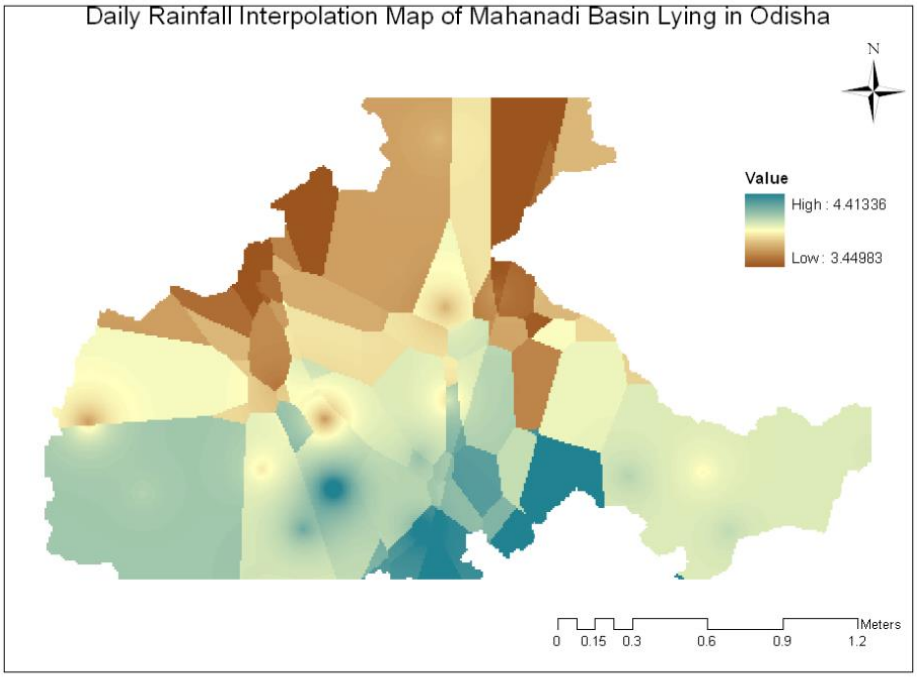

Figure 5.8: Daily Rainfall Interpolation by Ordinary Kriging Method

5.4 PERFORMANCE EVALUATION

The performance of the three interpolators e.g. IDW, Spline (regularized) and Ordinary Kriging (OK) methods are assessed and compared using cross validation. The idea consists of removing temporarily a rainfall observation randomly from the data set and "re-estimates" this value from remaining data using these three methods. The computed mean rainfall estimates were compared with the observed one and the error in the results have been estimated using mean error and root mean square error (RMSE) criteria. The governing equations are:

$$\text{Mean Error} = \frac{\sum_{i=1}^{n}(M_i - P_i)}{n} \tag{5.6}$$

$$\text{Root Mean Sqaure Error} = \sum_{i=1}^{n}\sqrt{\frac{(M_i - P_i)^2}{n}} \tag{5.7}$$

Table 5.1 indicates mean error and root mean square error of the three methods IDW, Spline (regularized) and Ordinary Kriging. Mean error should be close to zero and root mean square error should be as small as possible. As can be seen from the table, the Ordinary Kriging method provides best results with minimized error statistics.

Table 5.1: Performance Evaluation of IDW, Spline and Kriging Methods

Method	MEAN ERROR (mm/month)											
Month	**Jan**	**Feb**	**Mar**	**Apr**	**May**	**Jun**	**Jul**	**Aug**	**Sep**	**Oct**	**Nov**	**Dec**
Inverse Distance Weighting	0.15	0.33	0.15	-0.85	-1.43	-0.24	3.45	2.23	-0.62	-1.17	-1.02	-0.12
Regularized Spline	0.11	0.13	0.12	-0.32	-0.66	-0.66	2.58	-0.30	-0.18	-0.34	-0.56	-0.06
Ordinary Kriging	0.07	0.07	0.11	-0.20	-0.48	0.07	2.02	1.28	0.23	-0.07	-0.37	-0.11

Method	ROOT MEAN SQUARE ERROR (mm/month)											
Month	**Jan**	**Feb**	**Mar**	**Apr**	**May**	**Jun**	**Jul**	**Aug**	**Sep**	**Oct**	**Nov**	**Dec**
Inverse Distance Weighting	1.34	2.36	3.35	4.80	12.74	17.58	28.56	34.76	31.14	31.23	7.219	1.027
Regularized Spline	1.42	2.21	3.21	4.74	12.97	12.97	26.81	35.74	31.50	30.11	5.55	1.04
Ordinary Kriging	1.40	2.14	3.20	4.62	13.87	17.01	28.19	36.61	31.05	35.53	5.91	1.09

5.5 CONCLUSION

Both deterministic and geostatistical rainfall interpolation methods such as Inverse Distance Weighting, Spline and Kriging were used with monthly and daily rainfall data and the Ordinary Kriging method was selected for interpolation of monthly and daily rainfall over each subbasin as this method provided best results with minimized error statistics.

CHAPTER 6

DEVELOPMENT OF CURVE NUMBERS FOR DAILY AND MONTHLY RUNOFF SIMULATION AND PREDICTION

6.1 INTRODUCTION

There are numerous methods available for rainfall generated runoff modeling. Soil Conservation Services Curve Number (SCS-CN) technique is one of the oldest and simplest method for rainfall generated runoff moelling. Many modifications have been done in SCS-CN methods since its inception. Many developed models based on SCS-CN are in use and being referred by different researchers globally. In the present work, original SCS-CN, Mishra-Singh (MS) model (2002), Michel model (2005), and Sahu model (2007), being used commonly on the basis of SCS-CN concepts, with some modifications are used. Besides, modified and proposed empirical models, such as frequency distribution model based on probability of exceedance concept (FDM-PE), and SCS-CN method based on remote sensing and GIS data as inputs and median of ordered data for all the three antecedent moisture conditions (AMCs: AMC1, AMC2 and AMC3) are used in the present work (MM-SCS). Moreover, Artificial Neural Network based on Multi Layer Perceptron (ANN-MLP) has been used to generate a non-linear model function to test the applicability for simulating and predicting daily and monthly runoff data. Evaluation of each model has been done using different error statistics and correlation coefficient.

6.2 DESCRIPTION OF MODELS

6.2.1 SCS-CN Model: NEH

The SCS-CN method is developed in 1954 by the USDA Soil Conservation Service (Rallison 1980), and is described in the Soil Conservation Service (SCS) National Engineering

Handbook Section 4: Hydrology (NEH-4) (SCS 1985) (Ponce and Hawkins, 1996). The SCS-CN method is based on the water balance equation and two fundamental hypotheses. The first hypothesis states that the ratio of the actual amount of direct runoff to the maximum potential runoff is equal to the ratio of the amount of actual infiltration to the amount of the potential maximum retention. The second hypothesis states that the amount of initial abstraction is some fraction of the potential maximum retention.The water balance equation and the two hypotheses can be expressed mathematically, respectively, as follows.

$$P = Ia + F + Q \tag{6.1}$$

$$Q/(P - Ia) = F/S \tag{6.2}$$

$$Ia = \lambda S \tag{6.3}$$

where *P* is total precipitation, Ia is initial abstraction, *F is* cumulative infiltration excluding Ia, *Q is* direct runoff, *S* potential maximum retention or infiltration, and λ initial abstraction coefficient accounting for surface storage, interception, and infiltration before runoff begins. Combining Equations (6.1) and (6.2) the popular form of the existing SCS-CN method for direct runoff can be written as follows.

$$Q = (P - Ia)^2/(P - Ia + S) \tag{6.4}$$

As the method is practiced today, Q can be computed using equation (6.4) with the CN based on the land use and hydrologic soil group, and rainfall depth. Equation (6.4) is valid for $P > Ia$ and $Q = 0$ otherwise. With the initial abstraction included in equation (6.4), the actual retention $(P - Q)$ asymptotically approaches a constant value of $(S + Ia)$ as the rainfall increases unbounded.

The parameter λ can take any value ranging from 0 to ∞. But in the existing SCS-CN method, λ is assumed as equal to 0.2 for usual practical applications. Equation (6.4) after putting λ=0.2 contains only one unknown parameter, S, which ranges between 0 to ∞. For

convenience in practical applications, S is defined in terms of a dimensionless parameter, CN (Curve Number), which varies in a more restricted range 0-100. Parameter S (mm) in terms of CN can be expressed as

$$S = (25400/CN) - 254 \quad (6.5)$$

The parameter CN = 100 represents a condition of zero potential retention (S = 0), that is an impermeable watershed. Conversely, CN = 0 a theoretical upper bound represents to the potential retention ($S = \infty$), which is an infinitely abstracting watershed.

Many researchers attempted the practical design values validated by experience lying in a realistic range of 40 to 98 (Van-Mullem 1989). All the factors responsible for generation of runoff from rainfall in the watershed actually govern the curve number including hydro-meteorological and watershed characteristics. The major watershed characteristics such as soil type, land use/treatment classes, hydrologic soil group, hydrologic condition, and antecedent moisture condition significantly affect CN (Mishra and Singh 2003).

Of late, easy availability of spatially distributed digital database and use of GIS have accelerated the use of distributed curve numbers for runoff estimation. Composite (or area weighted) CN is estimated by compositing the area-weighted average CNs calculated for the entire watershed. To this end, satellite data of land use and soil maps obtained from various sources are overlaid to delineate polygons with unique land use and hydrologic soil group (HSG) combinations for determination of CN for each grid and then computation of the area-weighted average CN is as follows

$$CN = \frac{(CN_1 * A_1) + (CN_2 * A_2) + \cdots + (CN_n * A_n)}{A} \quad (6.6)$$

where A_1, A_2, … , A_n represent areas of polygons having CN value CN_1,CN_2, … ,CN_n, respectively; and A is the area of each grid = $A_1 + A_2 + \cdots + A_n$.

A square grid of area 24 X 24 square km is generated over the study area. The land use/land cover map used in the present study has been extracted for spatial resolution of 1 km. The soil map used in the present study has been extracted from the FAO/UNESCO Digital Soil Map of the World (DSMW) and has a spatial resolution of 5*5 arc minutes. Soil textures are classified by the percentage of sand, silt, and clay present in a soil. In the present study, according to the USDA soil textural classification, the six dominant soils found in the study area are classified into sandy loam, sandy clay loam and clay soil textures. Further these three soil textures are classified into A, C, and D hydrologic soil groups (HSGs). In the study area, no soil texture with HSG of B is found. HSG indicates the minimum rate of infiltration obtained for bare soil after prolonged wetting. Group A soils have low runoff potential and high infiltration rates even when thoroughly wetted. They consist chiefly of deep, well to excessively well drained sand or gravel and have a high rate of water transmission (greater than 0.30 in/hr). Group C soils have low infiltration rates when thoroughly wetted and consist chiefly of soils with a layer that impedes downward movement of water and soils with moderately fine to fine texture. These soils have a low rate of water transmission (0.05-0.15 in/hr). Group D soils have high runoff potential. They have very low infiltration rates when thoroughly wetted and consist chiefly of clay soils with a high swelling potential, soils with a permanent high water table, soils with a clay pan or clay layer at or near the surface, and shallow soils over nearly impervious material. These soils have a very low rate of water transmission (0-0.05 in/hr).

The original SCS-CN method computes the direct runoff by considering only the available rainfall on the current day without taking care of the effect of the moisture available prior to the storm. On the other hand, the curve numbers are sensitive to antecedent conditions (Ponce 1989). The curve number is usually represented for average antecedent moisture condition (AMC)-CN_{II} and for direct-runoff computation it is varied, with AMC generally described

using 5-day antecedent rainfall (P_5). For the first five days beginning from the first day of simulation, CN is taken as the curve number valid for AMC II (normal condition). As the time (day) advances, CN varies with AMC levels (Hawkins 1978; Mishra et al. 1998) dependent on the amount of antecedent rainfall (ANTRF). Antecedent rainfall is determined as follows

$$ANTRF_t = P_{t-1} + P_{t-2} + P_{t-3} + P_{t-4} + P_{t-5} \quad (6.7)$$

where t=current day, and P=rainfall of the respective day.

The SCS-CN method defines the antecedent moisture condition as an index of basin wetness. In particular AMC II is defined as "the average condition". However, determination of antecedent soil moisture content and classification into the antecedent moisture classes AMC I, AMC II and AMC III, representing dry, average and wet conditions, is an essential matter for the application of the SCS curve number procedure that is without a clear answer yet. The definition of antecedent moisture condition AMC II is the basis from which adjustments to the corresponding curve numbers for dry soils (AMC I) and wet soils (AMC III) are made.

AMC II (average or normal condition) is taken as the basis from which adjustments to daily curve numbers are made so that they correspond to AMC I or AMC III (Hjelmfelt 1991). The appropriate moisture group AMC I, AMC II and AMC III is based on a five-day antecedent rainfall amount and season category (dormant and growing seasons) (NEH-4, 1964). Different AMC class limits are provided for the dormant and growing seasons based on five-day antecedent precipitation, i.e., ANTRF (Mishra et al. 1998; Ponce 1989; Hawkins et al. 1985). Generally, June 1- October 31 is taken as the dormant season, and the remaining period of the year (November 1-May 31) as the growing season. Variation in curve numbers based on the total rainfall in the five days preceding the storm under consideration (Woodward and Croshney 1992), CN_t of t_{th} day which corresponds to CN_{II} is converted to CN_I or CN_{III}. There are many AMC-dependent CN-conversion formulas such as those of

Sobhani (1975), Chow et al. (1988), Hawkins et al. (1985), and Neitsch et al. (2002) are available in the literature. Generally, the Hawkins et al. (1985) AMC-dependent CN-conversion formulae is considered to convert the CN_{II} (normal condition) to CN_{I} (dry condition) or to CN_{III} (wet condition), depending on the magnitude of the 5-day antecedent rainfall amount. The CN-conversion formulae are expressed as

$$CN_{I} = CN_{II}/(2.281 - 0.01281CN_{II}) \quad (6.8)$$

$$CN_{III} = CN_{II}/(0.427 + 0.00573CN_{II}) \quad (6.9)$$

It is worth noting that the initial value of CN at the start of simulation, an optimized value, corresponds to AMC II. These equations are applicable in the range $55 \leq CN \leq 95$, which encompasses most estimated or experienced curve numbers (Ponce and Hawkins, 1996).

The main advantages (Mishra and Singh 2003a; Ponce and Hawkins 1996) of the SCS-CN method are it is a simple conceptual method for predicting direct surface runoff from a storm rainfall amount, and is well supported by empirical data and wide experience, it is easy to apply and useful for ungauged watersheds, the method relies on only one parameter CN, and the parameter CN is a function of the watershed characteristics and, hence, the method exhibits responsiveness to major runoff- producing watershed characteristics. However, the method has some limitations also which are: the three AMC levels used with the SCS-CN method permit unreasonable sudden jumps in CN, and hence corresponding sudden jumps in computed runoff is possible, there is a lack of clear guidance on how to vary antecedent moisture condition, there is no explicit dependency of initial abstraction on the antecedent moisture, the method doesn't contain any expression for time and ignores the impact of rainfall intensity and its temporal distribution and it is applicable to only small watersheds. Ponce and Hawkins (1996), for example, cautioned against its use to watersheds larger than 250 sq. km. Besides being fairly accurate in runoff predictions, the versatility of the SCS-CN method lies in the fact that it is simple, easy to understand and apply, stable, and capable of

accounting for several watershed runoff producing characteristics, such as soil type, land cover and practice, hydrologic condition, and antecedent moisture condition (AMC) (Ponce and Hawkins 1996; Mishra and Singh 2003b).

It is observed that variability of CN is also due to the effect of spatial variability of storm and watershed properties, temporal variability of storm, that is, storm intensity, quantity of measured data, that is, P-Q sets and antecedent rainfall and associated soil moisture (Ponce and Hawkins, 1996). The one to one relationship between CN and S renders the latter intrinsically related to antecedent moisture. Thus, potential retention is a measure of the ability of a given site to abstract and retain storm rainfall, provided the level of antecedent moisture has been factored into the analysis. In other words, potential retention and its corresponding curve numbers are intended to reflect not only the capacity of a given site to abstract and retain storm rainfall, but also (1) the recent history of antecedent rainfall or lack of it, which may have caused the soil moisture to depart from an average level (2) seasonal variation in runoff properties and (3) unusual storm conditions (Ponce and Hawkins, 1996).

If an event rainfall depth and the CN of a watershed are known, the runoff volume can easily be determined using equation (6.4) and (6.5). The potential maximum retention (S) for each of the maximum annual storm volume Q, and the rainfall volume P can be computed using the following expression too.

$$S = 5(P + 2Q - \sqrt{(4Q^2 - 5PQ)}) \quad (6.10)$$

This equation is an algebraic rearrangement of equation (6.4) with λ=0.2. For gauged watersheds where both rainfall and runoff volumes are known the Curve Number values can be determined using equations (6.5) and (6.10).

Indirect substitution of λ as 0.2 into Equation (6.4) yields the S-values for different P–Q sets. These values are mapped onto the CN-values using Equation (6.5). Geographic and other differences may dictate that the initial abstraction ratio λ be relaxed to the range validated by

local experience, say $0.0 \leq \lambda \leq 0.3$. For λ value other than 0.2, its variation can be expressed using the following relation, derived from the combination of Equation (6.4) and Equation (6.5).

$$S = P\left([2\lambda + C(1-\lambda)] - \sqrt{C[C(1-\lambda)^2 + 4\lambda]/2\lambda^2}\right) \quad (6.11)$$

where C is runoff factor, which is equal to Q/P.

6.2.2 Mishra-Singh (MS) Model

Mishra and Singh (1999) modified the popular form of the existing SCS-CN method (equation 6.4) for direct runoff and proposed its general form as:

$$Q = (P - I_a)^2/[S + a(P - I_a)] \quad (6.12)$$

where a is considered equal to 0.5.

Using the C=Sr concept, where C is the runoff coefficient (Q/(P-Ia)) and Sr is the degree of saturation, Mishra and Singh (2002) modified the equation of direct runoff for antecedent moisture M as:

$$Q = \frac{(P-I_a)(P-I_a+M)}{(P-I_a+M+S)} \quad (6.13)$$

where M is antecedent moisture (mm) and is computed as

$$M = 0.5[-(1+\lambda)S + \sqrt{(1-\lambda)^2S^2 + 4P_5S}] \quad (6.14)$$

Here, I_a is the same as in Equation (6.3) and P_5 denotes the amount of antecedent 5-day rainfall.

The combination of Equations (6.3), (6.13) and (6.14) is designated as the Mishra–Singh (MS) model. This method advantageously obviates sudden jumps in CNs and hence computes runoff through incorporation of the expression of M replacing the three AMCs. However, it does not show an explicit dependency of I_a on M. Further, in this method, S is

optimized as a parameter, which is, in fact, a varying quantity depending on M for a given watershed. Hence, it is not clear as to which moisture level/condition the optimized S would correspond to. Again Mishra et al. (2004) modified the existing SCS-CN method, which is based on the Soil Conservation Service Curve Number (SCS-CN) methodology but incorporates the antecedent moisture in direct surface runoff computations. They used the C=Sr concept, where C is the runoff coefficient (Q/(P − Ia)) and Sr= degree of saturation and modified the above Equation (6.13) for antecedent moisture M as

$$\frac{Q}{(P-I_a)} = \frac{(F+M)}{(S+M)} \tag{6.15}$$

By substituting Equation (6.2) into Equation (6.15) direct surface runoff becomes

$$Q = \frac{(P-Ia)(P-Ia+M)}{(P-Ia+M+S)} \tag{6.16}$$

According to Mishra and Singh (2004), by assuming λ equal to 0.2, M can be computed as

$$M = (P_5 - 0.2 * S_I)\, S_I / (P_5 + 0.8 * S_I) \tag{6.17}$$

where P_5 is the antecedent 5-day precipitation amount, and S_I is the potential maximum retention corresponding to AMC I, by assuming the watershed to be dry 5 days before the onset of the rain storm. Hence by taking $P_5 = 0$ and as $S_I = S + M$, Equation (6.10) becomes

$$M = 0.5[-1.2 * S + \sqrt{(0.64 * S^2 + 4 * P_5 * S)}] \tag{6.18}$$

In the above equation + sign before the square root is retained for M to be greater than or equalto zero. This equation can be generalized by replacing 0.2 by λ, and M can be expressed as

$$M = 0.5[-(1 + \lambda)S + \sqrt{(1-\lambda)^2 S^2 + 4 * P_5 * S)}] \tag{6.19}$$

The above equation forms the modified version of the Mishra–Singh model. Here, $P_5 \geq \lambda S$.

6.2.3 Michel Model

Initially according to Michel et al. (2005) the soil moisture accounting (SMA) procedure is based on the notion that higher the moisture store level, higher the fraction of rainfall that is converted into runoff. If the moisture store level is full, all the rainfall will become runoff. The following is the SMA equation

$$V = V_0 + P - Q \tag{6.20}$$

where V_0= soil moisture store level at the beginning of the rainfall event (mm), P = accumulated rainfall at time t along a storm (mm), Q = accumulated runoff at time t along a storm (mm), and V =soil moisture store level at time t, i.e. when the accumulated rainfall is equal to P (mm).They incorporated a new parameter 'S_a' by letting Sa be a set fraction of S (they recommended S_a= S/3). They also replaced V_0 by a fraction of S and finally suggested a one-parameter model to compute the surface runoff for the three AMCs.

Michel et al. (2005) pointed out inconsistencies in the original SCS-CN method, arising partly from the confusion between the intrinsic parameter and the initial condition and partly from the incorrect use of the SMA procedure. They described (V_0+I_a) as an intrinsic parameter (S_a) of the soil moisture model for computation of runoff as follows

If $V_0 \leq S_a - P$, then $Q = 0$. (6.21)

If $S_a - P < V_0 < S_a$, then $Q = \frac{(P+V_0-S_a)^2}{(P+V_0-S_a+S)}$. (6.22)

If $S_a < V_0 < S_a + S$, then $Q = P\left[1 - \frac{(S_a+S-V_0)^2}{S^2+(S_a+S-V_0)P}\right]$. (6.23)

Equations (6.21)–(6.23) constitute the Michel et al. (Michel) model. Despite the improvement over the popular form of SCS-CN method from the SMA view-point, the Michel model lacks an expression for the initial soil moisture store level (V_0).

Based on soil moisture accounting procedure (SMA), Michel et al. (2005) introduced a simplified one-parameter SCS-CN model for runoff computations for a given storm rainfall

event for the three AMCs. The simplified one-parameter SCS-CN procedure can be expressed as

For AMC I (V_0 =0.33S), $Q = P\frac{P}{(S+P)}$ (6.24)

For AMC II (V_0 =0.61S), $Q = P\frac{(0.48S+0.72P)}{(S+0.72P)}$ (6.25)

For AMC III (V_0 =0.87S), $Q = P\frac{(0.79S+0.46P)}{(S+0.46P)}$ (6.26)

6.2.4 Sahu Model

The antecedent or initial soil moisture (V_0) depends not only on P_5 but also on S. The dependency on S is based on the fact that the watershed with larger retention capacity S must retain higher moisture compared to the watershed with lesser S for a given P_5. An expression for initial soil moisture store level (V_0) is taken as AMC-dependent, which leads to a quantum jump in V_0 and, in turn, runoff computations. Therefore an expression for V_0 is suggested by Sahu et al. (2007) for continuous simulation.

For practical applications, Sahu et al. (2007) developed a one-parameter model, described by the following set of equations

If $P_5 \leq 0.1S$ then, $V_0 = 0.4P_5$ (6.27)

If $P_5 > 0.1S$ then, $V_0 = S[\frac{0.44P_5 - 0.004S}{P_5 + 0.9S}]$ (6.28)

From known V_0, Q can be computed as follows

If $V_0 + P \leq 0.1S$, then $Q = 0$. (6.29)

If $0.1S \leq V_0 + P \leq 0.1S + P$, then $Q = \frac{(P+V_0-0.1S)^2}{(P+V_0+0.9S)}$. (6.30)

If $0.1S \leq V_0 \leq 1.1S$, then $Q = P[1 - \frac{(1.1S-V_0)^2}{S^2+(1.1S-V_0)P}]$. (6.31)

6.2.5 Frequency Distribution based Probability of Exceedance (FDM-PE) Model

A prevailing application of the Curve Number method is to determine a given return period runoff for the same return period rainfall. This amounts to transforming a rainfall frequency distribution into a runoff frequency distribution (Hjelmfelt 1980). This leads to"frequency matching", which sorts P and Q depths separately and re-aligns them by common rank order, creating a new set of P, Q pairs. These P,Q pairs have equal sampled return periods and are called "ordered" data, with runoff Q not necessarily matched with the original rainfall P, thus obtaining a probabilistic-CN by means of equation (6.5). This is contrasted with "natural" data (P, Q events as observed naturally) (Hawkins et al. 1990, Van Mullem et al. 2002). A frequency distribution model applicable for all the cases (rainfall, runoff and curve number) has been developed to estimate probabilistic curve number (PCN).

6.2.6 Modified Median based- SCS (MM-SCS) Model

As explained in the original SCS-CN method, if an event rainfall depth and the CN of a watershed are known, the runoff volume can easily be determined using equation (6.4) and (6.5). The potential maximum retention (S) for each of the maximum annual storm volume Q, and the rainfall volume P can be computed using equation (6.10).

In the present case, the median CN from the sorted (in descending order) CN series is considered as AMC II (normal condition). Again, the median CNs of the sorted CN series corresponding to lower half and higher half are considered as AMC I (dry condition) and AMC III (wet condition) respectively. In fact, no equations and manipulations are required in this method to obtain AMC I and AMC III. The method is very simple and straight forward. Of, course, for un-gauged catchments, the method may not be applicable directly and CN values for AMC I, AMC II and AMC III may not be estimated due to non-availability of observed rainfall and runoff estimates. However, it can be developed using regional modeling and analysis.

6.2.7 Artificial Neural Network based Multi Layer Perceptron (ANN-MLP) Model

The ANN, as the name implies, employs the model construction of a neural network, a very powerful computational algorithm, which is used to simulate complex nonlinear relationships, especially in situations where the explicit form of the relation between the variables involved is unknown (Gallant 1993; Smith 1994). ANN is thus defined according to its model inputs and its architecture: the number of layers, the number of nodes in each layer, the activation function in each layer, and the manner in which the layers are interconnected.

However, one of the most unresolved questions in modeling of the rainfall-runoff process when applying ANNs is what architecture should be used to map the process effectively. The selection requires choosing an appropriate input vector, besides the hidden units and weights. Unlike the physically based models, the sets of variables that influence the system are not known a priori. Therefore, the selection of an appropriate input vector that will allow an ANN to map to the desired output vector successfully is not a trivial task. In most of the applications that are reported this has been done by a trial- and error-procedure (Fernando and Jayawardena, 1998). Sudheer et al. (2002) outlined a procedure for selecting an appropriate input vector in ANN rainfall-runoff models, based on statistical pre-processing of the data set. The proposed methodology has been illustrated by presenting an application of the procedure to an Indian River basin. The results reported by some researchers have also been analyzed to check the effectiveness of the proposed algorithm and then they concluded that their proposed algorithm would easily lead to a more compact network, thus avoiding a long trial- and-error procedure.

The architecture of a feed forward ANN can have many layers where a layer represents a set of parallel neurons. The basic structure of ANN usually consists of three layers: the input layer, where the data are introduced to the network; the hidden layer or layers, where data are processed; and the output layer, where the results of given outputs are produced. The neurons

in the layers are interconnected by strength called weights. The incoming data are processed by nonlinear functions at hidden and output layers to get the output. The commonly used nonlinear function is log sigmoid function (ASCE 2000a, b).

At present, the most common ANN architecture and algorithms being applied are multilayer feed forward, Hopfield networks, radial basis function network, recurrent network, self organization feature maps, and counter propagation networks. However, the multilayer feed forward networks are the most commonly used for hydrological applications (Dawson and Wilby 2001). In hydrology, multiple-layer perceptron (MLP) networks, a single hidden layer with a sigmoid transfer function and an output layer with a linear transfer function, are preferred for their simplicity and effectiveness (Anctil and Rat 2005; Hsu et al. 1995; Sivakumar et al. 2002). The MLP model architecture is often applied with the Levenberg-Marquardt back propagation algorithm, a second-order nonlinear optimization technique which is usually faster and more reliable than other back propagation variants (Demuth et al. 1992). The feed-forward operation computes an output for each input vector and then compares it with the actual value (Figure 6.1). The total error is calculated for all training sets

$$E = \sum_{m=1}^{M} E_m = \sum_{m=1}^{M} \sum_{k=1}^{N} (T_{mk} - O_{mk})^2 \quad (6.32)$$

Where E_m= error for the mthinput vector; M = number of input vectors; N = number of outputs; and O_{mk}, T_{mk}= observed and predicted values, respectively.

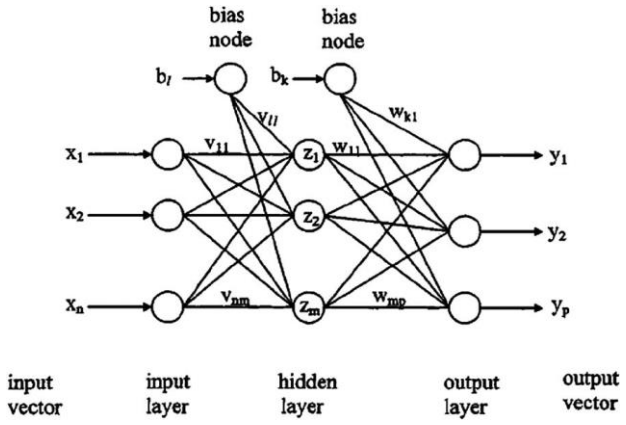

Figure 6.1: Standard FFNN with one hidden layer

6.2.7.1 The Architecture

The MLP architecture, a feed forward-type NN, is selected in this study because it usually has good model performance, and also because it is the most frequently used configuration in hydrology. The ANN networks consisting of an input layer, one single hidden layer composed of 3-12 nodes, and one output layer consisting of 1 node denoting the predicted runoff. Each ANN model has been tested on a trial-and-error basis for the optimum number of neurons in the hidden layer.

In ANN models, one major point is to determine the number of nodes in the input layer that provide the best calibrating results. The ANN model for the prediction of runoff is normally developed by using the same day rainfall, antecedent rainfall and antecedent runoff values of same stations as input vector (Cobaner et al. 2009). Determining the number of antecedent rainfall, and runoff values involves finding the lags of rainfall, and runoff values that have significant influence on the predicted runoff. These influencing values corresponding to the different lags can be very well-established through the statistical analysis of the data series. The input vector is selected generally by the trial-and-error method. The simple correlation between the dependent and independent variables helps in selecting the significant input vector to the model. The correlation analysis helps to find out the possible input variable for the modeling, but it does not give the exact lag values (Senthil Kumar et al., 2012). Generally the trial-and-error method is adopted to find out the significant lag values of the input variable. Sudheer et al. (2002) presented a statistical procedure that avoids the trial-and error procedure. They reported that the statistical parameters, such as autocorrelation function (ACF), partial autocorrelation function (PACF), and cross-correlation function (CCF), could be used to find out the significant lag values of input variables.

In this present work, an approach proposed by Sudheer et al. (2002) has been used. With respect to the ACF, PACF and CCF plots, the combinations containing different numbers of

input values of runoff and rainfall are considered in the input layer to predict the unique runoff value at the future time step in the output layer of the ANN model. Figure 6.2 and 6.3 shows PACF and CCF plots of daily and monthly runoff series respectively of Sundargarh sub-basin. Similar plots of other sub-basins are shown in Appendix III. A qualitative examination of the cross-correlation curves between the rainfall and runoff series revealed that antecedent rainfall heavily influences the runoff at a certain time. However, the rainfalls of consecutive days are also highly correlated and the rainfall occurred in recent past are required to be used as input to the ANN models. The neurons in the input layer of the ANN models represented different combinations of the various physical variables considered, and are chosen based on the correlation coefficients between rainfall (at different time steps) and the runoff data(Figure 6.2 and Figure 6.3).

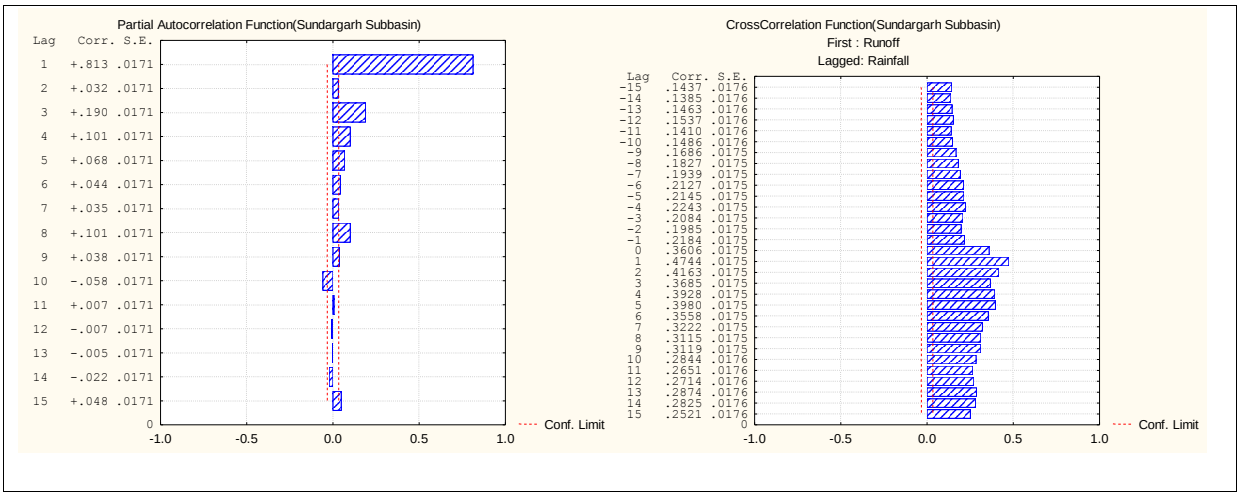

Figure 6.2 PACF and CCF Plots of Daily Runoff data of Sundargarh Sub-basin

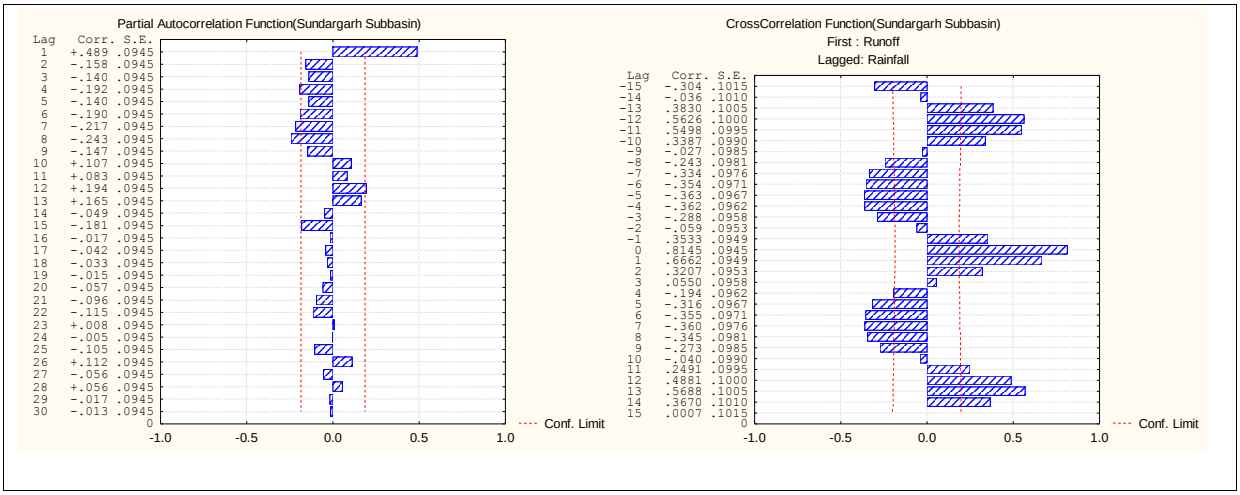

Figure 6.3 PACF and CCF Plots of Monthly Runoff data of Sundargarh Sub-basin

Similarly, an autocorrelation function (ACF) and partial autocorrelation function (PACF) suggests the influencing antecedent discharge patterns in the flow at a given time. The ACF and PACF with 95% confidence levels are used in diagnosing the order of the autoregressive process and are employed in ANN modeling too. The variables that did not have a significant effect on the performance of the model are trimmed off from the input vector, resulting in a more compact network.

6.2.7.2 Training of Daily and Monthly data using ANN Model

ANN training is the process of adjusting the weights and biases in order for the network to produce the desired output in response to every input pattern in a predetermined set of training patterns. Back-propagation which is a supervised training algorithm is by far the most commonly used method for training MLPs. It is popularized by Rumelhart et al. (1986), although earlier work had been done by Werbos (1974), Parker (1985), and LeCun (1985). Mathematically training a network means minimizing the error of an error function such as the sum of squares function. The process of calibrating (training and testing) the ANN inputs and outputs is carried out with the BP algorithm (Masters 1993; Haykin 1999). The weights are different in the hidden and output layers and their values can be changed during the

process of network training through an assigned specific error-correction learning rule. Once the training is done, testing and the validation stage began by using the optimum values found for the number of neurons in the input layer and hidden layer.

The whole rainfall and runoff data set are divided into three sets, 70% and 15% of the data are used to train and test the network, the rest 15% of the data are used to validate the network performance.

To prevent the networks from overtraining and to enhance the generalization capability of networks, the training termination criteria used testing techniques to stop the training when the testing error began to increase. The number of maximum training epochs is set to 1,000 and the training is terminated when there is no further improvement in testing after 100 epochs. The daily data from January 2000 to April 2009 are considered for the training, testing and validation of the model and data of each part are selected randomly. The ANN models are trained by using the automated neural networks function of "Statistica" software, developed by "Statsoft". The models developed for daily and monthly data of the five sub-basins are presented in Tables 6.1 and 6.2 respectively.

Table 6.1: ANN-MLP for Daily Rainfall generated runoff modeling

Subbasin	Input	Network Architecture
Kantamal	$Runoff_{t-1}$, $Runoff_{t-2}$,$Runoff_{t-3}$, $Rainfall_t$,$Rainfall_{t-1}$, $Rainfall_{t-2}$	6-10-1
Kesinga	$Runoff_{t-1}$, $Rainfall_t$,$Rainfall_{t-1}$	3-5-1
Tikarpada	$Runoff_{t-1}$, $Rainfall_t$,$Rainfall_{t-1}$, $Rainfall_{t-2}$, $Rainfall_{t-3}$, $Rainfall_{t-4}$, $Rainfall_{t-5}$	7-12-1
Naraj	$Runoff_{t-1}$, $Runoff_{t-2}$,$Runoff_{t-3}$, $Runoff_{t-4}$, $Rainfall_t$,$Rainfall_{t-1}$, $Rainfall_{t-2}$, $Rainfall_{t-3}$	8-9-1
Salebhatta	$Runoff_{t-1}$, $Runoff_{t-2}$,$Runoff_{t-3}$, $Rainfall_t$,	4-5-1
Sundargarh	$Runoff_{t-1}$, $Rainfall_t$,$Rainfall_{t-1}$	3-3-1

Table 6.2: ANN-MLP for Monthly Rainfall generated runoff modeling

Subbasin	Input	Network Architecture
Kantamal	$Runoff_{t-1}$, $Runoff_{t-2}$, $Rainfall_t$,$Rainfall_{t-1}$	4-9-1
Kesinga	$Runoff_{t-1}$, $Runoff_{t-2}$, $Rainfall_t$,$Rainfall_{t-1}$	4-10-1
Tikarpada	$Runoff_{t-1}$, $Runoff_{t-2}$, $Runoff_{t-11}$,$Rainfall_t$,$Rainfall_{t-1}$	5-9-1
Naraj	$Runoff_{t-1}$, $Runoff_{t-2}$, $Rainfall_t$,$Rainfall_{t-1}$	4-5-1
Salebhatta	$Runoff_{t-1}$, $Rainfall_t$,$Rainfall_{t-1}$	3-3-1
Sundargarh	$Runoff_{t-1}$, $Runoff_{t-12}$,$Rainfall_t$,$Rainfall_{t-1}$	4-5-1

6.3 EVALUATION OF DIFFERENT MODELS

6.3.1 SCS-CN Model: NEH

Figures 6.4 and 6.5 represent the land use/land cover map and the soil map of the study area. And tables 6.3 and 6.4 show the land use and land cover classification statistics and the soil classification statistics of the study area.

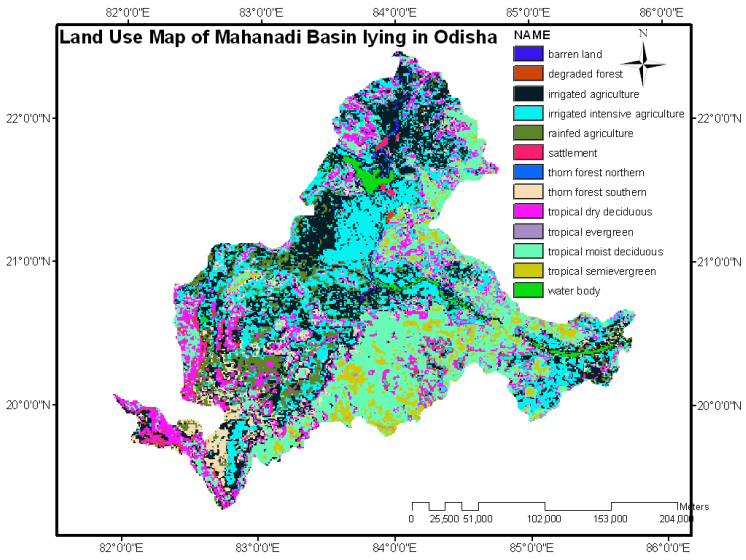

Figure 6.4: Land Use/Land Cover Map of Study Area

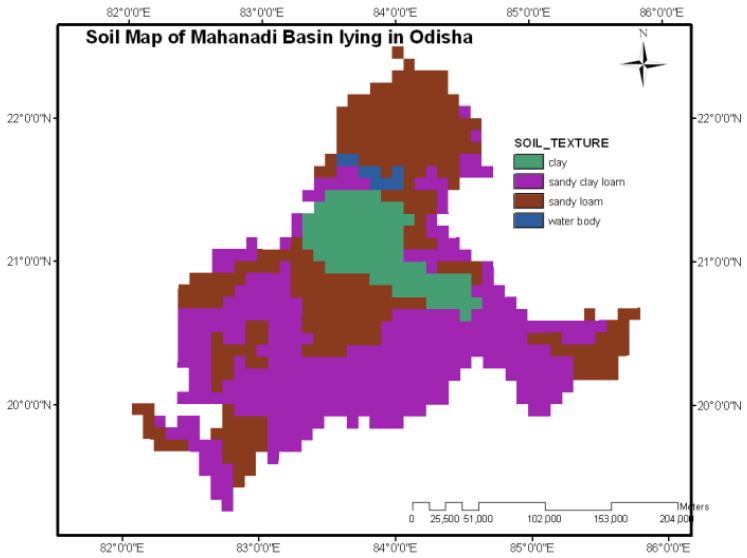

Figure 6.5: Soil Map of Study Area

Table 6.3: Land Use/Land Cover Classification Statistics of Study Area

LU/LC Class	TEF	TSEF	TMDF	TDDF	DF	TF	IIA	IA	RA	WB	BL	S
Percentage	0.53	4.61	22.84	11.47	1.54	5.55	23.16	21.80	6.62	1.18	0.40	0.32

Table 6.4: Soil Classification Statistics of Study Area

Soil	Orthic Acrisols	Lithosols	Ferric Luvisols	Chromic Luvisols	Eutric Nitosols	Chromic Vertisols	Water Bodies
Texture Class	Sandy Clay Loam	Sandy Clay Loam	Sandy Loam	Sandy Clay Loam	Sandy Clay Loam	Clay	
HSG	C	C	A	C	C	D	
Percentage	0.33	0.85	38.05	18.34	27.76	14.25	0.43

In the present study, the land use and soil coverage were merged using ARC-GIS software and all the polygons with particular land uses and a hydrologic soil group were selected at a time for assigning CN for AMC II condition. Thus, the generated CN coverage involves

different polygons with different CN values for AMC II condition. Then the generated CN coverage for AMC II condition was intersected with watershed grid for determination of average CN for AMC II condition. And finally average CN for AMC I and AMC III were computed using the equations (6.8) and (6.9) respectively. The CN was estimated by defining each and every hydrologic soil-land cover complex in the sub-basin, and then weighting to get the sub-basin average. Details of the CN values for different sub-basins are given in Table 6.5.

Table 6.5: CN of Sub-basins of the Study Area

	CN Corresponding to		
Subbasin	AMC II	AMC I	AMC III
Sundargarh	57.04	36.79	75.67
Salebhatta	70.59	51.28	84.90
Kesinga	72.42	53.60	85.98
Kantamal	69.82	50.79	84.21
Tikarpada	72.83	54.70	86.06

Using the CN from table 6.5, the potential retention S was calculated using equation (6.5) and then putting the calculated S value in equation (6.4), daily and monthly direct runoff were computed. Figure 6.6 shows daily simulation performance for the five sub-basins in terms of scatter plot. It can be observed that the computed runoff did not match well with the observed runoff. Figure 6.7 shows simulation performance for the five sub-basins in terms of scatter plot. Here it can be observed that the computed runoff matched better with the observed runoff.

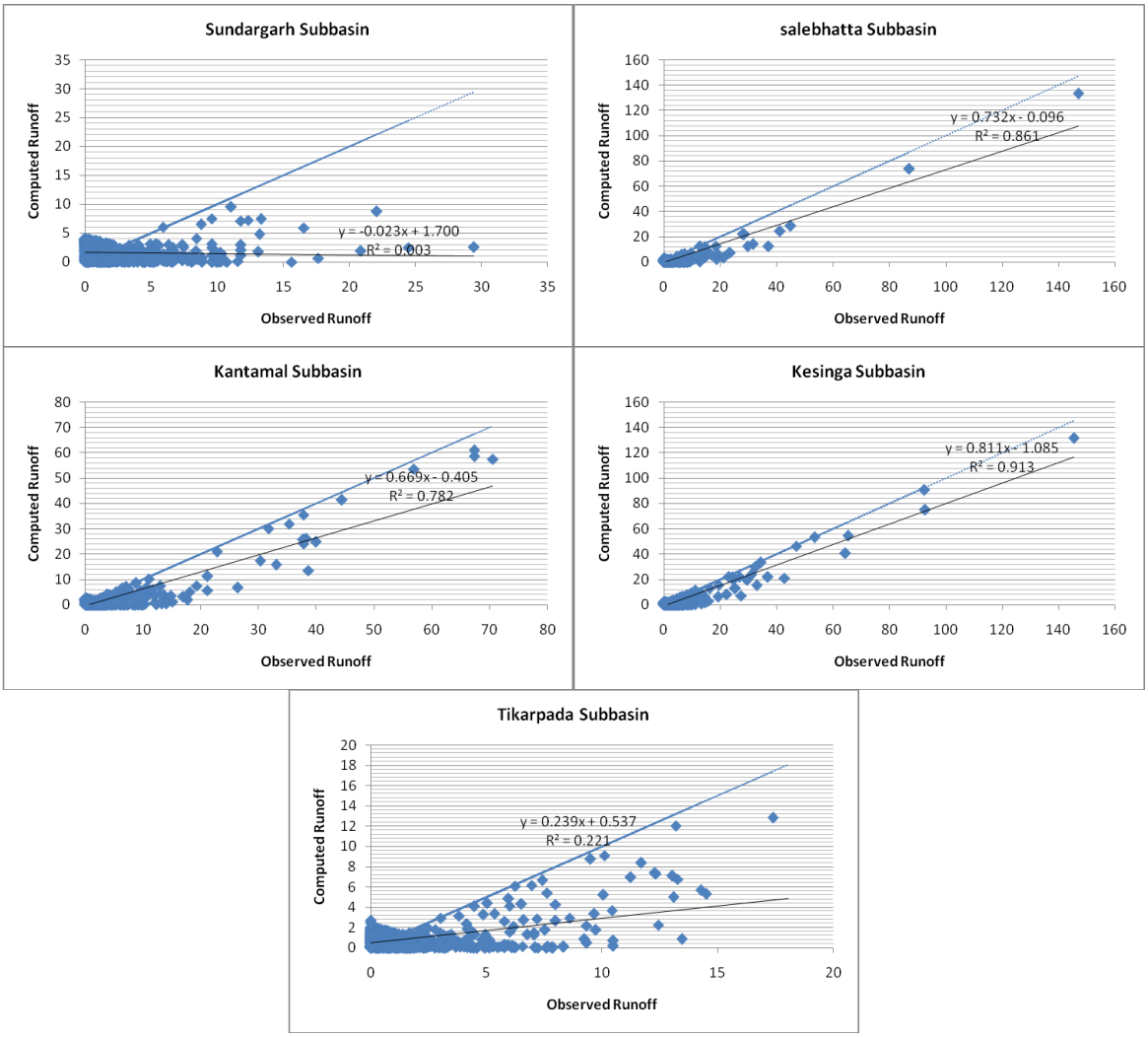

Figure 6.6 Daily Simulation Performances of Original SCS-CN Method

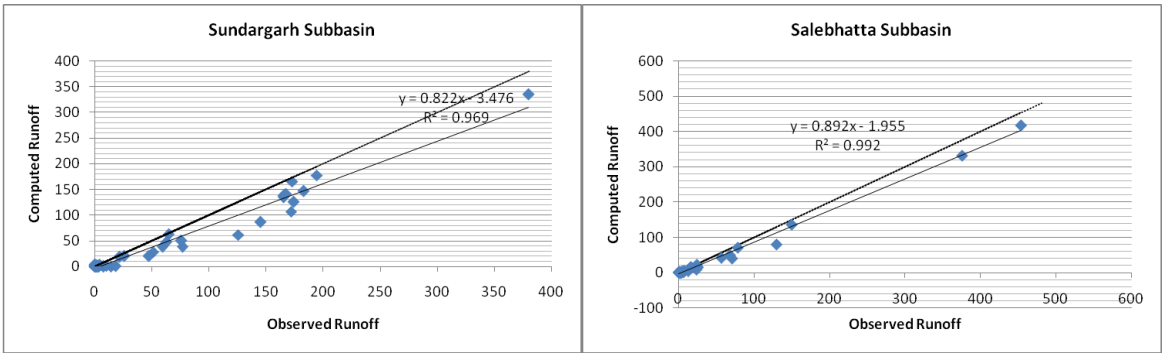

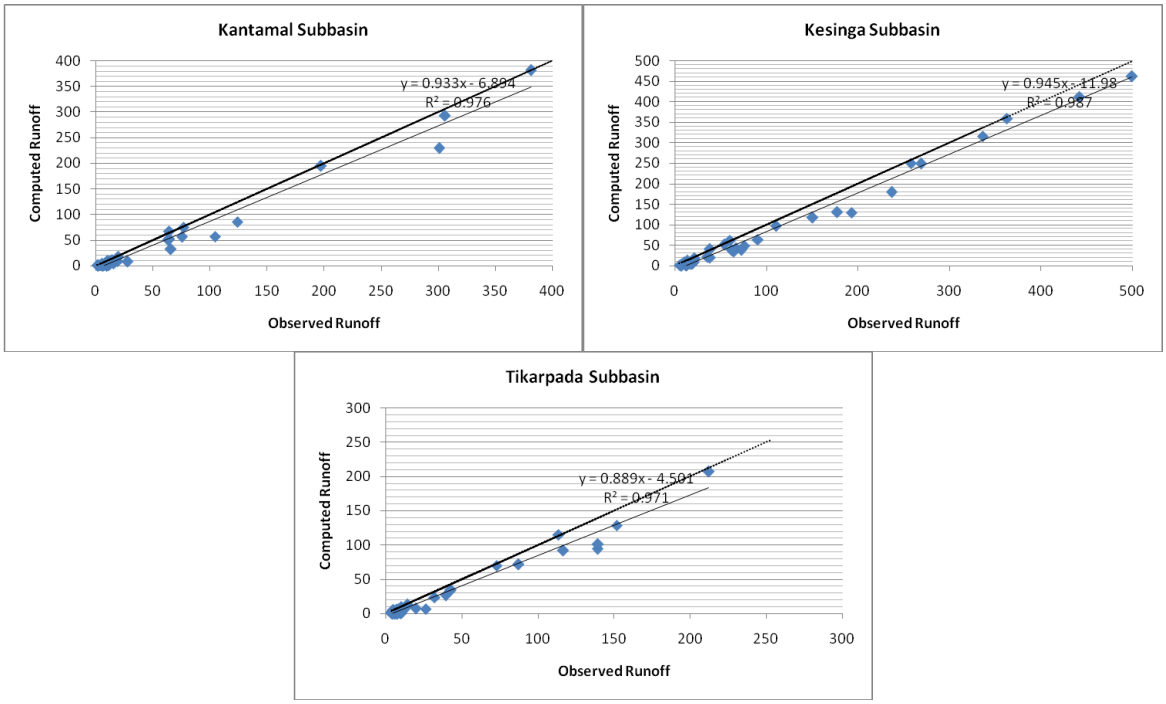

Figure 6.7 Monthly Simulation Performances of Original SCS-CN Method

6.3.2 Mishra-Singh (MS) Model

The original SCS-CN equation modified and substituted by equations (6.13) and (6.14) are used in the study area for all the sub-basin. For some reason, the results obtained are not very promising for daily runoff simulations. Figure 6.8 illustrate the results for daily simulation. The model is over estimating the runoff in most of the cases, which is not suitable for planning purpose. Further, the model is not able to estimate the runoff on monthly basis due to consideration of P_5 (5-day) cumulative rainfall for the analysis.

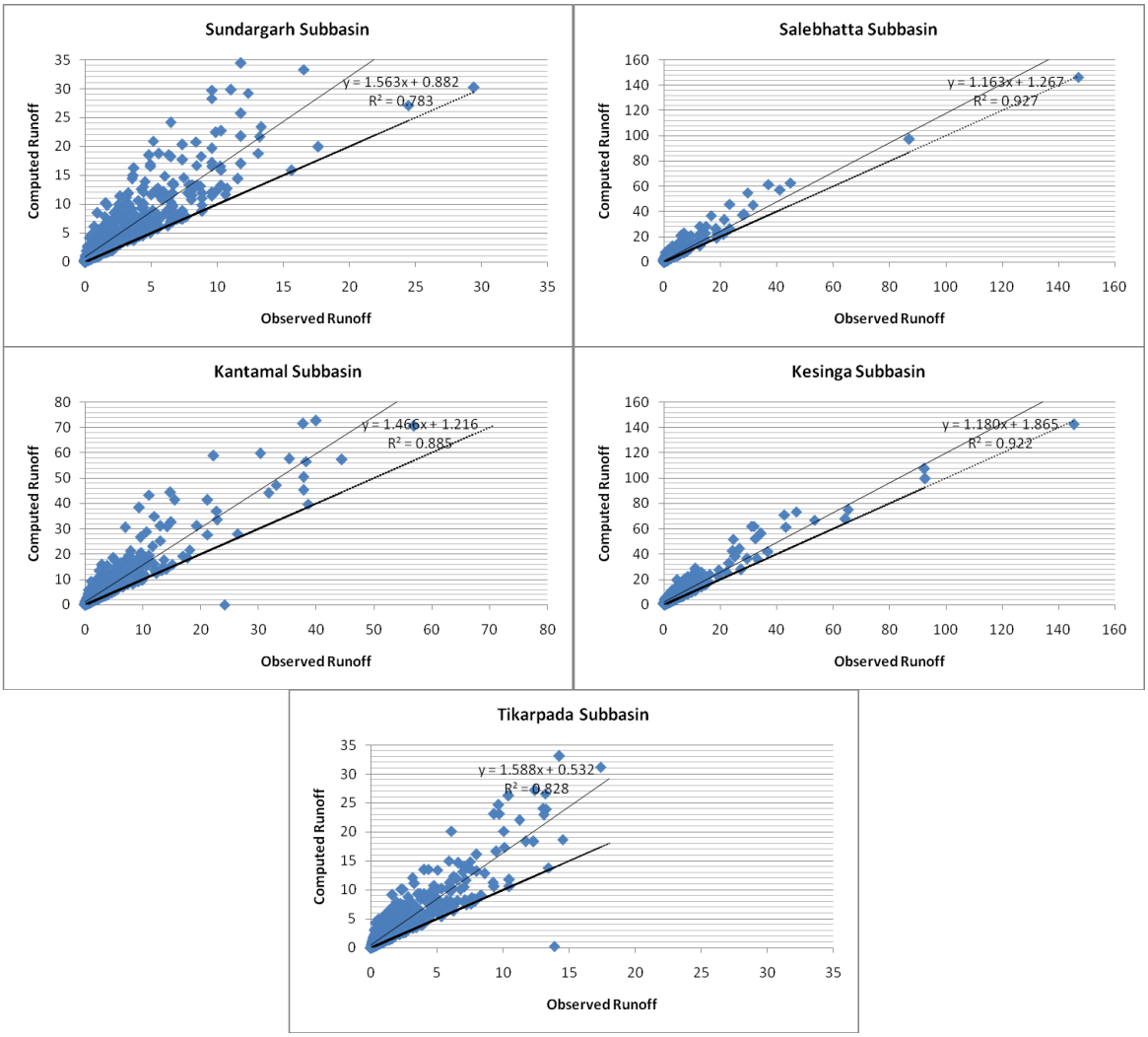

Figure 6.8 Daily Simulation Performances of Mishra-Singh Model

6.3.3 Michel Model

The Michel model estimates runoff using equations (6.21)-(6.26). The results obtained using Michel model for daily runoff is shown in Figure 6.9. In this case also, the results obtained are not very promising for daily runoff simulations. Further, the model is not able to estimate the runoff on monthly basis due to consideration of P_5 (5-day) cumulative rainfall for the analysis.

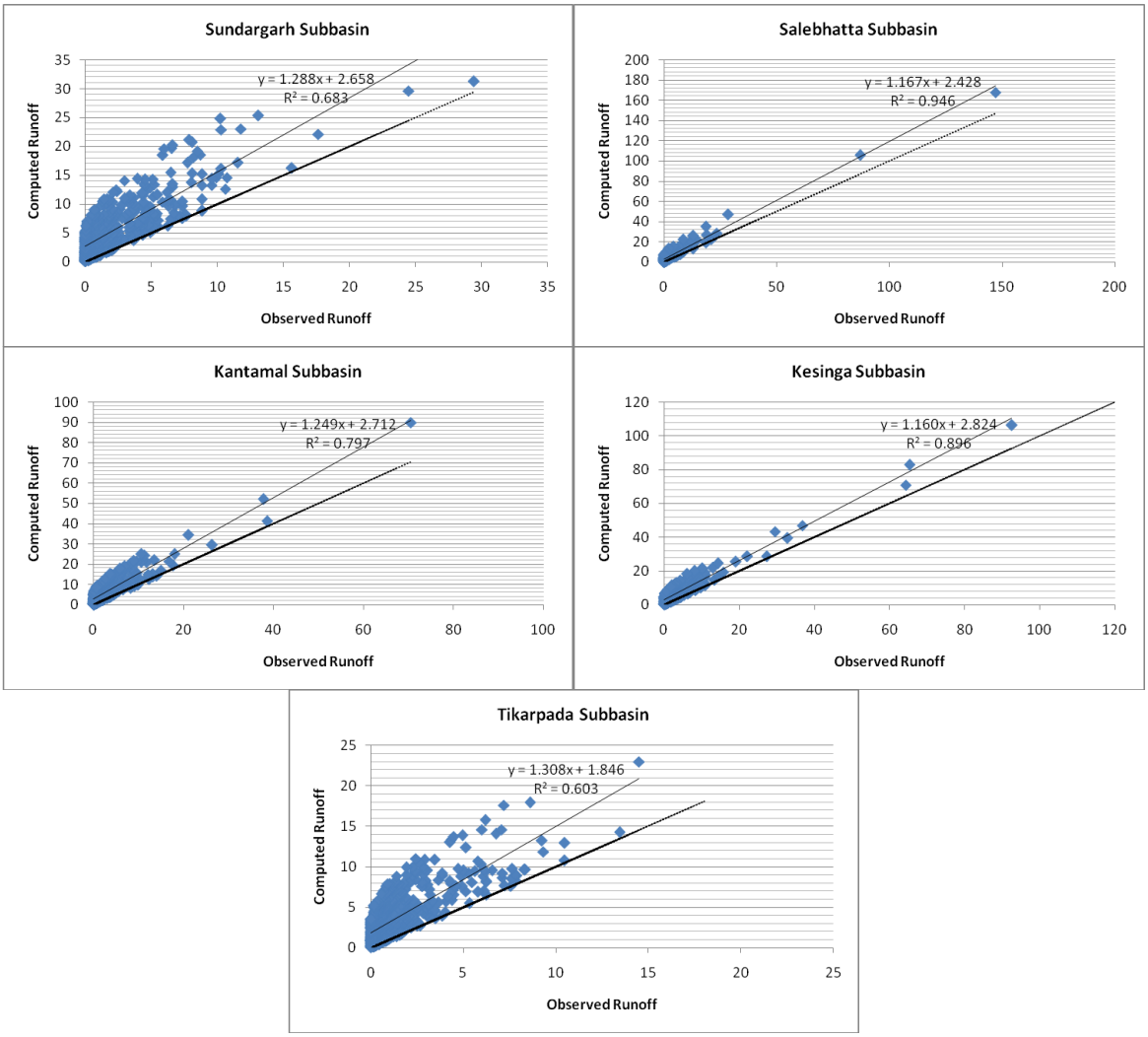

Figure 6.9 Daily Simulation Performances of Michel Model

6.3.4 Sahu Model

The Sahu model estimates runoff using equations (6.27)-(6.31). The results obtained using Sahu model for daily runoff is shown in Figure 6.10. In this case also, the results obtained are very poor in some of the sub-basins for daily runoff simulations. Further, the model is not able to estimate the runoff on monthly basis due to consideration of P_5 (5-day) cumulative rainfall for the analysis.

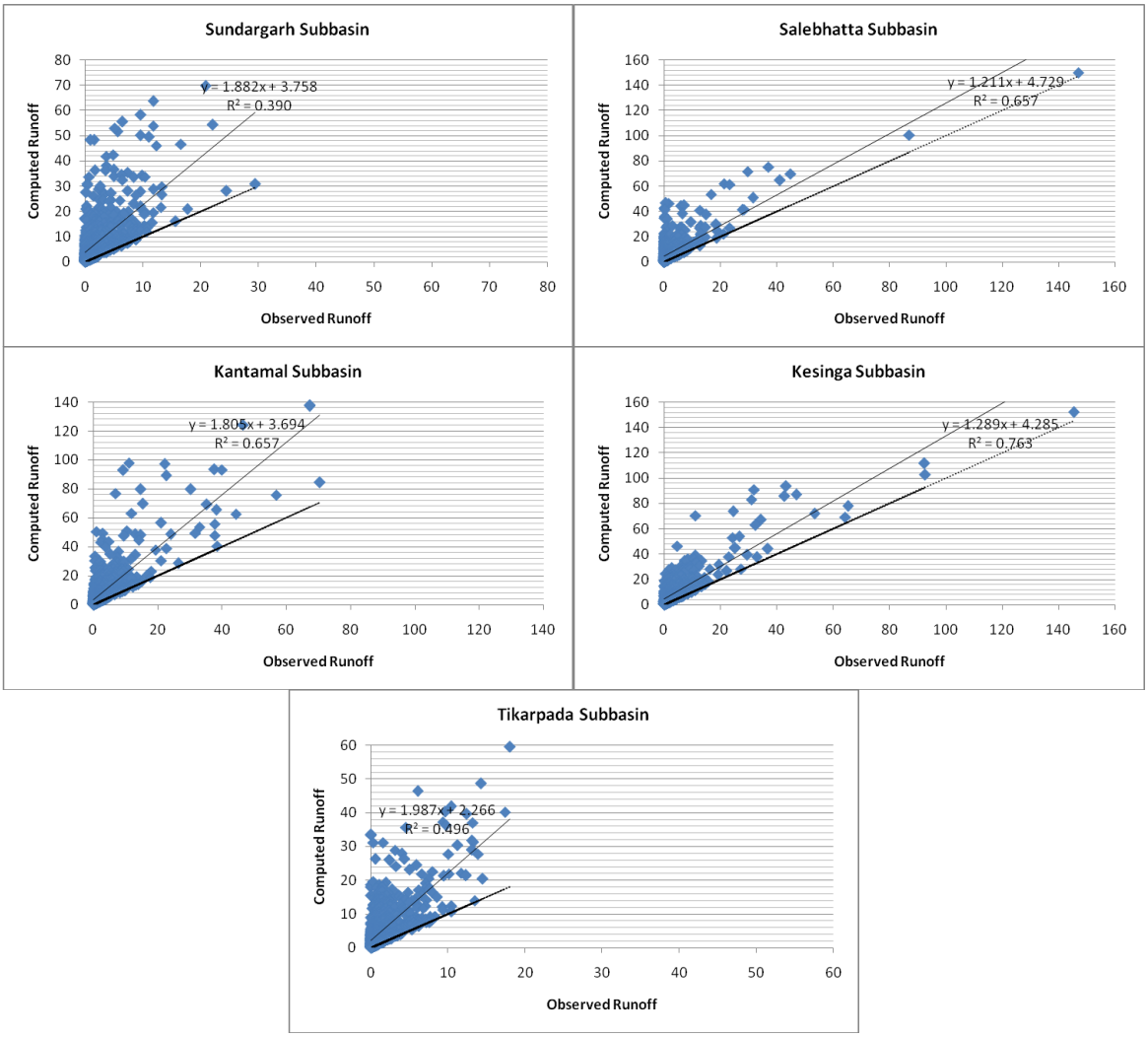

Figure 6.10 Daily Simulation Performances of Sahu Model

6.3.5 Frequency Distribution based Probability of Exceedance (FDM-PE) Model

The FDM-PE estimates runoff are obtained for each sub-basin by arranging rainfall data in descending order (according to probability of exceedance) and then estimating probabilistic CN (PCN) values using equation (6.10). Figure 6.11 illustrates the procedure for estimating PCN for Sundargarhl sub-basin. The equation can also be derived to estimate CN from known probability of exceedance as shown in Figure 6.11. Using PCN, the results obtained are very promising. As, this is a new concept, the results need to be verified further for other river basins too. The FDM-PE is able to estimate the runoff based on daily as well monthly rainfall data (Figure 6.12 and 6.13).

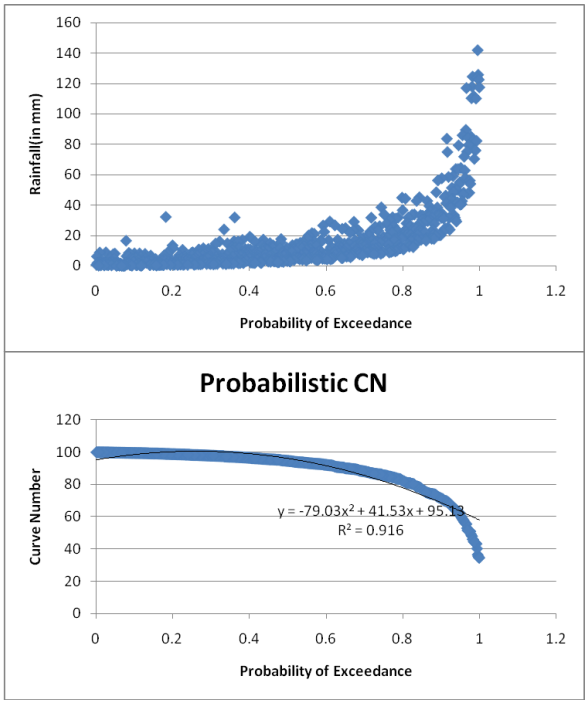

Figure 6.11: Probabilistic CN estimation using FDM-PE Model for Sundargarh Subbasin

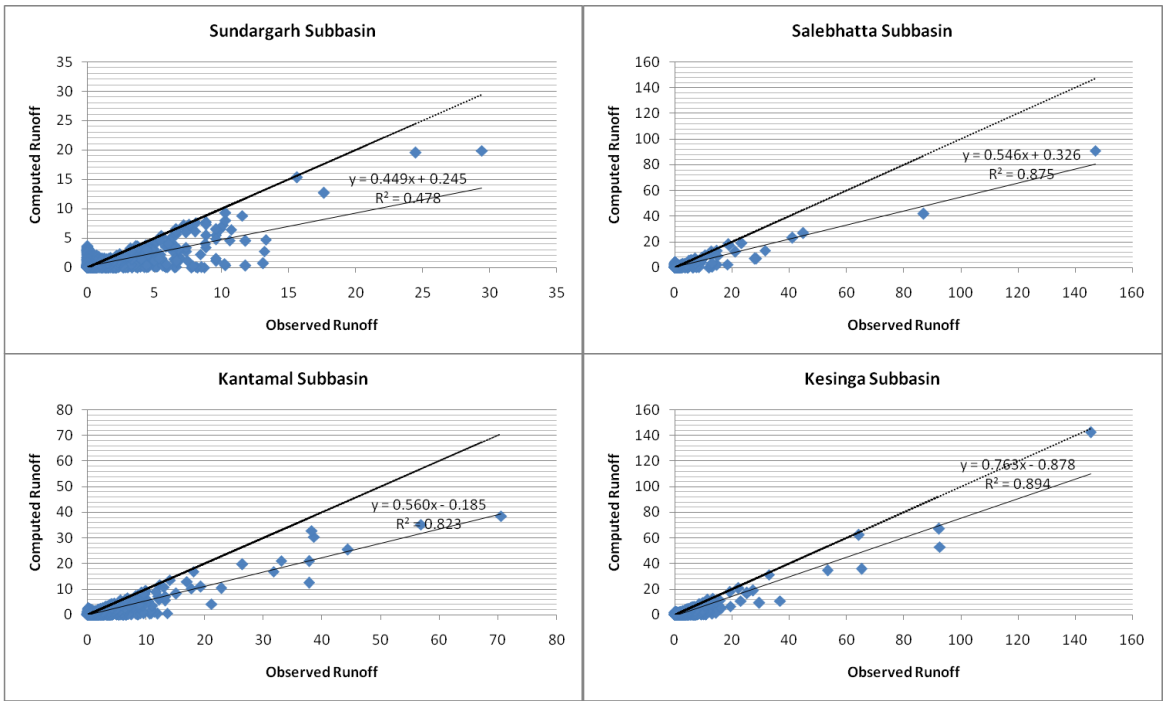

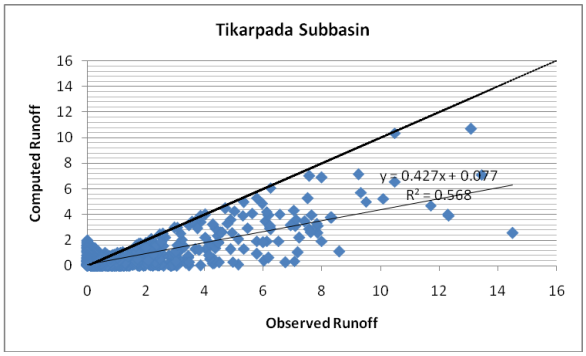

Figure 6.12 Daily Simulation Performances of FDM-PE Model

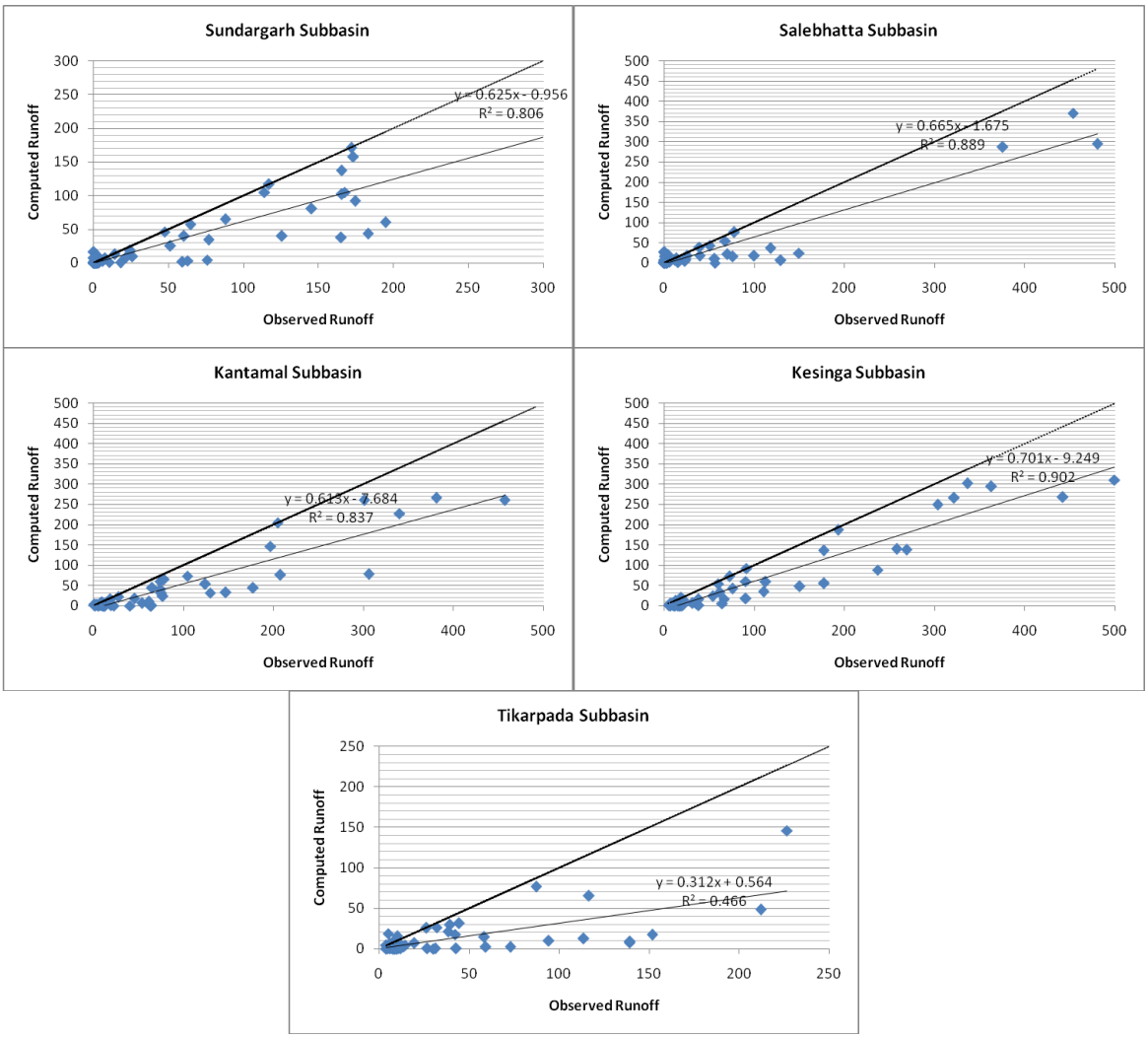

Figure 6.13 Monthly Simulation Performances of FDM-PE Model

6.3.6 Modified Median based- SCS (MM-SCS) Model

For gauged watersheds where both rainfall and runoff volumes are known the Curve Number values can be determined using equations (6.5). The observed rainfall and runoff data obtained on daily basis are used in equation (6.10) to obtain the values of S and values of Q are obtained using the equation (6.4).

Thereafter, the median CN from the sorted (in descending order) CN series is considered as AMC II (normal condition). Again, the median CNs of the sorted CN series corresponding to lower half and higher half are considered as AMC I (dry condition) and AMC III (wet condition) respectively. The results obtained using this method provided best results in comparison to other methods (Figures 6.14 and 6.15).

In fact, no equations and manipulations are required in this method to obtain AMC I and AMC III. The method is very simple and straight forward. Of, course, for un-gauged catchments, the method may not be applicable directly and CN values for AMC I, AMC II and AMC III may not be estimated due to non-availability of observed rainfall and runoff estimates. However, it can be developed using regional modeling and analysis.

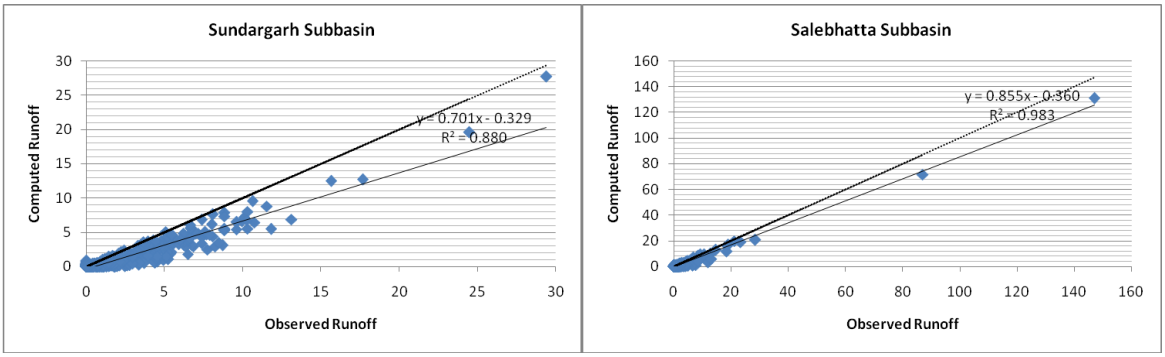

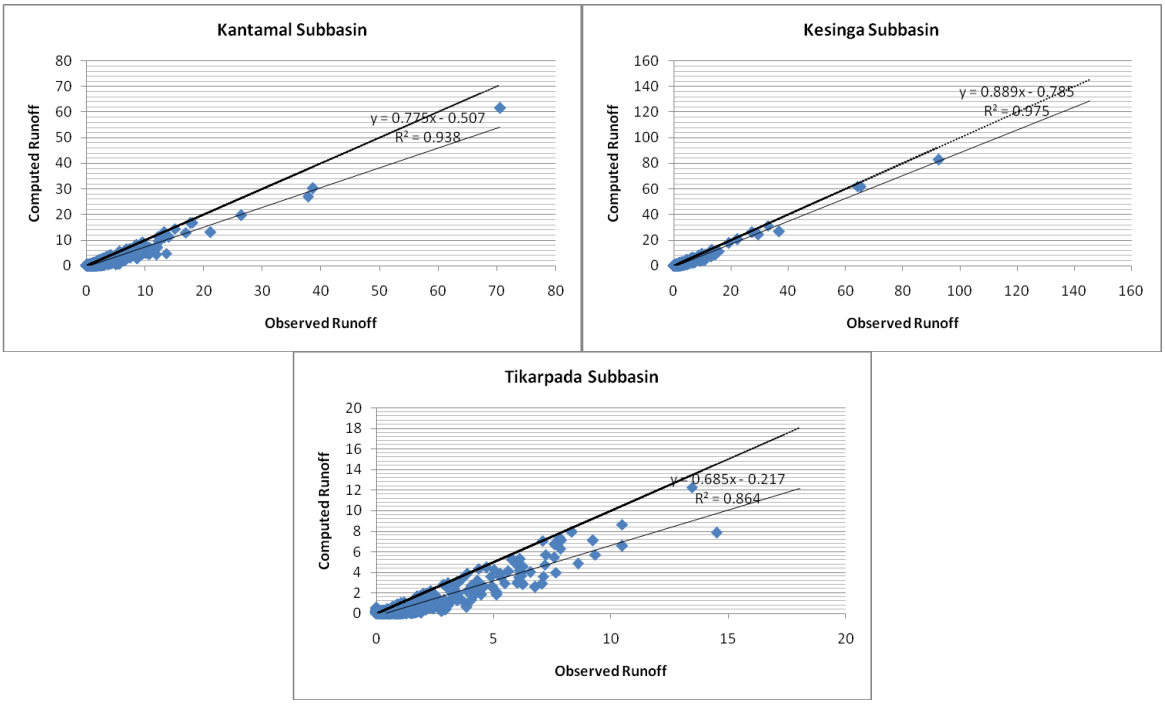

Figure 6.14 Daily Simulation Performances of MM-SCS Model

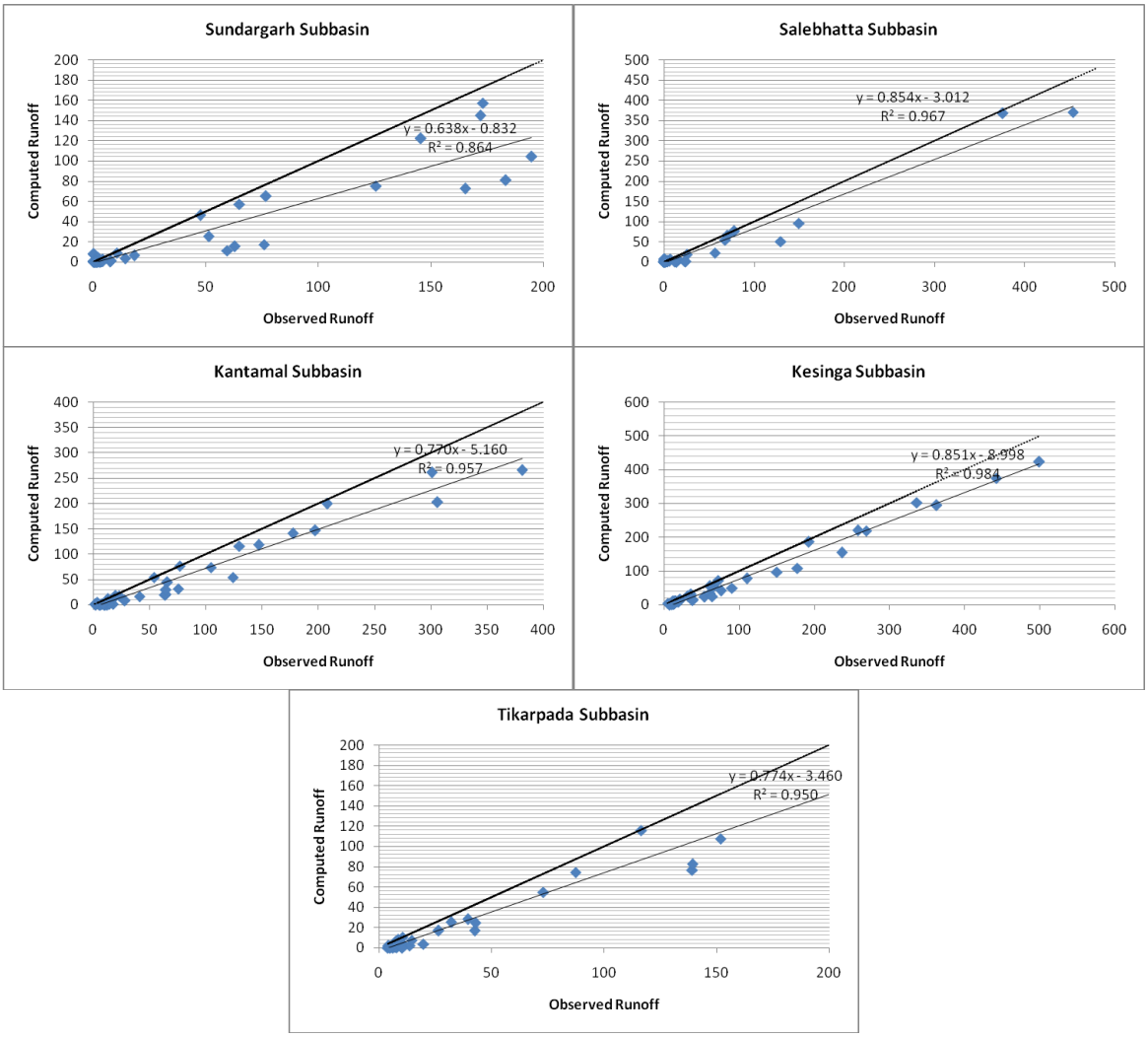

Figure 6.15 Monthly Simulation Performances of MM-SCS Model

Daily simulation performances of the methods described in sections 6.3.1 to 6.3.6 for all the stations are given in the appendix II. And monthly simulation performances of the methods described in sections 6.3.1, 6.3.5 and 6.3.6 for all the stations are also given in the appendix II.

6.3.7 Artificial Neural Network based Multi Layer Perceptron (ANN-MLP) Model

The MLP architecture, a feed forward-type NN, is selected in this study because it usually has good model performance, and also because it is the most frequently used configuration in hydrology. The ANN networks consisting of an input layer, one single hidden layer composed of 3-12 nodes, and one output layer consisting of 1 node denoting the predicted

runoff. Table 6.1 and 6.2 illustrate the AAN-MLP model structure in the present case for simulating daily and monthly rainfall data having different input variables. Figure 6.16 and 6.17 illustrates the results for daily and monthly simulation performances at validation stage, which are found to be inferior then MM-SCS method. However, the results are very promising and may be used for rainfall runoff analysis.

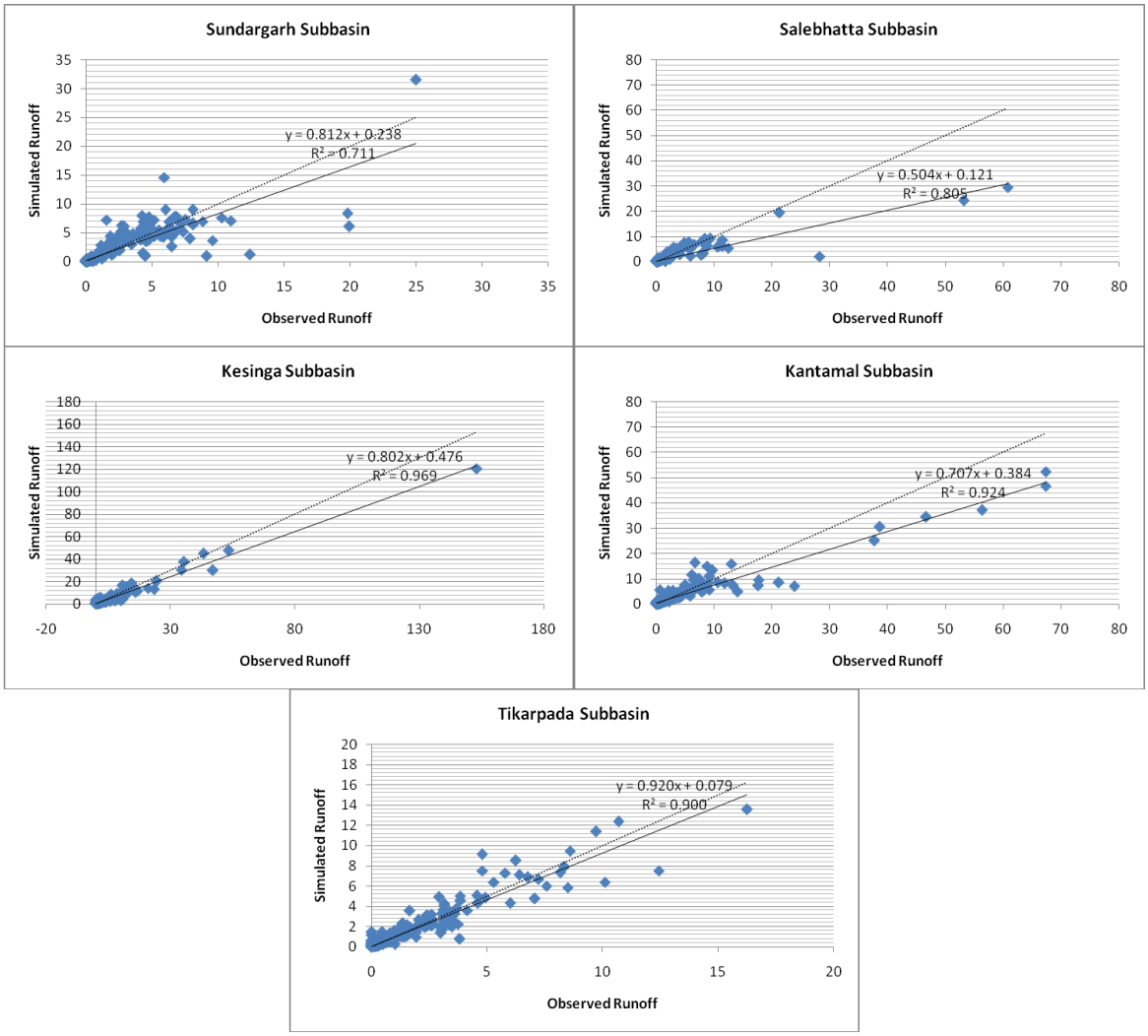

Figure 6.16 Daily Simulation Performances of ANN-MLP Model

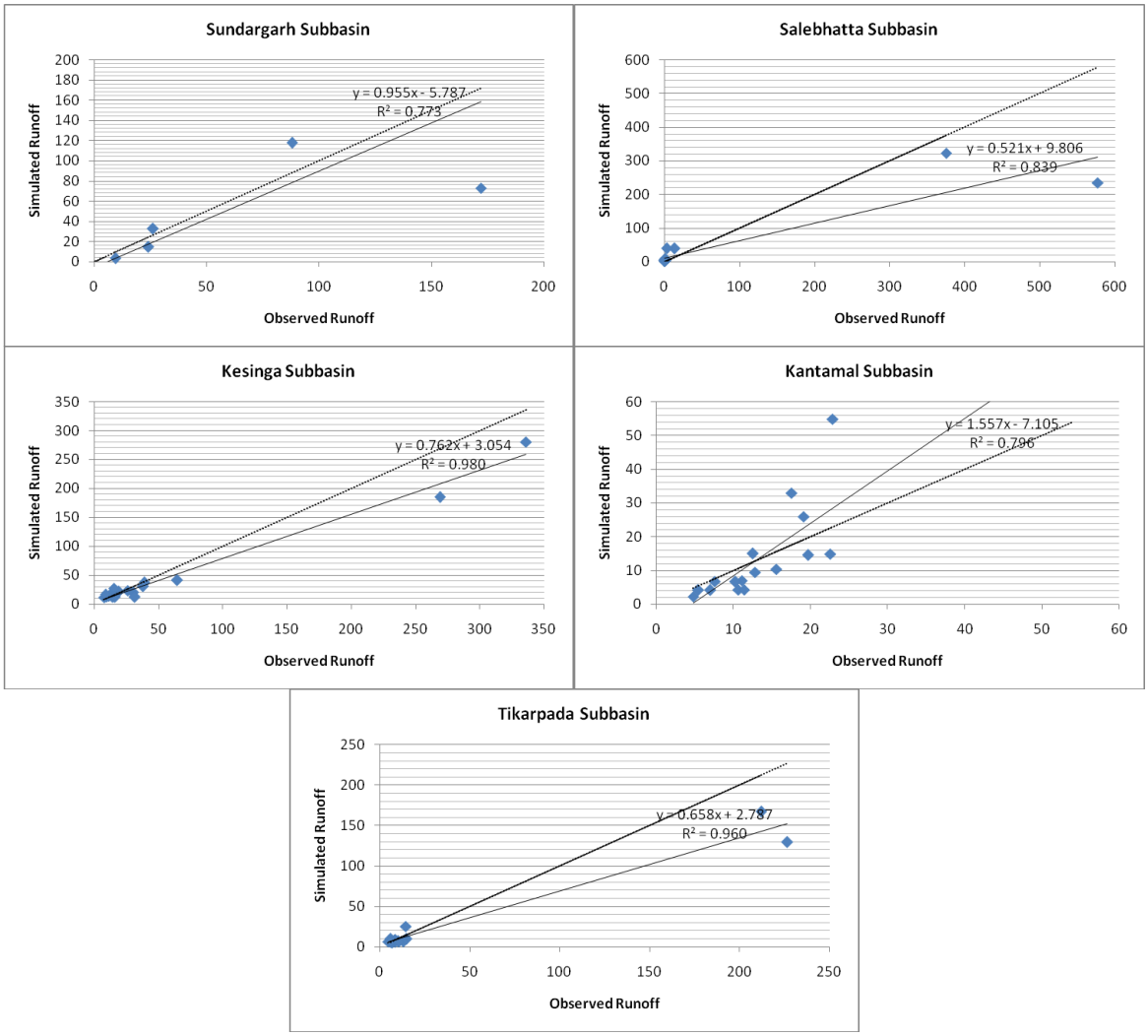

Figure 6.17 Monthly Simulation Performances of ANN-MLP Model

6.4 CONCLUSION

Two new approaches based on original SCS-CN method such as Frequency Distribution based Probability of Exceedance (FDM-PE) Model and Modified Median based- SCS (MM-SCS) Model were developed for simulation of daily and monthly runoff for five subbasins of the basin.MLP-ANN models were also developed for daily and monthly runoff simulation of the the five subbasins.

CHAPTER 7

DERIVATION OF CURVE NUMBERS FROM DAILY TO MONTHLY RAINFALL-RUNOFF DATA

7.1 INTRODUCTION

In the previous chapter, rainfall generated runoff has been estimated using seven different methods for daily and monthly rainfall-runoff data. Out of all the methods, MM-SCS model provided best results with the observed values of daily and monthly rainfall data. The other models FDM-PE and ANN-MLP proposed in the present work also provided fairly good results.

It is understood that, the CN value for estimating runoff potential for planning purposes at watershed, sub-basin and basin level is often a policy decision. The available approaches utilize either daily, weekly, half-monthly or monthly data or average physical characteristics of watersheds. Many researchers have demonstrated that the key parameter CN has variable components in a watershed (Hjelmfelt et al. 1982; McCuen 2002), and it varies with rainfall. The CN varies monthly, seasonally and annually. In a similar manner CN varies at daily, weekly and half-monthly basis too. It is, therefore, essential to carry out the required analysis to establish CN for the policy makers and decision makers.

7.2 DERIVATION OF CURVE NUMBERS FROM DAILY TO MONTHLY RAINFALL-RUNOFF DATA

Daily rainfall and runoff data for the period of ten years 2000-2009 has been used in the present analysis for the basins and sub-basins of Mahanadi river system lying in Odisha (Figure 7.1).

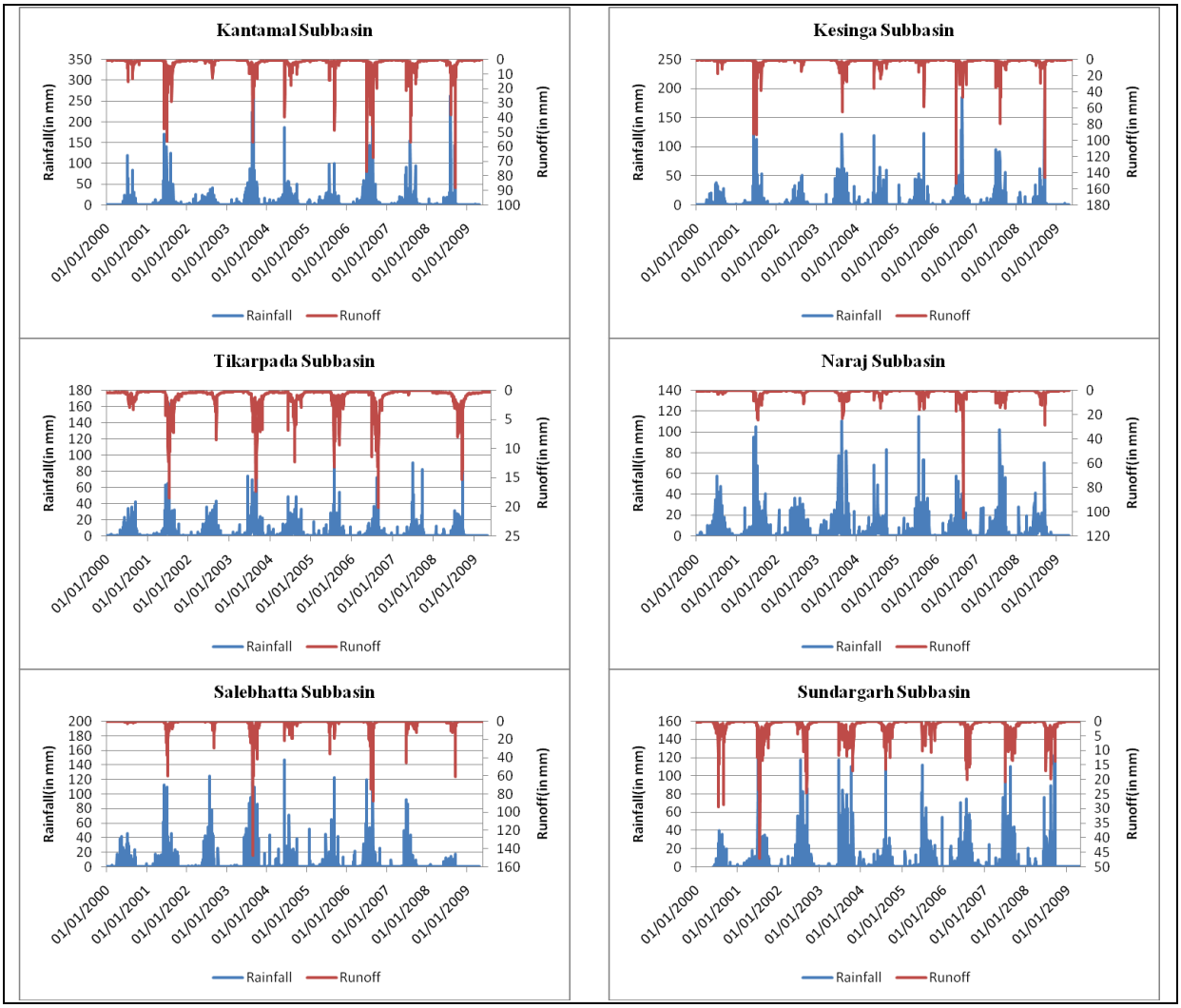

Figure 7.1: Time Series Plot of Daily Rainfall-Runoff of Sub-basins

The daily rainfall and runoff data for the stations and sub-basins are assumed to be represented by a linear relationship. This assumption means that the rainfall contributes fully to the net runoff (= rainfall excess) at the outlet of the considered basin in the time duration equal to the time of concentration (T_c). As a result, the routing of the rainfall-excess of the duration equal to or more than T_c for computation of actual (shape of) runoff hydrograph is not required. This basic premise also ignores the base flow contribution to the outlet, specifically in the non-monsoon season which refers to the period of no or scanty rainfall, and can lead runoff factor (C = Q/P) greater than 1, an unrealistic state assuming 1-day or more than 1-day routing depending on T_c value. Therefore, CN derivations from daily rainfall-

runoff events are considered for only those days when computed values of C are less than or equal to 1. The same concept is applied for all the other11 time spans for derivation of CN.

From previous studies, it has been observed that the monthly CN is much lower than daily CN and this reduction is subjected to runoff coefficient(C=Q/P). As runoff coefficient gradually decreases from daily time scale to monthly time scale due to increase in base flow contribution, the CN also gradually decreases from daily time span to monthly time span. It is found essential to estimate CN for different durations between 1-day to 30-day which is necessary for various purposes such as agriculture, flood control, drought mitigation etc. Daily rainfall and runoff data are summed up to get rainfall-runoff series for the 11 time spans i.e. 2-days, 3-days, 4-days, 5-days, 6-days, 7-days, 10-days, 15-days, 20-days, 25-days and 30-days time spans to derive Curve numbers for each n-day period. The CN has been derived using equations 7.1 and 7.2, also used in previous chapter is given below:

$$S = 5(P + 2Q - \sqrt{(4Q^2 - 5PQ)}) \quad (7.1)$$

$$S = (25400/CN) - 254 \quad (7.2)$$

The CN derived from equations (7.1) and (7.2), are used in MM-SCS to obtain CN for AMC I, AMC II and AMC III. A scatter plot of the curve numbers varying with storm duration from 1-day to 30-day for the five sub-basins is shown in Figure 7.2.

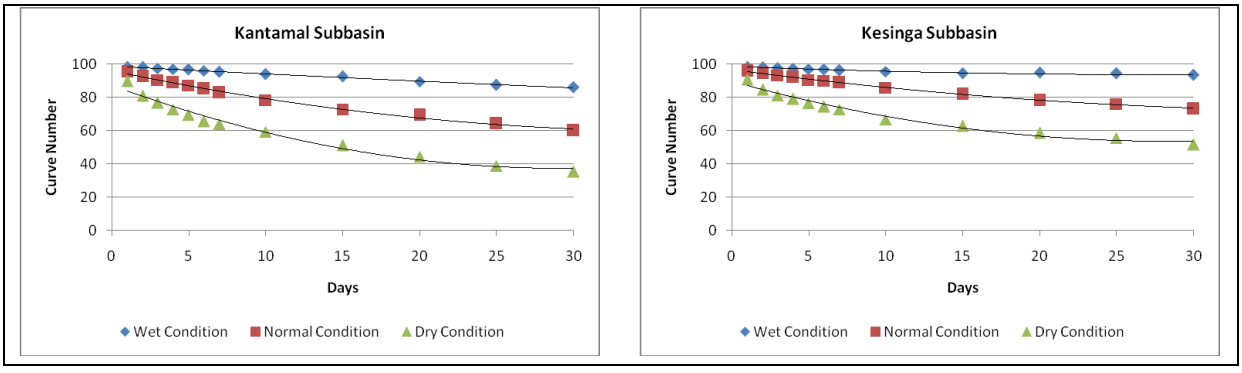

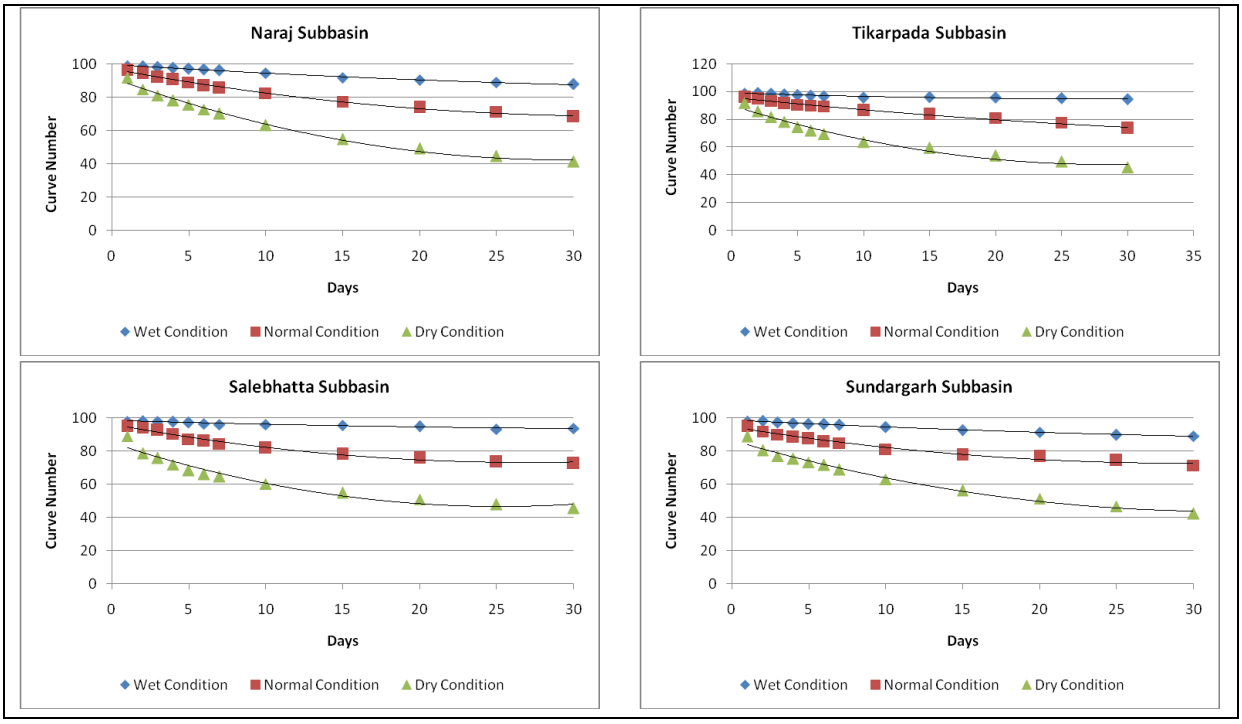

Figure 7.2: CN Variations with Rainfall Duration for Sub-basins

Through regression analysis the smooth curves are fitted and second order polynomial equations are derived for AMC I, AMC II and AMC III conditions. The derived second order polynomial equations for the all the five sub-basins having AMC I, AMC II and AMC III conditions at all five sub-basins of Mahanadi river system lying in Odisha are shown in equations (7.3) to (7.20).

Kantamal Sub-basin

$$y = 0.058x^2 - 3.415x + 87.16 \quad \text{AMC I} \quad (7.3)$$

$$y = 0.025x^2 - 1.934x + 96.01 \quad \text{AMC II} \quad (7.4)$$

$$y = 0.001x^2 - 0.482x + 98.72 \quad \text{AMC III} \quad (7.5)$$

Kesinga Sub-basin

$$y = 0.044x^2 - 2.527x + 89.22 \quad \text{AMC I} \quad (7.6)$$

$$y = 0.015x^2 - 1.226x + 96.62 \quad \text{AMC II} \quad (7.7)$$

$$y = 0.005x^2 - 0.339x + 98.53 \quad \text{AMC III} \quad (7.8)$$

Tikarpara Sub-basin

$y = 0.053x^2 - 3.012x + 90.30$ AMC I (7.9)

$y = 0.008x^2 - 0.974x + 95.96$ AMC II (7.10)

$y = 0.005x^2 - 0.293x + 98.86$ AMC III (7.11)

Naraj Sub-basin

$y = 0.056x^2 - 3.327x + 91.48$ AMC I (7.12)

$y = 0.025x^2 - 1.699x + 97.01$ AMC II (7.13)

$y = 0.005x^2 - 0.561x + 99.53$ AMC III (7.14)

Salebhata Sub-basin

$y = 0.060x^2 - 3.039x + 84.88$ AMC I (7.15)

$y = 0.032x^2 - 1.730x + 96.26$ AMC II (7.16)

$y = 0.003x^2 - 0.266x + 98.31$ AMC III (7.17)

Sundargarh Sub-basin

$y = 0.041x^2 - 2.679x + 86.44$ AMC I (7.18)

$y = 0.025x^2 - 1.475x + 94.35$ AMC II (7.19)

$y = 0.004x^2 - 0.454x + 98.45$ AMC III (7.20)

In these equations x is rainfall duration and y is curve number.

The derived equations obtaining curve numbers (CN) values for any given rainfall duration between 1-day to 30-days are tested for their applicability and CN values are re-estimated for different cumulative rainfall durations. Table 7.1 gives coefficient of determination and Nash and Sutcliffe simulation efficiency between observed and simulated CN values. The high values of R^2 and E_{NS} for all the sub-basins having AMC I, AMC II and AMC III suggest suitability and applicability of derived SCS-CN equations.

Table 7.1: Performance Efficiency of Developed Equation for Sub-basins

Subbasin	Coefficient of Determination(R^2)			Nash-Suttcliffe Simulation Efficiency (E_{NS})		
	Wet Condition	Normal Condition	Dry Condition	Wet Condition	Normal Condition	Dry Condition
Kantamal	0.996	0.995	0.978	0.994	0.995	0.977
Kesinga	0.955	0.998	0.978	0.938	0.998	0.978
Tikarpada	0.900	0.987	0.974	0.896	0.986	0.973
Naraj	0.994	0.981	0.979	0.992	0.977	0.976
Salebhatta	0.940	0.985	0.952	0.938	0.985	0.950
Sundargarh	0.995	0.980	0.983	0.994	0.979	0.983

Figure 7.3 shows simulation performance of the developed equations using monthly rainfall data for all the sub-basins as scatter plots. An independent dataset has been used in the validation stage, which was not used in the equation development stage. Even then, such high coefficient of determination values indicates high simulation performance of the developed equations. Table 7.2 gives the validation performance of the developed equations in terms of mean, standard deviation, coefficient of determination and model efficiency. It has been observed that for all the sub-basins mean and standard deviation of the simulated runoff are close to those of the observed runoff and the R^2 and E_{NS} values are also considerably high.

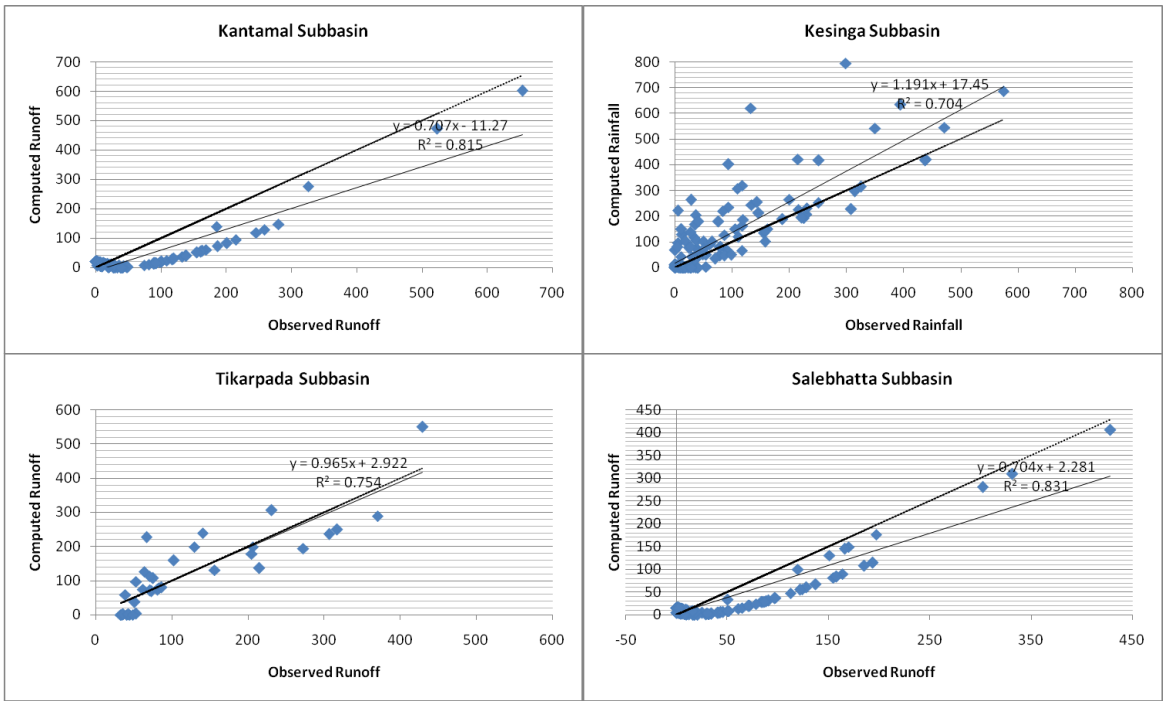

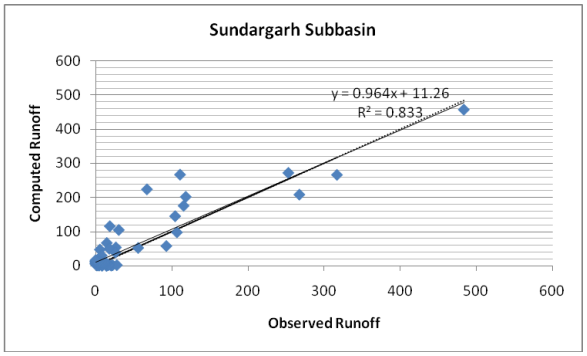

Figure 7.3: Validation of the derived CN using monthly data

Table 7.2: Error statistics of the derived CN equations

Subbasin	Mean		Standard Deviation		R^2	E_{NS}
	Observed Runoff	Simulated Runoff	Observed Runoff	Simulated Runoff		
Kantamal	63.828	33.911	100.920	79.133	0.815	0.591
Kesinga	74.112	105.779	109.249	155.079	0.705	0.659
Tikarpada	123.784	122.382	106.794	118.641	0.755	0.754
Salebhatta	34.031	26.270	64.966	50.220	0.832	0.670
Sundargarh	33.818	43.881	79.141	83.644	0.833	0.820

Similarly the developed equations were validated using daily rainfall data of the 14 stations of all the sub-basins for the year 2009 (Figure 7.4). The data which was not considered for CN derivation were used to test the validity of the model. Table 7.3 gives the simulation performance of the developed equations in terms of mean, standard deviation, coefficient of determination and model efficiency. It has been observed that for all the sub-basins mean and standard deviation of the simulated runoff are not so close to those of the observed runoff and the R^2 and E_{NS} values are also not considerably high.

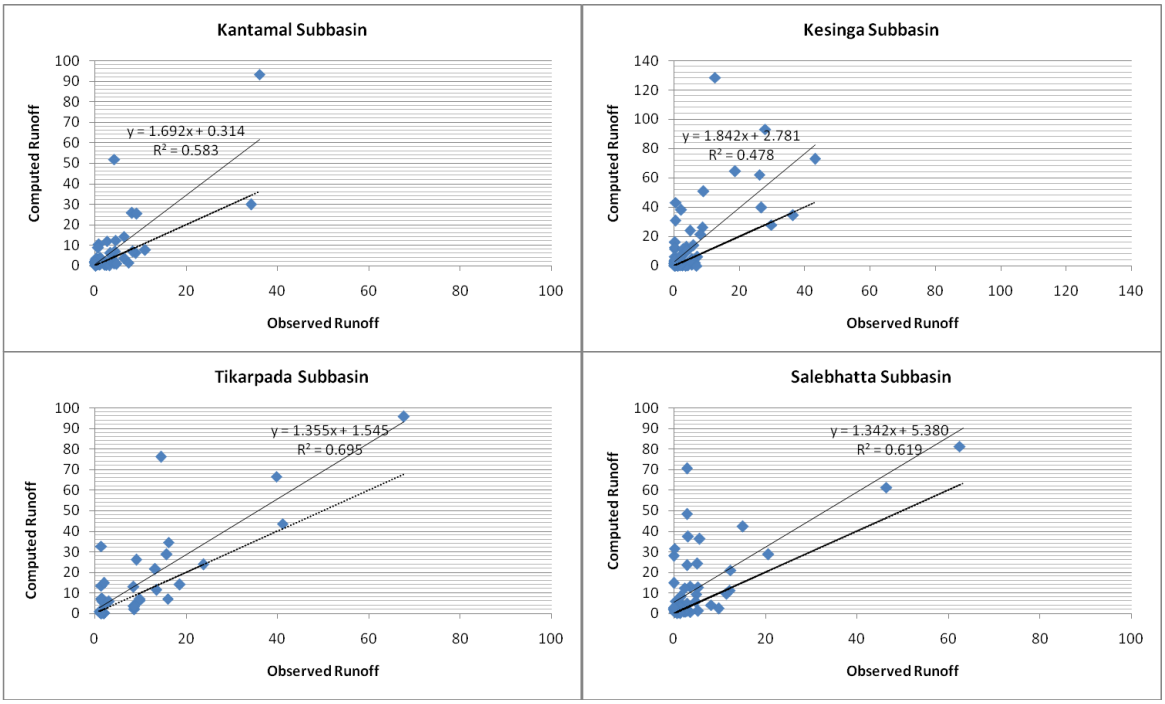

Figure 7.4: Daily Simulation Performance of Developed Equation

Table 7.3: Daily Simulation Performance of Developed Equation for Sub-basins

Subbasin	Mean		Standard Deviation		R^2	E_{NS}
	Observed Runoff	Simulated Runoff	Observed Runoff	Simulated Runoff		
Kantamal	3.487	6.168	6.453	14.286	0.582	0.469
Kesinga	4.113	10.318	8.113	21.613	0.477	0.349
Tikarpada	8.505	13.026	13.272	21.566	0.694	0.619
Salebhatta	5.327	12.547	12.360	21.108	0.619	0.517

7.3 CONCLUSION

Daily to monthly curve numbers were derived from daily to monthly rainfall-runoff data and equation were developed for wet, normal and dry conditions for four subbasins of the basins. Daily runoff was simulated using estimated daily curve number and efficiencies upto 0.69 were achieved.

CHAPTER 8

DEVELOPMENT OF RAINFALL FORECASTING MODELS

8.1 INTRODUCTION

In India, monthly rainfall data are easily available from different resources. These monthly data are very useful for the planning, development and management of available water resources. In previous chapters mean monthly rainfall over different sub-basins are obtained using Ordinary Kriging method of spatial interpolation and monthly runoff are derived from MM-SCS Model. In this context, if monthly rainfall forecasting models are developed, the monthly runoff estimates can be easily obtained, which is useful for planners and policy makers to make best use of available water resources.

8.2 AUTOREGRESSIVE INTEGRATED MOVING AVERAGE (ARIMA) MODEL

Typically various statistical tools are applied to auto-correlated time series of data for modeling and predicting future values in the monthly rainfall series. In general, autoregressive (AR), moving average (MA), autoregressive moving average (ARMA) and autoregressive integrated moving average (ARIMA) models are applied to time series of rainfall data. A model which depends only on previous outputs of a system to predict an output is called an autoregressive (AR) model. While a model which depends only on inputs to the system to predict an output is called a moving average (MA) model. The model derived from autoregressive and moving average processes may be a mixture of these two and of higher order than one as well, which is termed as a stationary ARMA model with its random shocks independent and normally distributed with zero mean and constant variance. An ARMA model can be noted as ARMA (p,q) where p is the number of AR parameters and

q is the number of MA parameters. It models only stationary dataset i.e. the dataset for which residuals are independent for all time period.

It is understood that all hydrologic datasets are not stationary in real life. Some datasets follow some sort of persistence or autocorrelation which is inherently present in it and cannot be removed. Some sorts of trend and cycle are also associated with such datasets. Modeling of non-stationary datasets with ARMA model looks difficult. Non-stationary datasets can be modeled through autoregressive and moving average processes through differentiation i.e. the dataset is differentiated until it becomes stationary. For real life data required differentiation is at maximum of the order of three to make it stationary.

ARIMA model is an extension of ARMA model in the sense that including autoregressive and moving average it has an extra part of differencing the time series. If a dataset exhibits long term variations such as trend, seasonality and cyclic components, differencing of dataset in ARIMA allows the model to deal with such long term variations. Two common processes of ARIMA in identifying patterns in time series data and forecasting are autoregressive and moving average.

Autoregressive process: Most time series consist of elements that are serially dependent. One can estimate a coefficient or a set of coefficients that describe consecutive elements of the series from specific, time-lagged (previous) elements. Each observation of the time series is made up of a random error component (random shock, ξ) and a linear combination of prior observations.

Moving average process: Independent from the autoregressive process, each element in the series can also be affected by the past error (or random shock) which is not considered by the

autoregressive component. Each observation of the time series is made up of a random error component (random shock, ξ) and a linear combination of prior random shocks.

The ARIMA model includes three types of parameters which are: the autoregressive parameters (p), the number of differencing passes (d), and moving average parameters (q). In the notation introduced by Box and Jenkins, models are summarized as ARIMA (p, d, q). For example, a model described as ARIMA (1,1,1) means it contains 1 auto regressive parameter and 1 moving average parameter for the time series after it is differenced once to attain stationary. The general form of the ARIMA model describing the current value X_t of a time series is:

$$\varphi_1 (B) (1-B) X_t = \theta_1 (B) e_t \quad (8.1)$$

where φ_1= Auto regressive parameter, and θ_1= Moving average parameter

Seasonal ARIMA is a generalization and extension of the ARIMA method in which a pattern repeats seasonally over time. In addition to the non-seasonal parameters, seasonal parameters for a specified lag (established in the identification phase) need to be estimated. Analogous to the simple ARIMA parameters, these are: seasonal autoregressive (P), seasonal differencing (D), and seasonal moving average parameters (Q). The seasonal lag used for the seasonal parameters is usually determined during the identification phase and must be explicitly specified. For example, a seasonal ARIMA model described as $(1,1,1)(1,1,1)^{12}$ includes 1 auto regressive parameter,1 moving average parameter,1 seasonal auto regressive parameter and 1 seasonal moving average parameter for the time series after it is differenced once at lag 1 and differenced once at lag 12. The general form of the seasonal ARIMA model describing the current value X_t of a time series is:

$$(1-\varphi_1 B)(1-\alpha_1 B^{12})(1-B)(1-B^{12}) X_t = (1-\theta_1 B)(1-\gamma_1 B^{12}) e_t \quad (8.2)$$

where φ_1=Non seasonal auto regressive parameter, α_1=Seasonal auto regressive parameter

X_t=Current value of the time series, B=Backward shift operator $BX_t=X_{t-1}$ and $B^{12}X_t=X_{t-12,}$

1-B=First order non seasonal difference, $1-B^{12}$=First order seasonal difference,

θ_1=Non seasonal moving average parameter, γ_1=Seasonal moving average parameter,

e_t =Current error term of the time series

Four basic stages of ARIMA and seasonal ARIMA in identifying patterns in time series data and forecasting are model identification, parameter estimation, diagnostic checking and forecasting.

At the model identification stage, number of autoregressive (p), seasonal autoregressive (P), moving average (q) and seasonal moving average (Q) parameters necessary to yield an effective model of the process are decided. The data are examined to check for the most appropriate class of ARIMA processes through selecting the order of the regular and seasonal differencing required to make the series stationary, as well as through specifying the number of regular and seasonal auto regressive and moving average parameters necessary to adequately represent the time series model. The major tools used in the identification phase are plots of the series, correlograms (plot of autocorrelation and partial autocorrelation verses lag) of autocorrelation function (ACF) and partial autocorrelation function (PACF). The ACF measures amount of linear dependence between observations in a time series that are separated by a lag k. The PACF plot helps to determine how many auto regressive terms are necessary to reveal seasonality of the series or to reveal trend either in the mean level or in the variance level of the series.

At the parameter estimation stage, the parameters are estimated using a function minimization algorithm, to minimize the sums of squared residuals and to maximize the likelihood (probability) of the observed series, given the parameter values. To compute the

sums of squares (SS*)* of the residuals, the approximate maximum likelihood method is chosen as this method is the fastest and can be used for very long data sets. The maximum likelihood method uses the following criteria in parameter estimation: (1) The estimation procedure stops when the change in all parameters estimate between consecutive iterations reaches a minimal change of 0.001 and (2) The estimation procedure stops when the sum of squared residual(SSR) between consecutive iterations reaches a minimal change of 0.0001.

At the diagnostic checking stage, the residuals from the fitted model are examined against adequacy. This is usually done by correlation analysis through the residual ACF plots and good-of-fit test by means of chi-square statistics. If the residuals are correlated, then the model parameters should be adjusted in the model identification stage. Otherwise the model is adequate to represent the time series.

At the forecasting stage, the estimated parameters are used to calculate new values of the time series and confidence intervals for those predicted values. The estimation process is performed on transformed (differenced) data, hence before the forecasts are generated; the series needs to be integrated to cancel out the effect of differencing so that the forecasts are expressed in values compatible with the input data. This automatic integration feature is represented by the letter "*I"* in the name of the methodology (ARIMA = Auto-Regressive Integrated Moving Average).

8.2.1 SARIMA Model Development

One hundred ten years of monthly rainfall data averaged over each station of the study area by the ordinary Kriging method has been divided into two components: a calibration data set consisting of the first 90 years data (1901-1990) and a validation data set consisting of the remaining 20 years data (1991-2010). The calibration data set is used for identification of

autoregressive and moving average parameters and estimation of the identified parameters. However, the validation data set is used at the diagnostic stage to calculate new values of the series and 90% confidence intervals for those predicted values using the estimated parameters.

For determining the most appropriate seasonal ARIMA model for a given variable, Box-Jenkins (1970) methodology is applied which includes: identification of model parameters, estimation of model parameters and forecasting of new values of the variable. The input time series for ARIMA is required to be stationary and should have a constant mean, variance, and autocorrelation with respect to time.

By nature, the monthly rainfall time series exhibit a yearly periodicity. By plotting the monthly rainfall time series, seasonality and non-stationarity can be revealed. In the present case also from the plot of autocorrelation verses lag of autocorrelation function (ACF), the appearance of a sinusoidal function with a 12-month period has been observed for the monthly rainfall time series data. The time series models are usually fitted to the decaying part of the autocorrelation function (Delleur et. al., 1978). In an ARIMA model fitted to the 12-lag differenced series, the observation at a particular month is related to the observations taken during the same month of previous years. This gives rise to a multiplicative model for 12 month seasonality, called seasonal ARIMA $(p,d,q)*(P,D,Q)^{12}$model. The (p,d,q) part is the non-seasonal ARIMA model and the $(P,D,Q)^{12}$ is the seasonal part of the ARIMA model. The autocorrelation functions for the 12-lag differenced series are obtained for the monthly rainfall series for each of the 23 stations of the basin and a significant correlation at lag 12 is found in all the cases.

The ACF and PACF plots of the series show a regular pattern and confirm that the data sets are not stationary (Figure 8.1). The normal probability plots and histograms of the series

show complete departure from the expected normal value. Similar plots for other sub-basins are given in Appendix IV. In order to fit an ARIMA model, stationary series both in mean and variance is needed. For stationary of variance of the time series, a Box-Cox or power transformation (α=0.5) is applied to it. The series is differenced seasonally at lag 12 due to the seasonality present in it. After differencing again plots the ACF and PACF are checked for stationary. The ACF and PACF plots of the differenced series do not show any regular pattern, which means that the series is stationary after having seasonal differencing. Therefore the $(p,0,q)(P,1,Q)^{12}$ ARIMA model could be identified for the seasonally differenced series.

Next the number of p, q, P and Q parameters are estimated for the $(p,0,q)(P,1,Q)^{12}$ model. The ACF and PACF plots of the $(p,0,q)(P,1,Q)^{12}$ model with first order seasonal differencing suggest that at initial stage our tentative model should be $(1,0,1)(1,1,1)^{12}$.Again the ACF and PACF plots of the residuals resulted from fitting the $(1,0,1)(1,1,1)^{12}$ model showed no regular pattern and confirmed that the model is an appropriate representation of the monthly observed data sets and could be used for rainfall forecasting.

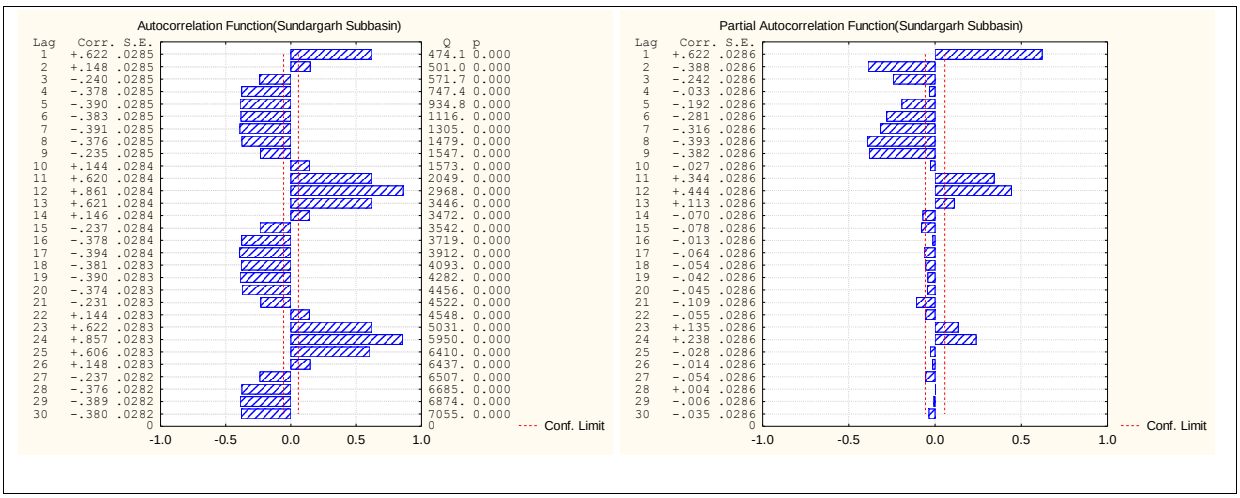

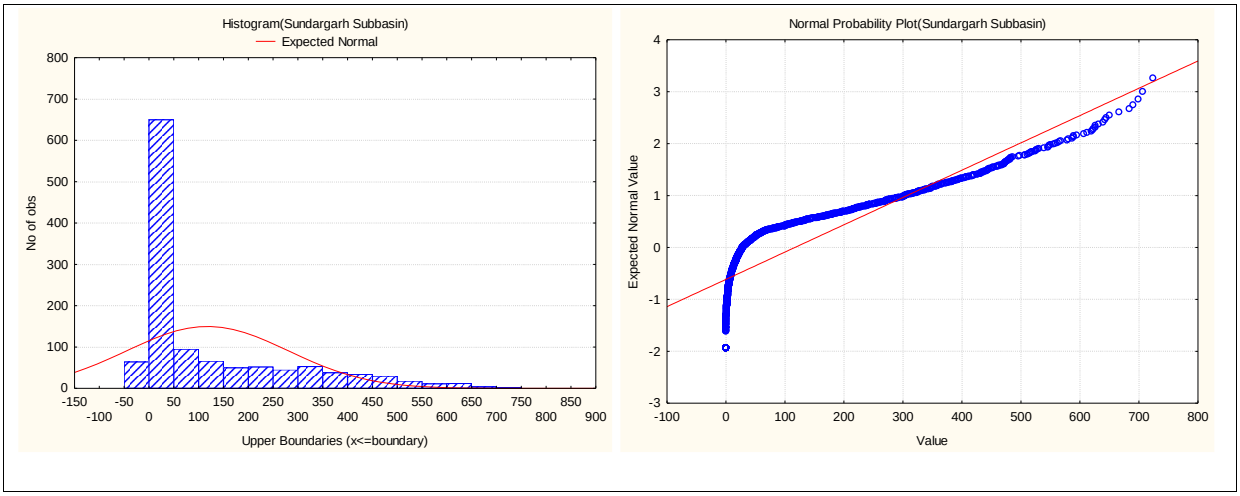

Figure 8.1: Time Series Plots of Monthly Rainfall Data of Sundargarh Sub-basin

Seasonal ARIMA $(P,D,Q)^{12}$ models resulted from differencing operations are useful for forecasting purposes. Therefore in order to analyze time series for mean monthly rainfall in the three sub-basins, the linear stochastic seasonal ARIMA models are used. Based on cross correlation, ACF and PACF, 9 different lumped data seasonal ARIMA models with various input combinations have been formulated to model the monthly rainfall and are evaluated by comparing the simulated rainfall with the hydrologic records. In all models box-cox transformed input time series are used. A non-seasonal lag of 1 and a seasonal lag of 12 are used for all models. Besides both non-differenced (d=0, D=0) and differenced (d=1, D=1) inputs are used in both the non-seasonal and seasonal parts of the models as listed out in Table 8.1.

Table 8.2: Seasonal ARIMA Models with different no. of parameter

Sl. No.	ARIMA Model	No. of Parameter	Sl. No.	ARIMA Model	No. of Parameter
1	$(1,0,1)(1,1,1)^{12}$	4	6	$(1,0,0)(1,1,0)^{12}$	2
2	$(1,0,1)(0,1,1)^{12}$	3	7	$(0,0,1)(1,1,1)^{12}$	3
3	$(1,0,1)(1,1,0)^{12}$	3	8	$(0,0,1)(0,1,1)^{12}$	2
4	$(1,0,0)(1,1,1)^{12}$	3	9	$(0,0,1)(1,1,0)^{12}$	2
5	$(1,0,0)(0,1,1)^{12}$	2			

The above mentioned 9 alternative seasonal ARIMA models are fitted to the time series of monthly rainfall data of 90 years (1901-1990) at each of 23 stations of the study area to select the best fitted one that can describe the inter-monthly variation of rainfall at that station. In ARIMA modeling we need to minimize the sum squared of residuals (SSR) between the actual and estimated values to represent the data most appropriately. But it is important to note that, the best ARIMA model should have the least number of parameters along with the minimum SSR. Therefore, in the stage of identifying the number of auto regressive and moving average parameters, the $(p,0,q)(P,1,Q)^{12}$ ARIMA model with least number of parameters is obtained. To accomplish the task, nine different $(p,0,q)(P,1,Q)^{12}$ ARIMA models with nine combinations of these four parameters are tested to find out the most appropriate model.

8.2.2 Model Performance Evaluation Criteria

8.2.2.1 Diagnostic checks

After different models has been fitted to the data, it is important to perform diagnostic checks to test the adequacy of each model. One way to accomplish this is through the analysis of residuals. It has been found that it is effective to measure the overall adequacy of the chosen model by examining a quantity Q known as Ljung-Box statistic (modified Box-Pierce statistic), (Yurekli et. al.; 2005, Sallehuddin et. al.; 2007, Mauludiyanto et. al.; 2010, Martins et. al.; 2011, Landeras et. al.; 2009) which is a function of autocorrelations of residuals and its approximate distribution is Chi-square. The diagnostic check stage determines whether residuals are independent or not. The residuals independence can be determined by obtaining the residual autocorrelation function (RACF) using the Q(r) statistic suggested by Ljung and Box (1978).A test of this hypothesis can be done for the model adequacy by choosing a level

of significance and then comparing the value of the calculated X^2 to the actual X^2 value from the table i.e. the Q(r) statistic is compared to critical values from Chi-square distribution. If the calculated value is less than the actual X^2 value, then the model is adequate, otherwise not i.e. if the model is correctly specified, residuals should be uncorrelated and Q(r) should be small (probability should be large). A significant Q(r) value indicates that the chosen model does not fit well. The Q(r) statistic calculated by the Ljung-Box statistic which can be expressed as

$$Q(r) = n(n+2)\sum r^2(j)/(n-j) \tag{8.3}$$

where n is the number of observations in the series and r (j) is the estimated correlation at lag j. Therefore, to obtain the best model, diagnostic checking of non-significance of autocorrelations of residuals via Ljung-Box test (modified Box-Pierce test) (Q-test based on Chi-square statistics) is performed.

8.2.2.2 Akaike Information Criterion

The criterion for selecting the most appropriate model in time series analysis is that several models appropriate for representing a given set of data may be used. Sometimes, the choice is easy, but other times, it may be much difficult. Therefore, numerous criteria are introduced for comparing models that are different from methods of model recognition. Some of them are based on statistics summarized from residuals that are computed from a fitted model. In the present study Akaike Information Criterion (AIC) is considered. AIC is an information criterion for model selection based on the statistical likelihood function.AIC can be computed from least square statistics, using the following expression

$$AIC = n\ log\ (SSR/n)\ +\ 2k \tag{8.4}$$

where SSR is the sum squared of residuals, n is the sample size and k is the number of parameters. The best model in a set can be the one which has the minimum AIC value.

8.2.2.3 Error analysis

There is no single performance criterion available to select the best model. Rather many performance criteria are used to select the best one. Each performance criteria indicates a particular capability of the model and hence various measures are used. But all the performance criteria are estimated based on the observed and predicted values. In the present study, to identify the best fitted model, the predicted values using the 9 different seasonal ARIMA models are compared to the observed data of the validation period (1991-2010).

In the present work, to evaluate the performance of the best ARIMA model at each station, two different measures are used to select the best model: coefficient of determination (R^2) and model efficiency (E_{NS}) which can be expressed as given below in the following equations.

$$R^2 = \frac{[\sum(R_o-\overline{R_o})(R_f-\overline{R_f})]^2}{\sum(R_o-\overline{R_o})^2\sum(R_f-\overline{R_f})^2} \tag{8.5}$$

$$E_{NS} = 1 - \frac{\sum(R_o-R_f)^2}{\sum(R_o-\overline{R_o})^2} \tag{8.6}$$

where R_o is the observed rainfall at time t, R_f is the forecasted rainfall at time t, and $\overline{R_o}$ and $\overline{R_f}$ are mean values of observed and forecasted rainfall series. The E_{NS} is the difference, on average, of the observed and predicted data and offers a general picture of the errors involved in prediction. R^2 gives impartial result as it takes mean values of both the observed and predicted data.

8.3 ARTIFICIAL NEURAL NETWORK (ANN) MODEL

Artificial Neural network (ANN) is a very sophisticated modeling technique capable of modeling extremely complex functions. Although we do need to have some heuristic knowledge of how to select and prepare data, how to select the appropriate neural network, and how to interpret the results, the level of knowledge needed to successfully apply neural networks is much lower than those needed in most traditional statistical tools and techniques.

8.3.1 Model Development

For the present study 110 years (1901-2010) of monthly rainfall data of 23 stations of the study area are used to train, test and validate a neural network and for this purpose a multilayer perceptron (MLP), has been used. The MLP networks are quite compact, execute quickly once trained but require iterative training. Before modeling of the data, it is preprocessed by limiting the numerical range of the input and target variables (rainfall values at different time steps), known as scaling process using linear transformations such that the original minimum and maximum of the target variable is mapped to the range (0, 1). The multilayer perceptron (MLP) neural networks have been generated using the sum of squares error function. The neurons of a network have activation functions that transform the incoming signals from the neurons of the previous layer using a mathematical function. The choice of the activation function, i.e., the precise mathematical function, is crucial in building a neural network model since it is directly related to the performance of the model. Here hyperbolic tangent (tanh) and identity functions for the hidden and output neurons respectively have been chosen as activation function for MLP networks. The hyperbolic tangent (tanh) is a symmetric s-shaped (sigmoid) function, whose output lies in the range (-1,

+1). With the identity function, the activation of the neurons is passed on directly as the output of the neurons and the output lies in the range $(-\infty, +\infty)$.

The process of adjusting the weights connecting the inputs to the hidden neurons and the hidden neurons to the output neurons so that the network can approximate the underlying functional relationship between the inputs and the targets is known as training. Neural networks are highly nonlinear tools that are usually trained using iterative training algorithms. MLP networks can be trained with various training algorithms, including Gradient Descent, Conjugate Gradient and BFGS (Broyden- Fletcher-Goldfarb-Shanno) Quasi-Newton Back Propagation. To choose the best training algorithm, MLP networks are developed with these three training algorithms using the 1^{st}-1080^{th} data of the original series. It has been observed that with BFGS the coefficient of determination (R^2) values of the MLP networks during the validation phase is highest and therefore the BFGS is the best one being selected as the training algorithm in this study. BFGS is much more efficient method than steepest descent method. It is a second derivative and line search method. Therefore this algorithm requires a smaller number of iterations to train a neural network given its fast convergence rate and more intelligent search criterion.

The performance of neural network is measured by how well it can predict unseen data not included in training data set. This process is known as generalization and neural network has the remarkable generalization ability. During training neural networks have tendency of over-fitting the training data accompanied by poor generalization. To combat the problem of over-fitting and tackling the poor generalization issue, testing data set is used which is never used for training. Instead, it is used as a mean of validating how well a network makes progress in modeling the input-target relationship as training continues. That means a neural network is optimized using a training data set. The testing data set is used to halt training to mitigate

over-fitting. The process of halting neural network training to prevent over-fitting and improving the generalization ability is known as early stopping. Just like the testing data set, a validation data set which is never used for training the neural network but is used to check the generalization ability of the neural network after the training is over. If the performance of the network is found to be consistently good on both the testing and validation data set, then it is reasonable to assume that the network generalizes well on unseen data. In this study the 110 years of mean monthly rainfall sample is divided sequentially into three parts: training sample, test sample which are two parts of calibration data set and the third part is validation data set. The train sample size, test sample size and validation sample size are from 1901-1990 (1080 observations), 1991-2002 (144 observations) and 2003-2010 (96 observations) respectively of the total sample size. The test sample is taken to prevent the network from over-fitting during training process and the validation sample is taken to evaluate the generalization ability of the trained network.

8.4 EVALUATION OF SARIMA MODEL

In the present study there are 1320 number of observations, out of which 1080 number of observations (1901-1990) are used for model calibration and the rest 240 number of observations (1991-2010) are used at the validation stage. After computing the SSR values, the AIC values for all the nine models are computed using the equation (8.4) with the number of parameters as mentioned in Table 8.1. The best model for each station is selected based on minimum AIC value. On the basis of the AIC values, $(0,0,1)^1(0,1,1)^{12}$ and $(1,0,0)^1(0,1,1)^{12}$ models provides best results in comparison to other models. The ACF and PACF plots of the residuals resulted from the $(1,0,0)(0,1,1)^{12}$ and $(0,0,1)^1(0,1,1)^{12}$ models do not show any regular pattern and confirm that the model is adequate to represent observed data and could be used to forecast the rainfall data. Summary of the best fitted SARIMA model for all the 23

stations is given in Appendix IV. Table 8.2 shows best fitted model architecture of each sub-basin along with their performance in terms of correlation coefficient in both calibration and validation stages.

Table 8.2: Best Fitted Seasonal ARIMA Model of Sub-basins

	Non-seasonal Differencing=0,Non-seasonal Lag=1, Seasonal Differencing=1,Seasonal Lag=12		
Subbasin	**Model Architecture**	**Calibration Performance**	**Validation Performance**
		Correlation Coefficient (R)	
Sundargarh	$(0,0,1)^1(0,1,1)^{12}$	1.000	0.923
Salebhatta	$(1,0,0)^1(0,1,1)^{12}$	1.000	0.808
Kesinga	$(1,0,0)^1(0,1,1)^{12}$	1.000	0.852
Kantamal	$(1,0,0)^1(0,1,1)^{12}$	1.000	0.836
Tikarpada	$(0,0,1)^1(0,1,1)^{12}$	1.000	0.850

In addition, we measured the goodness-of-fit of the $(1,0,0)(0,1,1)^{12}$ model by means of a quantity Q known as Ljung-Box statistic using equation (8.3), which is a function of autocorrelations of residuals and its approximate distribution is Chi-square. The p value for the autocorrelations of residuals from the $(1,0,0)(0,1,1)^{12}$ and $(0,0,1)^1(0,1,1)^{12}$ models up to lag 36 is above 0.05 for all the 23 stations, which indicates the acceptance of the null hypothesis of model adequacy at the 5% significance level. Therefore the set of autocorrelations of residuals are not significant. Finally, this concludes that the $(1,0,0)(0,1,1)^{12}$ and $(0,0,1)^1(0,1,1)^{12}$ ARIMA models are adequate to represent our data and could be used to forecast the upcoming rainfall data.

The coefficient of determination (R^2) is obtained from scatter plot of observed and simulated monthly rainfall for the validation data set using the best fitted seasonal ARIMA model for 23 rain gauge stations and it is found that that the coefficient of determination (R^2) is

satisfactory for all the stations. High value of R^2 reveals that the best fitted seasonal ARIMA model for each station has very well described its inter-monthly variation of rainfall.

The model efficiency (E_{NS}) is obtained for the validation data set using the best fitted seasonal ARIMA model for the 23 stations of Mahanadi river basin and it is found that the model efficiency (E_{NS}) of seasonal ARIMA for all the 23 stations is satisfactory. A model efficiency of ≥ 0.5 indicates acceptable performance. Therefore the best fitted seasonal ARIMA has very good ability to model and forecast the monthly rainfall series of the 23 stations.

After selecting $(1,0,0)(0,1,1)^{12}$ and $(0,0,1)^1(0,1,1)^{12}$ as the best ARIMA models, next task is to estimate values of its parameters p and Q. After estimating the parameters p and Q, rainfall values are computed and compared with the actual values. From comparison between the observed values and the ones resulted from the best fitted ARIMA models of each sub-basin using the estimated parameters, for the period between 2003 and 2010 of the validation stage, it is observed that the model is good enough to forecast rainfall, which may be used for proper utilization of the available water resources in future in Mahanadi river basin and sub-basins lying in Odisha.

Forecasting or predicting future is one of the main purposes for developing time series models. Therefore estimated values of the parameters p and Q were used to forecast 24 upcoming rainfall data .The forecasted values resulted from the best fitted ARIMA models of each sub-basin were compared with the real values of the period from 2011 to 2012. Figure 8.2 shows a comparison between the real values and the ones forecasted from the developed seasonal ARIMA model for the period between 2011 and 2012.The same figure shows a scatter plot between the observed rainfall and the forecasted rainfall for the same period.

From visual inspection of the graphical plot obtained for the actual series versus the predicted series, it was quite evident that the chosen model was good enough as the predicted series was very close to the actual series.

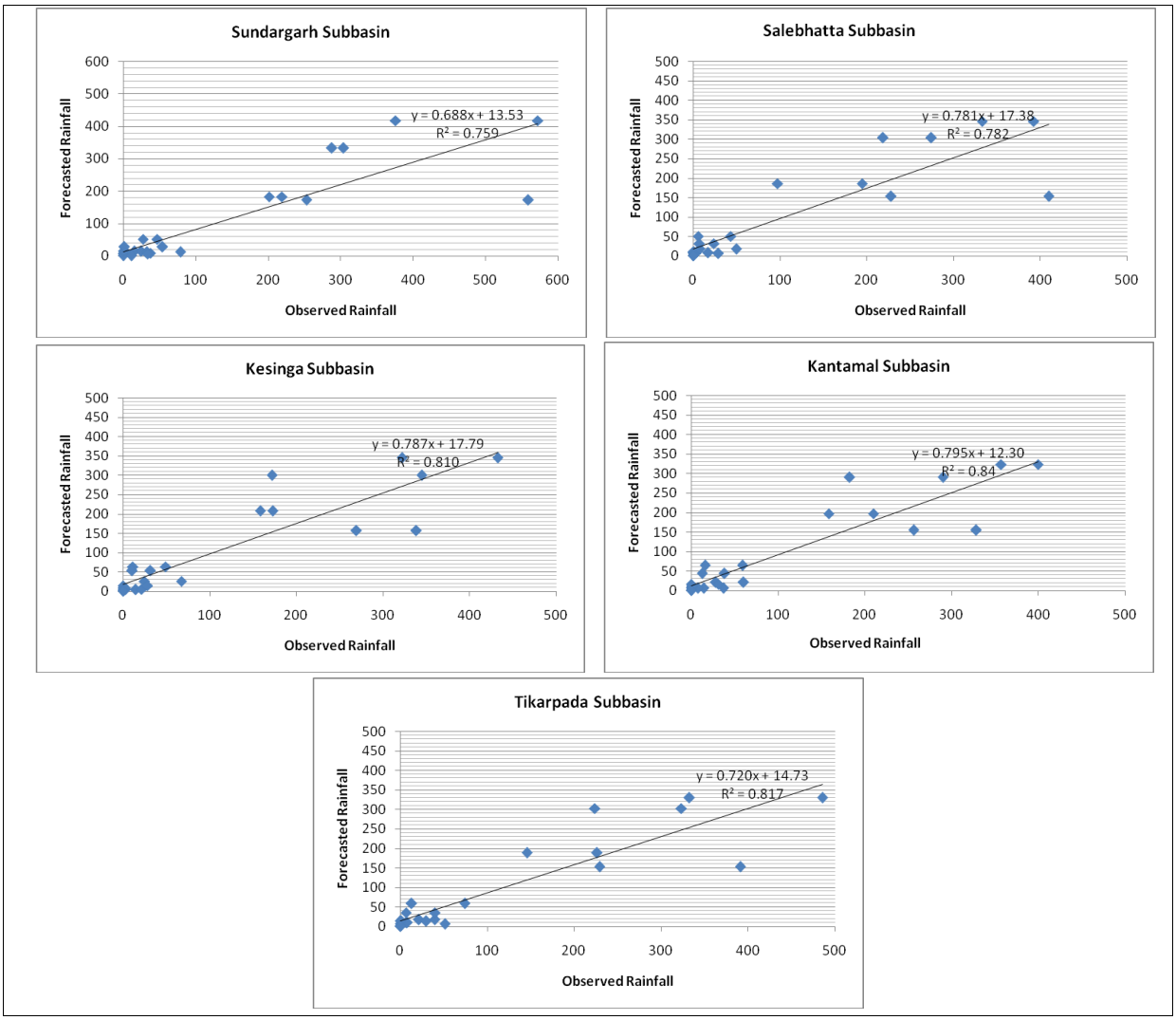

Figure 8.2: Forecasting Performance of Best Fitted SARIMA Model for Sub-basins

8.5 EVALUATION OF ANN MODELS

For the present study, 110 years (1901-2010) of monthly rainfall data of 23 stations of Mahanadi Basin are used to train, test and validate a neural network. Past studies have proven that a three-layer ANN model with one hidden layer is sufficient to handle any nonlinear data, if the number of hidden neurons is selected correctly. Therefore in this study, the three-

layer MLP (multi-layer perceptron) network is chosen. The time series contains a natural cycle of 12-months period and hence the data of present month has maximum correlation with the data of 12 months lag. For all the 23 stations the R^2 value increases fast with increase in the number of neurons in the input layer up to 12, but after 12 the R^2 value does not vary considerably for validation of the MLP network. Therefore, the optimum number of neurons in the input layer is chosen as 12. Therefore feed-forward MLP neural networks with an input layer of number of neurons from 1 to 12 (with time lag from t-1 to t-12), one hidden layer and an output neuron (of time t) are used. That means the network predicts rainfall for the next time step from a series of previous twelve time steps. The choice of optimal number of neurons in the hidden layer depends on the problem domain and is a trial and error procedure but, generally, it can be related to the number of neurons in the input layer. Therefore networks with hidden neurons from 2 to 8 have been tried to find out optimal design of the MLP neural network. The optimum number of neurons in the hidden layer is chosen based on R^2 value of the validation performance of the MLP network. Hence the best ANN model for each station is chosen with the numbers of neurons in the hidden layer giving maximum R^2 during validation phase of the MLP network. Summary of the optimum number of hidden layer neuron for all the 23 stations is given in appendix IV. Table 8.3 shows best fitted ANN architecture of each sub-basin along with their performance in terms of correlation coefficient in both calibration and validation stages.

Table 8.3: Best Fitted MLP ANN Model of Sub-basins

	Input= Rainfall$_{t-1}$, Rainfall$_{t-2}$, Rainfall$_{t-3}$, Rainfall$_{t-4}$, Rainfall$_{t-5}$, Rainfall$_{t-6}$, Rainfall$_{t-7}$, Rainfall$_{t-8}$, Rainfall$_{t-9}$, Rainfall$_{t-10}$, Rainfall$_{t-11}$, Rainfall$_{t-12}$			
Subbasin	**Network Architecture**	**Training Performance**	**Testing Performance**	**Validation Performance**
		Correlation Coefficient		
Sundargarh	12-8-1	0.938	0.942	0.825
Salebhatta	12-6-1	0.933	0.910	0.793
Kesinga	12-6-1	0.900	0.886	0.792
Kantamal	12-6-1	0.906	0.900	0.801
Tikarpada	12-2-1	0.913	0.913	0.779

Using the best fitted MLP ANN model described in the previous sections, monthly rainfall were predicted for the period from January 2011 to December 2012, in order to evaluate the forecasting performance of the developed model. To compare the forecasting performance of the best fitted ANN models with optimum number of hidden neurons of the MLP network, two error measures were introduced, the coefficient of determination (R^2) and model efficiency (E_{NS}) of the forecasting performance. The expressions of these two error measures have already been discussed in the seasonal ARIMA model section. R^2 value is influenced by distribution of forecasted data with original data and is an unbiased interpreter of the forecasting performance. The monthly rainfall prediction performances of the MLP ANN model in terms of coefficient of determination for the forecasting (2011-2012) period is shown in figure 8.3 for the six sub-basins.

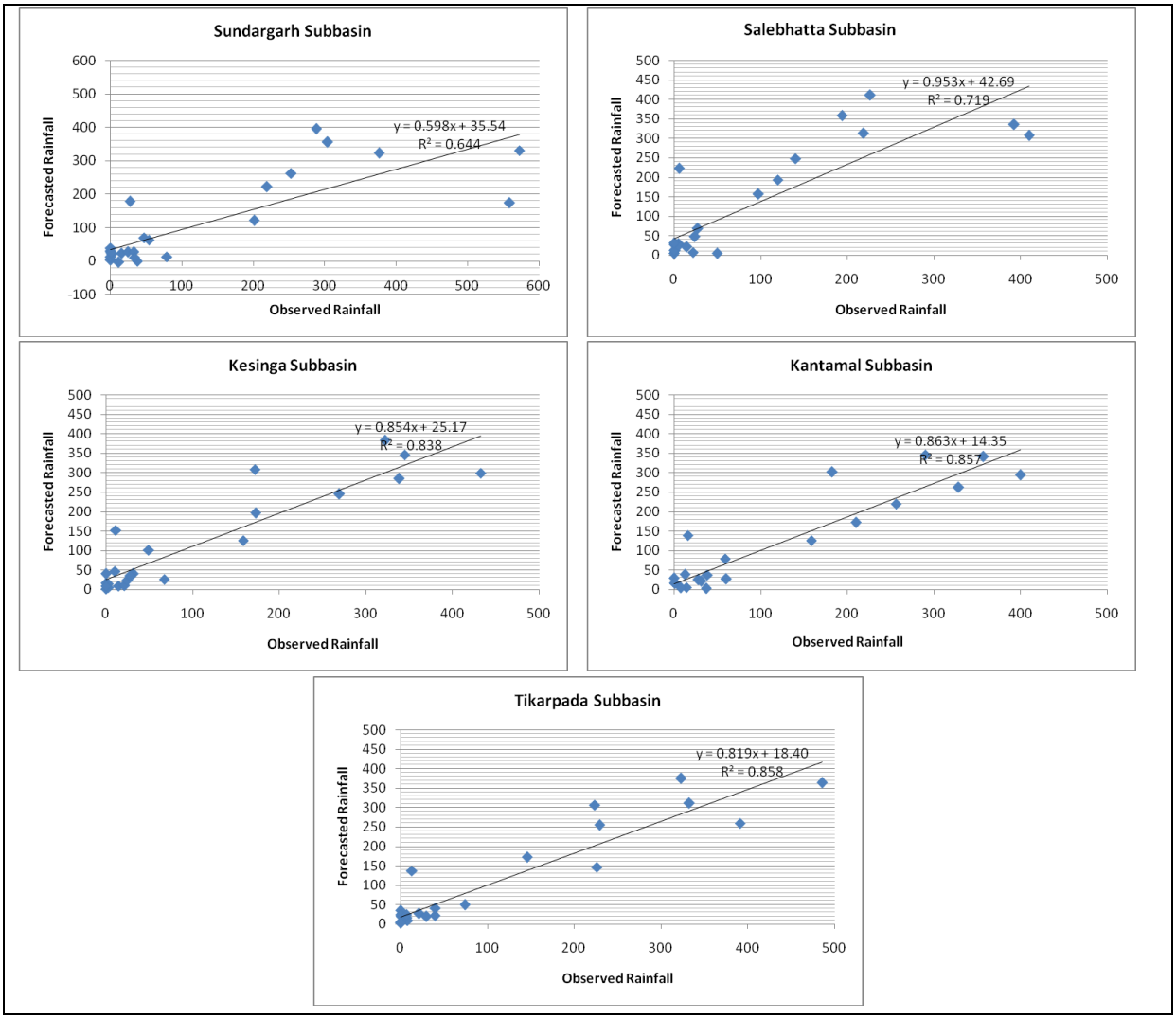

Figure 8.3: Forecasting Performance of Best Fitted MLP ANN for Sub-basins

8.6 PERFORMANCE COMPARISON OF SARIMA AND ANN MODELS

For comparison of performance measures of the two developed models, in terms of the statistical measure, model efficiency (E_{NS}) of the sub-basins were computed. The monthly rainfall prediction performances of both the SARIMA and MLP ANN models in terms of model efficiency for the forecasting period (2010-2012) are shown in table 8.4(a) and 8.4(b) for the five sub-basins. It can be observed that for Kantamal, Kesinga ,Tikarpada and Salebhatta sub-basins R^2 and E_{NS} values of MLP ANN are better than that of the seasonal

ARIMA model and for the Sundargarh sub-basins the R^2 and E_{NS} values of MLP ANN model is lower than the other model(though its value is relatively lower than that of other sub-basins) . Though the difference in R^2 and E_{NS} values for the two models is not so high, but the forecasting performance of MLP ANN model is considerably better.

Table 8.4(a): ARIMA and ANN Model Performance Comparison

Subbasin	Mean			Standard Deviation		
	Observed Rainfall	Forecasted Rainfall(ARIMA)	Forecasted Rainfall(ANN)	Observed Runoff	Forecasted Rainfall(ARIMA)	Forecasted Rainfall(ANN)
Sundargarh	130.771	103.621	113.827	176.346	139.421	131.472
Salebhatta	81.736	93.649	120.646	122.769	121.346	138.055
Kesinga	103.207	99.077	113.414	137.716	120.509	128.573
Kantamal	103.801	94.892	103.975	132.092	114.668	123.124
Tikarpada	110.526	94.399	108.960	147.325	117.426	130.309

Table 8.4(b): ARIMA and ANN Model Performance Comparison

Subbasin	R^2		E_{NS}	
	ARIMA	ANN	ARIMA	ANN
Sundargarh	0.759	0.645	0.581	0.349
Salebhatta	0.691	0.719	0.652	0.663
Kesinga	0.810	0.839	0.750	0.809
Kantamal	0.840	0.858	0.780	0.836
Tikarpada	0.818	0.858	0.682	0.816

Forecasting performance of the SARIMA and MLP ANN models for the six sub-basins in terms of time series representation is shown in figures 8.2 and 8.3 respectively. These graphs clearly indicate that both the SARIMA and the MLP ANN models are unable to touch the peaks in demonstrating monthly rainfall of Mahanadi river basin. From table 8.4, it can be observed that the MLP ANN model seemed to show better performance compared to the SARIMA with higher values of R^2 and E_{NS} for the forecasting period. No significant difference was observed between the two models in modeling and forecasting monthly rainfall with both the calibration and validation datasets. This again shows that although the two models are different in structure and algorithm, they are essentially using the same information i.e. previous monthly rainfall to forecast future rainfall values. The performance of ANN model may be even better if there were more information such as temperature and humidity etc. to make the system nonlinear and to map the nonlinear system through the MLP neural network. Therefore MLP ANN model is further considered for rainfall forecasting.

8.7 RUNOFF COMPUTATION WITH DEVELOPED CN EQUATION USING FORECASTED RAINFALL FROM SARIMA MODEL

Prediction of future rainfall is essential for development of water resources management scenarios, at watershed, sub-basin and basin scale. For rainfall forecasting reliable historic time series data is required. In the present study 110 years (1901-2010) of monthly rainfall data are analyzed to develop a theory-driven model and a data-driven model. Seasonal ARIMA and MLP ANN models were developed for forecasting of rainfall. Simulation performance of these two models at validation stage is very good. But SARIMA model is applied to forecast monthly rainfall of two years (2011-2012) and it is found that forecasting performance of this model is above satisfactory. From table 8.4 it can be stated that the SARIMA model can be adopted for future monthly rainfall prediction with up to 85% accuracy.

After forecasting of rainfall the next task in hydrological modeling is simulation of runoff with the forecasted rainfall. Therefore twenty four forecasted monthly rainfall values of two years from the SARIMA model are applied in the SCS-CN method to compute runoff. Forecasted monthly rainfall of stations was interpolated using Ordinary Kriging method to derive forecasted monthly rainfall of sub-basins. Observed monthly runoff values for these two years (2011 and 2012) of Sundargarh, Tikarpada, Salebhatta, Kantamal and Kesinga stations were applied at their respective sub-basins. For runoff computation CNs for the three AMCs was computed with the three developed equations of each sub-basin shown in chapter 7. Then using equations (6.5) and (6.4) respectively, potential retention S and direct runoff Q were computed. Finally the computed runoff was compared with the observed runoff.

Simulation performance of the SCS-CN method with forecasted rainfall from the developed SRIMA model for the five sub-basins is shown in Figure 8.4 in terms of scatter plot. Moderate coefficient of determination values indicates moderate simulation performance of the developed SARIMA model for rainfall forecasting. This figure also shows the time series plot of observed runoff and runoff computed with the SCS-CN method and it can be observed that the computed runoff could not match so well with the observed runoff. Extreme values could not be simulated very nicely. Some low values were over predicted and some high values were under predicted.

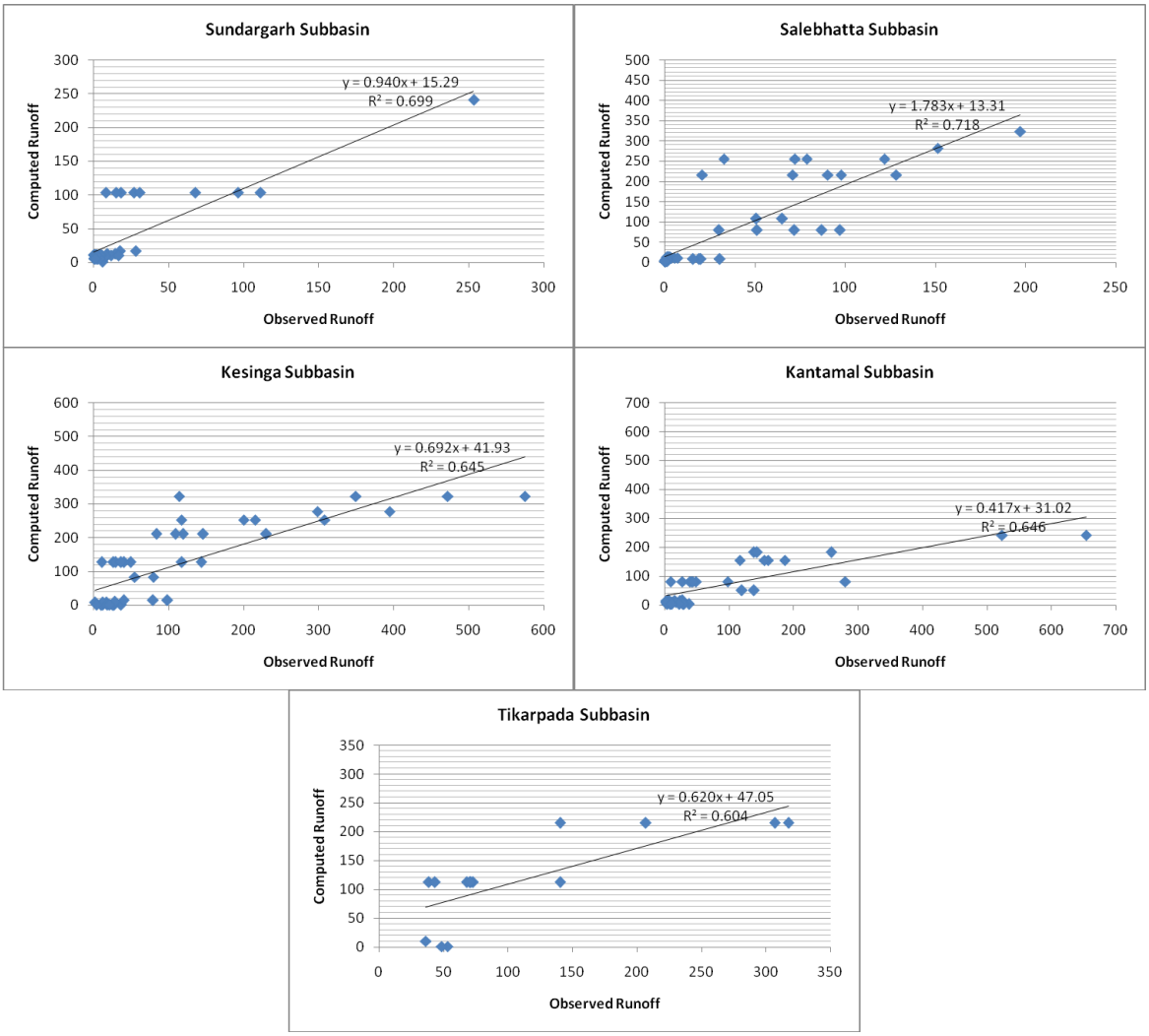

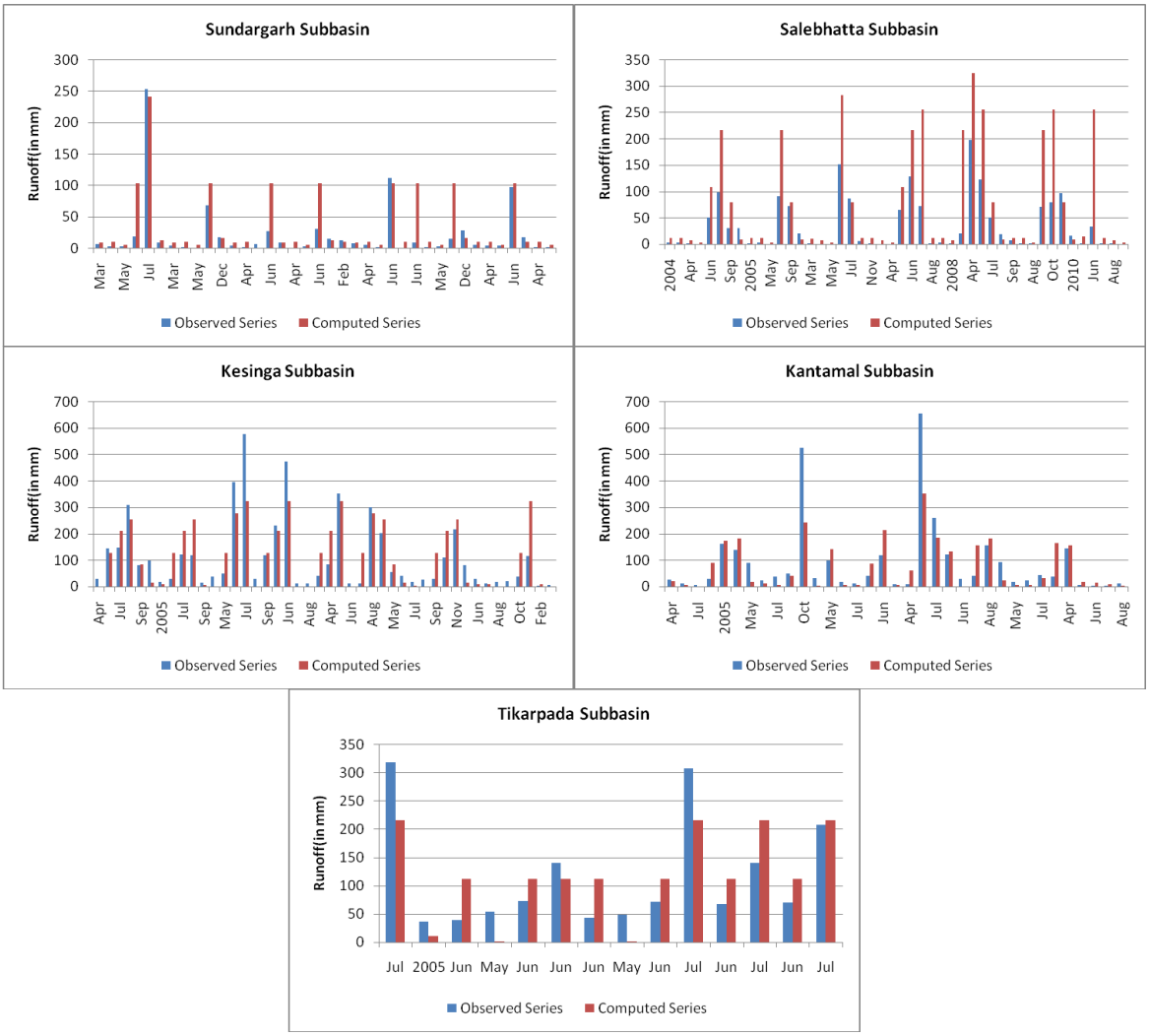

Figure 8.4: Simulation Performance of SCS-CN Method with SARIMA Monthly Forecasted Rainfall

8.8 CONCLUSION

Monthly rainfall was forecasted using seasonal ARIMA and MLP-ANN models and it was found that in case of monthly rainfall forecasting both the seasonal ARIMA and MLP-ANN models performances are comparable. Runoff was computed with developed CN equation using forecasted rainfall from both the SARIMA and MLP-ANN models and it was found that though performance of MLP-ANN was better than that of SARIMA,it was not considerably better.

CHAPTER 9

CONCLUSIONS

In the present work, rainfall and rainfall generated runoff has been estimated using various approaches for different functional analysis. The following conclusions are drawn.

1. The study area is delineated precisely into basin and sub-basins using Arc-SWAT, which is a very convenient and less time consuming way within the environment of Arc-GIS. Many Thematic maps are also developed in GIS environment precisely, which are very useful inputs in rainfall-runoff analysis. The thematic map developed from a variety of perspectives of the basin provides a view of the water shed and are used for hydrological analysis of Mahanadi river basin and sub-basins lying in Odisha, India.
2. The application of point rain gauge as precipitation input carries lots of uncertainties. Spatial interpolation, to estimate spatially continuous mean rainfall at sub-basin scale, using deterministic and geo-static approaches are found to be very effective in the study area. The geo-statistical interpolation methods, Ordinary Kriging (OK) with exponential semi-variogram model provided best results of daily and monthly rainfall with minimum mean and root mean square error (RMSE) values as given in Table 5.1.
3. The original SCS-CN model has been used in the present work by providing satellite based land use map and soil map delineated in GIS environment, as input. The results are found good for monthly rainfall-runoff simulation. However the method is found not appropriate for daily rainfall-runoff simulation.
4. Three models (Mishra-Singh, Michel and Sahu) modified on the basis of original SCS-CN are used for daily rainfall-runoff simulation. The results are found to under-estimate /

over-estimate the estimated runoff and are poorly correlated. These models are not applicable for monthly rainfall-runoff modeling.

5. Three models (FDM-PE, MM-SCS and ANN-MLP) are tested for their applicability along with other existing models. Out of seven models, MM-SCS model provided best results for daily and monthly rainfall-runoff data series. The other proposed models FDM-PE and ANN-MLP also provided reasonably good results. It is interesting to note that FDM-PE model provides best fit equation (Power equations) to estimate probabilistic curve number (PCN), which is very simple and useful, if established once for a basin or sub-basin.
6. It is understood that, the CN values for estimating runoff potential are policy decision. The CN varies at daily, weekly, half-monthly, monthly, seasonally and annually. It is found essential to carry out the required analysis to establish CN for any given rainfall duration between 1-day to 30-days for the policy makers and decision makers. The derived equations are tested for their applicability and CN values are re-estimated for different cumulative rainfall durations. The results shown in Table 7.1, substantiates the suitability of the developed second order regression polynomial equations for AMC I, AMC II and AMC III, which can be used directly for each sub-basin for any rainfall duration ranging between 1-day to 30-day.
7. In India, monthly rainfall data are easily available from different resources. In this context, if monthly rainfall forecasting models are developed, the monthly runoff estimates can be easily obtained, which is useful for planners and policy makers to make best use of available water resources. For this purpose, performance of SARIMA is tested and the models $(1,0,0)(0,1,1)^{12}$ and $(0,0,1)^{1}(0,1,1)^{12}$ are found to provide very good results with high correlation statistics and minimum errors. In addition, ANN-MLP has been used too for rainfall forecasting. The model

architecture 12-8-1, 12-6-1, 12-2-1 provided very good results. As can be seen from Table 8.2 and 8.3, the results obtained using both the methods are comparable.

8. After forecasting of rainfall the next task in hydrological modeling is the simulation of runoff with the forecasted rainfall. Therefore twenty four forecasted monthly rainfall values of two years from the SARIMA and MLP ANN models are applied in the SCS-CN method to compute runoff. The outcome of the forecasting models based on MLP ANN, is found to be better, but not much higher than the other model. It requires more input data sets and better training algorithm. Therefore the results obtained using SARIMA were accepted.

CHAPTER 10

SCOPE OF FUTURE STUDY

1. Further analysis is required to explore different deterministic and geo-static techniques suitable for spatial interpolation of rainfall.
2. Additional basin characteristics such as slope, geology, morphology and surface roughness features may be included to obtain more robust mean rainfall and runoff estimates.
3. In-situ soil moisture, wetness index, climate variability (evapo-transpiration, temperature, humidity, wind speed etc) and groundwater variables (infiltration rate, water table, hydraulic conductivity, field capacity etc) need to be included as input parameters in SCS-CN based methods.
4. Exhaustive analysis is needed to derive Curve Numbers for any rainfall duration by using more input rainfall data of longer durations.
5. Similarly, improvements are required in rainfall forecasting methodology and their application in runoff estimation.
6. The present study area covers Mahanadi basin lying in Odisha, India, which may be extended to the entire Mahanadi basin.

REFERENCES

Abrahart, R. J. and See, L. (2000) "Comparing neural network and autoregressive moving average techniques for the provision of continuous river flow forecasts in two contrasting catchments" Hydrological Processes, 14(11-12), 2157-2172.

Abtew, W. Obeysekera, J. and Shih, G. (1993) "Spatial analysis for monthly rainfall in South Florida" Journal of American Water Resources Association, 29(2), 179-188.

Akaike, Hirotugu. (1974) "A New Look at the Statistical Model Identification" IEE Transactions on Automatic Control, 19 (6), 716–723.

Abudu, S. Cui, C. King, J. P. Abudukadeer, K. (2010) "Comparison of performance of statistical models in forecasting monthly streamflow of Kizil River, China" Water Science and Engineering, 3(3), 269-281.

Abudu, S. King, J.P. and Pagano, T.C. (2010) "Application of Partial Least-Squares Regression in Seasonal Streamflow Forecasting", Journal of Hydrologic Engineering, 15(8), 612-623.

Abudu, S. King, J. P. and Bawazir, A. S. (2011) "Forecasting monthly streamflow of spring-summer runoff season in Rio Grande headwaters basin using stochastic hybrid modeling approach" Journal of Hydrologic Engineering, 16(4), 384–390.

Adamowski, J. and Karapataki, C. (2010) "Comparison of multivariate regression and artificial neural networks for peak urban water-demand forecasting: Evaluation of different ANN learning algorithms" Journal of Hydrologic Engineering, 15(10), 729–743.

Agnese, C. Grillone, G. and D'Asaro, F. (2008) "Comparison of temperature data collected in urban and agricultural areas surrounding" Italian Journal of Agrometeorology, 13 (1), 48-49.

Akhondi, E. (2001) “Analyzing curve number model in estimating flood by using geographical information systems” MA dissertation, The Faculty of Natural Resources and Maritime Sciences, Tarbiat-e-Modarres University.

Akhtar, M.K. Corzo, G.A. Andel, S.J.V. and Jonoski, A.(2009) “River flow forecasting with Artificial Neural Networks using satellite observed precipitation pre-processed with flow length and travel time information: case study of the Ganges river basin” Hydrology and Earth System Sciences Discussion, 6, 3385–3416.

Anctil, F. and Lauzon, N. (2004) “Generalisation for neural networks through data sampling and training procedures, with applications to streamflow predictions” Hydrology and Earth System Sciences, 8(5), 940–958.

Anctil, F. and Rat, A. (2005) “Evaluation of neural network streamflow forecasting on 47 watersheds” Journal of Hydrologic Engineering, 10(1), 85–88.

Andr´eassian, V. Perrain, C. Michel, C. Usart-Sanchez, I. and Lavabre, J. (2001) “Impact of imperfect rainfall knowledge on efficiency and the parameters of watershed models” Journal of Hydrology, 250, 206–223.

Ashri, A. A. M. Baki, A. M. and Atan, I. (2011) “Synthetic Simulation of Stochastic Rainfall-Runoff Model” UMTAS 2011, 140-146.

Asokan, S.M. and Dutta, D.(2008) “Analysis of water resources in the Mahanadi River Basin, India under projected climate conditions” Hydrological Processes. 22, 3589–3603.

Asokan, S. M. Jarsjö, J. and Destouni, G.(2010) “Vapor flux by evapotranspiration: Effects of changes in climate, land use, and water use” Journal of Geophysical Research,115,1-8.

Asokan, S. M. (2013) “Hydro-climatic change in irrigated world regions” Department of Physical Geography and Quaternary Geology, Stockholm University, Sweden.

Babul, S.K. Khadar, Karthikeyan, K. Ramanaiah, M. V. Ramanah, D. (2011) "Prediction Of Rain-Fall Flow Time Series Using Auto-Regressive Models" Advances In Applied Science Research, 2 (2), 128-133.

Baltas, E.A. Dervos, N.A. and Mimikou, M.A. (2007) "Technical Note: determination of SCS Initial Abstraction Ratio in an Experimental Watershed in Greece" Hydrology and Earth System Sciences, 11, 1825-1829.

Basistha, A. Arya, D.S. and Goel, N.K.(2008) "Spatial distribution of rainfall in Indian Himalayas - a case study of Uttarakhand region" Water Resources Management, 22(10), 1325-1346.

Beek, E.G. Stein, A. and Janssen, L.L.F. (1992) "Spatial variability and interpolation of daily precipitation amount" Stochastic Hydrol. Hydraul., 6(4), 304-320.

Bell, V.A. and Moore, R.J. (2000) "The sensitivity of catchment runoff models to rainfall data at different spatial scales" Hydrology and Earth System Sciences, 4(4), 653-667.

Beven, K.J. (2001) "Rainfall-runoff Modelling", The Primer, Wiley, Chichester.

Beven, K. (2001) "How far can we go in distributed hydrological modelling?" Hydrology and Earth System Sciences, 5, 1–12.

Birinci, V. and Akay, O. (2010) "A Study on Modeling Daily Mean Flow with MLR, ARIMA and RBFNN" BALWOIS 2010 - Ohrid, Republic of Macedonia.

Bo, X. Qing-Hai, W. Jun, F. Feng-Peng, H. and Quan-Hou, D. (2011) "Application of the SCS-CN Model to Runoff Estimation in a Small Watershed with High Spatial Heterogeneity" Pedosphere, 21(6), 738-749.

Boer, E. P. J. de Beurs, K. M. and Hartkamp, A. D. (2001) "Kriging and thin plate splines for mapping climate Variables" International Journal of Applied Earth Observation and Geoinformation, 3, 146–154.

Borga, M. and Vizzaccaro, A. (1997) “On the interpolation of hydrologic variables: formal equivalence of multiquadratic surface fitting and kriging” Journal of Hydrology, 195(1-4), 160-171.

Box, G. E .P. & Jenkins, G. M., (1970). Time Series Analysis, Forecasting and Control, Holden-Day, CA, San Francisco.

Brath, A. Montanari, A. and Toth, E. (2002) “Neural networks and non-parametric methods for improving realtime flood forecasting through conceptual hydrological models” Hydrology and Earth System Sciences, 6(4), 627-640.

Burrough, P. A. and McDonnell, R. A. (1998) “Principles of geographical information systems” Oxford University Press, Oxford. 333pp.

Bustami, R. Bessaih, N. Bong, C. and Suhaili, S. (2007) “Artificial Neural Network for Precipitation and Water Level Predictions of Bedup River” International Journal of Computer Science, 34(2), 1-6.

Buytaert W. (2006) “Spatial and temporal rainfall variability in mountainous areas: a case study from the South Ecuadorian Andes” Journal of Hydrology, 329(3-4), 413-421.

Carrera-Hernandez J.J. and Gaskin, S.J. (2007) “Spatio temporal analysis of daily precipitation and temperature in the Basin of Mexico” Journal of Hydrology, 336(3-4), 231-249.

Caruso, C. and Quarta, F. (1998) “Interpolation methods comparison” Computers and Mathematics with Applications, 35(12), 109-126.

Chang, T.J., Kavvas, M.L. and Delleur, J.W.(1984) “Modeling of sequences of wet and dry days by binary discrete autoregressive moving average processes” Journal of climate and applied meteorology,23,1367-1378.

Chapman, T. G. and Maxwell, A. I. (1996) “Baseflow separation-comparison of numerical methods with tracer experiments” Proceedings of Hydrological and water Resources Symposium, Institution of Engineers Australia, Hobart, Australia, 539-545.

Chatfield, C. (1996) “The Analysis of Time Series:-An Introduction” 5th Ed., Chapman and Hall, London.

Chattopadhyay, S. and Chattopadhyay, G. (2010) “Univariate modelling of summer-monsoon rainfall time series: Comparison between ARIMA and ARNN” Comptes Rendus Geoscience, 342(2), 100-107.

Chiew, F.H.S. Stewardson, M.J. Mcmahon, T.A. (1993) “Comparison of Six Rainfall-Runoff Modeling Approaches” Journal of Hydrology, 147, 1-36.

Chaubey, I. Haan, C.T. Grunwald, S. and Salisbury, J.M. (1999) “Uncertainty in the model parameters due to spatial variability of rainfall, Journal of Hydrology, 220(1-2), 48-61.

Chauhan, M. S. Kumar, V. Rahul, A. K.(2013) “Modeling and quantifying water use efficiency for irrigation project and water supply at large scale” International Journal of Advanced Scientific and Technical Research , 3 (5), 617-639.

Chen, F.W. and Liu, C.W. (2012) “Estimation of the spatial rainfall distribution using inverse distance weighting (IDW) in the middle of Taiwan” Paddy Water Environment.

Cheng, C.T. Wang, W.C. Xu D.M. and Chau K.W. (2008) “Optimizing hydropower reservoir operation using hybrid genetic algorithm and chaos” Water Resources Managemnet,7,895-909.

Chilès, J.P. and Delfiner, P. (1999) “Geostatistics: modelling spatial uncertainty” 1st ed. New York, USA: Wiley-Interscience.

Chiew, F.H.S., M.J. Stewardson, T.A. Mcmahon. (1993) “Comparison of Six Rainfall-Runoff Modeling Approaches” Journal of Hydrology, 147-136.

Chow, V.T. (1964) "Handbook of applied hydrology: a compendium of water-resources technology" 1st ed. New York, USA: McGraw-Hill, Inc.

Chow, V.T. Maidment, D.R. and Mays, L.W. (1988) "Applied Hydrology" International ed. Singapore: McGraw-Hill, Inc.

Cole, S. J. and Moore, R. J. (2008) "Hydrological modelling using raingage and radar-based estimators of areal rainfall" Journal of Hydrology, 358, 159– 181, 2008.

Collischonn, B. Collischonn, W. and Tucci, C. E. M. (2008) "Daily hydrological modeling in the Amazon basin using TRMM rainfall estimates" Journal of Hydrology, 360, 207–216, 2008.

Cressie, N. (1991) "Statistics for spatial data" 1st ed. New York, USA: Wiley.

Creutin, J.D. Delrieu, G.and Lebel, T. (1988) "Rain measurement by raingage-radar combination: a geostatistical approach" J. Atmos. Oceanic Technol., 5(1), 102-115.

CSE (2003) Climate Change and Orissa, Factsheet, Global Environmental Negotiations. (http://www.cseindia.org/programme/geg/mpdf/orissa.pdf).

Dadhwal, V.K. Aggrawal, S.P. and Mishra, N.(2010) "Hydrological simulation of Mahanadi river basin and impact of land use/land cover change on surface runoff using macro scale hydrological model" ISPRS TC VII Symposium – 100 Years ISPRS, Vienna, Austria, IAPRS, 38(7B),165-170.

D'Asaro, F. and Grillone G. (2010) "Runoff Curve Number method in Sicily: CN determination and analysis of the Initial abstraction ratio" Proceedings of the 4th Federal Interagency Hydrologic Modeling Conference, Las Vegas, Nevada, 06/27/2010-07/01/2010.

D'Asaro, F. and Grillone G. (2012) "Empirical investigation of Curve Number Method Parameters in the Mediterranean area" Journal of Hydrologic Engineering, ASCE, 17(10), 1141-1152.

D'Asaro, F. and Grillone G. (2013) "Curve Numbers Seasonal Variation in Sicily" Submitted to Journal of Hydrologic Engineering, ASCE.

Dastorani, M.T. Afkhami, H. Sharifidarani, H. and Dastorani, M. (2010) "Application of ANN and ANFIS Models on Dry land Precipitation Prediction (Case Study: Yazd in Central IRAN)" Journal of Applied Sciences, 10(20), 2387-2394.

Davidson, J. W. Savic, D. A. Walters, G. A. (2003) "Symbolic and Numerical Regression: Experiments and Applications" Journal of Information Science, 150(1-2):95-117.

Delleur, J.W. and Kavvas, M.L. (1978) "Stochastic Models for Monthly Rainfall Forecasting and Synthetic Generation" Journal of Applied Meteorology, 17, 1528-1536.

Demirel, M. C. Venancio, A. and Kahya, E. (2009b) "Flow forecast by SWAT model and ANN in Pracana Basin, Portugal" Adv. Eng. Software., 40(7), 467–473.

Demirel, M.C. Booij, M.J. and Kahya, E. (2012) "Validation of an ANN Flow Prediction Model

Using a Multistation Cluster Analysis", Journal of Hydrologic Engineering, 17(2), 262-271.

Deutsch, C.V. (1996) "Correcting for negative weights in ordinary kriging" Comput. Geosci.-Uk, 22(7), 765-773.

Diodato, N. (2005) "The influence of topographic co-variables on the spatial variability of precipitation over small regions of complex terrain" Int. J. Climatol., 25(3), 351-363.

Dirks, K.N. Hay, J.E. Stow, C.D. and Harris, D. (1998) "High-resolution studies of rainfall on Norfolk Island. Part 2: Interpolation of rainfall data" Journal of Hydrology, 208(3-4), 187-193.

Duc, L.V.(2009) "Applicability of Artificial Neural Network model for simulation of monthly runoff in comparison with some other traditional models" Science & Technology Development, 12(4), 94-106.

El-shafie, A. Mukhlisin, M. Najah, A.A. and Taha, M.R.(2011) “Performance of artificial neural network and regression techniques for rainfall-runoff prediction” International Journal of the Physical Sciences ,6(8), 1997-2003.

Fennessey, L.A. (2000) “The effect of inflection angle, soil proximity and location on runoff”, Ph.D. dissertation, Pennsylvania State University.

Fernando, D. A. K. and Jayawardena, A. W. (1998) “Runoff forecasting using RBF networks with OLS algorithm.” Journal of Hydrologic Engineering, 3(3), 203–209.

Faur`es, J. M. Goodrich, D. C., Woolhiser, D. A, and Sorooshian, S. (1995) “Impact of small-scale spatial variability on runoff modelling” Journal of Hydrology, 173, 309–326, 1995.

Gabellani, S., Boni, G., Ferraris, L., Hardenberg, J. V., and Provenzale, A. (2007) “Propagation of uncertainty from rainfall to runoff: A case study with a stochastic rainfall generator” Advances in Water Resources, 30, 2061–2071.

Galeati, G. (1990). A Comparison of Parametric and Non-Parametric Methods For Runoff Forecasting. Journal of Hydrological Sciences, 35:79-94.

Geetha, K. Mishra, S.K. Eldho, T.I. Rastogi, A. K. and Pandey, R. P. (2007) “Modifications to SCS-CN Method for Long-Term Hydrologic Simulation” Journal of Irrigation and Drainage Engineering, 133,475-486.

Geetha, G. and Selvaraj, R.S. (2011) “Prediction of monthly rainfall in Chennai using back propagation neural network” International Journal of Engineering Science and Technology, 3(1), 211-213.

Ghose,D.K. and Swain,P.C.(2011) “Erosion and sediment characteristics of peninsular river India,a case study” International Journal of Engineering Science and Technology,3(5),3716-3725.

Goodchild, M. University of California at Santa Barbara; Lecture on Spatial Interpolation; http://www.geog.ucsb.edu/~good/176b/a15.html

Goovaerts, P. (1997) “Geostatistics for natural resources evaluation” New York, USA: Oxford University Press.

Goovaerts, P. (1999) “Using elevation to aid the geostatistical mapping of rainfall erosivity” Catena, 34 (3-4), 227-242.

Goovaerts, P. (2000) “Geostatistical approaches for incorporating elevation into the spatial interpolation of rainfall” Journal of Hydrology, 228(1-2), 113-129.

Gorman, J. W. and Toman, R. J. (1966) “Selection of Variables For Fitting Equation To Data” Technometrics, 8(1): 27-51.

Grillone, G. Agnese, C. and D’Asaro, F. (2009) “Estimation of solar radiation in Sicily by daily data maximum and minimum temperature” Italian Journal of Agrometeorology, 14(2), 84-85.

Grillone, G. Agnese, C. and D'Asaro, F. (2012) “Estimation of Daily Solar Radiation from Measured Air Temperature Extremes in the Mid-Mediterranean Area” Journal of Irrigation and Drainage Engineering (ASCE), 138 (10), pp. 939-947.

Grillone, G. Baiamonte, G. D'Asaro, F. (2014) “Empirical determination of the average annual runoff coefficient in the Mediterranean area” American Journal of Applied Sciences, 11 (1), 89-95.

Groisman, P.Y. and Legates, D.R. (1994) “The accuracy of United States precipitation data” Bull. Am. Meteorol. Soc., 75(2), 215-227.

Gronewold, A.D. Clites, A.H. Hunter, T.S. and Stow, C.A.(2011) “An appraisal of the Great Lakes advanced hydrologic prediction system” Journal of Great Lakes Research,37,577-583.

Gujarati, D. N. (1995) “Basic Econometrics” 5th Ed., McGraw-Hill Book Co., New York.

Gupta, P.K. Punalekar, S. Panigrahy, S. Sonakia, A. and Parihar, J.S. (2012) "Runoff Modeling in an Agro-Forested Watershed Using Remote Sensing and GIS" Journal of Hydrologic Engineering, 17(11), 1255-1267.

Haberlandt, U. and Kite, G.W. (1998) "Estimation of daily space-time precipitation series for macroscale hydrological modeling" Hydrological Processes, 12(9), 1419-1432.

Haberlandt, U. (2007) "Geostatistical interpolation of hourly precipitation from rain gauges and radar for a large-scale extreme rainfall event" Journal of Hydrology, 332(1-2), 144-157.

Haquea, M.M. Rahmana, A. Hagarea, D. and Kibriab, G. "Principal Component Regression Analysis in Water Demand Forecasting: An Application to the Blue Mountains, NSW, Australia" Journal of Hydrology and Environment Research, 1(1), 49-59.

Hawkins, R.H. (1978a) "Effects of rainfall intensity on runoff curve numbers" Proc., 1978 Meeting of the Arizona Section of the American Water Resources Association, Flagstaff, Arizona, 53-64.

Hawkins, R.H. (1978b) "Discussion to 'Infiltration formula based on SCS curve number" Journal of Irrigation and Drainage Engineering, ASCE, 104(4), 464-467.

Hawkins, R.H. (1984) "A comparison of predicted and observed runoff curve numbers", Symposium Proceedings, Water Today and Tomorrow, Flagstaff AZ. ASCE, New York, 702-709.

Hawkins, R. H., Hjelmfelt, A.T., and Zevenberger, A.W. (1985) "Runoff probability, storm depth, and curve numbers" Journal of Irrigation and Drainage Engineering, ASCE, 111(4), 330-340.

Hawkins, R.H. (1990) "Asymptotic determination of curve numbers from rainfall-runoff data", Symposium Proceedings, Watershed Planning and Analysis in action, Durango CO, ASCE, New York, 67-76.

Hawkins, R.H. (1993) "Asymptotic determination of runoff curve numbers from data", Journal of Irrigation and Drainage Engineering, ASCE, 119(2), 334-345.

Hawkins, R.H. and Ward, T. J. (1998) "Site and cover effects on event runoff, Jornada Experimental Range, New Mexico", Symposium Proceedings, Conference on Rangeland Management and Water Resources, Reno, NV. American Water Resources Associations, 361-370.

Hawkins, R.H, Ward, T. J. Woodward, D.E. and Van Mullem, J.A. (2009) "Curve Number Hydrology: state of practice" American Society of Civil Engineers, Reston, Virginia (USA), 106pp, ISBN 978-0-7844-1044-2.

Hawkins, R.H. Ward, T. J. Woodward, D.E. and Van Mullem, J.A. (2010) "Continuing evolution of Rainfall-Runoff and the Curve Number Precedent", Proceedings of Fourth Federal Interagency Hydrologic Modeling Conference, Las Vegas, Nevada, 2010.

Heany, J.P. Huber, W.C. Nix, S.J. (1976) "Storm water management model: level I-preliminary screening procedures" EPA Rep. No. 66/2-76-275. U.S. Environ. Protection Agency (U.S.EPA), Cincinnati, Ohio.

Helman,K.(2011) "SARIMA models for temperature and precipitation time series in the Czech Republic for the period 1961-2008" Journal of Applied Mathematics,4(3),281-290.

Hengl, T. Geuvelink, G.B.M. and Stein, A. (2003) "Comparison of kriging with external drift and regression kriging" Enschede, The Netherlands: ITC.

Hevesi, J.A. Flint, A.L. Istok, J.D. (1992a) "Precipitation estimation in mountainous terrain using multivariate geostatistics. Part I: structural analysis" Journal of Applied Meteorology, 31, 661–676.

Hevesi, J.A. Flint, A.L. Istok, J.D. (1992b) "Precipitation estimation in mountainous terrain using multivariate geostatistics. Part II: Isohyetal maps" Journal of Applied Meteorology, 31, 677–688.

Hjelmfelt, A.T. (1980) "Empirical Investigation of Curve-Number Technique", ASCE, Journal of the Hydraulics Division, 106(9), 1471-1476.

Hjelmfelt, A.T. (1991) "Investigation of curve number procedure", Journal of Hydrological Engineering, ASCE, 117(6), 725-737.

Hofstra, N. Haylock, M. New, M. Jones, P. and Frei, C. (2008) "Comparison of six methods for the interpolation of daily, European climate data" Journal of Geophysical research, 113, 1-19.

Hsieh, W. W. Yuval, Li, J. Shabbar, A. and Smith, S. (2003) "Seasonal prediction with error estimation of Columbia River streamflow in British Columbia" Journal of Water Resources Planning and Management, 1292, 146–149.

Hsu, K., Gupta, H. V. Sorooshian, S. (1995). Artificial Neural Network Modeling Of The Rainfall-Runoff Process, Water Resources Research, 31(10): 2517-2530.

Huang, N.Q. Babel, M.S. Weesakul, S. and Tripathi, N.K. (2009) "An artificial neural network model for rainfall forecasting in Bangkok, Thailand" Hydrology and Earth System Sciences, 13, 1413-1425.

Huang, W. Xu, B. and Hilton, A.C. (2004) "Forecasting flows in Apalachicola River using neural Networks" Hydrological Processes, 18, 2545–2564.

Hutchinson, M.F. (1998) "Interpolation of rainfall data with thin plate smoothing splines-Part I: Two dimensional smoothing of data with short range correlation" Journal of Geographic Information and Decision Analysis, 2(2), 139-151.

Imrei, C.E. Durucan, S. and Korre, A. (2000) "River flow prediction using artificial neural networks: generalization beyond calibration range" Journal of Hydrology, 233, 138-153.

Integrated Hydrological Data Book (non-classified river basins) (2009), Central Water Commission, New Delhi.

Integrated water resources development- A plan for action(1999), Report of The National Commission for Integrated Water Resources Development, Ministry of Water Resources, New Delhi.

Isaaks, E.H. and Srivastava, R.M. (1990 "An introduction to applied geostatistics" New York, USA: Oxford University Press.

Iseri, Y. Dandy, G.C. Maier, H.R. Kawamura, A. and Jinno, K. (2005) "Medium term forecasting of rainfall using artificial neural networks" International Congress on Modeling and Simulation, 1834-1840.

IWMI (International Water Management Institute)(2000a) "World water supply and demand 1995 to 2025" Draft report prepared for World Water Vision. Colombo, Sri Lanka: IWMI.

Jain, A. and Indurthy, S.K.V. (2003) "Comparative Analysis of Event-based Rainfall-runoff

Modeling Techniques-Deterministic, Statistical, and Artificial Neural Networks", Journal of Hydrologic Engineering, 8(2), 93-98.

Jain, A. and Srinivasalu, S. (2004) "Development of effective and efficient rainfall-runoff models using integration of deterministic, real-coded genetic algorithms and artificial neural network techniques" Water Resources Research, 40, 1-12.

Jain, A. and Srinivasalu, S. (2006) "Integrated approach to model decomposed flow hydrograph using artificial neural network and conceptual techniques" Journal of Hydrology, 317(3-4), 291-306.

Jain, M.K. Mishra, S.K. and Singh, V.P. (2006) "Evaluation of AMC dependent SCS - CN based models using watershed characteristics" Journal of Water Resources Management, 20(4), 531-555.

Jakeman, A.J. Hornberger, G.M. (1993) "How much complexity is warranted in a rainfall-runoff model" Water Resources Research, 29, 2637–2649.

Jha, R. and Jaiswal, R.K. (1992) "Analysis of rainfall pattern in a catchment" IAH Journal of Hydrology (India), Roorkee.

Jha, R. Sharma, K.D. and Neupane, B. (2009) "Technique for Supporting the Identification and Remediation of Water Scarcity Issues and Global Change Impact on Water Resources in India" International Journal of Hydrologic Environment (IHES), Korea, 5(1), 1-11.

Johnson, G.L. and Hanson, C.L. (1995) "Topographic and atmospheric influences on precipitation variability over a mountainous watershed" Journal of Applied Meteorology, 34(1), 68-87.

Johnston, K. Ver Hoef, J. M. Krivoruchko, K. and Lucas, N. (2010) "Using ArcGIS Geostatistical Analyst" ESRI, Redlands, CA.

Kabiri, R. Chan, A. Ramani, B. (2013) “Comparison of SCS and Green-Ampt Methods in Surface Runoff-Flooding Simulation for Klang Watershed in Malaysia” Open Journal of Modern Hydrology, 3, 102-114.

Kaluarachchi, J.J. Parker, J.C. and Lenhard, R.J. (1990) “A numerical model for areal migration of water and light hydrocarbon in unconfined aquifers” Adv. Water Resour. 13, 29-40

Kar, A.K. Winn, L.L. Lohani, A.K. and Goel, N.K. (2012) “Soft Computing–Based Workable Flood Forecasting Model for Ayeyarwady River Basin of Myanmar” Journal of Hydrologic Engineering, 17(7), 807-822.

Karamouz, M. Fallahi, M. Nazif, S.and Farahani, M.R. (2009) “Long lead rainfall prediction using statistical downscaling and artificial neural network modeling” Transaction A: Civil Engineering, 16(2), 165-172.

Karnieli, A. and Gurion, B. (1990) “Application of kriging technique to areal precipitation mapping in Arizona” Geojournal, 22(4), 391-398.

Kastelec, D. and Kosmelj, K. (2002) “Spatial interpolation of mean yearly precipitation using universal kriging” Developments in Statistics, 149-162.

Kelway, P. S. (1974) “A scheme for assessing the reliability of interpolated rainfall estimates” Journal of Hydrology, 21, 247-267.

Khalili, N. Khodashenas, S.R. Davary, K. and Karimaldini, F. (2011) “Daily rainfall forecasting for Mashhad synoptic station using artificial neural networks” International Conference on Environmental and Computer Science, 19, 118-123.

Kihoro, J.M., Otieno, R.O. and Wafula, C. (2004) “Seasonal time series forecasting: a comparative study of ARIMA and ANN models” African Journal of Science and Technology, Science and Engineering Series, 5(2), 41-49.

Kobold, M. and Su˘selj, K. (2005) “Precipitation forecasts and their uncertainty as input into hydrological models” Hydrology and Earth System Sciences, 9, 322–332.

Koteshwaram,P. and Alvi, S.M.A.(1969) “Secular trends and periodicities in rainfall at west coast stations in India” Current Science,38(10),229-231.

Kottek, M. and Rubel, F. (2008) “Co-kriging global daily rain gauge and satellite data” Geophysical Research, 10.

Kumar, R. Singh, R.D. and Sharma, K.D. (2005) “Water Resources of India” Current Science, 89(5), 794-811.

Kumar, D. N. Reddy, M. J. and Maity, R.(2007) “Regional Rainfall Forecasting using Large Scale Climate Teleconnections and Artificial Intelligence Techniques” Journal of Intelligent Systems,16(4),307-322.

Kumar, A. Rajpoot, P. S. (2013) “Assessment of hydro-environmental loss as surface runoff using CN method of Pahuj River Basin Datia, India” Proceedings of the International Academy of Ecology and Environmental Sciences, 3(4), 324-329.

Kuo, J.T. And Y.H. Sun (1993) “An Intervention Model for Average 10 Day Stream Flow Forecast And Synthesis” Journal of Hydrology, 151,35-56.

Kyriakidis, P.C., Kim, J. and Miller, N.L. (2001) “Geostatistical mapping of precipitation from rain gauge data using atmospheric and terrain characteristics” Journal of Applied Meteorology, 40(11), 1855-1877.

Lall, U. and Bosworth, K. (1993) “Multivariate Kernel Estimation of Functions of Space and Time Hydrologic Data” In: Hipel, KW (Ed.), Stochastic and Statistical Methods in Hydrology and Environmental Engineering, Springer Velag/ Kluwer, New York.

Landeras, G. Ortiz-Barredo, A. and López, J. J. (2009) "Forecasting Weekly Evapotranspiration with ARIMA and Artificial Neural Network Models" Journal of Irrigation and Drainage Engineering, ASCE, 135(3), 323-334.

Langu, E.M. (1993) "Detection of Changes in Rainfall and Runoff Patterns" Journal of Hydrology, 147,153-167.

Lanza, L.G. Ramirez, J.A. and Todini, E. (2001) "Stochastic rainfall interpolation and downscaling" Hydrology and Earth System Sciences, 5(2), 139-143.

Leander, R., Buishand, T. A., van den Hurk, B. J. J. M, and de Wit,M. J. M. (2008) "Estimated changes in flood quantiles of the river Meuse from resampling of regional climate model output" Journal of Hydrology, 351, 331–343.

Lin, J.Y. Cheng, C.T. and Chau, K.W. (2006) "Using Support Vector Machine for Long Term Discharge Prediction" Hydrological Sciences Journal, 43, 47-66.

Ljung, G. M. and Box, G. E. P. (1978) "On a measure of lack of fit in time series models" Biometrika, 65, 297-303.

Lloyd, C.D. (2005) "Assessing the effect of integrating elevation data into the estimation of monthly precipitation in Great Britain" Journal of Hydrology, 308(1-4), 128-150.

Looper, J.P. and Vieux, B.E. (2011) "An assessment of distributed flash flood forecasting accuracy using radar and rain gauge input for a physics-based distributed hydrologic model" Journal of Hydrology, 412-413, 114-132.

Luo, X. Xu, Y. and Shi, Y. (2011) "Comparison of interpolation methods for spatial precipitation under diverse orographic effects" IEEE.

Ly, S. Charles, C. and Degre, A. (2011) "Geostatistical interpolation of daily rainfall at catchment scale: the use of several variogram models in the Ourthe and Ambleve catchments, Belgium" Hydrology and Earth System Sciences, 15, 2259-2274.

Magar, R.B. and Jothiprakash, V. (2011) “Intermittent reservoir daily-inflow prediction using lumped and distributed data multi-linear regression models” Journal of Earth System Sciences, 120(6), 1067-1084.

Mahsin, Md. Akhter, Y, Begum, M. (2012) “Modeling Rainfall In Dhaka Division Of Bangladesh Using Time Series Analysis” Journal of Mathematical Modelling and Application, 1(5), 67-73.

Mair, A. and Fares, A. (2011) “Comparison of Rainfall Interpolation Methods in a Mountainous Region of a Tropical Island” Journal of Hydrologic Engineering, 16(4), 371-383.

Makridakis, S. Wheelwright, S.S. and Hyndman, R.J. (1998) “Forecasting: Methods and Applications” John Wiley, New York.

Mandapaka, P.V. Krajewski, W.F. Mantilla, R. and Gupta, V.K. (2009) “Dissecting the effect of rainfall variability on the statistical structure of peak flows” Adv. Water Resour., 32(10), 1508-1525.

Manfreda, S. Giordano C. and Iacobellis, V. (2003) “Stima dei deflussi di base mediante un filtro fisicamente basato” Proceedings of Giornata di Studio: Metodi Statistici e Matematici per l'Analisi delle Serie Idrologiche, Rome, Italy, 247-258.

Marqu´ınez, J. Lastra, J. and Garc´ıa, P. (2003) “Estimation models for precipitation in mountainous regions: the use of GIS and multivariate Analysis” Journal of Hydrology, 270, 1–11.

Martins, O. Y. Ahaneku, I. E. Mohanned , S. A. (2011) “Parametric Linear Stochastic Modeling of Benue River Flow Process” Open Journal of Marine Science, 3, 73-81.

Martins, O. Y. Sadeeq, M. A. and Ahaneku, I. E. (2011) “ARMA Modelling of Benue River Flow Dynamics: Comparative Study of PAR Model” Open Journal of Modern Hydrology, 1, 1-9.

Masih, I. Maskey, S. Uhlenbrook, S. and Smakhtin, V. (2011) "Assessing the impact of areal precipitation input on streamflow simulations using the SWAT model" Journal of American Water Resources Assocoation, 47(1), 179-195.

Mateos, V.L. Garchia, J.A. Serrano, A. and Gallego, M.D.L.C.(2002) "Transfer function modeling of the monthly accumulated rainfall series over the Iberian peninsula"Atmosfera,15,237-256.

Matheron, G. (1971) "The theory of regionalized variables and its applications" Paris : École Nationale Supérieure des Mines de Paris.

Mauludiyanto, A. Hendrantoro, G. Purnomo, M. H. Ramadhany, T. and Matsushima, A. (2010) "ARIMA Modeling of Tropical Rain Attenuation on a Short 28-GHz Terrestrial Link" IEEE Antennas and Wireless Propagation Letters, 9, 223-227.

McKnight, T. L. and Hess, D. (2000) "Physical Geography: A Landscape Appreciation" edited by Prentice Hall (Upper Saddle River, New Jersey), 624 pp.

Meher, J. and Jha, R. (2011a) "Analysis of spatio-temporal variability of rainfall over mahanadi river basin" International Conference SWRMCCA, 17-19 February, NIT Durgapur

Meher, J. and Jha, R.(2011b) "Time series analysis of rainfall data over Mahanadi River basin," Emerging Science, 3(6), 22-32.

Meher, J. and Jha, R. (2013). Time Series Analysis of Monthly Rainfall Data of Mahanadi River Basin, India. International Journal of Science in Cold and Arid regions, China 2013, 5(1): 0073–0084 DOI: 10.3724/SP.J.1226.2013.00073

Michel, C. Vazken, A. Perrin, C. (2005) "Soil conservation service curve number method: how to mend a wrong soil moisture accounting procedure" Water Resources Research, 41, 1–6.

Mishra, S. K., Goel, N. K., Seth, S. M., and Srivastava, D. K. (1998) "An SCS-CN based long term daily flow simulation model for a hilly catchment" International Symposium of Hydrology of Ungauged Streams in Hilly Regions for Small Hydropower Development, AHEC, University of Roorkee, 59-81.

Mishra, S.K. and Singh, V.P. (1999) "Another Look at SCS-CN method" Journal of Hydrologic Engineering, 4(3), 257-264.

Mishra, S.K. Jain, M.K. and Singh, V.P. (2004) "Evaluation of the SCS-CN-Based Model Incorporating Antecedent Moisture" Water Resources Management, 18, 567–589.

Mishra, S. K. Geetha, K. Rastogi, A. K. and Pandey, R. P. (2005a) "Long-term hydrologic simulation using storage and source area concepts" Hydrological Processes, 19(14), 2845–2861.

Mishra, S. K. Pandey, R. P. Jain, M. K. &. Singh, V. P. (2008) "A Rain Duration and Modified AMC-dependent SCS-CN Procedure for Long Duration Rainfall-runoff Events" Water Resources Management, 22,861–876.

Mockus, V. (1964) Personal communication, Letter to Orrin Ferris dated March 5, 1964, 5 pp., USDA, NRCS, Washington DC (USA).

Mohammadi, K. Eslami, H. R. and Dardashti, S. D.(2005) "Comparison of Regression, ARIMA and ANN Models for Reservoir Inflow Forecasting using Snowmelt Equivalent (a Case study of Karaj)" J. Agric. Sci. Technol. , 7,17-30.

Montgomery, D.C. L.A. Johnson (1967). Forecasting and Time Series Analysis. McGraw-Hill, New York.

Moral, F.J. (2010) "Comparison of different geostatistical approaches to map climate variables: application to precipitation" Int. J. Climatol., 30(4), 620-631.

Moulin, L. Gaume, E. and Obled, C. (2009) "Uncertainties on mean areal precipitation: assessment and impact on streamflow simulations" Hydrology and Earth System Sciences, 13, 99–114.

Mukerji, A. Chatterjee, C. and Raghuwanshi, N. S. (2009) "Flood forecasting using ANN, neuro-fuzzy, and neuro-GA models" Journal of Hydrologic Engineering, 14(6), 647–652.

Naill, P.E. and Momani, M. (2009) “Time Series Analysis Model for Rainfall Data in Jordan: Case Study for Using Time Series Analysis” American Journal of Environmental Sciences, 5(5), 599-604.

Nalder, I.A. and Wein, R.W. (1998) “Spatial interpolation of climatic normals: test of a new method in the Canadian boreal forest” Agricultural and Forest Meteorology, 92(4), 211-225.

Namias, J. (1968) “Further studies of drought over north-eastern united states” Proceeding of conference on the drought in the north-eastern United States, 57-94.

Naoum, S. and Tsanis, I.K. (2004) “Ranking spatial interpolation techniques using a GIS-based DSS” Global Nest: the International Journal, 6(1), 1-20.

Nayak, P.C. Sudheer, K.P. and Jain, S.K.(2007) “Rainfall-runoff modeling through hybrid intelligent system” Water Resources Research,43,1-17.

Nicotina, L. Celegon, E.A. Rinaldo, A. and Maran,i M.(2008) “On the impact of rainfall patterns on the hydrologic response” Water Resources Research, 44(12).

N.O.A.A. (1972) National Weather Service River Forecast System forecast procedures. TM NWS HYDRO-14, US Department of Commerce, Washington DC.

Noakes, D. J. McLeod, A. I. and Hipel, K. W. (1985) “Forecasting monthly riverflow time series” International Journal of Forecasting, 1(2), 179-190.

Noto, L. La Loggia, G. and Pirrello, M. (2001) “Un Sistema Informativo Territoriale per l’analisi del rischio idraulico delle infrastrutture viarie”, Atti della 5a Conferenza Nazionale ASITA, Rimini, Italy, 2001.

Nourani,V. Komasi, M. and Alami, M.T. (2012) “Geomorphology-based genetic programming approach for rainfall-runoff modeling” Journal of Hydroinformatics.

Nourani, V. Komasi, M. and Alami, M.T. (2012) “Hybrid wavelet-genetic programming approach to optimize ANN modeling of rainfall-runoff process” Journal of Hydrologic Engineering, 17(6), 724-741.

Obled, C. Wendling, J. and Beven, K. (1994) “The sensitivity of hydrological models to spatial rainfall patterns: an evaluation using observed data” Journal of Hydrology, 159(1-4), 305-333.

Orissa Community Tank Development and Management Society, Hydrological Assessment, Final Report, 2007.

Otok, B.W. and Suhartono (2009) “Development of Rainfall Forecasting Model in Indonesia by using ASTAR, Transfer Function, and ARIMA Methods” European Journal of Scientific Research, 38 (3), 386-395.

Panahi, A. (2013) “Evaluating SCS-CN Method in Estimating the Amount of Runoff in Soofi Chay basin Using GIS” Life Science Journal, 10(5s), 271-277.

Peel, M. C. Finlayson, B. L. and McMahon T. A. (2007). “Updated world map of the Koppen-Geiger climate classification”, Hydrology and Earth System of Sciences, 11, 1633-1644.

Phillips, D.L. Dolph, J. and Marks, D. (1992) “A comparison of geostatistical procedures for spatial analysis of precipitation in mountainous terrain” Agric. For. Meteorol., 58(1-2), 119-141.

Ponce, V.M. (1989) “Engineering hydrology, principles and practices” Prentice Hall, Englewood Cliffs, N.J.

Ponce, V.M. and Hawkins, R.H. (1996) “Runoff Curve Number: Has it reached maturity?” Journal of Hydrologic Engineering, ASCE, 1(1), 11-19.

Rabenja, A.T. Ratiarison, A. Rabeharisoa, J.M. (2009) “Forecasting of the rainfall and the discharge of the Namorona river in Vohiparara and fft analyses of these data”4th International Conference in High-Energy Physics, Antananarivo ,Madagascar,1-12.

Refsgaard, J.C. (1996) “Terminology, modelling protocol and classification of hydrological model codes” In: Abbott M.B. & Refsgaard J.C., eds. Distributed hydrological modelling. Dordrecht, the Netherlands: Kluwer Academic Publishers, 17-39.

Ramamurthy, K.V. Sonam,M.K. and Muley,S.S. (1987) “Long term variation in the rainfall over upper Narmada catchment”Mausam,38(3),313-318.

Reshma, T. Kumar, P.S. Babu, M.J.R.K. and Kumar, K.S. (2010) “Simulation of Runoff in Watersheds using SCS-CN AND Muskinggum-Cunge Methods using Remote Sensing and Geographical Information Systems” International Journal of Advanced Science and Technology, 25, 31-42.

Ripley, B. D. (1981) “Spatial statistics” John Wiley Sons, New York.

Risley J. Gannett, M. Lea, J. and Roehl. E. (2005) “An analysis of statistical methods for seasonal flow forecasting in the Upper Klamath River Basin of Oregon and California” USGS Scientific Investigations Report, 2005-5177.

Ruelland, D. Ardoin-Bardin, S. Billen, G. and Servat, E. (2008) “Sensitivity of a lumped and semi-distributed hydrological model to several methods of rainfall interpolation on a large basin in West Africa” Journal of Hydrology, 361, 96–117.

Sahai, A.K. Soman, M.K. and Satyan, V. (2000) “All India summer monsoon rainfall prediction using an artificial neural network” Climate Dynamics, 16, 291-302.

Sahu, R. K. Mishra, S. K. Eldho, T. I. and Jain, M. K. (2007) “An advanced soil moisture accounting procedure for SCS curve number method” Hydrological Processes, 21(21), 2872–2881.

Salas, J. D. (1992) “Analysis and modeling of hydrologic time series” In: D.R. Maidment (editor-in-chief), Handbook of Hydrology, McGraw-Hill, Inc., USA.

Salas, J. D., Deulleur, J. W., Yevjevich, V. Lane, W. L. (1980) “Applied Modeling of Hydrologic Time Series” Water Resources Publications, Littleton, CO.

Sallehuddin R., Shamsuddin S. M. H., Hashim, S. Z. M. Abraham, A.(2007) “Forecasting time series data using gray relational artificial neural network and auto regressive integrated model” Neural Network World ,6, 573-605.

Schiemann R. (2011) “Geostatistical radar-raingauge combination with nonparametric correlograms: methodological considerations and application in Switzerland” Hydrology and Earth System Sciences, 15(5), 1515-1536.

Schuurmans, J. M. and Bierkens, M. F. P. (2007) “Effect of spatial distribution of daily rainfall on interior catchment response of a distributed hydrological model, Hydrology and Earth System Sciences, 11, 677– 693.

Schuurmans, J.M. Bierkens, M.F.P. Pebesma, E.J. and Uijlenhoet, R. (2007b) “Automatic prediction of high-resolution daily rainfall fields for multiple extents: the potential of operational radar” Journal of Hydrometeorology, 8(6), 1204-1224.

Segond, M.L. Wheater, H.S. and Onof, C. (2007) “The significance of spatial rainfall representation for flood runoff estimation: a numerical evaluation based on the Lee catchment” UK.J. Hydrol., 347(1-2), 116-131.

Sevruk, B. (1997) “Regional dependency of precipitation-altitude relationship in the Swiss Alps” Clim. Chan,ge, 36(3-4), 355-369.

Shah, S.M.S. O’Connell, P.E. and Hosking, J.R.M. (1996a.) “Modelling the effects of spatial variability in rainfall on catchment response. 1. Formulation and calibration of a stochastic rainfall field modelJournal of Hydrology, 175(1-4), 67-88.

Shah, S.M.S. O’Connell, P.E. and Hosking, J.R.M. (1996b) “Modelling the effects of spatial variability in rainfall on catchment response. 2. Experiments with distributed and lumped models” Journal of Hydrology, 175(1-4), 89-111.

Shamseldin, A. Y. Nasr, A. E. and O’Connor, K. M. (2002) “Comparison of different forms of the multi-layer feed-forward neural network method used for river flow forecasting” Hydrology and Earth System Sciences, 6(4), 671–684.

Shamsnia,S.A. Shahidi,N. Liaghat,A. Sarraf,A. and Vahdat,S.F.(2011)"Modeling of weather parameters using stochastic methods(ARIMA Model)(Case Study: Abadeh Region, Iran)"International Conference on Environment and Industrial Innovation, Singapore, 12: 282-285.

Shrestha, R. R. Theobald, S. and Nestmann, F. (2005) "Simulation of flood flow in a river system using artificial neural networks" Hydrology Earth Syst. Sci., 9(4), 313–321.

Sicilian Informative Agrometeorological Service (SIAS), (2002) "Sicilian Climatologic Atlas", Department of Agriculture of Sicilian Autonomous Region, Sicily.

Simanton, J.R. Hawkins, R.H. Mohseni-Saravi, M. and Renard, K.G. (1996) "Runoff Curve Number Variation with Drainage Area, Walnut Gulch, Arizona" Transaction of ASAE, American Society of Agricultural Engineers, 39 (4), 1391-1394.

Sinclair, M.R. Wratt, D.S. Henderson, R.D. and Gray, W.R. (1997) "Factors affecting the distribution and spillover of precipitation in the Southern Alps of New Zealand -a case study" J. Appl. Meteorol., 36(5), 428-442.

Singh, V. P. (1989) "Hydrologic Systems: Volume 2-Watershed modeling" Prentice Hall, Englewood Cliffs, New Jersey.

Singh, V.P. (1995) "Watershed modeling" In: Singh V.P., ed. Computer models of watershed hydrology. Colorado, USA: Water Resources Publications, 1-22.

Singh, V. P. (1997) "Effect of spatial and temporal variability in rainfall and watershed characteristics on stream flow hydrograph" Hydrological Processes, 11, 1649–1669.

Singh, V.P. and Frevert, D.K. (eds.) (2006) "Watershed Models" CRC Press, Boca Raton, Florida.

Singh, P.K. Yaduvanshi, B.K. Patel, S. and Ray, S. (2013) "SCS-CN Based Quantification of Potential of Rooftop Catchments and Computation of ASRC for Rainwater Harvesting", Water Resources Management, 27, 2001-2012.

Singhrattna, N. Rajagopalan, B. Clark, M. and Kumar, K.K. (2005) "Seasonal forecasting of Thailand summer monsoon rainfall" International Journal of Climatology, 25, 649–664.

Solomatine, D. P. and Price, R. K. (2004) "Innovative approaches to flood forecasting using data driven and hybrid modeling" Proceedings, 6th International Conference on Hydroinformatics, World Scientific, Singapore, 1639–1646.

Solomatine, D. P. Maskey, M. and Shrestha, D. L. (2007) "Instance-based learning compared to other data-driven methods in hydrological forecasting" Hydrological Processes, 22(2), 275–287.

Somvanshi, V.K. Pandey, O.P. Agrawal, P.K. Kalanker, N.V. RaviPrakash, M. and Chand, R. (2006) "Modeling and prediction of rainfall using artificial neural network and ARIMA techniques" Journal of Indian geophysics Union, 10(2), 141-151.

Song, X. Kong, F. Zhan, C. and Han, J. (2012) "Hybrid optimization rainfall-runoff simulation based on Xinanjiang model and Artificial Neural Network" Journal of Hydrologic Engineering, 17(9), 1033-1041.

Soulis, K. X. Valiantzas, J. D. Dercas, N. and Londra, P. A. (2009) "Analysis of the runoff generation mechanism for the investigation of the SCS-CN method applicability to a partial area experimental watershed" Hydrology and Earth System Sciences Discussion, 6, 373–400.

Soulis, K.X. and Valiantzas, J.D. (2012) "SCS-CN parameter determination using rainfall-runoff data in heterogeneous watersheds- the two-CN system approach" Hydrology and Earth System Sciences, 16, 1001–1015.

Sovoe, S. (2011) "Modeling West African total precipitation depth: a statistical approach" ISI 2011, 58th World Statistics Congress of the International Statistical Institute, Dublin, Ireland.

Srivastava, P. McNair, J.N. and Johnson, T.E. (2006) “Comparison of process-based and artificial neural network approaches for streamflow modeling in agricultural watersheds” Journal of the American Water Resources Association, 42(2):545-563.

Stewart, D. Canfield, E. and Hawkins, R.H. (2012) “Curve Number Determination methods and Uncertainty in Hydrologic Soil groups from Semiarid Watershed Data” Journal of Hydrologic Engineering, ASCE, 17(11), 1180-1187.

Sudheer, K. P. Gosain, A. K. and Ramasastri, K. S. (2002) “A data-driven algorithm for constructing artificial neural network rainfall-runoff models” Hydrological Processes, 16, 1325–1330.

Sumi, S.M. Zaman, F. Hirose, H. (2012) “A rainfall forecasting method using machine learning models and its application to the Fukuoka city case” International Journal of Applied Mathematics and Computer Science, 22(4),841–854.

Syed, K. H. Goodrich, D. C. Myers, D. E. and Sorooshian, S. (2003) “Spatial characteristics of thunderstorm rainfall fields and their relation to runoff” Journal of Hydrology, 271, 1–21.

Tabios, G.Q. and Salas, J.D. (1985) “A comparative analysis of techniques for spatial interpolation of precipitation” Water Resour. Bull., 21, 265-380.

Taesombat, W. and Sriwongsitanon, N. (2009) “Areal rainfall estimation using spatial interpolation techniques” Science Asia, 35, 268-275.

Takagi, T. and Sugeno, M. (1985) “Fuzzy identification of systems and its application to modeling and control” IEEE, Transactions on Systems, Man and Cybernetics, 15, 116–132.

Takeli, Y.I. Akgul, S. Dengiz, O. Akuzum, T. (2006) “Estimation of Flood Discharge for Small watershed Using SCS Curve Number and Geographic Information system” International Congress on River Basin Management, 527-538.

Tan, S.B.K. Lo, E.Y. Shuy, E.B. Chua, L.H.C. and Lim, W.H. (2009) "Hydrograph separation and development of empirical relationships using single parameter digital filters" Journal of Hydrologic Engineering, ASCE, 14(3), 271-279.

Tao, T. Chocat, B. Liu, S. and Xin, K. (2009) "Uncertainty analysis of interpolation methods in rainfall spatial distribution-A case of small catchment in Lyon" Journal of Water Resources and Protection, 2, 136-144.

Tedela, N. H. McCutcheon, S. C. Campbell, J. L. Swank, W. T. Adams. M. B. and Rasmussen, T. C. (2012) "Curve Numbers for Nine Mountainous Eastern United States Watersheds: Seasonal Variation and Forest Cutting", Journal of Hydrologic Engineering, 17(11), 1199-1203.

Tedela, N. H. McCutcheon, S. C. Rasmussen, T. C. Hawkins, R. H. Swank, W. T. Campbell, J. L. Adams, M. B. Jackson, C. R. and Tollner, E. W.(2012) "Runoff Curve Numbers for 10 Small Forested Watersheds in the Mountains of the Eastern United States" Journal of Hydrologic Engineering, 17(11), 1188-1198.

Titmarsh, G.W. Pilgrim, D.H. Cordery, I. and Hossein, A.A. (1989) "An examination of design flood estimations using the US Soil Conservation Services Method", Proceedings Hydrology and Water Resources Symposium, Christchurch NZ, 10/23/1989-30/10/1989, 247-251.

Titmarsh, G.W. Cordery, I. and Pilgrim, D.H. (1995) "Calibration procedures for rational and USSCS design hydrographs", Journal of Hydraulic Engineering, ASCE, 121(1), 61-70.

Titmarsh, G.W. Cordery, I. and Pilgrim, D.H. (1996) "Closer to 'Discussion on Calibration procedures for rational and USSCS design hydrographs", Journal of Hydraulic Engineering, ASCE, 122(3), p. 177.

Tiwari, M.K. Song, K.Y. Chatterjee, C. and Gupta, M.M.(2012) "River-Flow Forecasting Using Higher-Order Neural Networks", Journal of Hydrologic Engineering, 17(5), 655-666.

Tobin C. et al., 2011. Improved interpolation of meteorological forcings for hydrologic applications in a Swiss alpine region. Journal of Hydrology, 401(1-2), 77-89.

Tobler, W. (1970) "A computer movie simulating urban growth in the Detroit region" Economic Geography, 46(2), 234-240.

Todini, E. Pellegrini, F. and Mazzetti, C. (2001) "Influence of parameter estimation uncertainty in Kriging Part 2 – Test and case study applications" Hydrology and Earth System Sciences, 5, 225–232.

Tokar, A.Z. Johnson, P.A. (1999) "Rainfall-runoff modeling using artificial neural network" Journal of Hydrologic Engineering, ASCE 4(3), 232–239.

Tokar, A. S. and Markus, M. (2000) "Precipitation runoff modeling using artificial neural networks and conceptual models" Journal of Hydrologic Engineering, 5(2), 156-161.

Toth, E. Brath, A. and Montanari, A. (2000) "Comparison of short-term rainfall prediction models for real-time flood forecasting" Journal of Hydrology, 239,132-147.

Tseng, F.M. Y, H.C. Tzeng, G.H.(2002) "Combining neural network model with seasonal time series ARIMA model" Technological Forecasting & Social Change,69,71–87.

Tudisca, S. Di Trapani, A.M. Sgroi, F. Testa, R. and Squatrito, R. (2013a) "Economic analysis of PV systems on buildings in Sicilian farms" Renewable and Sustainable Energy Reviews 28, 691-701.

Tudisca, S. Di Trapani, A.M. Sgroi, F. and Testa, R. (2013b) "The cost advantage of Sicilian wine farms" American Journal of Applied Sciences 10 (12), 1529-1536.

Tudisca, S. Di Trapani, A.M, Sgroi, F. and Testa, R. (2014) "Organic farming and economic sustainability. The case of Sicilian durum wheat" Quality – Access to Success, 14 (138), 93-96.

Tularam, G.A. and Ilahee, M. (2010) “Time Series Analysis of Rainfall and Temperature Interactions in Coastal Catchments” Journal of Mathematics and Statistics 6 (3), 372-380.

Vandaele, W. (1983) “Applied Time Series And Box-Jenkins Models” Academic Press, Orlando, FL.

USDA, SCS (1964, 1972, 1985). National Engineering Handbook, Sec. 4 Hydrology. Washington D.C. (USA)

USDA, NRCS (2004, 2009). National Engineering Handbook, Part 630 Hydrology. Washington D.C.(USA)

Van De Beek, C.Z. Leijnse, H. Torfs, P.J.J.F. and Uijlenhoet, R. (2011) “Climatology of daily rainfall semi-variance in The Netherlands” Hydrology and Earth System Sciences, 15(1), 171-183.

Van Mullem, J.A. Woodward, D.E. Hawkins, R.H. Hjelmfelt, A.T. and Quan, Q.D. (2002). “Runoff Curve Number Method: Beyond the Handbook” Proceedings of Second Federal Interagency Hydrologic Modeling Conference, Las Vegas, Nevada, 2002.

Velasco-Forero, C.A. Sempere-Torres, D. Cassiraga, E.F. and Gomez-Hernandez, J.J. (2009) “A non-parametric automatic blending methodology to estimate rainfall fields from rain gauge and radar data” Adv. Water Resour., 32(7), 986-1002.

Verworn, A. and Haberlandt, U. (2011) “Spatial interpolation of hourly rainfall - effect of additional information, variogram inference and storm properties” Hydrology and Earth System Sciences,15(2), 569-584.

Viola, F. Noto, L. V. Cannarozzo, M. and La Loggia, G. (2011) “Regional flow duration curves for ungauged sites in Sicily” Hydrology and Earth System Science, 15, 323-331.

Wang, W. C. Chau, K. W. Cheng, C. T. and Qiu, L. (2009) "A comparison of performance of several artificial intelligence methods for forecasting monthly discharge time series" Journal of Hydrology, 374(3–4), 294–306.

Wang, Y.M. Kerh, T. and Traore, S.(2009) "Neural network approach for modeling river suspended sediment concentration due to tropical storms" Journal of Global Nest,11,457-466.

Watson, D.F. and G.M. Philip. (1985) "A refinement of inverse distance weighted interpolation" Geo-Processing, 2, 315- 327.

Webster, R. and Oliver, M.A. (2007) "Geostatistics for environmental scientists" 2nd ed. Chichester, UK: John Wiley & Sons.

Weesakul, U. and Lowanichchai, S. (2005) "Rainfall Forecast for Agricultural Water Allocation Planning in Thailand" Thammasat International Journal of Science and Technology, 10(3), 18-27.

Woodward, D.E. and Gburek, W.J. (1992) "Progress report ARS/SCS runoff curve number work group" Proc., ASCE Water Forum,92, ASCE, New York, 378-382.

Woodward, D.E. Hawkins, R.H. Hjelmfelt, A.T. Van Mullem, J.A. and Quan, Q.D. (2002). "Curve Number Method: Origins, Applications and Limitations" Proceedings of Second Federal Interagency Hydrologic Modeling Conference, Las Vegas, Nevada, 2002.

Woodward, D.E. Van Mullem, J.A. Hawkins, R.H. and Plummer A. (2010) "Curve Number Completion Study" Consultant's report to USDA, NRCS, Beltsville MD, 38pp.

Wu, J. S. Han, J. Annambhotla, S. and Bryant, S. (2005) "Artificial neural networks for forecasting watershed runoff and stream flows" Journal of Hydrologic Engineering, 10(3), 216–222.

Wu, C.L. Chau, K.W. and Li, Y.S. (2009) "Methods to improve neural network performance in daily flows prediction" Journal of Hydrology, 372(1-4), 80-93.

Yaghoobzadeh, M. (2008) “Determining the curve number of watered field by using GIS and RS. Case in point: watered field of Mansoorabad (birjand)” MA dissertation, the department of water engineering, Kerman Shahid Bahonar University.

Yonaba, H. Anctil, F. and Fortin, V. (2010) “Comparing sigmoid transfer functions for neural network multistep ahead streamflow forecasting.” Journal of Hydrologic Engineering, 15(4), 275–283.

Yu, B. (1998) “Theoretical justification of SCS method for runoff estimation” Journal of Irrigation and Drainage Engineering, 124(6), 234–238.

Yu, B. (2012) “Validation of SCS Method for Runoff Estimation” Journal of Hydrologic Engineering, 17(11), 1158-1163.

Yurekli, K. Kurunc, A. and Ozturk, F. (2005) “Testing the Residuals of an ARIMA Model on the Cekerek Stream Watershed in Turkey” Turkish Journal of Engineering and Environmental Science, 29, 61-74.

Yurekli,K. Kurung,A. and Cevik,O.(2004) “Simulation of Drought Periods using Stochastic Models” Turkish Journal of Engineering and Environmental Sciences,28,181-190.

Zavoianu, I. (1985) “Morphometry of Drainage Basins.” Developments in Water Science, v. 20. Elsevier, Amsterdam, 238 pp.

Zealand, C.M. Burn, D.H. Simonovic, S.P. (1999) “Short term streamflow forecasting using artificial neural networks” Journal of Hydrology, 214, 32–48.

Zhan, X. and Huang, M.L. (2004) “ArcCN-Runoff: an ArcGIS tool for generating curve number and runoff maps” Environmental Modeling and Software, 19(10), 875-879.

Zhang, Q. Wang, B.D. He, B. Peng, Y. Ren, M.L. (2011) “Singular spectrum analysis and ARIMA hybrid model for annual runoff forecasting” Water Resources Management, 25, 2683-2703.

Zimmerman, D. Pavlik, C. Ruggles, A. and Armstrong, M. (1999) “An experimental comparison of ordinary and universal kriging and inverse distance weighting” Math. Geol., 31(4), 375-390.

Zlatanović, N. Gavrić, S. (2013) “Comparison of an automated and manual method for calculating storm runoff response in ungauged catchments in Serbia” Journal of Hydrology and Hydromechanics, 61(3), 195–201.

APPENDIX I

Watershed Characteristics

Watershed	Average Slope (%)	Longest Flow Path(km)	Mean Elevation(m)	Perimeter(km)	Area(Km^2)
1	197149.9	0.567902	264	49.50608	1524.918
2	59153.09	0.043689	207	8.962832	55.39949
3	143908.9	0.615635	287	45.21645	1422.093
4	54919.14	0.087081	218	9.748716	91.74278
5	177630.5	0.558139	267	36.64189	884.8161
6	87334.61	0.075592	209	8.574567	59.44719
7	242240.7	0.938071	234	71.73071	3704.935
8	105708.3	0.67022	197	47.94834	1153.936
9	178746.7	0.802716	155	61.59841	2832.032
10	260669.6	0.206362	424	17.93034	245.9439
11	122528.2	0.925745	173	59.65709	2258.581
12	102872.1	0.041963	122	4.677887	18.12912
13	205997.5	1.310262	186	90.43291	3944.771
14	83698.73	0.379932	117	25.7237	531.1333
15	78833.49	0.542902	128	36.64656	752.8403
16	218041.2	0.387132	151	29.24147	675.3121
17	63863.79	0.068689	79	6.235623	24.18846
18	72948.44	0.267851	133	19.09981	298.38
19	49873.71	0.066963	100	3.89668	14.09377
20	183160.1	0.765093	110	61.20079	2026.707
21	198936.4	0.768249	271	53.03788	1624.683
22	462445.2	0.536591	445	42.48457	1336.373
23	91711.75	0.596058	168	41.71272	1205.397
24	184979.2	0.440584	154	34.70057	813.3113

25	99687.83	0.15434	166	10.91351	110.8717
26	385915.3	0.931168	213	53.7957	2346.228
27	315939.6	0.317014	157	31.58041	690.3577
28	435859.3	1.029196	732	66.65053	2058.063
29	733340.3	0.66302	190	57.6877	1776.933
30	55565	0.060355	147	5.066152	28.22381
31	166639.2	0.529391	85	35.07012	645.0041
32	102443.4	0.046844	46	3.901358	14.09377
33	232306.2	0.128748	158	9.748716	76.62497
34	134314.1	0.694086	266	43.67275	1487.6
35	147310.8	0.502665	179	43.28449	1063.23
36	146103	0.207496	211	19.89038	284.2501
37	92888.2	0.199755	178	16.37728	187.4845
38	668081.1	0.937775	118	77.96634	1829.297
39	614003.6	0.314992	389	24.55891	491.8148
40	281726.8	0.212673	68	16.75619	220.7435
41	54948.32	0.155474	162	11.69004	86.62272
42	238108.3	0.970567	98	66.27162	2665.797
43	518653.9	0.852716	319	62.36091	1359.599
44	473949.6	0.575102	278	42.87751	1540.012
45	464652.8	0.569332	593	59.62434	2146.721
46	418568.5	0.82599	256	60.4383	1953.251
47	184917.1	0.317014	166	24.94717	518.0392
48	390808.5	0.438858	149	61.20547	2374.427
49	138372.1	0.805279	211	47.9577	1526.821
50	71737.4	0.07214	198	7.021508	42.34196
51	341439.7	0.685457	222	45.60004	986.7015
52	349652.9	0.780279	246	51.8497	1516.944

53	119319.8	0.077022	203	6.628566	48.38882
54	428269.4	1.065093	227	83.43011	4012.047

APPENDIX II

Derived Daily CN of Stations

Station	Probability Based Curve Number			Median Based Curve Number			Catchment Characteristics Based Curve Number		
	Wet Condition	Normal Condition	Dry Condition	Wet Condition	Normal Condition	Dry Condition	Wet Condition	Normal Condition	Dry Condition
Badapandusar	99.137	93.476	66.947	97.086	93.476	86.168	85.873	72.189	53.226
Baghupali	97.692	81.804	52.152	91.270	81.804	66.154	79.608	62.504	42.223
Bansajal	99.259	91.120	63.616	95.978	91.120	81.689	83.683	68.652	48.982
Bargaon	98.642	90.714	63.732	95.784	90.714	80.943	87.132	74.302	55.900
Bisipada	99.550	91.150	63.393	95.993	91.150	81.746	87.132	74.302	55.900
Burat	99.399	91.796	66.604	96.299	91.796	82.950	86.404	73.073	54.332
Chatikuda	99.334	91.444	65.974	96.132	91.444	82.291	82.337	66.560	46.599
Kadaligarh	98.170	88.173	59.906	94.547	88.173	76.422	83.683	68.652	48.982
Magurbeda	99.219	90.192	62.871	95.533	90.192	79.992	84.460	69.887	50.432
Maneswar	98.372	86.230	57.991	93.575	86.230	73.138	80.544	63.869	43.661
Naraj	99.453	92.887	66.423	96.812	92.887	85.025	76.234	57.800	37.518
Rampur	96.212	86.395	54.170	93.584	86.248	73.168	75.294	56.547	36.327
Surubali	99.037	91.133	57.803	95.984	91.133	81.713	82.890	67.413	47.559
Takara	98.563	88.537	62.934	94.726	88.537	77.055	84.555	70.038	50.613
Takla	99.065	89.686	61.951	95.288	89.686	79.083	84.702	70.276	50.897
Tulaghat	98.547	85.956	55.641	93.436	85.956	72.686	82.890	67.413	47.559
Tumulibud	99.502	93.784	72.751	97.229	93.784	86.772	70.216	50.166	30.619

Daily Simulation Performances of Three CN Derivation Methods and Three Developed Models of Stations

Station	Correlation Coefficient of Observed Runoff with Runoff for					
	Probability-CN	Median-CN	Catchment Characteristics-CN	MS Model	Sahu Model	Michel Model
Badapandusar	0.315	0.832	0.610	0.878	0.809	0.340
Baghupali	0.670	0.908	0.777	0.964	0.487	0.650
Bansajal	0.952	0.944	0.971	0.946	0.839	0.817
Bargaon	0.845	0.966	0.908	0.941	0.776	0.876
Bisipada	0.007	0.587	0.045	0.703	0.305	0.251
Burat	0.898	0.969	0.926	0.885	0.645	0.798
Chatikuda	0.744	0.961	0.844	0.914	0.743	0.868
Kadaligarh	0.908	0.929	0.867	0.906	0.702	0.687
Magurbeda	0.890	0.981	0.890	0.872	0.491	0.779
Maneswar	0.846	0.945	0.730	0.879	0.621	0.640
Naraj	0.799	0.967	0.519	0.791	0.448	0.812
Rampur	0.650	0.962	0.616	0.914	0.672	0.804
Surubali	0.842	0.978	0.867	0.847	0.576	0.809
Takara	0.442	0.904	0.602	0.826	0.349	0.517
Takla	0.929	0.982	0.919	0.950	0.785	0.890
Tulaghat	0.814	0.966	0.916	0.911	0.731	0.841
Tumulibud	0.750	0.919	0.301	0.915	0.615	0.674

Derived Monthly CN of Stations

Station	Probability Based Curve Number			Median Based Curve Number			Catchment Characteristics Based Curve Number		
	Wet Condition	Normal Condition	Dry Condition	Wet Condition	Normal Condition	Dry Condition	Wet Condition	Normal Condition	Dry Condition

Badapandusar	81.410	40.738	13.138	60.672	39.881	22.385	85.873	72.189	53.226
Baghupali	83.610	43.680	8.166	64.332	43.680	25.217	79.608	62.504	42.223
Bansajal	92.701	61.353	21.351	78.686	61.353	40.836	83.683	68.652	48.982
Bargaon	92.459	72.057	19.005	85.708	72.057	52.856	87.132	74.302	55.900
Bisipada	94.344	47.433	16.219	67.726	47.433	28.177	87.132	74.302	55.900
Burat	96.074	56.668	16.281	74.100	55.161	34.848	86.404	73.073	54.332
Chatikuda	95.912	67.622	25.683	81.107	64.862	44.524	82.337	66.560	46.599
Kadaligarh	91.367	62.871	14.648	79.749	62.871	42.404	83.683	68.652	48.982
Magurbeda	95.849	56.539	21.233	75.157	56.539	36.127	84.460	69.887	50.432
Maneswar	92.364	59.906	15.043	77.652	59.906	39.380	80.544	63.869	43.661
Naraj	96.517	57.225	25.893	75.676	57.225	36.775	76.234	57.800	37.518
Rampur	93.731	61.800	11.702	78.917	61.680	41.170	75.294	56.547	36.327
Surubali	93.749	48.820	24.540	68.805	48.677	29.197	82.890	67.413	47.559
Takara	92.643	46.182	18.836	65.969	45.461	26.601	84.555	70.038	50.613
Takla	97.287	68.280	30.174	83.350	68.280	48.344	84.702	70.276	50.897
Tulaghat	95.665	50.397	13.411	69.066	48.981	29.449	82.890	67.413	47.559
Tumulibud	94.424	57.064	11.700	75.555	57.064	36.623	70.216	50.166	30.619

Monthly Simulation Performances of Three CN Derivation Methods of Stations

Station	**Correlation Coefficient of Observed Runoff with Runoff for**		
	Probability-CN	Median-CN	Catchment Characteristics-CN
Badapandusar	0.114	0.845	0.980
Baghupali	0.867	0.986	0.998
Bansajal	0.903	0.982	0.992
Bargaon	0.955	0.999	0.999
Bisipada	0.177	0.769	0.965
Burat	0.862	0.991	0.995

Chatikuda	0.818	0.983	0.985
Kadaligarh	0.901	0.996	0.998
Magurbeda	0.733	0.898	0.978
Maneswar	0.647	0.983	0.987
Naraj	0.884	0.967	0..967
Rampur	0.416	0.964	0.975
Surubali	0.896	0.954	0.982
Takara	0.419	0.897	0.956
Takla	0.954	0.987	0.979
Tulaghat	0.895	0.978	0.995
Tumulibud	0.303	0.986	0.979

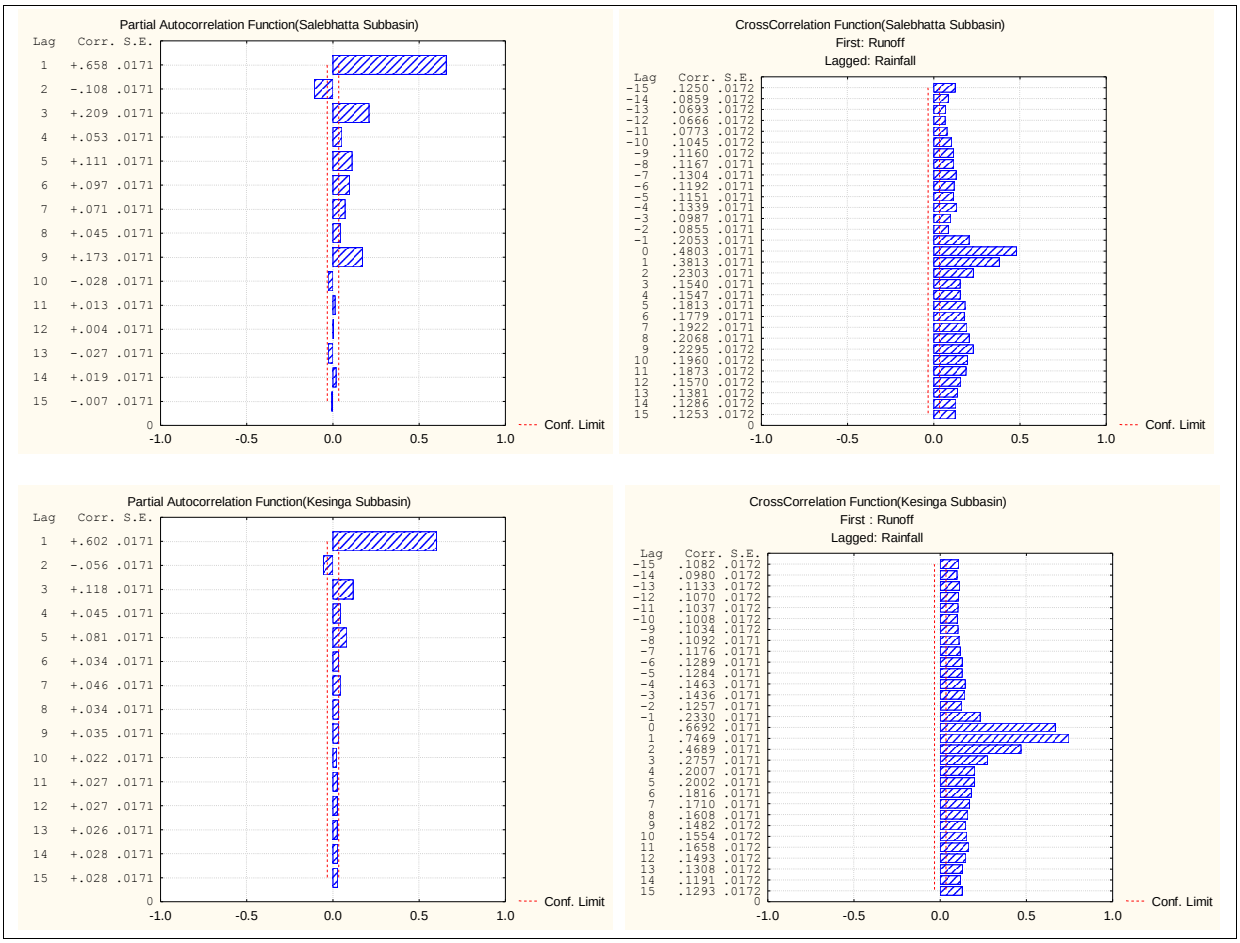

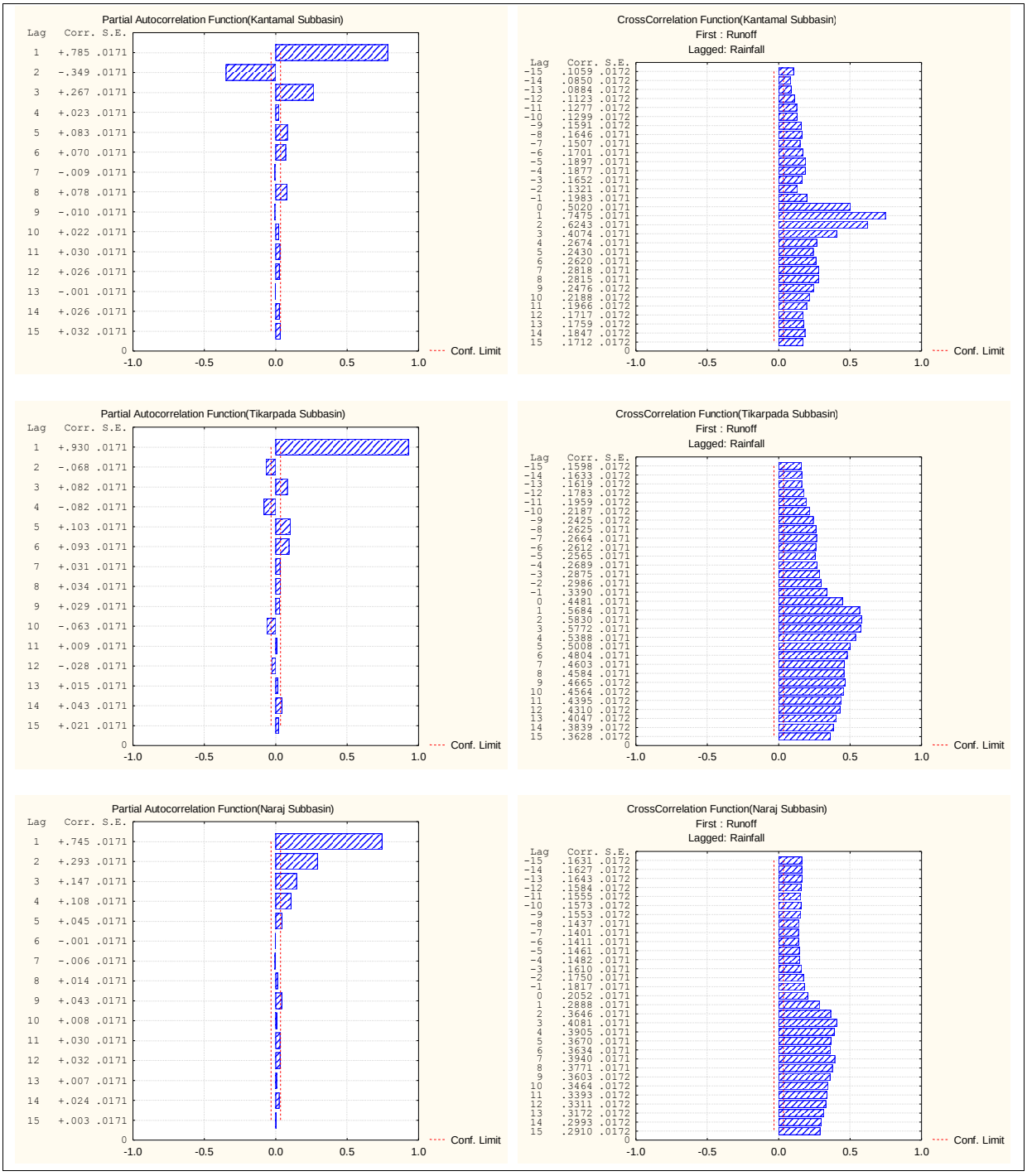

PACF and CCF Plots of Daily Runoff Time Series of Sub-basins

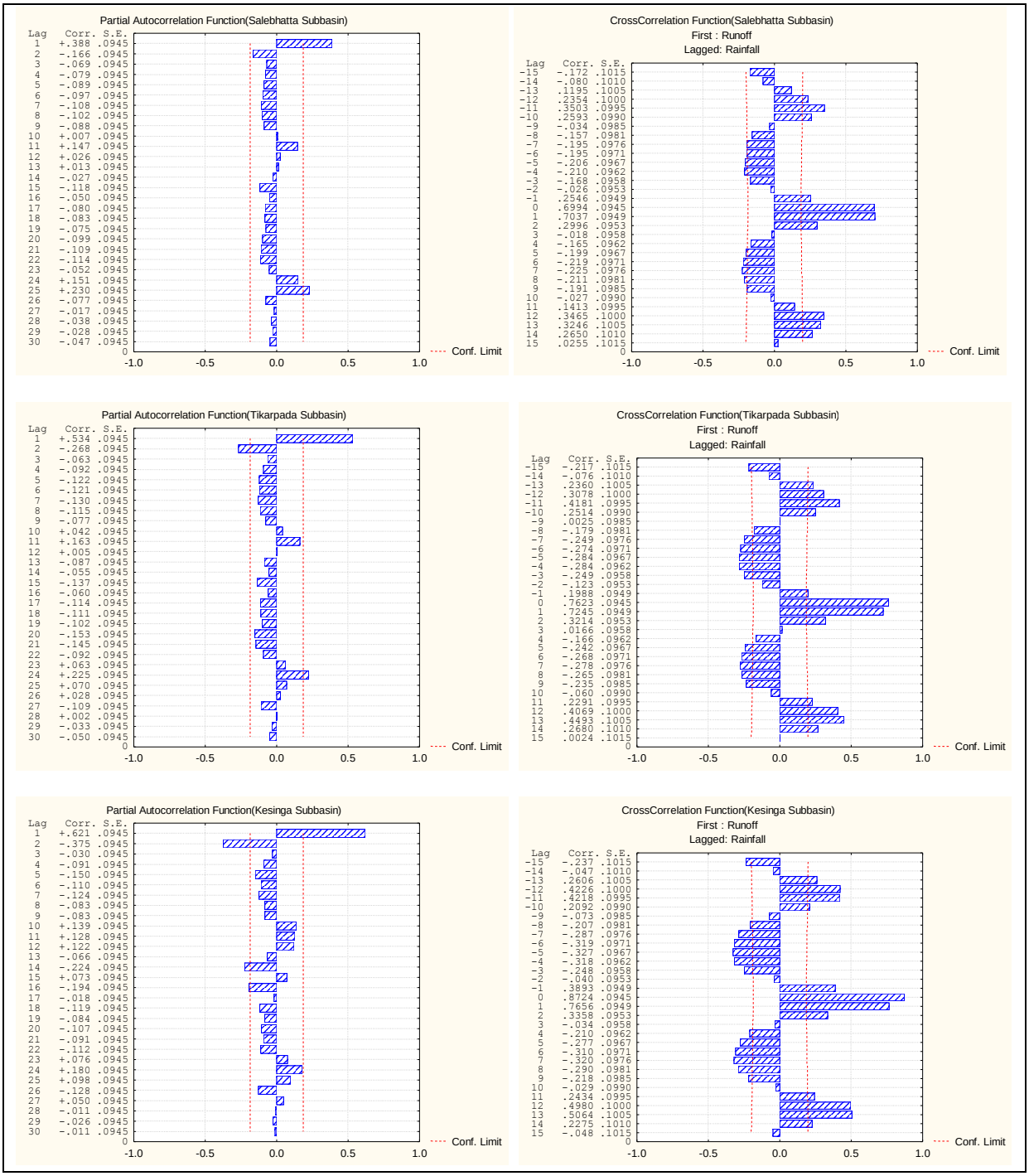
Partial Autocorrelation Function(Salebhatta Subbasin)
Lag Corr. S.E.
1 +.388 .0945
2 -.166 .0945
3 -.069 .0945
4 -.079 .0945
5 -.089 .0945
6 -.097 .0945
7 -.108 .0945
8 -.102 .0945
9 -.088 .0945
10 +.007 .0945
11 +.147 .0945
12 +.026 .0945
13 +.013 .0945
14 -.027 .0945
15 -.118 .0945
16 -.050 .0945
17 -.080 .0945
18 -.083 .0945
19 -.075 .0945
20 -.099 .0945
21 -.109 .0945
22 -.114 .0945
23 -.052 .0945
24 +.151 .0945
25 +.230 .0945
26 -.077 .0945
27 -.017 .0945
28 -.038 .0945
29 -.028 .0945
30 -.047 .0945
-1.0 -0.5 0.0 0.5 1.0
Conf. Limit
CrossCorrelation Function(Salebhatta Subbasin)
First : Runoff
Lagged: Rainfall
Lag Corr. S.E.
-15 -.172 .1015
-14 -.080 .1010
-13 .1195 .1005
-12 .2354 .1000
-11 .3503 .0995
-10 .2593 .0990
-9 -.034 .0985
-8 -.157 .0981
-7 -.195 .0976
-6 -.195 .0971
-5 -.206 .0967
-4 -.210 .0962
-3 -.168 .0958
-2 -.026 .0953
-1 .2546 .0949
0 .6994 .0945
1 .7037 .0949
2 .2996 .0953
3 -.018 .0958
4 -.165 .0962
5 -.199 .0967
6 -.219 .0971
7 -.225 .0976
8 -.211 .0981
9 -.191 .0985
10 -.027 .0990
11 .1413 .0995
12 .3465 .1000
13 .3246 .1005
14 .2650 .1010
15 .0255 .1015
-1.0 -0.5 0.0 0.5 1.0
Conf. Limit
Partial Autocorrelation Function(Tikarpada Subbasin)
Lag Corr. S.E.
1 +.534 .0945
2 -.268 .0945
3 -.063 .0945
4 -.092 .0945
5 -.122 .0945
6 -.121 .0945
7 -.130 .0945
8 -.115 .0945
9 -.077 .0945
10 +.042 .0945
11 +.163 .0945
12 +.005 .0945
13 -.087 .0945
14 -.055 .0945
15 -.137 .0945
16 -.060 .0945
17 -.114 .0945
18 -.111 .0945
19 -.102 .0945
20 -.153 .0945
21 -.145 .0945
22 -.092 .0945
23 +.063 .0945
24 +.225 .0945
25 +.070 .0945
26 +.028 .0945
27 -.109 .0945
28 +.002 .0945
29 -.033 .0945
30 -.050 .0945
-1.0 -0.5 0.0 0.5 1.0
Conf. Limit
CrossCorrelation Function(Tikarpada Subbasin)
First : Runoff
Lagged: Rainfall
Lag Corr. S.E.
-15 -.217 .1015
-14 -.076 .1010
-13 .2360 .1005
-12 .3078 .1000
-11 .4181 .0995
-10 .2514 .0990
-9 .0025 .0985
-8 -.179 .0981
-7 -.249 .0976
-6 -.274 .0971
-5 -.284 .0967
-4 -.284 .0962
-3 -.249 .0958
-2 -.123 .0953
-1 .1988 .0949
0 .7623 .0945
1 .7245 .0949
2 .3214 .0953
3 .0166 .0958
4 -.166 .0962
5 -.242 .0967
6 -.268 .0971
7 -.278 .0976
8 -.265 .0981
9 -.235 .0985
10 -.060 .0990
11 .2291 .0995
12 .4069 .1000
13 .4493 .1005
14 .2680 .1010
15 .0024 .1015
-1.0 -0.5 0.0 0.5 1.0
Conf. Limit
Partial Autocorrelation Function(Kesinga Subbasin)
Lag Corr. S.E.
1 +.621 .0945
2 -.375 .0945
3 -.030 .0945
4 -.091 .0945
5 -.150 .0945
6 -.110 .0945
7 -.124 .0945
8 -.083 .0945
9 -.083 .0945
10 +.139 .0945
11 +.128 .0945
12 +.122 .0945
13 -.066 .0945
14 -.224 .0945
15 +.073 .0945
16 -.194 .0945
17 -.018 .0945
18 -.119 .0945
19 -.084 .0945
20 -.107 .0945
21 -.091 .0945
22 -.112 .0945
23 +.076 .0945
24 +.180 .0945
25 +.098 .0945
26 -.128 .0945
27 +.050 .0945
28 -.011 .0945
29 -.026 .0945
30 -.011 .0945
-1.0 -0.5 0.0 0.5 1.0
Conf. Limit
CrossCorrelation Function(Kesinga Subbasin)
First : Runoff
Lagged: Rainfall
Lag Corr. S.E.
-15 -.237 .1015
-14 -.047 .1010
-13 .2606 .1005
-12 .4226 .1000
-11 .4218 .0995
-10 .2092 .0990
-9 -.073 .0985
-8 -.207 .0981
-7 -.287 .0976
-6 -.319 .0971
-5 -.327 .0967
-4 -.318 .0962
-3 -.248 .0958
-2 -.040 .0953
-1 .3893 .0949
0 .8724 .0945
1 .7656 .0949
2 .3358 .0953
3 -.034 .0958
4 -.210 .0962
5 -.277 .0967
6 -.310 .0971
7 -.320 .0976
8 -.290 .0981
9 -.218 .0985
10 -.029 .0990
11 .2434 .0995
12 .4980 .1000
13 .5064 .1005
14 .2275 .1010
15 -.048 .1015
-1.0 -0.5 0.0 0.5 1.0
Conf. Limit

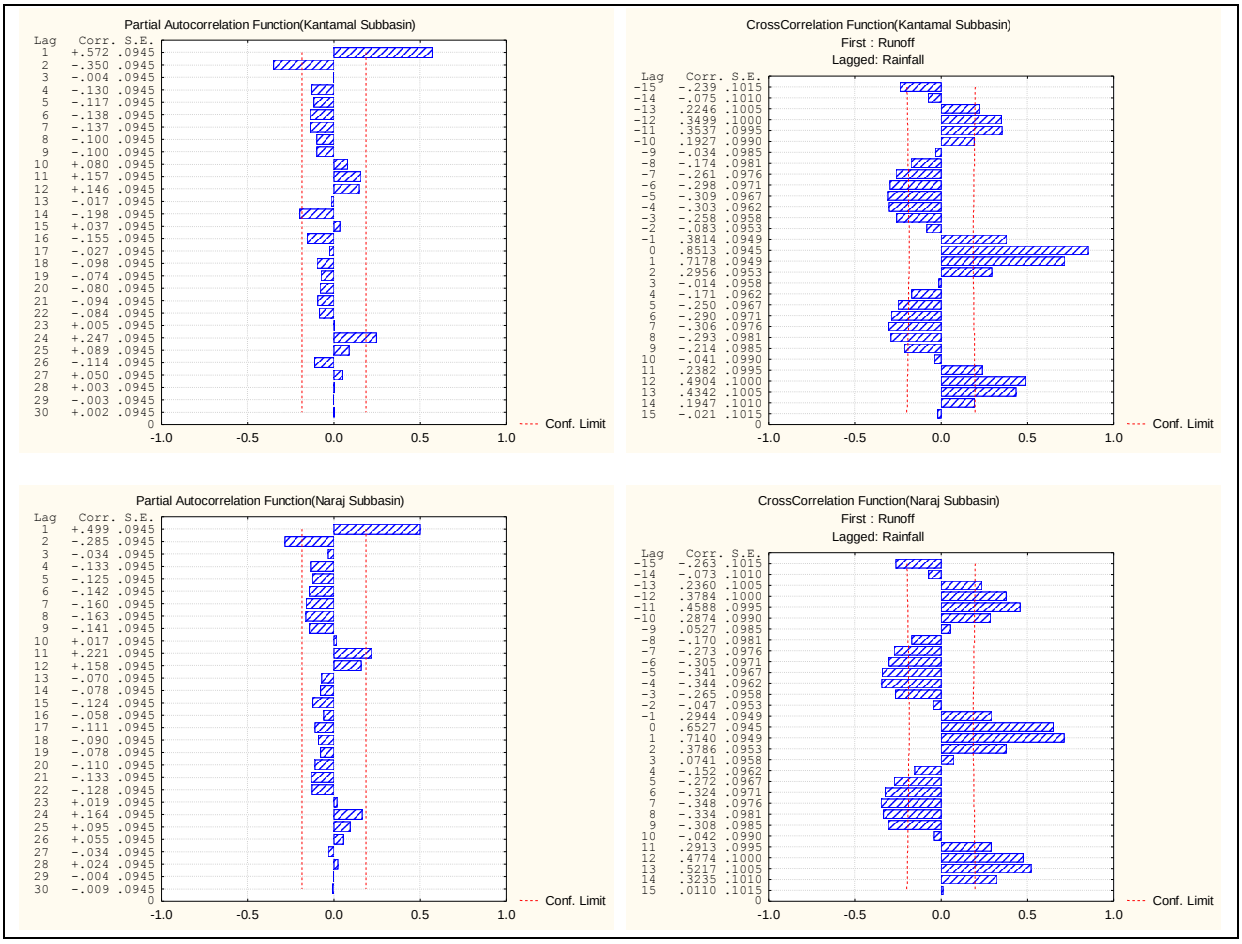

PACF and CCF Plots of Monthly Runoff Time Series of Sub-basins

Optimized Neural Network Structure of Daily Rainfall-Runoff Models for Stations

Station	Input	Network Architecture	Training Performance	Testing Performance	Validation Performance
			Correlation Coefficient		
Badapandusar	$Runoff_{t-1}$,$Rainfall_t$,$Rainfall_{t-1}$	3-6-1	0.952622	0.895081	0.883660
Baghupali	$Runoff_{t-1}$, $Runoff_{t-2}$,$Runoff_{t-3}$, $Rainfall_t$,$Rainfall_{t-1}$	5-5-1	0.964467	0.905719	0.961573
Bansajal	$Runoff_{t-1}$, $Rainfall_t$	2-7-1	0.867596	0.971063	0.926563
Bargaon	$Runoff_{t-1}$, $Runoff_{t-2}$,$Runoff_{t-3}$, $Rainfall_t$,$Rainfall_{t-1}$	5-7-1	0.832116	0.905426	0.816451
Bisipada	$Runoff_{t-}$	3-8-1	0.889366	0.961788	0.889581

	$_{1}$,Rainfall$_{t}$,Rainfall$_{t-1}$				
Burat	Runoff$_{t-1}$,Rainfall$_{t}$	2-6-1	0.932643	0.852241	0.695227
Chatikuda	Runoff$_{t-1}$,Rainfall$_{t}$,Rainfall$_{t-1}$	3-7-1	0.802113	0.829324	0.833666
Kadaligarh	Runoff$_{t-1}$,Rainfall$_{t}$,Rainfall$_{t-1}$	3-3-1	0.538364	0.824117	0.545724
Magurbeda	Runoff$_{t-1}$,Rainfall$_{t}$,Rainfall$_{t-1}$	3-8-1	0.887770	0.788330	0.572845
Maneswar	Runoff$_{t-1}$,Rainfall$_{t}$	2-5-1	0.668776	0.797439	0.621700
Naraj	Runoff$_{t-1}$, Runoff$_{t-2}$,Runoff$_{t-3}$, Runoff$_{t-4}$, Rainfall$_{t}$,Rainfall$_{t-1}$, Rainfall$_{t-2}$, Rainfall$_{t-3}$	8-11-1	0.838748	0.940569	0.950569
Rampur	Runoff$_{t-1}$,Rainfall$_{t}$,Rainfall$_{t-1}$	3-6-1	0.920238	0.956834	0.951579
Surubali	Runoff$_{t-1}$,Rainfall$_{t}$	2-4-1	0.911878	0.902365	0.913115
Takara	Runoff$_{t-1}$,Rainfall$_{t}$,Rainfall$_{t-1}$	3-10-1	0.756132	0.630685	0.697855
Takla	Runoff$_{t-1}$,Rainfall$_{t}$,Rainfall$_{t-1}$	3-8-1	0.871863	0.838230	0.820649
Tulaghat	Runoff$_{t-1}$,Rainfall$_{t}$	2-8-1	0.797698	0.843584	0.800136
Tumulibud	Runoff$_{t-1}$,Rainfall$_{t}$	2-3-1	0.849080	0.828812	0.975035

Optimized Neural Network Structure of Monthly Rainfall-Runoff Models for Stations

Station	**Input**	**Network Architecture**	**Training Performance**	**Testing Performance**	**Validation Performance**
			Correlation Coefficient		
Badapandusar	Runoff$_{t-1}$, Rainfall$_{t}$,Rainfall$_{t-1}$, Rainfall$_{t-2}$	4-10-1	0.970510	0.888590	0.985080
Baghupali	Runoff$_{t-1}$, Rainfall$_{t}$,Rainfall$_{t-1}$	3-8-1	0.753767	0.507449	0.324110
Bansajal	Runoff$_{t-1}$, Runoff$_{t-12}$	4-6-1	0.889786	0.542577	0.802705

	,$Rainfall_t$,$Rainfall_{t-1}$				
Bargaon	$Runoff_{t-1}$, $Rainfall_t$,$Rainfall_{t-1}$	3-5-1	0.761034	0.694489	0.960666
Bisipada	$Runoff_{t-1}$, $Runoff_{t-2}$,$Runoff_{t-12}$,$Rainfall_t$,$Rainfall_{t-1}$	5-10-1	0.854087	0.885012	0.823119
Burat	$Runoff_{t-1}$, $Rainfall_t$,$Rainfall_{t-1}$	3-9-1	0.789030	0.827558	0.878641
Chatikuda	$Runoff_{t-1}$, $Runoff_{t-2}$, $Rainfall_t$,$Rainfall_{t-1}$	4-3-1	0.903001	0.748038	0.960032
Kadaligarh	$Runoff_{t-1}$, $Rainfall_t$,$Rainfall_{t-1}$	3-4-1	0.690388	0.697327	0.998803
Magurbeda	$Runoff_{t-1}$, $Rainfall_t$,$Rainfall_{t-1}$	3-3-1	0.959014	0.914909	0.996835
Maneswar	$Runoff_{t-1}$, $Rainfall_t$	2-4-1	0.958333	0.816375	0.930031
Naraj	$Runoff_{t-1}$, $Runoff_{t-2}$, $Rainfall_t$,$Rainfall_{t-1}$	4-7-1	0.900733	0.712729	0.953313
Rampur	$Runoff_{t-1}$, $Runoff_{t-2}$, $Rainfall_t$	3-5-1	0.843734	0.401993	0.933423
Surubali	$Runoff_{t-1}$, $Runoff_{t-2}$, $Rainfall_t$,$Rainfall_{t-1}$	4-9-1	0.906211	0.705282	0.982581
Takara	$Runoff_{t-1}$, $Rainfall_t$,$Rainfall_{t-1}$	3-4-1	0.871319	0.620951	0.996230
Takla	$Runoff_{t-1}$, $Runoff_{t-2}$, $Rainfall_t$,$Rainfall_{t-1}$	4-5-1	0.880287	0.123139	0.993362
Tulaghat	$Runoff_{t-1}$, $Rainfall_t$,$Rainfall_{t-1}$	3-4-1	0.688083	0.308826	0.995064
Tumulibud	$Runoff_{t-1}$, $Rainfall_t$,$Rainfall_{t-1}$	3-9-1	0.504002	0.723149	0.582130

APPENDIX III

Computed Daily and Monthly CN from equations for Stations

Station	Daily Curve Number Derived from Developed Equation			30-Day Curve Number Derived from Developed Equation		
	Wet Condition	Normal Condition	Dry Condition	Wet Condition	Normal Condition	Dry Condition
Badapandusar	97.399	88.45	73.791	56.19	37.99	28.58
Baghupali	95.334	89.452	74.511	84.72	60.8	43.22
Bansajal	96.062	89.28	75.49	75.24	42.88	28.8
Bargaon	96.748	91.15	77.777	68.56	51.71	32.74
Bisipada	96.836	87.788	74.253	73.81	44.52	26.49
Burat	96.824	90.386	79.992	89.11	60.98	33.65
Chatikuda	98.125	92.039	81.543	87.25	72	51.76
Kadaligarh	96.942	89.742	76.272	80.76	58.77	39.79
Magurbeda	96.555	88.076	74.433	71.76	43.88	26.96
Maneswar	96.244	88.614	75.385	82.44	52.48	26.52
Naraj	97.143	91.744	78.882	88.82	81.13	64.73
Rampur	96.129	88.976	77.282	87.4	58.7	44.86
Surubali	97.581	90.563	77.491	68.32	50.05	35.47
Takara	94.009	85.148	70.61	76.29	42.17	25.95
Takla	96.156	90.837	78.701	82.41	64.07	47.41
Tulaghat	94.02	84.439	67.43	81.26	44.39	26.83
Tumulibud	97.604	93.926	86.592	92.79	69.16	45.18

Performance Efficiency of Developed Equation of Stations

Station	Coefficient of Determination(R^2)			Nash-Suttcliffe simulation efficiency (E_{NS})		
	Wet Condition	Normal Condition	Dry Condition	Wet Condition	Normal Condition	Dry Condition
Badapandusar	0.991	0.996	0.990	0.991	0.996	0.990
Baghupali	0.845	0.911	0.904	0.809	0.906	0.894
Bansajal	0.991	0.996	0.990	0.991	0.996	0.990
Bargaon	0.982	0.998	0.990	0.981	0.998	0.990
Bisipada	0.997	0.983	0.973	0.997	0.983	0.972
Burat	0.973	0.987	0.992	0.972	0.987	0.992
Chatikuda	0.957	0.995	0.980	0.956	0.994	0.979
Kadaligarh	0.932	0.983	0.985	0.928	0.983	0.985
Magurbeda	0.993	0.992	0.983	0.992	0.992	0.983
Maneswar	0.906	0.988	0.991	0.897	0.988	0.991
Naraj	0.955	0.955	0.813	0.954	0.953	0.773
Rampur	0.852	0.985	0.978	0.840	0.985	0.977
Surubali	0.994	0.997	0.979	0.993	0.997	0.978
Takara	0.967	0.988	0.976	0.966	0.988	0.971
Takla	0.952	0.985	0.988	0.947	0.985	0.988
Tulaghat	0.986	0.995	0.970	0.985	0.995	0.970
Tumulibud	0.951	0.996	0.997	0.949	0.996	0.996

APPENDIX IV

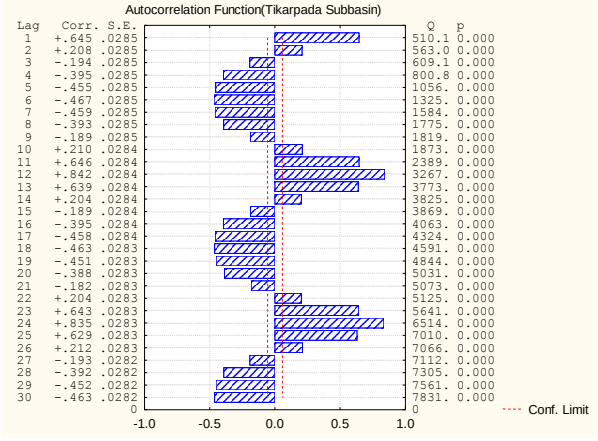
Autocorrelation Function(Tikarpada Subbasin)
Lag Corr. S.E. Q p
1 +.645 .0285 510.1 0.000
2 +.208 .0285 563.0 0.000
3 -.194 .0285 609.1 0.000
4 -.395 .0285 800.8 0.000
5 -.455 .0285 1056. 0.000
6 -.467 .0285 1325. 0.000
7 -.459 .0285 1584. 0.000
8 -.393 .0285 1775. 0.000
9 -.189 .0285 1819. 0.000
10 +.210 .0284 1873. 0.000
11 +.646 .0284 2389. 0.000
12 +.842 .0284 3267. 0.000
13 +.639 .0284 3773. 0.000
14 +.204 .0284 3825. 0.000
15 -.189 .0284 3869. 0.000
16 -.395 .0284 4063. 0.000
17 -.458 .0284 4324. 0.000
18 -.463 .0283 4591. 0.000
19 -.451 .0283 4844. 0.000
20 -.388 .0283 5031. 0.000
21 -.182 .0283 5073. 0.000
22 +.204 .0283 5125. 0.000
23 +.643 .0283 5641. 0.000
24 +.835 .0283 6514. 0.000
25 +.629 .0283 7010. 0.000
26 +.212 .0283 7066. 0.000
27 -.193 .0282 7112. 0.000
28 -.392 .0282 7305. 0.000
29 -.452 .0282 7561. 0.000
30 -.463 .0282 7831. 0.000
Conf. Limit

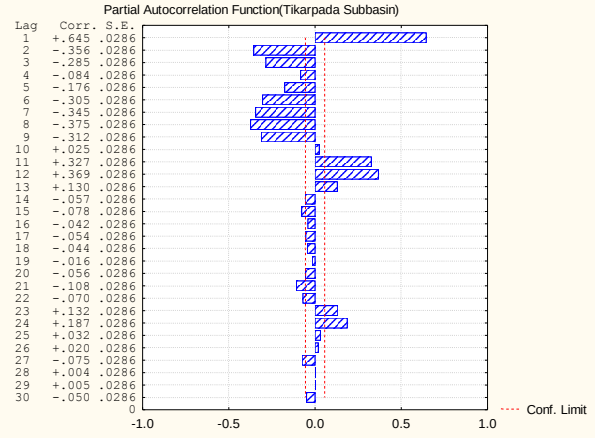
Partial Autocorrelation Function(Tikarpada Subbasin)
Lag Corr. S.E.
1 +.645 .0286
2 -.356 .0286
3 -.285 .0286
4 -.084 .0286
5 -.176 .0286
6 -.305 .0286
7 -.345 .0286
8 -.375 .0286
9 -.312 .0286
10 +.025 .0286
11 +.327 .0286
12 +.369 .0286
13 +.130 .0286
14 -.057 .0286
15 -.078 .0286
16 -.042 .0286
17 -.054 .0286
18 -.044 .0286
19 -.016 .0286
20 -.056 .0286
21 -.108 .0286
22 -.070 .0286
23 +.132 .0286
24 +.187 .0286
25 +.032 .0286
26 +.020 .0286
27 -.075 .0286
28 +.004 .0286
29 +.005 .0286
30 -.050 .0286
Conf. Limit

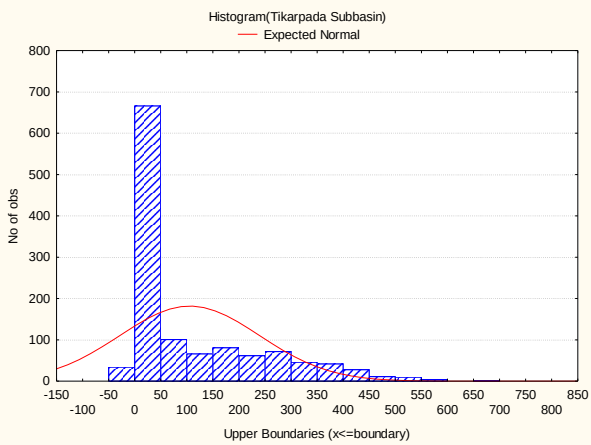
Histogram(Tikarpada Subbasin)
Expected Normal
No of obs
Upper Boundaries (x<=boundary)

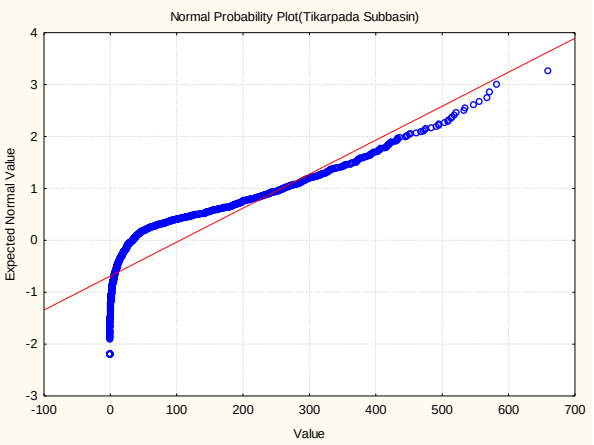
Normal Probability Plot(Tikarpada Subbasin)
Expected Normal Value
Value

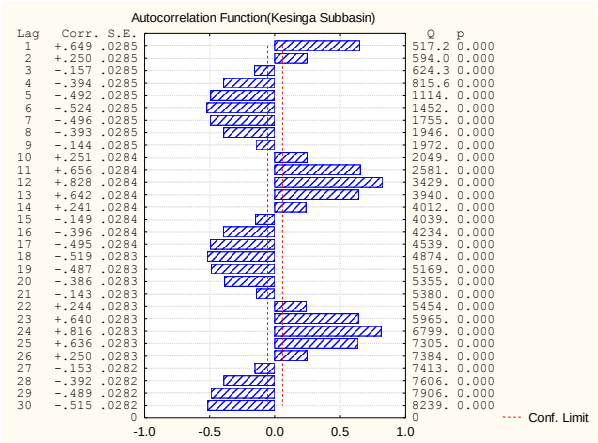
Autocorrelation Function(Kesinga Subbasin)
Lag Corr. S.E. Q p
1 +.649 .0285 517.2 0.000
2 +.250 .0285 594.0 0.000
3 -.157 .0285 624.3 0.000
4 -.394 .0285 815.6 0.000
5 -.492 .0285 1114. 0.000
6 -.524 .0285 1452. 0.000
7 -.496 .0285 1755. 0.000
8 -.393 .0285 1946. 0.000
9 -.144 .0285 1972. 0.000
10 +.251 .0284 2049. 0.000
11 +.656 .0284 2581. 0.000
12 +.828 .0284 3429. 0.000
13 +.642 .0284 3940. 0.000
14 +.241 .0284 4012. 0.000
15 -.149 .0284 4039. 0.000
16 -.396 .0284 4234. 0.000
17 -.495 .0284 4539. 0.000
18 -.519 .0283 4874. 0.000
19 -.487 .0283 5169. 0.000
20 -.386 .0283 5355. 0.000
21 -.143 .0283 5380. 0.000
22 +.244 .0283 5454. 0.000
23 +.640 .0283 5965. 0.000
24 +.816 .0283 6799. 0.000
25 +.636 .0283 7305. 0.000
26 +.250 .0283 7384. 0.000
27 -.153 .0282 7413. 0.000
28 -.392 .0282 7606. 0.000
29 -.489 .0282 7906. 0.000
30 -.515 .0282 8239. 0.000
Conf. Limit

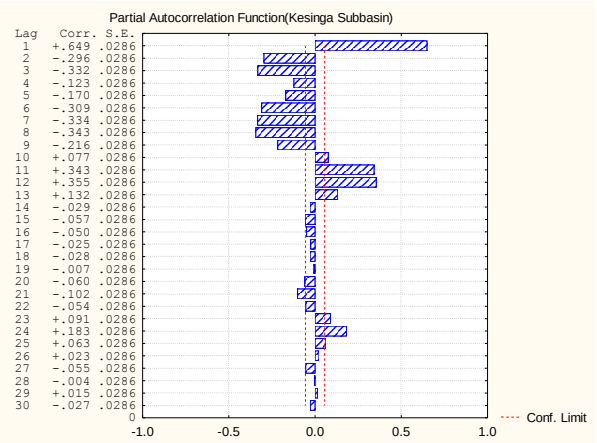
Partial Autocorrelation Function(Kesinga Subbasin)
Lag Corr. S.E.
1 +.649 .0286
2 -.296 .0286
3 -.332 .0286
4 -.123 .0286
5 -.170 .0286
6 -.309 .0286
7 -.334 .0286
8 -.343 .0286
9 -.216 .0286
10 +.077 .0286
11 +.343 .0286
12 +.355 .0286
13 +.132 .0286
14 -.029 .0286
15 -.057 .0286
16 -.050 .0286
17 -.025 .0286
18 -.028 .0286
19 -.007 .0286
20 -.060 .0286
21 -.102 .0286
22 -.054 .0286
23 +.091 .0286
24 +.183 .0286
25 +.063 .0286
26 +.023 .0286
27 -.055 .0286
28 -.004 .0286
29 +.015 .0286
30 -.027 .0286
Conf. Limit

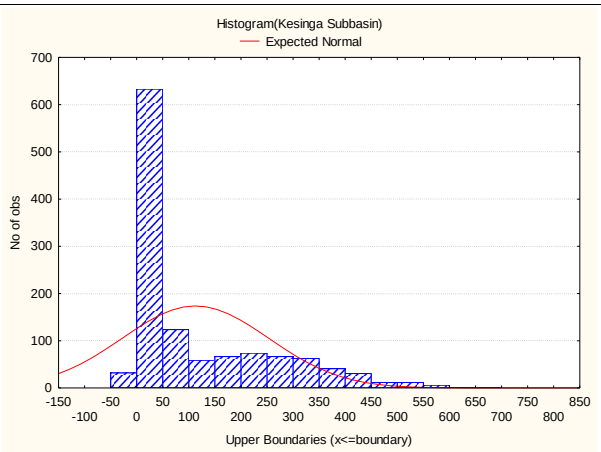
Histogram(Kesinga Subbasin)
Expected Normal
No of obs
Upper Boundaries (x<=boundary)

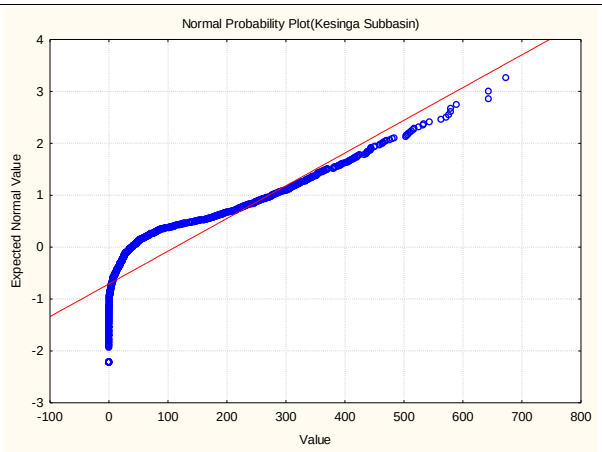
Normal Probability Plot(Kesinga Subbasin)
Expected Normal Value
Value

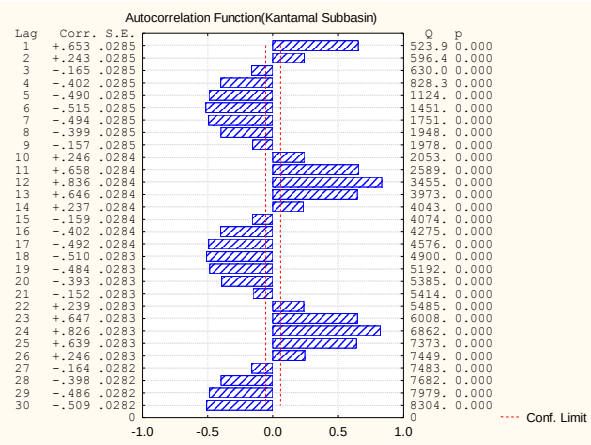
Autocorrelation Function(Kantamal Subbasin)
Lag Corr. S.E. Q p
1 +.653 .0285 523.9 0.000
2 +.243 .0285 596.4 0.000
3 -.165 .0285 630.0 0.000
4 -.402 .0285 828.3 0.000
5 -.490 .0285 1124. 0.000
6 -.515 .0285 1451. 0.000
7 -.494 .0285 1751. 0.000
8 -.399 .0285 1948. 0.000
9 -.157 .0285 1978. 0.000
10 +.246 .0284 2053. 0.000
11 +.658 .0284 2589. 0.000
12 +.836 .0284 3455. 0.000
13 +.646 .0284 3973. 0.000
14 +.237 .0284 4043. 0.000
15 -.159 .0284 4074. 0.000
16 -.402 .0284 4275. 0.000
17 -.492 .0284 4576. 0.000
18 -.510 .0283 4900. 0.000
19 -.484 .0283 5192. 0.000
20 -.393 .0283 5385. 0.000
21 -.152 .0283 5414. 0.000
22 +.239 .0283 5485. 0.000
23 +.647 .0283 6008. 0.000
24 +.826 .0283 6862. 0.000
25 +.639 .0283 7373. 0.000
26 +.246 .0283 7449. 0.000
27 -.164 .0282 7483. 0.000
28 -.398 .0282 7682. 0.000
29 -.486 .0282 7979. 0.000
30 -.509 .0282 8304. 0.000
Conf. Limit

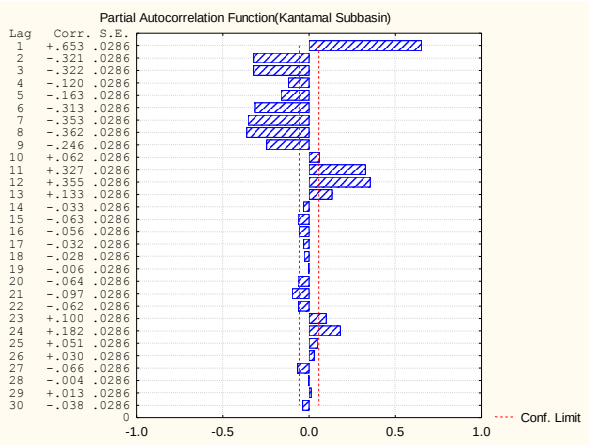
Partial Autocorrelation Function(Kantamal Subbasin)
Lag Corr. S.E.
1 +.653 .0286
2 -.321 .0286
3 -.322 .0286
4 -.120 .0286
5 -.163 .0286
6 -.313 .0286
7 -.353 .0286
8 -.362 .0286
9 -.246 .0286
10 +.062 .0286
11 +.327 .0286
12 +.355 .0286
13 +.133 .0286
14 -.033 .0286
15 -.063 .0286
16 -.056 .0286
17 -.032 .0286
18 -.028 .0286
19 -.006 .0286
20 -.064 .0286
21 -.097 .0286
22 -.062 .0286
23 +.100 .0286
24 +.182 .0286
25 +.051 .0286
26 +.030 .0286
27 -.066 .0286
28 -.004 .0286
29 +.013 .0286
30 -.038 .0286
Conf. Limit

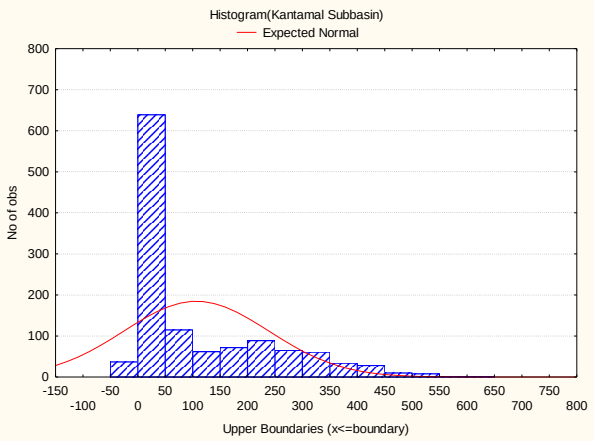
Histogram(Kantamal Subbasin)
Expected Normal
No of obs
Upper Boundaries (x<=boundary)

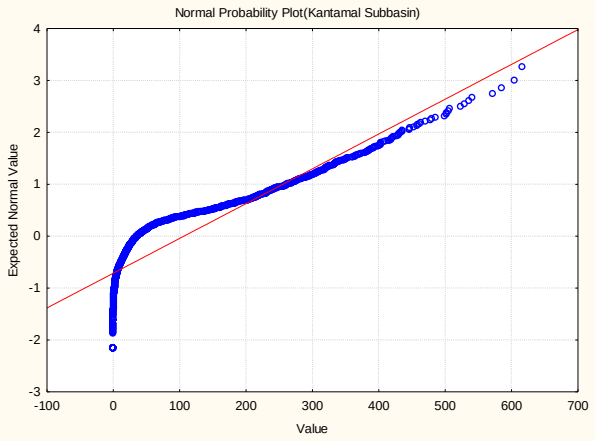
Normal Probability Plot(Kantamal Subbasin)
Expected Normal Value
Value

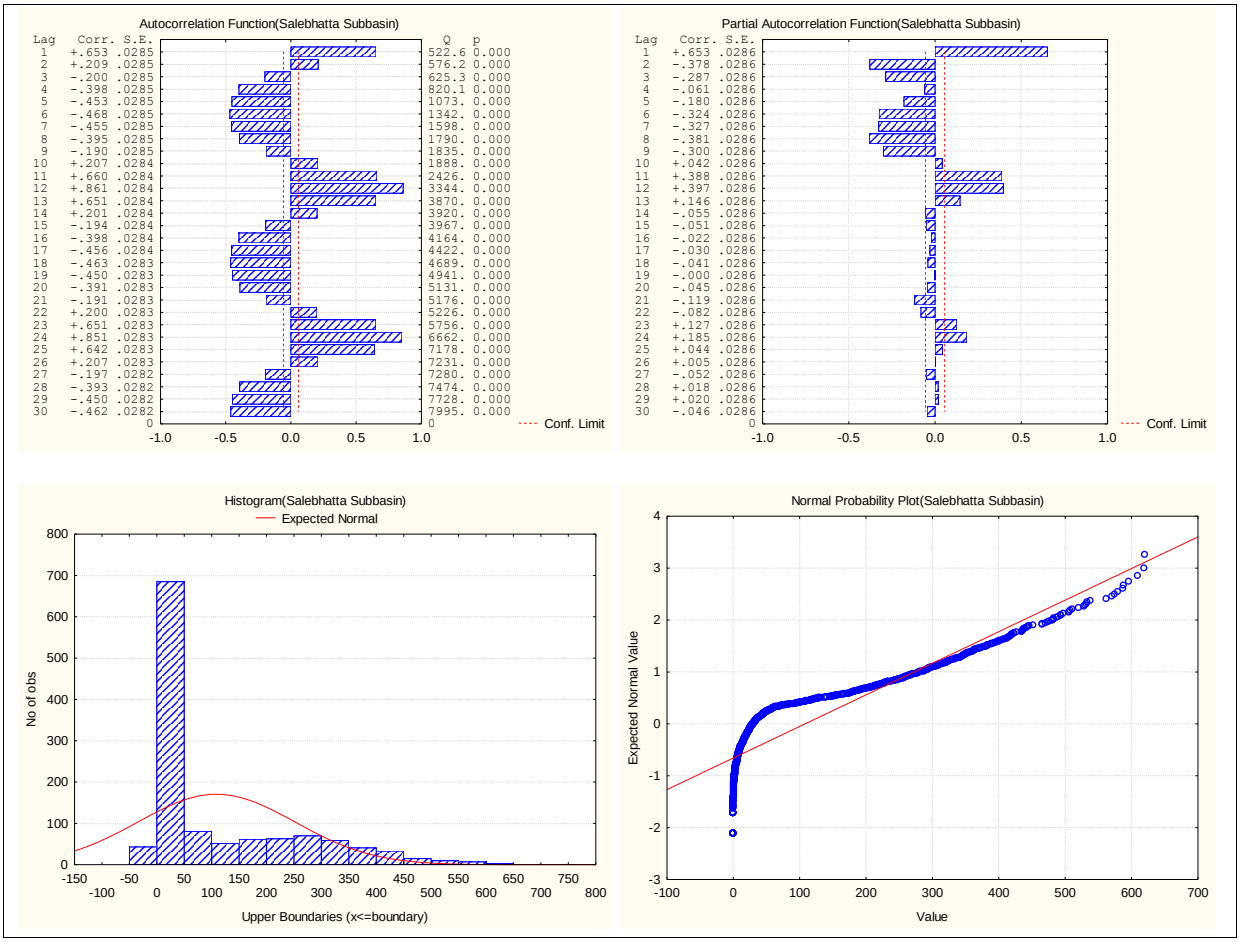

Time Series Plots of Monthly Rainfall Data

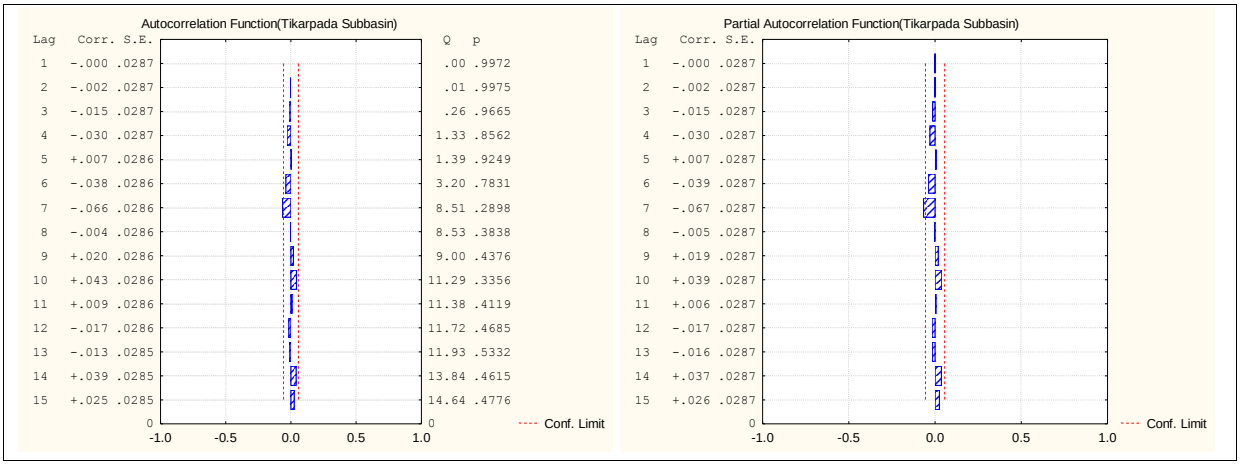

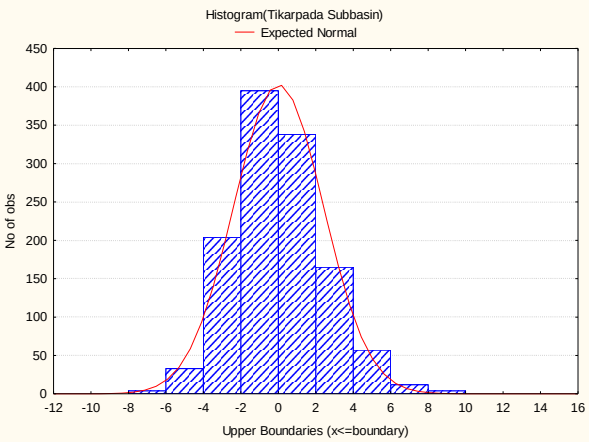
Histogram(Tikarpada Subbasin)
Expected Normal
No of obs
Upper Boundaries (x<=boundary)

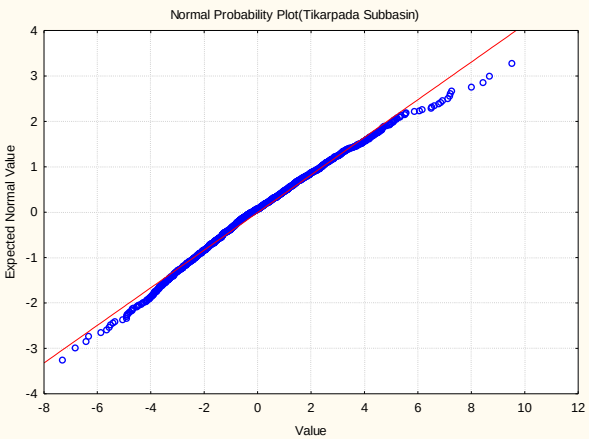
Normal Probability Plot(Tikarpada Subbasin)
Expected Normal Value
Value

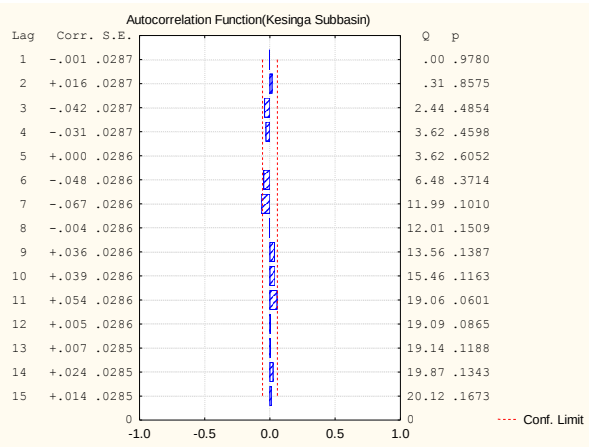
Autocorrelation Function(Kesinga Subbasin)
Lag Corr. S.E. Q p
1 -.001 .0287 .00 .9780
2 +.016 .0287 .31 .8575
3 -.042 .0287 2.44 .4854
4 -.031 .0287 3.62 .4598
5 +.000 .0286 3.62 .6052
6 -.048 .0286 6.48 .3714
7 -.067 .0286 11.99 .1010
8 -.004 .0286 12.01 .1509
9 +.036 .0286 13.56 .1387
10 +.039 .0286 15.46 .1163
11 +.054 .0286 19.06 .0601
12 +.005 .0286 19.09 .0865
13 +.007 .0285 19.14 .1188
14 +.024 .0285 19.87 .1343
15 +.014 .0285 20.12 .1673
Conf. Limit

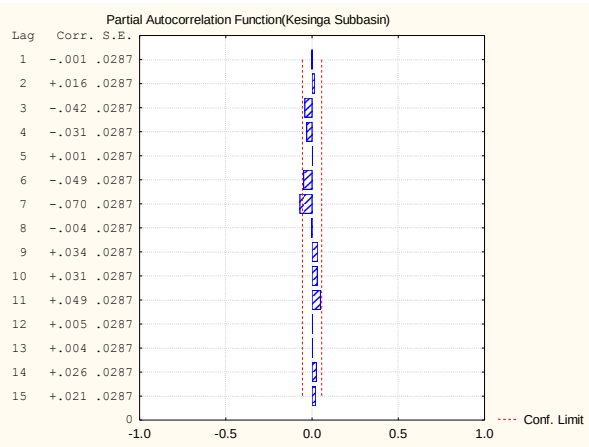
Partial Autocorrelation Function(Kesinga Subbasin)
Lag Corr. S.E.
1 -.001 .0287
2 +.016 .0287
3 -.042 .0287
4 -.031 .0287
5 +.001 .0287
6 -.049 .0287
7 -.070 .0287
8 -.004 .0287
9 +.034 .0287
10 +.031 .0287
11 +.049 .0287
12 +.005 .0287
13 +.004 .0287
14 +.026 .0287
15 +.021 .0287
Conf. Limit

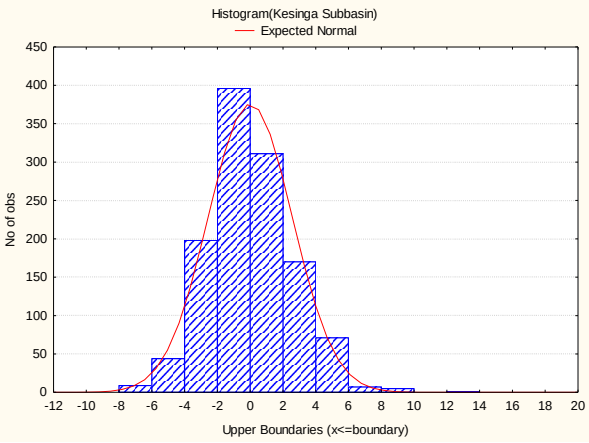
Histogram(Kesinga Subbasin)
Expected Normal
No of obs
Upper Boundaries (x<=boundary)

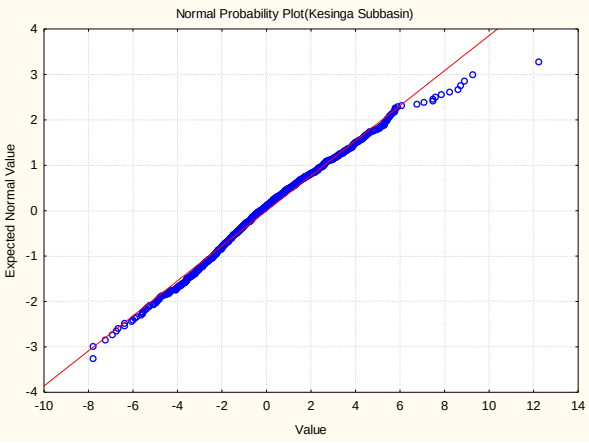
Normal Probability Plot(Kesinga Subbasin)
Expected Normal Value
Value

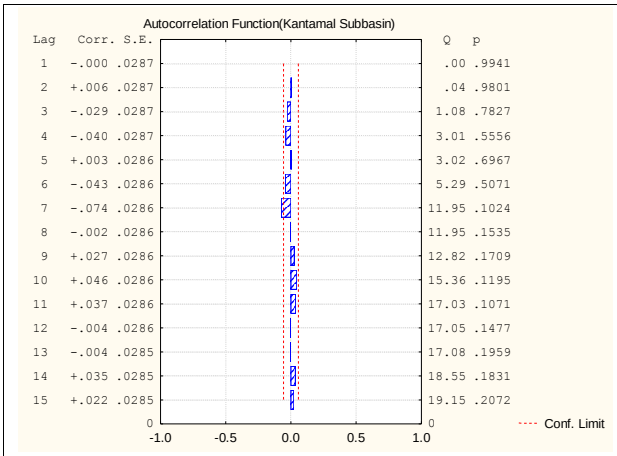
Autocorrelation Function(Kantamal Subbasin)
Lag Corr. S.E. Q p
1 -.000 .0287 .00 .9941
2 +.006 .0287 .04 .9801
3 -.029 .0287 1.08 .7827
4 -.040 .0287 3.01 .5556
5 +.003 .0286 3.02 .6967
6 -.043 .0286 5.29 .5071
7 -.074 .0286 11.95 .1024
8 -.002 .0286 11.95 .1535
9 +.027 .0286 12.82 .1709
10 +.046 .0286 15.36 .1195
11 +.037 .0286 17.03 .1071
12 -.004 .0286 17.05 .1477
13 -.004 .0285 17.08 .1959
14 +.035 .0285 18.55 .1831
15 +.022 .0285 19.15 .2072
-1.0 -0.5 0.0 0.5 1.0
Conf. Limit

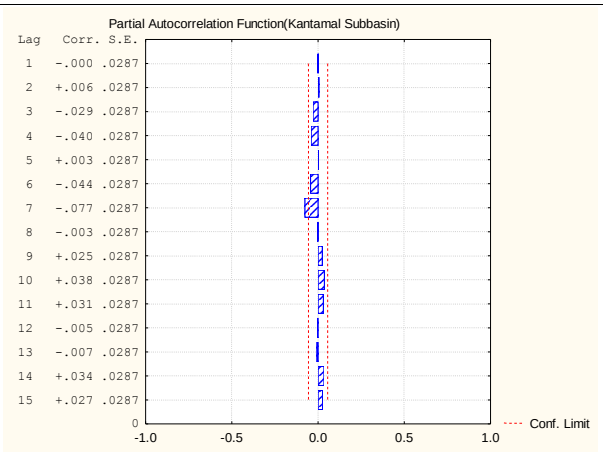
Partial Autocorrelation Function(Kantamal Subbasin)
Lag Corr. S.E.
1 -.000 .0287
2 +.006 .0287
3 -.029 .0287
4 -.040 .0287
5 +.003 .0287
6 -.044 .0287
7 -.077 .0287
8 -.003 .0287
9 +.025 .0287
10 +.038 .0287
11 +.031 .0287
12 -.005 .0287
13 -.007 .0287
14 +.034 .0287
15 +.027 .0287
-1.0 -0.5 0.0 0.5 1.0
Conf. Limit

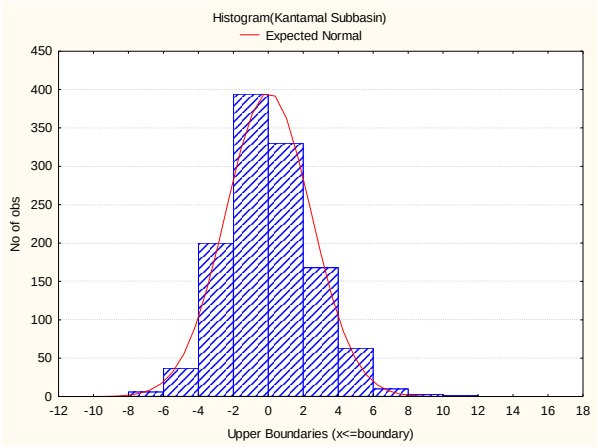
Histogram(Kantamal Subbasin)
Expected Normal
No of obs
Upper Boundaries (x<=boundary)

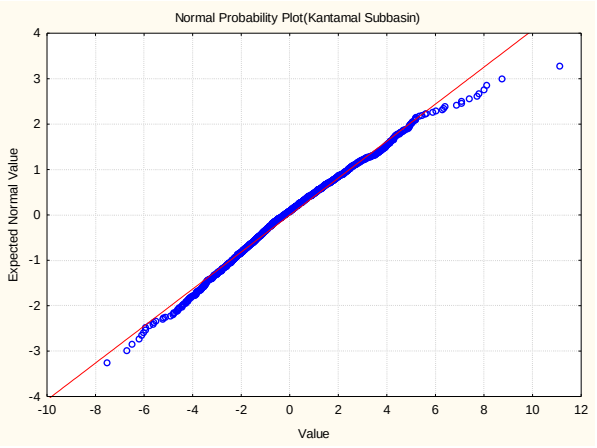
Normal Probability Plot(Kantamal Subbasin)
Expected Normal Value
Value

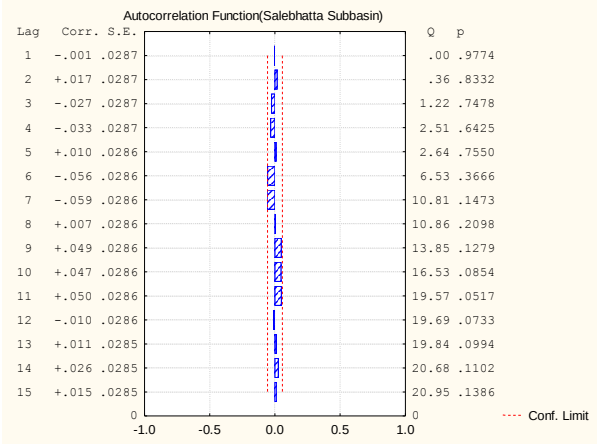
Autocorrelation Function(Salebhatta Subbasin)
Lag Corr. S.E. Q p
1 -.001 .0287 .00 .9774
2 +.017 .0287 .36 .8332
3 -.027 .0287 1.22 .7478
4 -.033 .0287 2.51 .6425
5 +.010 .0286 2.64 .7550
6 -.056 .0286 6.53 .3666
7 -.059 .0286 10.81 .1473
8 +.007 .0286 10.86 .2098
9 +.049 .0286 13.85 .1279
10 +.047 .0286 16.53 .0854
11 +.050 .0286 19.57 .0517
12 -.010 .0286 19.69 .0733
13 +.011 .0285 19.84 .0994
14 +.026 .0285 20.68 .1102
15 +.015 .0285 20.95 .1386
-1.0 -0.5 0.0 0.5 1.0
Conf. Limit

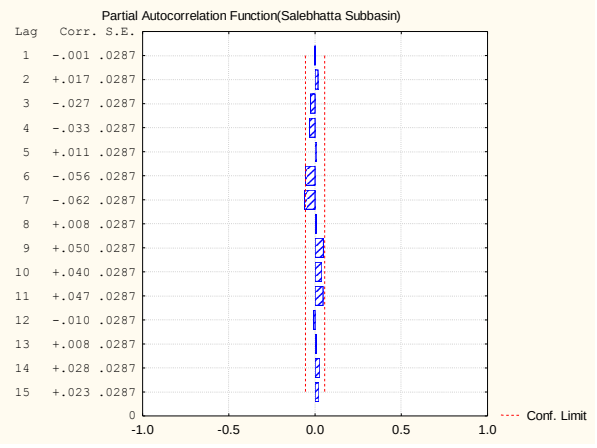
Partial Autocorrelation Function(Salebhatta Subbasin)
Lag Corr. S.E.
1 -.001 .0287
2 +.017 .0287
3 -.027 .0287
4 -.033 .0287
5 +.011 .0287
6 -.056 .0287
7 -.062 .0287
8 +.008 .0287
9 +.050 .0287
10 +.040 .0287
11 +.047 .0287
12 -.010 .0287
13 +.008 .0287
14 +.028 .0287
15 +.023 .0287
-1.0 -0.5 0.0 0.5 1.0
Conf. Limit

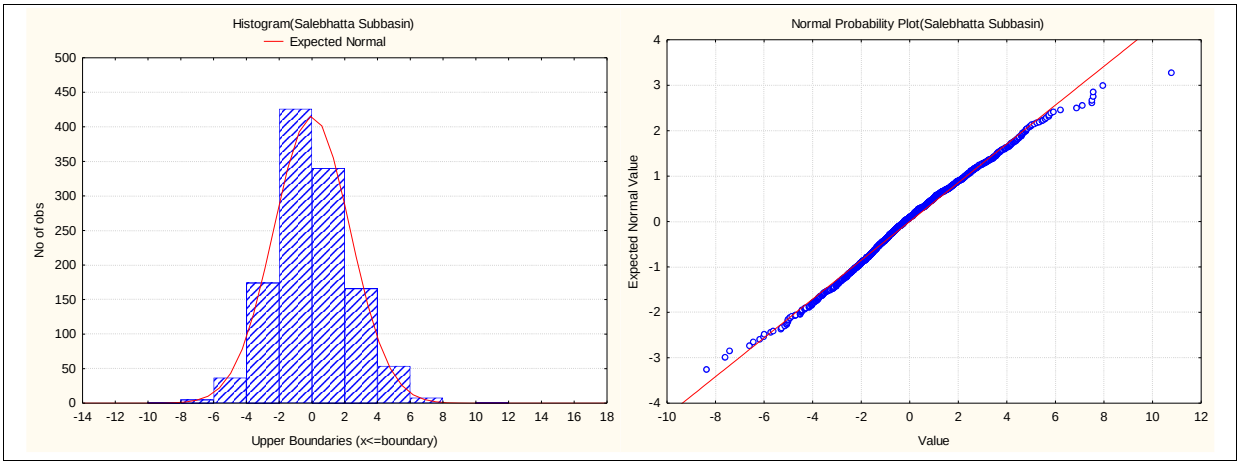

Diagnostic Check Plots of Residual from Best Fitted Seasonal ARIMA Model

Best Fitted SARIMA Model of Stations

Station	Network Architecture
Angul	$(0,0,1)^1(0,1,1)^{12}$
Balangir	$(1,0,0)^1(0,1,1)^{12}$
Bargarh	$(1,0,0)^1(0,1,1)^{12}$
Boudh	$(0,0,1)^1(0,1,1)^{12}$
Cuttack	$(0,0,1)^1(0,1,1)^{12}$
Debgarh	$(0,0,1)^1(0,1,1)^{12}$
Dhenkanal	$(0,0,1)^1(0,1,1)^{12}$
Ganjam	$(0,0,1)^1(0,1,1)^{12}$
Jagatsingpur	$(1,0,0)^1(0,1,1)^{12}$
Jajpur	$(0,0,1)^1(0,1,1)^{12}$
Jharsuguda	$(0,0,1)^1(0,1,1)^{12}$
Kalahandi	$(1,0,0)^1(0,1,1)^{12}$
Kandhamal	$(0,0,1)^1(0,1,1)^{12}$
Kendrapada	$(1,0,0)^1(0,1,1)^{12}$
Khordha	$(0,0,1)^1(0,1,1)^{12}$
Nabarangpur	$(1,0,0)^1(0,1,1)^{12}$
Nayagarh	$(0,0,1)^1(0,1,1)^{12}$
Nuapada	$(1,0,0)^1(0,1,1)^{12}$
Puri	$(1,0,0)^1(0,1,1)^{12}$
Rayagada	$(0,0,1)^1(0,1,1)^{12}$
Sambalpur	$(0,0,1)^1(0,1,1)^{12}$
Sonepur	$(0,0,1)^1(0,1,1)^{12}$
Sundargarh	$(0,0,1)^1(0,1,1)^{12}$

Best Fitted MLP ANN Model of Stations

Station	Network Architecture
Angul	12-8-1
Balangir	12-5-1
Bargarh	12-7-1
Boudh	12-6-1
Cuttack	12-6-1
Debgarh	12-8-1
Dhenkanal	12-6-1

Ganjam	12-4-1
Jagatsingpur	12-7-1
Jajpur	12-5-1
Jharsuguda	12-5-1
Kalahandi	12-6-1
Kandhamal	12-5-1
Kendrapada	12-6-1
Khordha	12-2-1
Nabarangpur	12-8-1
Nayagarh	12-2-1
Nuapada	12-4-1
Puri	12-4-1
Rayagada	12-5-1
Sambalpur	12-7-1
Sonepur	12-5-1
Sundargarh	12-7-1

Published and Under Review Papers

- J. Meher and R. Jha(2013) "Time series analysis of monthly rainfall data for the Mahanadi River basin, India" Sciences in Cold and Arid Regions, 5(1),73-84.

- J. Meher and R. Jha(2013) **"**Development of ARIMA model for shifting monthly rainfall trends in Mahanadi basin, India" KSCE. (Under Review)

- J. Meher and R. Jha (2014)"Mapping Monthly Precipitation in Mahanadi River Basin using GIS" *International Journal of Earth Sciences and Engineering.*(Under Review)

- R. Jha and J. Meher(2014) "IWRM on reduced sweet water flow at sites in Mahanadi River System, India: Past, Present and Future" *International Journal of Water Resources Development, Taylor & Francis, USA*. (Accepted for publication in July 2014)

- J. Meher and R. Jha(2011) "Time series analysis of rainfall data over Mahanadi River basin" Emerging Science,3(6),22-32,2011.

- J. Meher and R. Jha(2012) "Critical evaluation of ANN algorithms for predicting monthly rainfall time series" International conference "HYDRO 2012",IIT Bombay.

- J. Meher and R. Jha(2011) "Analysis of spatio-temporal variability of rainfall over Mahanadi river basin", International conference "Sustainable water resources management and climate change adaptation" , NIT Durgapur.